A Mechanical Study of Synthetic Soft Tissue Membranes for Prosthesis.

By

Richard Charles Arm

A thesis submitted in partial fulfilment of the requirements of Nottingham Trent University for the degree of Doctor of Philosophy

December 2023

Director of studies: Dr Hughes-Riley **Supervisor:** Dr Moghaddassian Shahidi

Acknowledgments

I would like to offer my thanks and gratitude to my supervisory team, Dr Hughes-Riley, Dr Shahidi, and consultants Dr Coulter and Professor Mahoney for their advice, guidance and assistance. Thanks to the School of Art and Design at NTU, Emeritus Professor Dias and Professor Marsden.

Thanks to my family- Mother Tannia, wife Karyn and daughter Mimi for all their love, support, patience and encouragement.

- For Elora -

Research Activities

Memberships:

1. The Royal Society of the Arts Fellow (FRSA)
2. The Higher Education Academy Fellow (FHEA)
3. Member of the Society of Surgical Simulation (No SSIM-0449)
4. Member of the British Association for the study of the Liver (No 4574)
5. Member of the British Society of Strain Measurement
6. Member of the Association for Simulated Practice in Healthcare
7. Member of EGE University, Scientific Committee

Exhibitions:

1. 2023 – Exhibitor at European annual Cardiothoracic Society conference, Vienna, Austria.
2. 2019 – Exhibitor at Emergency Services Show, NEC, Birmingham, UK.
3. 2017 – Exhibitor at DSEI 2017 Alongside RCDM and the Tri-service Defence Medical Services.
4. 2017 – Awarded Transforming Surgical Education Award from Royal College of Surgeons.
5. 2016 - Exhibitor at The Tomorrow Fair, Saatchi Gallery/ The Design Museum, London, UK.
6. 2016 - Exhibitor at LATi: From earth to space and beyond, Loughborough University, UK.
7. 2016 – Exhibitor at Melbourne Victoria Museum of Natural History, Melbourne, Australia.
8. 2016 – International press coverage of thoracic trauma trainer. Global.
9. 2016 - Exhibitor of thoracic trauma trainer at Trauma Innovations, Birmingham, UK.

Journal Articles

1. Arm, R., Shahidi, A., Pislaru, A., Marasinghe, K., Bibb, R., & Hughes-Riley, T. (2024). Mechanical Behavior of Oil-Saturated Silicone Membranes for Adipose Tissue Synthesis in Clinical and Theatrical Prosthesis. Prosthesis, 6(6), 1340-1358.
2. Hughes-Riley, T., Shahidi, A.M…Arm, R., Oliveira, C., Holmquist, L.E. and Dias, T. (2024). Wearable Electronic Textiles for Healthcare, Wellbeing, and Protective Applications. In *Extended Abstracts of the CHI Conference on Human Factors in Computing Systems* (1-5).
3. Arm., R (2024). Research applications case study 6—Biomodelling with bio-inspired soft materials. In, Bibb, R., Eggbeer, D., Paterson, A., & Mohammed, M. I. (2024). *Medical Modeling: The Application of Advanced Design and Additive Manufacturing Techniques in Medicine*. Elsevier.
4. Lugoda, P., Arm, R., Wooler…Navaraj, W. (2024). HaptiYarn: development of an actuator yarn that can transform everyday textiles into haptic devices. IEEE Transactions on Haptics.
5. Agbiki, T., Arm, R., Hewson, D… Morgan, S. P. (2024). Fabrication and assessment of a bio-inspired synthetic tracheal tissue model for tracheal tube cuff leakage testing. *BJA Open*, *10*, 100290.
6. Gaddum, N., Dillon-Murphy, D., Arm, R., et al (2022). In silico modelling of aortic strain and strain rate in aortic coarctation treated with stent angioplasty with comparison to clinical cohorts. *Applications In Engineering Science*, 12: 100123. DOI: 10.1016/j.apples.2022.100123
7. Arm R, Shahidi A, Clarke C, Alabraba, E. (2022) Synthesis and characterisation of a cancerous liver for presurgical planning and training applications. BMJ Open Gastroenterology 2022;9: DOI: 10.1136/bmjgast-2022-000909
8. Abeywardena, C., Vanheusden, F., Walker, K., Arm, R., Zhang, Q., (2020). Fetal movement counting using optical fibre sensors. *Sensors*, 21 (1): 48. ISSN 1424-8220 DOI:10.3390/s21010048.
9. Arm, R., Shahidi, A., Dias, T. (2019). 'Mechanical Behaviour of silicone membranes saturated with short-strand, loose polyester fibres for prosthetic and surrogate skin applications.' Materials. DOI 10.3390/ma12223647
10. P. Mahoney, D. Carr, R. Arm. (2018). Ballistic impacts on an anatomically correct synthetic skull with a surrogate skin/soft tissue layer. International Journal of Legal Medicine. 132, 2, pp 519–530 DOI: 10.1007/s00414-017-1737-9

Conference proceedings

Arm, R., Shahidi, A., Clarke, C. (2021). Creating a surrogate artificial liver using 3D printing and mechanical characterisation of hepatic tissues for tumour removal education. Gut 2021;70: A51. DOI:10.1136/gutjnl-2021-BASL.78

Conference presentations

1. 2022 – Presenter at Roentgenfest (clinical imaging) annual conference, Nottingham, UK. (November)
2. 2022 – Presenter at Medical Technologies and Advanced Materials Conference, Nottingham, UK. (November)
3. 2022 – Presenter at CHEAD and Laboratory tour. Nottingham, UK. (July)
4. 2022 – Presenter at Board of Governors research. NTU, Nottingham, UK. (July)
5. 2022 – Presenter at Annual Research Conference, NTU, Nottingham, UK. (March)
6. 2019 – Presenter (main stage), at TCT 2019, NEC Birmingham, UK.
7. 2019 – Presenter at Think BIG Future Healthcare and Technology. Institution of Engineering and Technology, UK.
8. 2019 – Presenter at Medical Technology and advanced materials conference 2019, NTU Clifton, Notts, UK.
9. 2018 – Presenter at SPMIC (Sir Peter Mansfield Imaging Centre) Imaging, SPMIC, UK..
10. 2017 – Presenter at Society for Tri-service Anaesthetic Trainees conference, MoD, Edinburgh, UK.
11. 2017 – Presenter at Medilink conference for 3D printing in medicine, Nottingham, UK.
12. 2017 - Presenter and exhibitor at Surgeons Education day, Royal College of Surgeons, London.
13. 2017 – Keynote presenter/ exhibitor for The National Centre for Crafts and Design, UK.
14. 2016 – Presenter at Crafts Council event at Manchester Museum of Science and Industry, UK.
15. 2016 - Presenter at Policom, 'Applied polymeric composites' EGE University, Izmir, Turkey.

Patents:

1. Prosthetic silicone sleeve liner

Publication number: 20170216058

2. Silicone adhesive bra

Publication number: 20190274369

Abstract

Polydimethylsiloxane (PDMS) gels and elastomers are also known as Silicones. These materials are well documented in the literature especially in scientific journals, but PDMS gels employed by prosthetists often have adulterating agents in them that can affect their mechanical behaviour. Experienced prosthetists have been adding loose fibres, embedding fabrics and adding oil to polydimethylsiloxane (PDMS) gels for decades, building a deep understanding of the benefits and drawbacks, but literature documenting these additives' use is rare. Coloured, loose fibres are often used to pigment it, textiles are employed to reinforce it and oil is used to soften it, but the technical know-how of PDMS gel manipulation, has remained the embodied, tacit knowledge of the prosthetist, remaining unpublished and unquantified.

In this thesis, conclusive, data-based evidence is used to examine the technical aspects and mechanical influence of adding fibres, fabrics and oils to PDMS gels. Using industry agreed test standards and accessible technologies, this work presents an unabridged exploration of PDMS gel characteristics that would be familiar and useful to the experienced and inexperienced prosthetist alike.

New knowledge generated by this investigation defines the hardening effect of fibres and how textile addition, orientation and tension have a direct, measurable influence on a range of mechanical characteristics. Beyond simply adding strength, fibres and fabrics can be used to create membranes that are visually and mechanically similar to human skin. Additionally, data-based evidence reveals previously unknown material characteristics of oil saturated PDMS gels and mechanical tests demonstrate how they can be used to create more realistic, synthetic soft tissues and organs for surgical training models.

This work explicitly contributes new knowledge to the field of functional prosthetics by describing the mechanisms for control over key behavioural traits linked to the performance of organic counterparts such as extensibility, elasticity, anisotropy, and viscoelasticity.

Content

Surrogate- to elect in another's place. *Something that replaces or is used instead of something else.*

Chapter 1

Introduction

This thesis is a scientific investigation into the mechanical behaviour of synthetic surrogate materials intended for clinical and theatrical prosthetic applications. Soft, synthetic membranes, informed by nature's own designs, were created with elastomeric composites, which would be familiar to prosthetists. The membranes were mechanically characterised using repeatable standardised test methods, to improve communication amongst disparate user groups. Novel material characteristics are reported with a focus on mechanical, tactile responses to physical stress and deformation.

This is not a biomechanical investigation or an exercise in theoretical, mathematical modelling. It is a pragmatic account of the mechanical consequence of elastomeric property manipulation: The purpose of which, is to demonstrate the versatility of surrogate soft tissues, in a manner that is understandable by an interdisciplinary audience.

1.1 Background

The term, 'Soft prosthetics', has quite different meanings and uses for different disciplines. While theatrical prosthetics are typically used to change an actors appearance for a performance, most often to simulate injury (moulage) or alter the face, clinical prosthetics are used for a wider range of purposes. [1, 2, 3] Rehabilitation of patients suffering from facial disfigurement, implantable soft prosthetics used in cosmetic surgery and assistive devices, all aid the individual. [2, 4, 5] But a new use for the word is bucking trends in medical training. Prosthetics in surgical simulation and medical modelling, utilises all the tools of the theatrical and clinical prosthetist, in new ways, that have yet to be fully explored.

Although they have much in common, the two disciplines of theatrical and clinical prosthetics rarely interact. Most theatrical prosthetists are trained as make-up artists, whereas most clinical prosthetists are trained, initially, as dental technicians - worlds apart from one another. [1, 2, 3] One thing that brings all these groups together, is the use of silicone-based elastomers, like polydimethylsiloxane (PDMS). Colourless, non-toxic and mechanically acrobatic; PDMS gels are used by the experienced prosthetist as an integral part of their daily work in simulating soft tissues. Native translucency of PDMS lends itself to subtle intrinsic pigmentation with coloured fibres, and its low viscosity means it readily accommodates embedded textiles that can be used to resist tears and change its

physical characteristics. Other interesting qualities are more reliant on its simple molecular structure, which can be easily altered with the addition of hardeners and softeners to tune gel compliance. Knowledge of these properties, relevant to prosthetists, remains the tacit, embodied know-how of niche user groups, virtually undocumented in academic literature.

Fuelling the need for a deeper understanding of altered PDMS gel behaviour, are the requirements of surgical simulation and medical modelling.[4] This emerging field in healthcare simulation practice has built the foundation of a new industry, able to provide realistic models of anatomy for a variety of meaningful purposes that will be explored in this thesis. Key to continuing growth in this new interdisciplinary sector, is the adoption of skills and technologies borrowed from other disciplines. The technical support of specialist clinicians, manipulation of medical imaging data, additive manufacturing (3D printing), and more recently, material science and craft-based, prosthetics and special effects know-how.[5, 6, 7, 8]

Implementation of these skills and technologies has already resulted in a tantalising range of innovative and impactful outputs, from emergency surgery task training,[8, 9, 10] to elective surgical rehearsal,[11] (shown in figure 1.1) medical device development,[6] and even forensic reconstructions in legal medicine.[7]

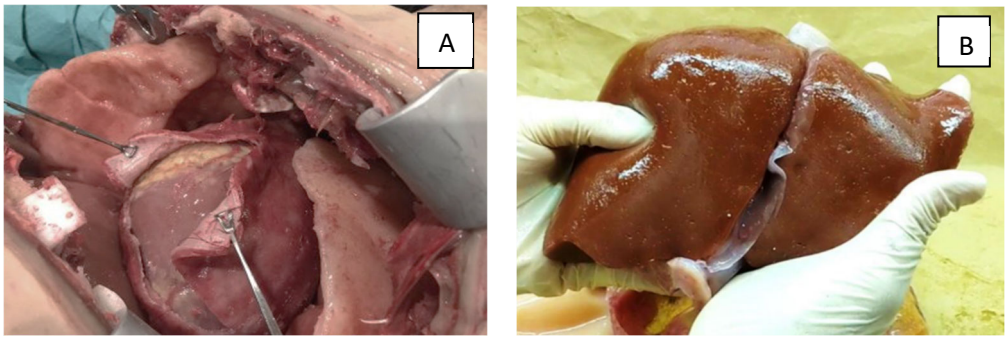

Figure 1.1 Examples of medical modelling using PDMS gels with fibres, textiles and oil. *Image 'A' shows a medical model made with PDMS gels embedded with fibres and textiles to produce 'Simbodies PRO', a surgery training tool produced by Simbodies global- Safeguard Medical Group. (Licenced from Nottingham Trent University since 2018). Image 'B' shows a medical model made with PDMS gels, dispersed in oil to produce a 'cancerous liver' that can be used to train surgeons in tumour resection. Both reproduced from patient data, 3D printing and traditional moulding and casting techniques (Authors own images.)*

Testament to the rapid growth in this sector, the global healthcare simulation market was estimated to be worth $1.9 billion in 2022, a figure set to more than double over the next 5 years to $4.2 billion.[12] So, to foster continuing growth in this sector, development of more realistic, more accessible and more affordable methods for surrogate soft tissue production and characterisation are desperately needed.

When prosthetists are selecting an appropriate PDMS gel to match the tactility of native tissues they are trying to simulate, mechanical data is provided by the manufacturer, alongside the material, so that users can predict a materials behavioural properties with some degree of reliability.[3] However, most PDMS elastomers are highly elastic and extremely extensible, so prosthetists almost always employ additives to change the appearance and characteristics of the PDMS gel, with experience as the only impetus for success. This was not such an issue for theatrical prosthetists, whose work only needs to look convincing on the stage or screen for a short time. For medical modelling scenarios, where surrogate tissues need to look and perform like the real thing, material properties and tactility are important factors.

When properties like hardness or elasticity are important to the end-users, more attention needs to be paid to PDMS composite characteristics. Afterall, surgeons, in particular, rely on tactile and visual cues to conduct their work.[13, 14] Therefore, a better understanding of the influence that additives have on PDMS gels can help designers make more informed decisions about how best to emulate different types of soft tissues for soft medical modelling. For example, the ability to reduce the elasticity of PDMS is important when simulating the effect of aging in soft tissue membranes, like blood vessels,[5] and skin.[15] And the ability to reliably control hardness can be equally valuable, when recreating the variable hardness of human skin, and other soft tissue membranes and connective tissues.[16, 17, 18, 19] In addition, maxillofacial prosthetists are expected to consider the patients' soft tissue compliance and facial mobility, specific to each patient, whilst maintaining a robust design, resistant to daily wear and tear.[20]

As the motives and applications for PDMS prosthetics are discipline dependent, related material properties are discussed amid disparate, topical strands of research throughout this thesis. For example, there is a wealth of literature concerning soft tissue characteristics that can help us recognise and understand the causes for certain types of

mechanical behaviour. Biomechanical data in turn, highlights how nature's own design can help us understand the role of heterogeneity in PDMS composites. Perhaps more importantly, these design prompts may teach us how to control and predict PDMS composite behaviour in new ways.

Despite our deep understanding of soft tissue behaviour, precise mechanical profiling of PDMS equivalents remains elusive.

Because human skin is the most widely documented soft tissue in the literature, due to its accessibility, it has been used as a benchmark for characterisation in this thesis. Although this work is not about trying to emulate skin specifically, data on skin was used because it is sufficiently detailed to build physical models from.

So, three types of bio-inspired, surrogate human membranes were produced: Thin and fibrous membranes inspired by the epidermis, soft yet strong membranes inspired by the dermis, and flaccid, oily membranes inspired by subcutaneous fat. Mechanical thresholds, identified in the literature, were used to inform initial surrogate material choices, while membrane creation was based on technical experience of the author.

1.2 Thesis Aim

Establish new knowledge on the specification, design, fabrication and mechanical characteristics of PDMS-based composites, familiar to prosthetists.

1.3 Research questions

This research focuses on quantifying the mechanical response of PDMS composite membranes that are familiar to clinical and theatrical prosthetists. Additives and fabrication methodologies that are used by these groups remains tacit, embodied knowledge, previously developed through trial and error and experiential learning, largely undocumented in academic literature. This gap in the knowledge base, hampers development of realistic surrogate materials that are able to mimic the tactile, and mechanical characteristics of soft tissues.

To bridge the gap in knowledge, a series of research questions were investigated in this thesis:

1. **What are the mechanical characteristics of PDMS gel membranes saturated with loose, short-strand fibres?**

   Addition of loose fibres are used in everyday production of soft tissue prosthetics, but their influence on PDMS mechanical properties is unknown. What are the mechanical implications of their inclusion in PDMS blends?

2. **What are the mechanical characteristics of multi-layered PDMS gel membranes embedded with textiles?**

   Embedded textiles are often employed in the fabrication of prosthetics for the purpose of reinforcement, repairability and durability enhancement, but what are the mechanical advantages or disadvantages of their employment, and can their mechanical properties be controlled?

3. **What are the mechanical characteristics of oil saturated PDMS gel membranes?**

   PDMS oil is often added to PDMS gels to reduce their viscosity, they also soften the PDMS gel too, although the amounts required, and their mechanical influence remains unknown. How much oil is needed to simulate very soft tissues and what other changes are wrought by oil dispersal in PDMS gels?

To answer the research questions effectively, a series of experiments were designed to determine the mechanism of behavioural changes in PDMS membranes. These experiments are outlined below.

1.4 Objectives

The objective of this work are:

1. Mechanically characterise single-layered PDMS membranes saturated with variable amounts of loose, short-strand fibres.
2. Investigate the mechanical influence of single and multi-layered PDMS membranes, that

have been embedded with textiles.

3. Characterise the mechanical influence of oil saturation in single-layered PDMS membranes.

To achieve these objectives, data on soft tissues behaviour was used to identify the target mechanical properties of organic materials. Surrogate materials that imitate target mechanical properties were fabricated as a series of membranes. Each PDMS membrane was prepared in a manner that complied with the requirements of internationally agreed test standards. These test standards are mentioned in the next section but are discussed in detail in Chapter 3.

1.5 Research methodology

To achieve the aim and objectives, quantitative research methods were used to cultivate data from the literature to identify gaps in the knowledge. The literature review (Chapter 2) provides a detailed background to the development of our understanding of soft tissue behaviour. Existing knowledge on soft tissue characteristics, (identified in the literature) was used to influence the development of suitable surrogate materials. The literature review was essential to identifying disparities and errors in published data too. Most importantly it helped to identify gaps in the knowledge and defined limitations of current state-of-the-art in soft tissue surrogacy. PDMS membranes that were produced as part of this investigation, were reliant on the data provided by key literature sources.

When creating the PDMS membranes to be tested, additives familiar to prosthetists were employed to improve engagement and relevance for the target audience. Experimental Chapters 4, 5 and 6 document specific membrane fabrication techniques, useful to a wider audience. Chapter 5 builds on concepts proved in Chapter 4. Chapter 6 explores aspects of membrane behaviour not feasible with methods proven in Chapters 4 and 5. Once suitable membranes were prepared, a range of standards were selected to characterise their behaviour. Deployed standards were used to determine changes in mechanical behaviour based on variables that are encountered during preparation and fabrication of prostheses', such as the amount of filler used or the tension/orientation of fabric during the embedding process. The precise tests standard parameters are described in more detail, in Chapter 3.

Generally, though, mechanical characterisation of all membranes focusses on multiple aspects of mechanical behaviour including- hardness (Shore hardness), elasticity (Young's modulus, MPa), strength (ultimate tensile strength), and overall stress strain behaviour throughout extension to failure.

The standard does not dictate how the amount of Force is expressed, Force is more tangible to prosthetists than MPa but doesn't change the profile of the curves (for easy conversion, if required). Finally, MPa is given for each material separately, so if MPa values are required by the reader, a chart is available, alongside the curves used to illustrate extensibility behaviour. In this way, readers have the best of both, when it comes to provision and interpretation of data. Additionally, all the graphs not presented in the main document are included in the appendices.

Mechanical characterisation also includes multi-axial profiling to determine changes in viscoelasticity, like hysteresis to determine changes in the membranes over time, in cyclic loading events, force decay/degradation (creep), permanent deformation (bagging or plastic deformation).

1.6 Thesis Outline

In this section, a general outline is provided first, to contextualise the research questions. This is followed by a breakdown of the thesis as a chapter-by-chapter account. Finally, an overview of the entire thesis is supplied as a chart for easy navigation of content.

In the next chapter, a literature review offers a detailed account of the mechanical behaviour of living soft tissues, and suitable soft elastomeric surrogate behaviour. Both elements are presented as a double narrative that takes the reader on a journey of discovery concerning the development in our understanding of each topic, through the lens of scientific relevance. The literature review is presented as an appropriately engaging background to the thesis and provides a justifiable context for this work and future work.

Next, the methods and standards are described (in Chapter 3) to frame the research methodology for experimental chapters that follow.

The experimental chapters cover work that took place in three phases:

- In the first phase of the investigation, loose, short-strand fibres were blended with two PDMS gels in varying amounts.
- In the second phase of this work, two PDMS membranes, with known properties, were used to embed textiles. Membranes were tested with varying layer compositions, textile tensions and orientations.
- In the final phase, PDMS oils were added in incremental amounts to a PDMS gel.

The thesis concludes with a summary of all findings related to the research questions, difficulties faced during the research and a topical discussion on its implications for future work, to benefit the interdisciplinary prosthetist.

1.6.1 Structure of the thesis

This thesis is broken into seven chapters. Each chapter builds on the previous chapter and concludes with a summary of the findings of this work.

Chapter 1 - Introduction

Prepares the reader for the subject matter and ambition of the thesis. The background is presented and introduces the target audience. It serves to define gaps in knowledge, and how the gaps can be bridged with targeted experimentation by proposing solutions inspired by nature. The structure of the thesis is outlined with a brief overview of each chapter.

Chapter 2 - Literature review

This chapter has been structured as two parallel chronological narratives documenting the development in our understanding of soft tissue behaviour, alongside the technological development of surrogate materials that have been previously used as surrogates.

The chapter concludes with a table of key literature sources, and a summary of important behavioural traits that need to be considered in the development of soft tissue surrogate membranes.

Chapter 3 - Methods and materials

This chapter covers all aspects of the test standards used in the experimental chapters. It documents everything from preparation conditions and storage, to test analysis and criteria for reporting data. Material preparation is discussed in general terms and expanded further in each experimental chapter on a topical basis.

Chapter 4 - Mechanical behaviour of silicone membranes saturated with short strand, loose fibres

In this chapter, the behaviour of two single-layered membranes saturated with varying amounts of loose fibres were tested and characterised. Results of mechanical testing were presented as per the standards laid out in Chapter 3.

Chapter 5 - Mechanical behaviour of multi-layered, reinforced silicone membranes for clinical and theatrical prosthesis

This chapter is composed of two parts, one part focuses on yarns embedded in PDMS membranes, while the other focuses on fabric embedded in PDMS membranes. The introduction, fabrication and results of experiments with yarns, comprises Part one. Because the outcomes for membranes embedded with fabric were quite different from yarns, results were split into two parts, to maintain clarity and brevity, each part focuses on one of two yarn architecture variations in embedded textiles. Therefore, the second part of this chapter focuses only on results of PDMS membranes that were embedded with fabric (knitted from the yarn characterised in the first part). All specimens were tested in the same way, only with different tensions, orientations and number of layers.

Chapter 6 – Mechanical effects of oil dispersal on silicone gel membrane behaviour

In this chapter, changes in the mechanical properties of PDMS gel, when incremental amounts of oil were added, is documented. Base PDMS gel used in this experiment was similar to that used in the previous experimental chapters.

Chapter 7 – Conclusions

The thesis is concluded by drawing together all of the results from the experimental

chapters and comparing them to the literature discussed in Chapter 2. The chapter offers insights into further potential development in this area and possible future work.

The reader is finally directed to related published work in this field by the author.

An overview of this thesis is summarised in figure 1.2.

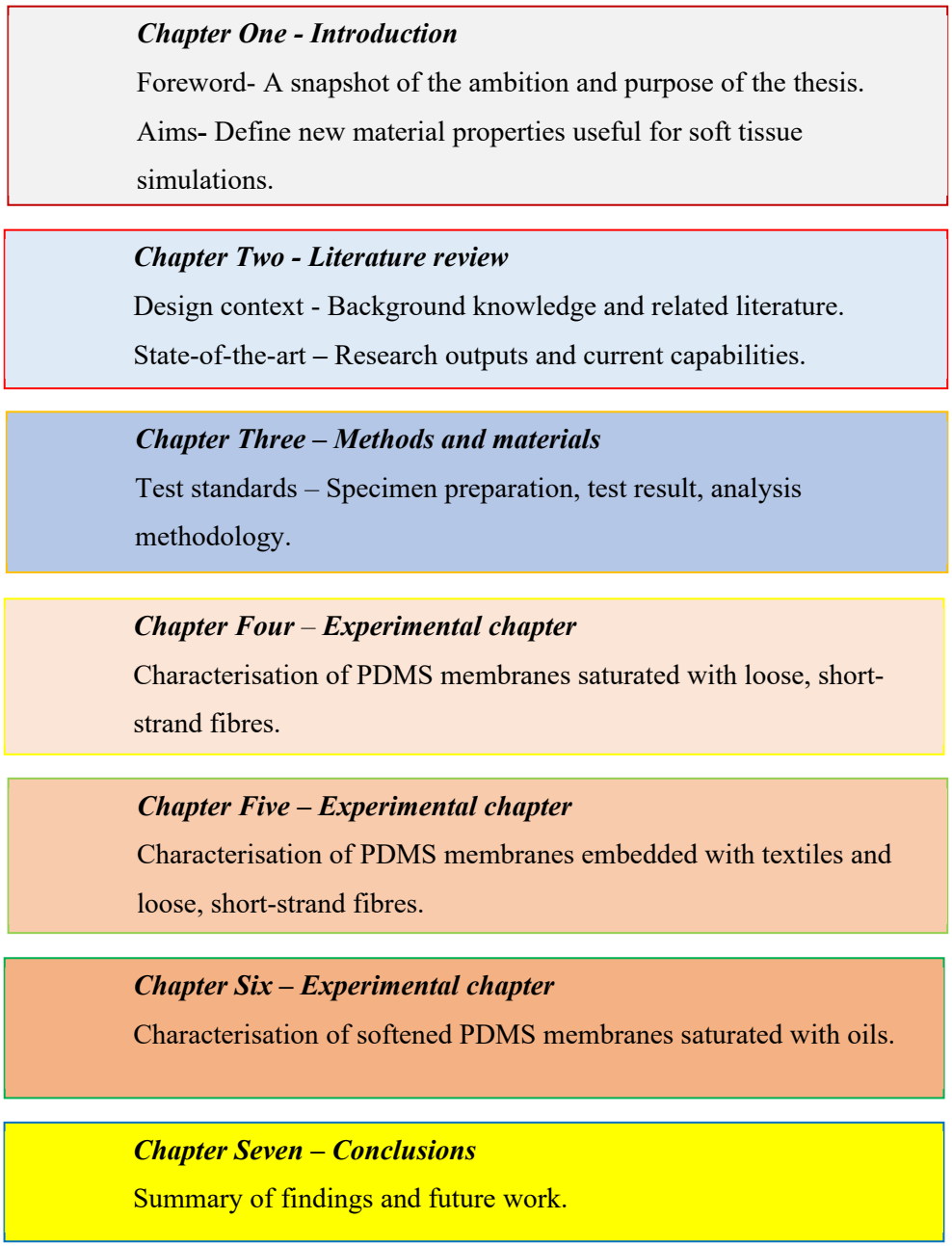

Figure 1.2 Diagram of the thesis structure.

Image describing content on a chapter-by-chapter basis in order of appearance.

Chapter 2

Literature review

2.1 Introduction

This chapter is a review of interdisciplinary literature, structured as two co-dependent narratives. Firstly, a chronology of human understanding of soft tissue membranes is presented, from the earliest visual documentations of soft tissue properties to the latest concepts in soft tissue biomechanics. Secondly, a narrative of the development in our understanding of soft elastomeric materials is provided. Both topics are examined as a background to the experimental work presented in this thesis. Prior art is also discussed throughout, in the context of incumbent technologies, production techniques and test methodologies, relevant to the work. In the second part of this chapter, each PDMS additive is discussed in turn, framing the experimental chapters, and is accompanied by a selection of relevant literature on organic counterparts. This section begins with a discourse on disorganised fillers that are considered as single-layered fibrous membranes. Secondly, organised fillers are presented in the context of multi-layered, fibre-filled membranes, reinforced with directional yarns and fabrics. And thirdly, softening of PDMS gels is discussed in relation to the dispersal of oil in the gel mixture. Each topic touches on behavioural phenomena associated with both natural and synthetic soft membranes to help contextualise the work and provide insights into PDMS composite behaviour. A detailed review of behavioural phenomena associated with soft materials (and phenomena that have never been associated with soft materials before) is also used to prepare the reader for interpretation of the results, contained in the experimental chapters (Chapter 4, 5 and 6). Finally, this chapter concludes with a summary of key texts from the literature that outline the test methods, analysis, and validation of results. These are discussed with a particular focus on the most relevant data obtained from similar studies involving organic soft membranes. The test standards highlighted by the most relevant studies are catalogued in acknowledgement of the literature, but the specifics of each test methodology will be discussed in more detail in the following chapter (Chapter 3). Each chapter of this thesis unpacks the mechanical behaviour of PDMS membranes that have been adapted for prosthesis fabrication progressively over time, and the techniques are engrained in disciplinary practice rather than specific literature. There are a handful of magazines and books that discuss prosthetic recipes, methodologies, and the visual effects of additives such as fibres, fabrics, and oils, but the mechanical changes that occur through the use of such

ingredients has never been documented before. Therefore, each topic is discussed from an interdisciplinary viewpoint with a focus on describing behavioural traits of natural and synthetic soft membranes. A detailed literature review conducted in 2015, on the mechanical properties of soft tissues, found that less than 20 investigations were published per year, prior to 1990, but by 2013 this number exceeded 300 new publications per year: indicating a clear growth in interest and understanding of soft tissue behaviour over the last 30 years.[21]

The next section examines the development of our understanding of soft tissue mechanics to help frame the proceeding section about mimicking its behaviour. It is important to communicate here, that, as the most accessible, and best documented soft membrane, much of the literature contained in this review concerns the behaviour of human skin. But this thesis is not about simulating human skin. It is about mimicking soft tissue membrane behaviour using materials familiar to clinical and theatrical prosthetists.

2.2 Development of soft tissue mechanics

For millennia, physicians and surgeons have learned their craft on people, both living and dead, while scientists and artists studied the flesh in exquisite detail in pursuit of a means to synthesise it for clinical or artistic purposes.[22] Our understanding of soft tissue mechanics has grown exponentially over the last 500 years, from drawings in a sketchbook to digital images captured by the scanning electron micrograph (Fig. 2.1). And yet our understanding of the materials required to emulate their behaviour remains in its infancy.

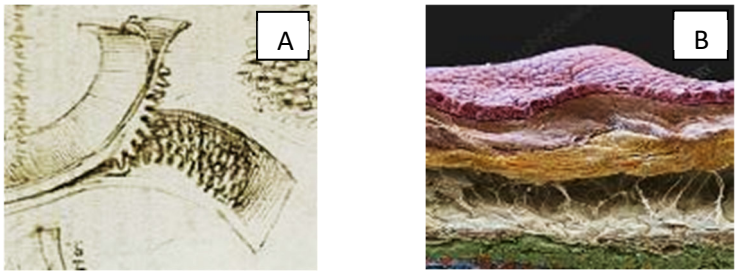

Figure 2.1 Studies on soft tissue membranes separated by 500 years of science.
Both images show the distinct layers of different thicknesses were noticed during dissection. Image 'A' shows a drawing from Da Vinci's sketchbook (1510-12). Image 'B' shows a Scanning Electron Micrograph of the same topical soft tissue membrane, 500 years later. Image 'B'- [Eye of Science, Science Photo Library.] Available at *www.sciencephoto.co./media/1305080/view*

Until the 19th Century, much about human anatomy was understood from a qualitative viewpoint. Medical practitioners and anatomists of the time appreciated the structure and mechanical properties of soft tissues membranes in some depth. In one of the first, early discourses in soft tissue membranes, Gordon[23] gives an unabridged account of the skins' different layers that he observed during the dissection of cadavers. Prior to his publication, cadaver dissection and lectures on anatomy were the gold standard in soft tissue explorations (fig 2.2).

Figure 2.2 17th Century cadaver dissection. *An anatomy lesson, captured by Dutch master 'Rembrandt', shows medical students engrossed in the dissection of a fresh cadaver. [Van Rijn, R. 1632. 'The Anatomy Lesson of Dr. Nicolaes Tulp']*

Cadaver dissection, as shown in Figure 2.2, has remained largely the same to this day and is still common practice in medical schools and laboratories studying soft tissues. Much of what we know about the properties of soft tissues and structures was learned using this process, until quite recently, when non-destructive methods of gathering information have become accessible. Imaging apparatus like Computed Tomography (CT) and Magnetic Resonance Imaging (MRI) and mechanical apparatus like the durometer and cutometer have allowed for living tissue to be measured with great accuracy.

Prior to these 20th century breakthroughs, scientists like Gordon (1815)[23] paved the way for others like Struthers (1848)[24], who was the first to scientifically determine that each layer of the skin contributed to its mechanical response to deformation.
A decade later, Gray and Carter (1858)[25] published their first edition of the staple of modern medical practitioners- *Gray's Anatomy*, which contained the first comprehensive

visual account of human anatomy, in print. It also included a detailed description of human skin, suggesting its mechanical behaviour was similar to other soft tissue membranes such as the brain's meninges, organ pleura, the gut wall and blood vessels, but it was not yet understood how soft membranes grew and repaired.

The answer was found a few years later, in 1861 by Karl Langer,[26] who discovered that human skin contained lines of directional collagen fibre growth, that are formed during foetal development. These lines are visible as grooves in the skins surface that indicate the skins fibre direction, thickness, and determine extensibility specific to each region of the body. 'Langer lines' as they became known, allowed the skin to stretch more in the perpendicular direction, relative to the Langer lines, and stretch less along them, suggesting anisotropic directional extensibility. Building on Langer's discovery, towards the end of the 19th century, tissue specific studies were beginning to build a more detailed picture of the importance of fibres, fibre architecture and their orientation in soft tissue membranes, especially the skin.[27, 28]

However, the technology required to identify the precise mechanical properties of the skin, like extensibility or elasticity simply did not exist yet. The lack of standardised test methods and universal equipment required to test most soft materials, hampered the progress of investigators, who were unable to reliably compare data.

Test methods and materials would not be standardised until the emergence of the American Society for Testing and Materials (ASTM) in 1898, and a few years later the British equivalent, the British Standards Institute (BSI) in 1901. These were followed sometime after by the creation of the international equivalent- The International Organisation for standardisation, in 1947.

Standardised characterisation devices for soft tissues first became available in 1912, when Schade invented the first mechanical indentation device specifically designed to measure the elasticity of the skin.[29] Although the apparatus was cumbersome and used a rudimentary data gathering methodology, it was a simple and widely accessible device, remaining largely unchanged for the next 50 years or so.

By the mid-20th century, Rothman[30] and Ridge[31,32] identified the skin to be an anisotropic, viscoelastic material and recommended five key mechanical tests to help determine the characteristic behaviour of human skin. Tensile strength, extensibility, creep, stress

relaxation and Young's modulus (elasticity).

These early investigations into the mechanical behaviour of soft tissue membranes formed the basic understanding of the materiality and structural behaviour of membranes like skin,[32, 33, 34] blood vessels,[35] natural fibres and animal skin.[36, 37, 38] This work was responsible for identifying some of the most important, fundamental characteristics of fibrous soft tissue membranes, helping create more reliable methods for gathering mechanical data. Ridge and colleagues, in particular, noticed many similarities between the distinctive behaviour of natural fibres in textiles and the behaviour of fibres like elastin and collagen, found in soft tissue membranes.

In the late 20th century, it was found that the majority of the skins mass was made up of 'ground substance', a soft, gel-like material that contains elastin (2% dry-weight volume) and collagen (30% dry-weight volume).[39] These fibres were found to be chiefly responsible for its complex behavioural response to mechanical loading. Both fibre types perform separate, but overlapping mechanical duties, that lend strength to the skin during deformation. It was found that collagen in particular determined the skins' response to deformation, especially at higher strains (3-5%).[39] This was because the 'wavy' architecture of collagen fibres played a crucial role in the anisotropic, viscoelastic characteristics exhibited by skin during mechanical testing, especially in extension.

One literature source suggests that skin (of the breast) behaves as a linear isotropic material under strains of 50 %,[40] while elastin was found to be almost perfectly linear in its response to elastic deformation up to 150% and is present as thin strands in the skin. Collagen forms the leading architecture for soft tissue formation, created from twisted helical fibrils that organise themselves into 3-dimensional tissue structure.[41] These collagen structures untangle and stretch as the skin extends, rearranging themselves back into coiled structures as the skin relaxes causing both elastic and viscoelastic response to loading at different strain rates.

Similarities were also found in other membranes like the pericardium too. Lee[42] and colleagues proposed that the changes in viscoelastic response of the pericardium was due to the volume fraction of fibres present in the membrane specimens tested.

Other researchers have found that when skin is stretched up to 3% in extension, the collagen fibres remained 'wavy' offering little resistance to loading causing the skin to

behave more like an elastic material.[43] As the amount of strain increased, the collagen fibres gradually straightened until they were aligned with the direction of stress, at which point they would take up the strain previously born by the elastin fibres, making the skin respond with a short elastic reaction under low strain and non-linear at higher strains;[44] As the skin was stretched to its limit, it became stiffer, an effect now known as 'strain hardening'.[45] Today, it is broadly agreed that soft tissue membranes are heterogenous, time-dependent, viscoelastic, and anisotropic in their behaviour under loading. The phenomena of strain hardening and softening, in (synthetic) soft material mechanics is now known as the Mullins effect and the Payne effect.[46, 47]

Such phenomena are discussed in more detail later in this chapter, alongside the influence of preconditioning and hysteresis in cyclic tests. In essence, these behavioural traits are all attributed to mechanical loading history and the presence of fillers in the soft membrane's composition, such as intrinsic fibre type, organisation, density, and direction.[41, 48, 49, 50]

It is also well known that these characteristics also have many variable factors that might influence test results such as tissue type, thickness, location, temperature, hydration and test speed, as well as loading history (preconditioning).[51, 52]

Reliably gathering data to compare results from similar studies is difficult without an agreed standardisation of test parameters and equipment. Although several studies have adopted some aspects of agreed test standards, usually those reserved for elastomers or elasticated fabrics, few adhere to the proper standard test methods for characterisation, as demonstrated when discussing the relevant literature later.

Finally, it is well known that soft membranes can be mathematically modelled by the hyperelastic models proposed by many different research groups over the years.[41, 53, 54, 55, 56, 57] Despite this, mathematical modelling of materials and continuum mechanics was not the focus of the work presented in this thesis. Instead, the data presented in the experimental chapters (Chapters 4, 5 and 6) only use rigorous mechanical characterisation methodologies to determine tactile material properties, except where clear trends are observed in the data. In such instances, linear regression models were created but only to aid in understanding predictability beyond the values presented in the experiments.

2.3 The structure of soft tissue membranes in humans

Skin is the largest, heaviest and most accessible membrane of the human body, it is the largest organ in humans and its structure is unique to mammals. In humans, the skin is made of two behavioural membranes, the epidermis (epithelium or cuticle) and the dermis (corium or cutis vera) and varies in thickness (0.05 mm – 10 mm).[58] It is thickest on the back (up to 10 mm), thinner elsewhere (1 mm to 3 mm), and is thinnest on the eyelids. The hypodermis is mostly made of subcutaneous fat or adipose tissue that varies widely in thickness depending on site and individuals' body mass index, but it is absent in the eyelids and male genitalia. Other, human (serous) membranes, pleural membranes or visceral lamina are found principally around the heart (pericardium), lungs (pleura), abdominal cavity (peritoneum), testis (tunic vaginales) and (exclusive to gestating females) in the amnion (amniotic sac). In the case of the heart, the pericardium is made of two layers of collagen and elastin fibres totalling around 1 mm thick and is a tough, fibrous, and viscoelastic membrane.[42] In the case of the amniotic sac, the membrane comprises of two layers of collagen (amnion and chorion) collectively described as a thin, time-dependant, viscoelastic membrane.[59]

Most human, multi-layered membranes composed of elastin and collagen inevitably demonstrate similar mechanical characteristics, typically exhibiting flexibility, elasticity, viscoelasticity, and time-dependency.[52, 60] Each membrane type and corresponding layer has its own specific function, and like most biological membranes, their function is intrinsically linked to their multi-layered structure.[61]

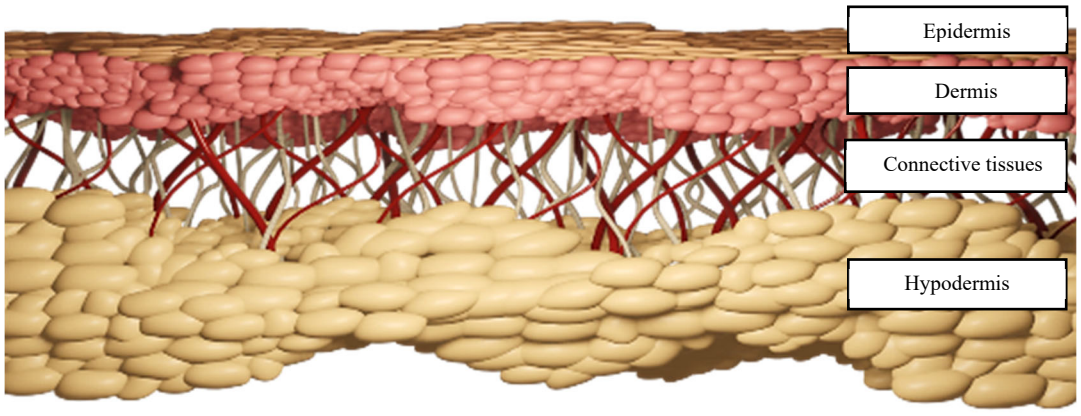

Figure 2.3 Cross-sectional model of human skin.

Anatomy of the skin showing the two 'true' skin layers of the epidermis and dermis, connective tissues, and the fatty hypodermis, as labelled.

Therefore, in order to replicate the mechanical behaviour of these membranes, it is necessary to discuss their form and function.

Shown in Figure 2.3, the multi-layered structure of the skin is made up of several layers. The epidermis forms the protective outer membrane while the dermis forms the softer, 'living' layer beneath. The structure of the epidermis is free of blood vessels and mainly comprised of compacted, dead skin cells made almost entirely of keratin (90 % to 95 %),[52] which creates a stiff membrane ranging mostly between 100 µm and 1.5 mm, protecting the softer, underlying dermis. It is thickest on the palms of the hands and soles of the feet where it is usually around 1.5 mm but can be much thicker in individuals that regularly walk barefoot.[52]

Skin is naturally thicker on the posterior of the torso and outer surfaces of the limbs and is generally thicker in males than in females overall. In essence though, the epidermis is a thin, 'stiff', viscoelastic membrane.[62, 63] The dermis, however, is highly heterogenous and contains all the biologically active elements of the skin such as hair follicles, oil and sweat glands, nerve endings, blood vessels and lymph vessels. It is more viscoelastic, softer, and more extensible than the epidermis. It also contains large amounts of coiled collagen and elastin fibres.[63]

In summary, there is a wealth of literature on the structure, physical limitations, and characteristics of skin and other soft tissue membranes. Available literature offers the diligent prosthetist useful design queues for the development of synthetic membranes that mimic their behaviour. Some of the most useful studies in the literature focus on the tensile testing of excised skin specimens,[15, 16, 39, 50] however, results vary widely as do the individuals they were sourced from, and while numerous contributory factors have been debated in the literature, it is broadly agreed that the variable, fibrous structure of skin, is responsible for its unique viscoelastic response to strain.[45, 64]

Finally, it is important to consider living skin as a whole organ that is subject to varying two and three-dimensional loading and that they are continually compressed and stretched during motion. To build an accurate imitation of soft membrane behaviour with surrogate materials, simple measurements of hardness must be complimented by more complex measurements taken from uni-axial and multi-axial data.

Next, the developmental chronology of soft materials is discussed and how our

understanding of these materials might help inform synthesis of accurate physical models of soft tissues.

2.4 Development of soft tissue surrogates

Up until the 20th century, the discipline of prosthetics remained the domain of the carpenters, tanners and blacksmiths until the invention of modern rubbers. In this section, we discuss some of the landmark discoveries in elastomeric technologies, as a background to this work.

Throughout the 19th century, as demand for rubber increased, with the popularisation of the automobile, natural rubber industries boomed, despite the social atrocities associated with its procurement.[23] Due to the rising costs of rubber (both fiscally and morally) the big rubber companies began pouring money into development of new synthetic rubbers that could be manufactured on demand.

During that golden age of material exploration, Charles Goodyear filed a patent for gum elastic layered shoe soles with embedded fabric layers to resist tears.[65] Then, in 1851 he was also credited with the invention of the 'modern' tyre, produced by heating natural rubber with added sulphur and carbon fillers, a process known as *vulcanisation*, key to improved tyre grip and durability.[66]

Most investigations into the development of alternative soft, elastomeric materials like polysulfides, polyurethanes, polyvinylchloride and fluorocarbons were dominated by automotive, aerospace, medical and cosmetics industries, but none were soft enough to be a candidate for soft tissue surrogacy.[67, 68] The development of silicone-based elastomers was initially no different. In 1901, chemistry professor, Frederick Kipping, stumbled upon this new group of elastomers while attempting to engineer a ketone polymer of silicon, later synthesising the elastomer in 1927.[69, 70] Due to its silicon/ketone heritage, he originally called the compound *Silicoketone*, but later shortened it to *'Silicone'*.[71]

Building on Kipping's early work, Hyde developed the world's first, fully synthetic elastomer that would go on to be the largest group of commercially produced silicones, called *Polydimethylsiloxane* (PDMS).[72] Unlike natural rubbers, silicones have a variety

of possible curing mechanisms: thermal, ultra-violet, and cross-linking (hydrosilylation).[73] In the case of PDMS curing (from its fluid state to a solid state) the addition polymerisation process occurs using two viscous, but pourable fluids, one a bulk polymer the other a diluted platinum-based cross-linker (or catalyst).[74] Once mixed at the stoichiometric ratio, curing takes place in a dependable and repeatable fashion with fixed mechanical properties.

Modern PDMS elastomers are very different from natural rubber, in that they are chemically and thermally stable, non-toxic, and highly adaptable due to their simplistic formulation of silicon and oxygen molecules as long-chain polymers.[73] During (silicones) development, Kipping was the first to realise that it could be engineered into liquids, solids, and gels with astonishing versatility, thanks to its close elemental relationship to carbon and oxygen.[72, 75] Kipping went on to publish over 50 papers on the topic in the first half of the twentieth century.[71, 72, 76] It was quickly realised that the dispersion of filler particles in silicones, changed the mechanical characteristics of soft silicones, like PDMS.[77, 78] Such changes included anisotropic behaviour, with evidence of permanent deformation and significant gains in elastic modulus.[79, 80]

The work of pioneers like Kipping[71], Hyde[72] and Rochow[75] helped to outline the versatile mechanical behaviour of silicon-based organic chemistry and its suitability as a surrogate material for soft organs and skin.[81] Although unaware of this at the time, their work shaped the foundation of prosthetic materials that were capable of soft tissue mimicry. (For a comprehensive account of silicone chemistry and technology, readers are directed to Noll 2012).[73]

2.5 The emergence of modern prosthetics

Since its introduction, natural rubber dominated for over 50 years. In 1864, early prosthetists- Kingsley and Preterre, reported on the use of vulcanised natural rubber for maxillofacial clinical prosthesis.[82, 83, 84] Natural rubber's availability diminished when most raw materials became scarce during the first and second world wars, accelerating development of synthetic alternatives.[83, 85] During the same period, the foundations of modern surgery were being laid by battlefield surgeons, and with it, an improved understanding of soft tissues was being developed; how they could be damaged, repaired

and healed. Soft tissue trauma management and rehabilitation of the injured, perpetuated the need for new, improved, compliant maxillofacial prosthetics.[86] The priority for post-war maxillofacial prosthetists was to reintegrate facially disfigured veterans with society, not reproduce the properties of facial soft tissues.[83, 86] Early silicone-based elastomers were ignored by the therapeutic prosthetics community until 1960 when Barnhart published his work in *'somato-prosthesis'* (silicone prosthesis).[87] Soon after, in 1962, plastic surgeons implanted the first silicone breast implant, cementing its analogous characteristics as a suitable soft tissue surrogate;[88] however, the materials and methods required to maximise the mechanical benefit of PDMS use in prostheses remained limited, as did their commercial availability.

Around the same time, the first synthetic patient simulators were introduced in 1960 to improve accessibility to basic training in emergency patient care, specifically for cardiopulmonary resuscitation training.[89] These manikins were first made by the European toy makers *Laerdal,* who used their toy making experience to produce rigid, plastic, life-sized manikins with articulated mechanical joints. [89] Little attention was paid to creating a realistic skin.

By the 1970's, silicone gels were gaining notoriety as cosmetic implants thanks to the increasing popularity of plastic surgery,[90] but the maxillofacial prosthesis industry was still dominated by other cheaper materials like polyvinyl chloride (PVC) composites. [91]

During the 1980's, clinical maxillofacial prosthetists began to explore other softer materials and in 1980, Lewis and Castleberry[92] concluded that a 25-35 Shore A hardness silicone with a tensile strength between 6.9 MPa and 13.8 MPa would be ideal for facial prosthesis.[92] Today, prosthetics are mostly produced with 10 Shore hardness PDMS, or softer, so early silicones would be considered rather stiff by most modern prosthetists, but available technology of the time, was limited.[3, 94] In parallel, theatrical prosthetics were making huge advances, especially in the horror movie genre, Nair[95] and colleagues give a thorough account of natural rubber use in theatrical prosthesis in the run up to the end of the 20th century. By the start of the 21st century, improved silicone formulations like PDMS, were already well established and growing in popularity in theatrical prosthesis as well as clinical limb prosthesis (as seen in figure 2.4).

Figure 2.4 Examples of surrogate appendages, therapeutic prosthetics*. A range of PDMS prosthetic hands, feet and fingers for therapeutic use by amputees. Prosthetics like these are usually passive, cosmetic appliances rather than functional replacements for the missing body part.* [*Artistic photography of prosthetic limb components from http://www.ortho-europe.com Photographed by Paul Wenham Clarke. http://www.wenhamclarke.com/]*

2.6 Soft prosthetics

Currently, modified PDMS gels are especially popular amongst clinical maxillofacial and theatrical prosthetists, who use them to mimic most soft tissue types.[3, 96, 97, 98] Usually supplied as a two-part kit (base and catalyst), PDMS gels can be mixed by hand and poured into a mould to form almost any shape required. They can be readily pigmented with fibres or strengthened with fabrics, while the mechanical properties like hardness and elasticity can also be changed with the introduction of various additives:[3, 99] Some of these aspects will be expanded later in this chapter.

In this section, the various materials and motives that drive development of soft tissue prosthetics are discussed.

PDMS gel models have previously been shown to simulate some of the mechanical properties of soft tissues reported in the literature.[100, 101] More specifically, PDMS gels with shore hardness of A-10 and 00-30 have previously been used to simulate skin,[102, 103, 104, 105, 106] muscle,[8, 107, 108], heart valves,[109] and internal organs and soft connective tissues[3, 8, 11, 107, 110] and even organic soft robotics.[111] Frustratingly, few of these studies reference the standard and rarely disclose manufacturing methodology or specimen preparation conditions, making any direct comparison unreliable.

When human cadavers are unavailable for medical training or product testing, substitute animal tissues are considered suitable alternatives. Porcine,[103, 112, 113, 114] bovine,[115] and murine tissues,[116] are all commonly used as alternatives for human tissues for medical

training. Porcine tissues are most often used for surgical training because of their similarity to human tissues.[114, 117, 118] *Wetlab Ltd*. (Warwickshire, UK) commercially provide animal tissues for this purpose. In some countries, surgical training on live animals is still commonplace.[119, 120, 121] Porcine skin (living and dead) is often used for surgical suture training due to its low cost and wide availability.[112, 122] The use of cadavers is limited to licenced training centres, and animal tissues pose a biohazard to users, but also present considerable ethical and religious constraints too.[123] For these reasons, substitute materials have previously been used to create surrogate soft tissues to bridge the gap in user consumption. Materials such as oil, lard, gelatine, alginate, carrageenan, and agar are common organic alternatives.[124 - 128] Due to their biodegradability and changeable mechanical characteristics over time, organic materials are also unsuitable for continual or periodic clinical use or commercial production of training products, where storage and transportation are a consideration.[129] Synthetic alternatives like polyurethanes (PU), polyvinyl alcohol/acetate (PVA/c), hydrogels and PDMS gels are preferable to organic counterparts due to their synthetic nature (i.e.. they do not biodegrade as organic materials do). Unfortunately, their behavioural response to deformation is poorly understood, especially concerning the use of softening agents that help fabricators adjust their native hardness to suit their application.

Today, PDMS gel formulations are used for all sorts of prosthetic applications that are analogous to a variety of soft tissues, testament to their widespread use and versatility, but the mechanical properties of these materials are still surprisingly poorly documented, considering their popularity. Advances in production techniques and reductions in manufacturing costs have also fuelled the development of next-generation, hyper-realistic surgical training manikins. Medical imaging data, additive manufacturing and novel post-print production techniques has been paired with soft PDMS gels, to enabled life-like imitations of soft tissues for surgical training applications. Companies such as UK-based *Simbodies Global (est. 2014) (*shown in fig. 2.5), *Trauma Simulation LTD (est. 2015) and Lifecast Body Simulations (est. 2017)* all quickly capitalised on the need for improved, risk-free, task-based training on medical manikins, especially in training field surgical teams for deployment. Not surprisingly, none of these companies report the precise mechanical behaviour of the materials used in their creations.

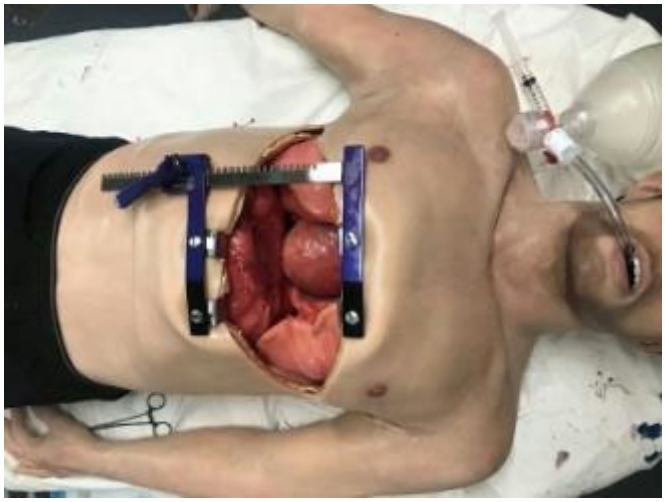

Figure 2.5 Simbodie PRO prototype surgical manikin during user trials, 2017.

Produced by Linzi Foxcroft and Richard Arm (the author), these manikins are currently manufactured under licence by Simbodies Global (Thirsk, N. Yorkshire). Simbodies PRO manikins are the world's first, commercially available, tether less, full body surgical manikin to facilitate emergency thoracic surgery training for first responders and military field surgical teams. (authors own image)

2.7 Additive manufacturing of soft materials

Recent approaches used to simulate soft tissues using modern production techniques rely on additive manufacturing (AM or 3D printing), especially for creating soft models of congenital heart diseases for task-based training.[130, 131, 132, 133] These types of clinical prosthetic/medical modelling have a greater emphasis on form rather than function and are produced with little acknowledgement of the real tissue properties. The complex geometries and multiple, thin walled, interlocking vasculature structures of the cardiovascular system, make traditional, craft-based production techniques almost impossible. AM offers realistic solutions, but with some trade-offs. Firstly, soft AM materials are not capable of reproducing multi-layered structures or very soft tissues. Herzberger[134] and colleagues give a detailed account of these limitations for AM, briefly, almost all flexible AM materials rely on thermoplastic urethane elastomers (TPU) rather than 'true elastomers' like PDMS.[134] TPU's for AM, are more mechanically similar to soft plastics, than true elastomers like PDMS. The elasticity characteristic of PDMS elastomers is lacking in current polyurethane technology. AM production of soft materials is limited to three main types of production. Fused deposition modelling

(FMD), Stereolithography (SLA) and selective laser sintering (SLS). FDM relies on hot melt filament extrusion, photo-curing soft polymers made by SLA, or thermoform polyurethane powder fused with SLS.[134] Generally TPU's are harder, weaker, less elastic, and far less versatile than PDMS gels, and they cannot be easily altered by the user, vital for material tunability.[135] In their extensive review of AM soft tissue surrogates, Yoo and colleagues also point out that surgeons find TPU models, like the one shown in figure 2.6, are stiff and difficult to suture.[133]

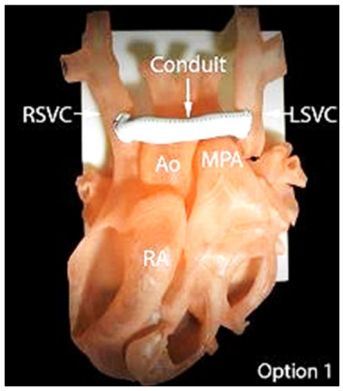

Figure 2.6 AM TPU model of defective human heart used for patient-specific surgical simulation. *[Hussein, N., Kasdi, R., Coles, J. G., & Yoo, S. J. (2020).][133] TPU selective laser sintered (AM) heart model of a patient with congenital heart disease. A flexible elastomeric model that can be cut and sutured to rehearse procedures.*

TPU's are also difficult to colour and do not lend themselves to textile reinforcement due to the method of their production.[136] There has been increasing interest in the field of printable PDMS elastomers over the last five years or so, and some research has successfully produced tuneable AM PDMS elastomers using fillers and thermal curing.[135, 137] Some investigators have even had some success with soft commercial PDMS gels (with hardness's of A10 and OO-30):[138, 139] However, AM specific PDMS material technology is still in its infancy though and there are no commercially viable materials or printers able to print PDMS gels directly.

Although limited in their versatility, SLS printers are commercially available and capable of printing in soft materials, so they tend to be popular in the medical modelling community as the models they produce need little specialist post-production attention to turn into a useful product.[132] Despite the lack of forthcoming data, these new industries

arguably represent the emergence of a new discipline that merges clinical and theatrical prosthetics, with material science. Despite this the key problem remains; skilled practitioners, proficient in the arts of advanced soft prosthesis fabrication, rarely document their embodied knowledge, especially where commercially sensitive intellectual property is concerned. Nevertheless, the foundation of a new discipline has been laid and now meaningful transfer of knowledge and dialogue is happening between these communities. [140, 141, 142, 143, 144]

In the next section, the behaviour of soft fibrous tissues membranes is presented to help identify similarities and how they might be used to improve our understanding and characterisation of surrogate behaviour. Each new topic has a central theme related to the type of fillers commonly used to change the properties of commercial PDMS elastomers; loose, disorganised fillers like fibres, organised fillers like textiles and liquid fillers like oil. Other liquid fillers commonly used by prosthetists, such as PEIE (softeners) *Smith's prosthetic deadener®* (*Polytek®* Development Corp', PA, USA) are covered by the manufacturers material data sheets.

2.8 Behaviour of loose fillers in elastomers

When testing natural and synthetic elastomers that are purely elastic, investigators often rely on Hooke's law to determine its elasticity,[145, 146] most often communicating results in the form of a Young's modulus value. [147, 148] Hooke's law works perfectly well for isotropic, linear materials and to a certain extent, anisotropic, viscoelastic materials, but only at low strains, and within their recoverable elastic region.[149, 150] When fillers are added to rubber, the mechanical response to loading changes as it begins to respond more like organic soft membranes; this was first noticed by Holt in 1932. [151] In his experiments on early rubbers for tyre producers, Holt noticed that loose particle filled rubbers, like carbon black filled (natural) rubber, struggled to recover after repeated deformation during compression and tension in cyclic tests. [151] Cyclic tests were designed to determine the mechanical performance of rubber under repeated use and deformation. During these experiments, Holt noticed that permanent deformation began to affect rubber performance after the first few loading cycles, gradually changing its elastic response with each additional cycle. The effect became known as dynamic strain ageing or softening.[151]

2.8.1 Bio-inspired, disorganised fibrous membranes

The softening effect is now a well-known feature of soft tissues as well as soft elastomers, in preconditioning scenarios.[152, 153, 154] Fung attributes softening of soft tissue to the presence of fibres such as elastin and collagen, somewhat similar to Holt's observations of carbon black filled rubber. Similarly, fillers like fumed silica, commonly used as a bulking agent in PDMS elastomers, has been shown to reduce susceptibility to tearing in PDMS membranes but it is not useful for pigmentation due to its colour.[141, 142, 143] As fumed silica is only available in white and causes opacity in PDMS, other particulate fillers are often used as intrinsic PDMS pigments. Loose, short-strand fibres made from nylon, polyester or rayon plastic (flocking fibres) are commonly used in both clinical and theatrical soft tissue prostheses fabrication to achieve depth and texture to coloured prosthesis.[3, 155, 156] Furthermore, a survey of 43 maxillofacial prosthetists revealed that most use these loose, short-strand fibres, to intrinsically pigment their prostheses in their daily practice.[157] Addition of loose fibre fillers is preferred to liquid pigments because many colours of fibres can be combined to produce a more realistic skin tone with depth of colour while maintaining native material translucency.[3, 158, 159] See figure 2.7

In previous studies on filled PDMS elastomers (>20A Shore hardness), the mechanical influence of embedded short-strand rayon fibres, was previously reported, but essential quantitative data on the relationship between fibre quantity and the mechanical properties

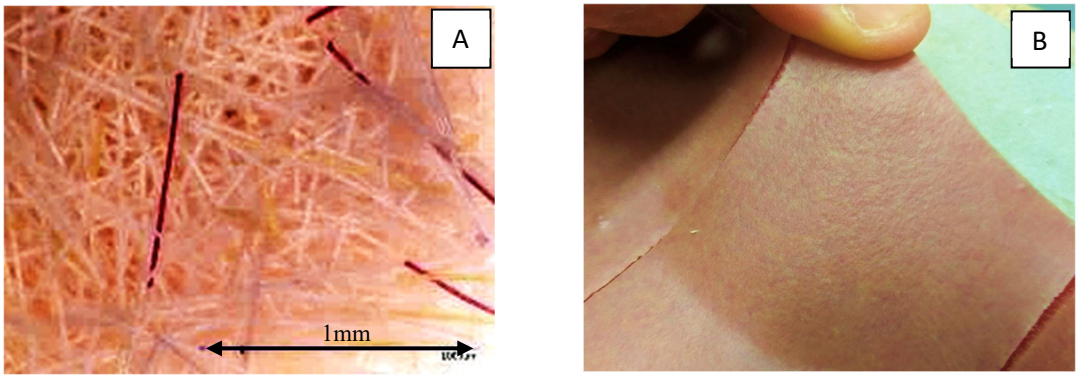

Figure 2.7 Loose flocking fibres used to pigment and texturize PDMS membranes.
Image 'A' shows a microscopic view of flocking fibres at 200x magnification. Image 'B' shows a closeup view of a multi-layered PDMS membrane saturated with flocking fibres. Demonstrating the tonal, textural value of multi-coloured, loose fibre saturation. Ordinarily, the PDMS appears smooth and colourless.

of PDMS was not relayed. [158, 160] They did not report on the behavioural influence of fibre addition or offer explicit, repeatable production methods.

Short-strand fibre flock saturation in PDMS elastomeric gels (shown in figure 2.7) was also noted by Debreceni[3] and Montgomery[157] but they only mentioned aesthetic benefits and trends in soft prosthesis.

2.9 Fibre-reinforced elastomeric composites

Fibre-reinforced elastomeric composites are often employed in non-cosmetic medical implants. Medical grade elastomers (ethylene-propylene-diene-monomer) used in the manufacture of medical devices such as vascular stents, heart valves and assistive devices, draw design inspiration from the arrangement and function of natural fibres such as collagen and elastin, found in the body.[161, 162] The amount of collagen and elastin found in the skin effects its characteristic performance. Their influence on the mechanical properties of soft tissues can be reliably measured by determining parameters such as hardness, elasticity, and extensibility.[41, 45, 163, 164, 165] Soft, synthetic elastomers (lacking fibre reinforcement), such as pure PDMS gels, have an exaggerated isotropic, viscoelastic elongation under load (>1000%) whereas soft, biological membranes like human skin (that contain fibres) exhibit less elongation under load (<150%). This will be discussed in more detail in the experimental chapters of this thesis.

It is tempting to argue then, that by varying the amount, and arrangement, of embedded textile in other elastomers, like PDMS gel, we may gain control of its mechanical behaviour. A recent study suggests that through use of embedded textile elements, one might even limit extensibility and improve strength by redistributing mechanical loading and interrupting the propagation of tears as load increases.[161] Other studies into the suitable percentage of fibre saturation in other elastomers show that low volumes (by weight) of 2 % to 2.5 % introduce changes in mechanical behaviour, particularly in hardness and elastic modulus.[163, 164] Despite this, emulating the characteristics of soft tissues with fibre-filled elastomers cannot be limited to mimicking simple hardness and isotropic, elastic modulus, and other mechanical tests, like multi-axial tests, are needed.

Multi-axial deformation is inherent to the tactility of soft tissue membranes, as they

stretch and move over underlying, three-dimensional structures of the body. For example, the heterogeneity of membranes like skin and some of the causes of its inconsistent behaviour across the body, is due to variable thickness and it's time-dependent response to strain changes are dependent on age, gender, sample site and many other variables including fibre type, density and distribution.[166]

These variables are further confounded by the presence of incompressible fluids, hydrated or perfused tissue and embedded vascular structures.[167] In addition, the volume, distribution and orientation of fibres such as collagen and elastin is changeable, layer-by-layer.[168]

Taking these variables and complexities into account, alongside the diverse test methods and equipment, it is easy to understand the broad mechanical threshold of elasticity (Young's modulus) of human skin given in the literature (4.5 kPa to 30 MPa).[16, 39, 50, 169, 170, 171, 172, 173, 174, 175]

Understandably, this breadth of available data makes selection of the correct modulus difficult when attempting to reproduce these values with synthetic mediums. Despite the wealth of biomedical data on the mechanical properties of skin and skin simulants, there are still no available equivalent studies that investigate the mechanical behaviour of fibre embedded PDMS gel membranes as soft tissue surrogates. [45, 62, 63, 64, 168, 176, 177]

2.10 Organic fibrous structures

In this section, the characteristics of organic fibres and reinforced, soft membranes are discussed in the context of the literature. The various advances that have been made to emulate certain aspects of fibrous tissue behaviour, using synthetic mediums, are reported. Fibres like elastin and collagen, which are found in skin and other soft tissues, have a directionally biased linear structure that mostly follows the direction of the underlying muscle structures. These linear structures are known as Langer's lines.[26] It is well established that the direction of the fibre alignment in soft tissues like human skin has a great effect on its behaviour during mechanical deformation.[50, 64, 172, 173] The characteristic behaviour of organic membranes is notoriously complex, especially when considered as a multi-layered composite material, where each layer contributes its own

mechanical characteristics to the cumulative effect on overall membrane behaviour. Studies have shown that multi-functionality offered by multi-layered membranes with stiffer fibrous layers and softer extensible layers, as seen in blood vessels and skin, for example, prevent premature rupture during mechanical loading.[178]

The epidermis and dermis have very different mechanical attributes when examined in isolation. Accounting for 77% of human skin, collagen has a big effect on performance characteristics like strength and recovery after loading.[41, 179] Unsurprisingly, elastin also has an important role to play in the mechanical elasticity of skin, despite only comprising 4 % the skin. Together these substances contribute to the overall membrane characteristics. It has been established that these volumes change a little with age, but it is widely agreed that collagen in particular accumulates damage over time, gradually deteriorating by 25 % between the ages of 25 and 65.[52, 180] As the collagen volume decreases during this period, the overall thickness also decreases as the underlaying structure diminishes, causing age-related wrinkles.[180] Despite degradation of density and tension over time, these fibres remain mechanically functional and repairable for a lifetime, influencing the mechanical behaviour of the skin.[18, 52, 180] Type 1 collagen fibrils (20 nm – 40 nm in diameter) that are found in human skin and other membranes, form collagen fibres (0.2 µm – 12 µm in diameter) that, when relaxed, appear twisted and bunched or crimped.[41] As the skin is stretched, these fibres straighten and become stiff as they approach their mechanical limit, similar to mechanical loading of synthetic elastane.[26, 181, 182] A visual comparison of the structure can be seen in figure 2.8.

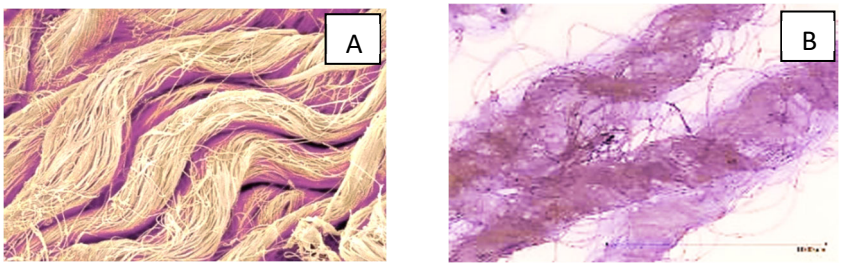

Figure 2.8 A comparison of Collagen and elastane fibres- *Image 'A' shows collagen fibre bundles of the dermis of the skin, taken using a Scanning Electron Micrograph (scale undisclosed). Image 'B' shows elastane yarns at 200x magnification (scale shown in image) to demonstrate the visible structural similarity between elastane yarns and collagen fibres. Image 'A' – [by Nishinaga, S. / Science Photo Library]. Available at Collagen fibres, SEM - Stock Image - C008/7530 - Science Photo Library*

Langer's lines are a consequence of fibre direction during formation of the skin, and it has been shown, for example, that skin exhibits greater extensibility in certain regions such as the scapula (shoulder blade) and back of the knee.[50]

The ability to control the extensibility in specific regions should be considered an important factor when attempting to emulate the mechanical properties of soft tissue membranes like skin. In such regions, the Langer's lines align in uniform parallel formation, delivering greater skin mobility between these lines, hence, the skin is a directional membrane that stretches more perpendicular to the direction of the lines and less in parallel to the lines.[26, 181, 182, 183] The organisation of these fibrous lines of tension are well known to influence its resistance to deformation, elongation and tearing.[30, 178, 184, 185, 186, 187, 188] Finally, when extending the skin in uni-axial tests it was found that the extensibility of juvenile skin was 50%,[30] while other, more recent studies found it to be 100%, in a wider age range.[31, 174, 189, 190,

Extensibility is an important aspect of soft tissue behaviour and is a mechanical characteristic that is well understood in textile manufacturing and textile-based prosthetics and implantables. In the next two sections, the mechanical benefits offered by textile elements are presented and examples of its application are discussed.

2.11 Bio-inspired, organised fibrous membranes (knitted elastane)

Elastane is well known for its elastic stretch and recovery in support of bodily soft tissues, hence its popularity in compression and sportswear garments.[191, 192, 193] Taking advantage of knitted elastane characteristics, a recent study demonstrated how embedded elastane yarns could be used to control the mechanical characteristics of polyurethane-based elastomers.[194]

Knitted textiles have three distinct directions that produce different mechanical characteristics when stretched: Wales, coarse and bias, broadly speaking, vertical, horizontal and diagonal, respectively (illustrated in detail in Chapter 5). Changes in response to loading in each direction are most evident in the elastic modulus and extensibility, in particular.[195] When stretched in the wales direction, knitted fabric has a higher elastic modulus but lower extensibility, while in the coarse direction it exhibits

the greater extensibility and a lower modulus, features which can be further exaggerated in the bias direction.[196]

There are three common terms in use for elastane fabric. Elastane is a more general term that describes the co-polymer yarns that are made into the fabric. *Spandex* is simply an acronym of expands, later coined by users.[197] Finally, *Lycra* is a brand name associated with the inventor of elastane- Joseph Shivers, in 1958 for DuPont Corporation. Lycra® (DE, USA).[198]

Most elastane yarns are made from a cylindrical, hyperelastic polyurethane (PU) core, wound with a loosely wrapped, unspun, non-extensible, micro-filament, nylon strands.[199] When stretched, the PU core extends with typical Hookean elasticity, as the inextensible nylon wrapping gradually straightens, it takes up an increasing amount of the loading force until straightened, whereupon it receives the entire loading force until failure.[194] The properties and behaviour of elastane yarn are expanded in Chapter 5.

2.12 Textile reinforced elastomers in medical device design

Realising the potential of fibre reinforced elastomers, designers of implantable devices like cardiovascular prosthesis have been capitalising on the mechanical benefits for decades. Endoprostheses, for example, have been used to treat vascular ruptures and dissections using woven nylon yarn reinforced with elastomers since the 1990's, especially in cases of abdominal aortic aneurysms (AAA).[200] PDMS elastomers were embedded with a woven lattice structure of monofilament textiles that could reliably reproduce the mechanical characteristics of soft tissue membranes like the human aorta. In their investigation, Zhalmuratova[181] and colleagues used fabric reinforced elastomers to mimic the mechanical properties of aortic tissue to induce the Windkessel effect, required for continual vascular bloodflow.[181] In their study, the well-known properties of stiffness and inextensibility in arterial vasculature, formed the basis for informed development of the synthetic membranes they produced.[201, 202, 203]

Embedded woven fibre architecture works well for devices like stiffer arteries, but it is not suitable for softer tissues like skin, which need to stretch.

Knitted fabric structures, however, are anisotropic and their extensibility is dependent on

orientation, just like human skin.[50] The structure of knitted textiles also makes it permeable to liquids, which is ideal for creating mechanical bonds with PDMS gels during the lamination process.

The mechanical advantages offered by fabric reinforced PDMS elastomers are well appointed by prosthetic sleeve designers. There are numerous design applications with various fabric types and similar production methodologies usually involving the bonding of a fabric layer to the outer surface of the microparticle polymer filled PDMS liner (1785 patents). Some examples of the type of fabric used includes- silk and fibreglass,[204] knitted lycra,[205, 206] or knitted silicone yarn.[207, 208] Some inventions also site more stretch in one direction (circumferentially) than another (longitudinally) for the purpose of preventing the liner elongating with the weight of the prosthetic limb during use.[204, 208]

2.13 Textile reinforced, synthetic membranes

Several studies on the influence of knitted structures and two-dimensional, directional elastomeric yarns showed great potential as clinical soft tissue surrogates, but the complexity of their preparation and related costs will likely preclude widespread uptake by clinical and theatrical prosthetists and design communities.[209, 210, 2011, 212]

Wang[213] recognised the value of PDMS/fabric composites for use as a robust membrane in robotic skins too, supporting their claims with standardised mechanical testing. Using single binding gel, Zhalmuratova[181,182] and colleagues also found that, when embedded in a soft PDMS gel (‘*Eco-flex 0050’ Polytek, USA*), woven fabric offered increased strength in membranes for robotic applications as well as aortic prosthesis. They also noticed that the textile structure and yarn elasticity contributed to the characteristic ‘J’-shaped or ‘deckchair’-shaped anisotropic stress/strain curves (in uni-axial testing).[45] This topic will be expanded in Chapter 5.

One commercialised example of fabric being used to reinforce PDMS-based soft tissue surrogates include cardiovascular models produced by *The Chamberlain Group*. They use coloured, soft PDMS gels, embedded with knitted elastane fabric (shown in figure 2.9), as a means of reinforcing the models, to prevent tearing during surgical training exercises. Naturally, the production methodology and intellectual property are protected

with a patent (US 6,685,481 B2).[214] The presence of fabric and its mechanical influence appears to not feature in their homogeneous designs though, as other anatomical details are also ignored, like differing tissue hardness, accurate colouration, thickness, and modulus.

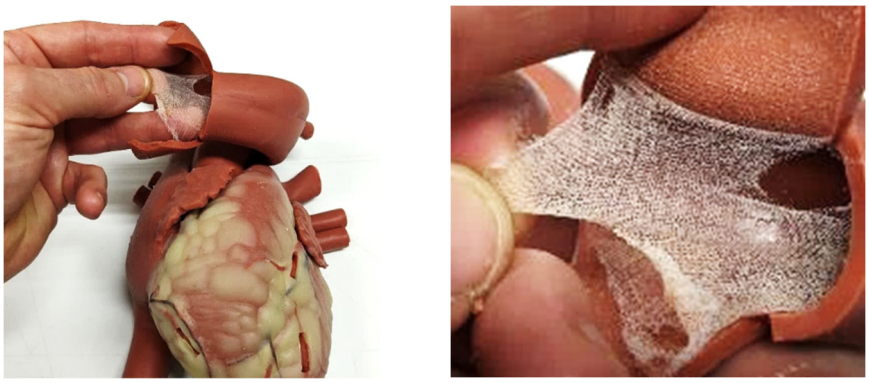

Figure 2.9 PDMS heart model reinforced with knitted elastane fabric.
Image 'A' shows the commercially available heart model, produced in the USA with a patented design by The Chamberlain Group (US 6,685,481 B2).
Image 'B' shows a close-up view of the single-layered PDMS gel construction and the knitted elastane substructure bonded to the surface of the interior.

Investigations into the characteristics of fabric reinforced PDMS membranes, has previously been reported, but all neglected to describe guidance from any specific test standard. Interestingly though, some researchers must have recognised test standard value as they all adopted some elements from the standards, such as specimen dimensions or test speeds.[152, 181, 182, 210, 211, 212, 213, 215]

Crucial to organised filler or textile use is bonding of the lamina. Bonding of elastomeric layers to one another, as well as bonding between the elastomer to the embedded fillers or textiles, takes two distinct forms, mechanical and molecular.[216] In mechanical bonding, a changeable, weaker bond is formed as the PDMS gel flows through, and around, macroscopic gaps in the permeable filler/textile structure. The shape and size of these gaps (between the individual yarns) are dependent on the type of yarn used and the method of textile construction.[181]

PDMS gel can only form molecular bonds with other cross-linked PDMS surfaces, so it stands to reason that the PDMS gel will form stronger molecular bonds where the PDMS

gel is able to interface directly with underlaying PDMS surfaces.[217] Esteves' work in this area suggests that the initially fixed shape and area are also changeable, at both the preparation phase as tension is applied during embedding, and at the testing phase as the specimens are deformed and the gaps change shape.[217]

To summarise, the examples discussed in this section draw many parallels with the curious mechanical behaviour of soft tissue membranes in that they are heavily influenced by the concentration and arrangement of natural fibres like collagen and elastin.[218, 219, 220] While collagen bundles are crimped and coiled in their relaxed state, they stiffen when straightened under tension.[221] Elastin (like elastane), is highly elastic, as its name suggests, but is weak and breaks easily when its elastic limit is exceeded.[41] Natural fibres found in organic membranes, like skin, have a directionally bias structure that helps limit their extensibility, much like fabric reinforced elastomers. Organic fibres present in soft tissues are even similarly bound together in a soft viscous gel like material referred to as 'ground substance'.[41, 222] Coalesced by the ground substance, fibre architecture and gel composition complement one another, mechanically speaking.[223]

Next, we look at the behaviour of very soft tissues that have little or no real structure or strength.

2.14 Characteristic behaviour of very soft, oily tissues

In contrast to fibrous soft tissues that require embedded fibres and textiles to limit extensibility of synthetic surrogates, very soft oily tissues have a much different set of requirements for synthetic emulation.

As the most easily accessible and commonly handled very soft tissue, fat, or at least subcutaneous adipose tissue (SAT), found just under the skin, represents the best documented very soft tissue in the literature.[224, 225, 226, 227] Physiologically speaking, SAT is a deposit of fragile, thin-walled cells that accumulate just under the skin adjacent to the dermis.[228] Due to its proximity to the skin it is sometimes referred to as the hypodermis. Strictly speaking though, it is not part of the skin, nor is it connected to the skin in the same way that the epidermis is connected to the dermis.[229] SAT is only loosely connected to the skin, mainly due to its softness, friable nature, and poor structural

integrity.[230] The physiologic union of the dermis and the fat is called the dermal-fat interface or the 'apical layer'. This is an extremely thin layer of fatty tissue that loosely connects the skin to the underlying fat.[230] The interconnecting structures that join the skin to the underlying anatomy pass through the SAT layer, joining the dermis to the fat via capillary blood and lymphatic vessels, and tiny nerve endings.

For this reason, the skin can be easily debrided from the underlying fat in blunt dissection, but also from the muscle facia below the fat. In contrast, the epidermis and dermis are very difficult to separate without significant chemical or mechanical abrasion.[230]

In summary, very soft, oily tissues should be considered, treated and characterised as a separate soft tissue membrane. In practical, synthetic surrogate applications like clinical or theatrical prosthetics, they could be weakly bonding to the more substantial layers of soft tissue to keep them in place while providing enhanced membrane mobility with their self-lubricating qualities.

Nineteenth-century clinical investigators of fatty tissues were quick to recognise that its mechanical behaviour was similar to that of an oily gel. Due to its oily nature, it is incompressible and immiscible with water-based substances like blood. Due to oil's well-known temperature-dependant mechanical characteristics, fat is highly temperature-dependent in its response to deformation too.[23] In 2010 - 2012 Comley and Fleck provided a detailed review of the mechanical properties of adipose anatomy, documenting the response of SAT to mechanical stresses, however, their observations were based on non-standard test methods using custom-made equipment, making repeatability and comparison of physical attributes, amongst research groups, somewhat problematic.[231, 232, 233] Nevertheless, Comley and Fleck showed that SAT had Young's modulus of 0.011 ± 0.006 MPa, exhibiting a non-linear, stress-strain curve up to 30 % (extension) in uni-axial elongation. [231, 232, 233]

Indentation (hardness) by durometer tests on fat samples from human patients found visceral fat to be softer than adipose fat.[234] Unfortunately, once again, indentation tests and result analysis failed to adhere to a standard, rendering results without comparative merit. Most studies that use bespoke test equipment have unfortunately failed to share full details of their test apparatus' construction and specimen conditions like hydration

and temperature, conditions well-known to affect the hardness and elastic response of both organic soft tissues and synthetic elastomers.[41, 235]

Mechanical tests on other very soft tissues, where elevated hardness is an indication of disease, in conditions like liver fibrosis and skin sclerosis, hardness has been previously measured by indentation with a Shore hardness durometer.[17, 236, 237, 238, 239] In the same way, the fat pad of the heel has also been characterised by durometer hardness tests too.[240]

Chanda[210] built on Tong's[240] findings to create a synthetic, PDMS-based model that was able to mechanically mimic the fat pad. The value of test standards, especially indentation by durometer, are recognised and reported, but no examples of adipose fat hardness measurements could be found in the literature.

Perhaps such scarcity is due to biomechanical researchers not recognising the real value of transferability offered by agreed standards, or perhaps the format offered by the standard lacks sufficient detail for their study. Whatever the reason, despite the dearth of conforming literature, specific to adipose tissues, tests like indentation by durometer demonstrate how standardised measuring techniques are key to repeatability in development of soft tissue surrogates. Critically, widespread access and affordability of durometers and the results they produce can be validated and repeated with the same universal standards and equipment.

Due to the gap in the literature, an objective of this chapter is to identify adjustable material characteristic properties, so that they might be used to simulate their biological counterparts.

2.15 Bio-inspired, very soft membranes

In this section, the various compatible liquid fillers available for PDMS gels are introduced. This is followed by a review of the literature with a particular focus on the use of PDMS oil and how PDMS oil dispersal in PDMS gel can be used to influence mechanical properties like hardness and elastic modulus, to mimic the properties of very soft tissue reported in the literature.

Various, commercially available liquid additives are used in conjunction with PDMS

elastomers for prosthetic applications. Liquid additives are used to alter the characteristics of the elastomer, usually during preparation.

PDMS oil is more widely recognised for its non-toxic lubrication properties in sports equipment, engineering, and cosmetics, as well as its anti-foaming effects in food preparation.[20, 241] PDMS oil is also used in clinical applications, like ocular therapy, most notably for use in retinal tamponade studies, due to its excellent optical clarity.[242, 243, 244]

While PDMS oils are well known for their optical and lubricating properties in other disciplines, they are poorly understood when adapting them for prosthetic use in the simulation of soft tissues.[245, 246, 247, 248] In an attempt to prevent biocontamination and fouling of medical devices researchers have previously created a bio-inspired, self-lubricating 'mucus membrane' using PDMS gels, diluted with oil. Howell and Cui were among the first to report on the self-lubricating and self-healing properties of oil saturated PDMS elastomers. [247, 248] Since then, other studies have used fabric reinforced, cured PDMS membranes, soaked in oil, when investigating antibacterial, non-sticking properties for wound dressings.[250, 251] Sotiri also noticed that changing the stoichiometric ratio of the two-part PDMS elastomer (*Dow Sylgard 184*) had a greater effect on softening and elasticity, than the viscosity of oil.[251] This was mostly due to swelling of the PDMS caused by prolonged submersion in an oil bath though, rather than true dispersion in the gel matrix that is achieved by mixing the oil in with the PDMS gel during its preparation.

The most common method employed by other researchers for softening PDMS elastomers, involves altering the manufacturers stoichiometric ratios, [251, 252, 253] however this causes unreliability, instability, poor repeatability, and post-cure material flow.[74]

To maintain material integrity, it is important to use the manufacturers specified stoichiometric ratios and use recommended additives as required.

Importantly, softeners like ethoxylated polyethyleneimine (PEIE) also introduce other mechanical side effects during the cross-linking process. Adding softener promotes intrinsic material tackiness, which increases adhesivity as more softener is added, which is a problem when trying to emulate very soft tissues that are often slippery and limp to

handle.[177] PEIE also increases viscoelasticity and reduces hardness that will be discussed later in this chapter.[3, 254]

Due to their lubricating qualities, the dispersal of oil in gel does not result in increased tackiness. The softening effect of PDMS oil has previously been mistaken for PEIE-based softeners like 'Smith's prosthetic deadener' due to the similar softening properties;[255] however these are very different materials that yield different results when mixed. Most notably, PDMS oil cannot cross-link with the PDMS gel as PEIE does. Instead, the added oil is free to migrate through the cured gel, resulting in an oily, self-lubricating gel whereas PEIE cross-links with the PDMS forming a permanent, sticky bond.[256]

Researchers at the Optical and Biomedical Engineering Laboratory,[257] (University of Western Australia) recognised some influential properties of PDMS oil dispersion in PDMS elastomers. They established that dispersal of PDMS gel in PDMS oil created very soft, viscoelastic tissues like fat, connective visceral tissues, or soft friable internal organs. [257] The mixing ratios specified on the OBEL website claim that between 100 % and 600 % (by weight) oil dispersal in a relatively firm 45 Shore A hardness PDMS rubber yielded moduli between 0.3MPa and 0.01MPa, respectively. [257] Hardness results were within range of most very soft tissues given in the literature, but a lack of reported test methodologies or standards, restricts validation of the results.

PDMS gels and oil have also been successfully used at higher oil percentages to simulate soft tissues, specifically for medical imaging training. For example, Oldenburg[258] used 900 % oil in a PDMS firm 44 Shore A hardness PDMS rubber to simulate human skin in magnetic resonance imaging scenarios. Liang[259] used similar percentages of oil to create soft tissues phantoms for magnetic resonance elastography imaging, noting that the elastic modulus of the cured PDMS changed from 0.359 MPa to 0.012 MPa as the amount of oil was increased from 100 % to 900 %, respectively. Other similar investigations used a firm PDMS, with a 43 Shore A hardness, to look at the changes in tensile and shear characteristics with the addition of 10 - 30% oil dispersal, where a significant softening effect was observed.[260] Once again, in both of these studies, no test standards were mentioned or adhered to, making validation and further development problematic.

PDMS oil has also been used as a mixed viscosity reducer. In one study, up to 50 % oil (by weight) was added to a PDMS gel to reduce the mixed viscosity. Investigators noticed that the modulus of the composite reduced as the percentage of oil was increased, which was in agreement with other similar studies.[261] Other investigations have explored the potential of PDMS oil as a thinning agent to reduce the mixed viscosity of PDMS elastomers. Ustbas[262] and colleagues formulated blends of PDMS gel and PDMS oil to simulate the optical properties of breast tissues for medical imaging. They observed a softening effect as the amount of oil was increased from 50 % to 83 %.[262]

Others have also reported the mechanical changes in PDMS gels resulting from additions of PDMS oil. Zhang[263] and colleagues, added 25% oil to their PDMS gel to reduce viscosity and aid the dispersal of dry filler particles, like fumed silica and starch. Zhang's study is unique in the literature (concerning PDMS gel composites), as it used a repeatable methodology, based on known, agreed test standards.[263] In particular, Zhang's team used two standards- tensile testing, that adhered to ASTM D 412-16 and shore hardness tests that adhered to ASTM D2240-15.

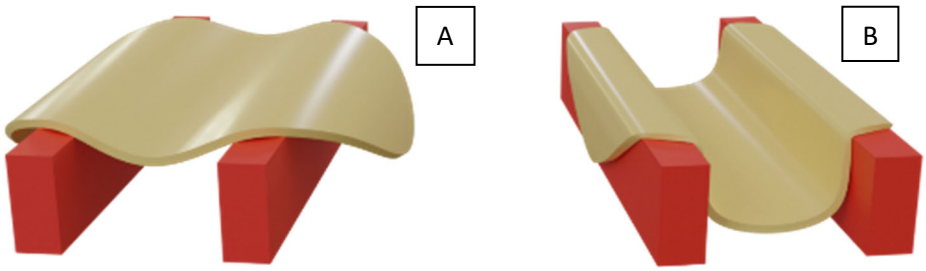

Figure 2.10 Demonstration of the slumping effect caused by dispersal of PDMS oil.
When cast as a thin membrane, PDMS gels still exhibit high elasticity and some rigidity shown in image 'A'. When PDMS oil is added to PDMS gel, it disrupts the cross-linking process required for curing. The disruption does not stop the curing process, but it does disrupt the molecular structure. The presence of oil is known to cause dangling chains of polymers that have only one attached end and one free end that is highly mobile. This mobility causes the PDMS gel to lose its elasticity, allowing it to slump under its own weight, shown in image 'B'.

Interestingly, the unique, self-lubricating properties of oil saturated PDMS elastomers has been linked to its molecular structure (when cured), where the presence of oil prevents the elastomer from fully cross-linking. More specifically, dispersal of PDMS oil in a cross-linked PDMS gel causes what are known as 'daggling chain polymers'.[263]

Dangling chains are unfixed ends in the polymer chain, allowing for greater mass mobility as some of the free polymer chains struggle to form a molecular bond with one another. From a prosthetist's viewpoint, this causes a characteristic softening and slumping effect that becomes more pronounced as more oil is added.[11, 264] (as shown in figure 2.10) Slumping or relaxation phenomena is a trait typically associated with very soft, organic tissue behaviour, like SAT, the spleen and the liver.[11, 265]

In this section, it has been shown how PDMS gels can be manipulated in various ways to change the native mechanical properties of a variety of PDMS gels. There remains a clear gap in the knowledge about the precise effect of PDMS oil dispersal in PDMS gels. It is not known precisely how oil dispersal effects hardness, elasticity or other physical qualities important to prosthetists' emulation of human SAT and other very soft tissues or organs.

Next, we examine some of the known mechanical phenomena observed in soft membranes, when they are subjected to mechanical loading, in the context of the literature.

2.16 Behavioural phenomena of soft membranes

The mechanical behaviour of soft, multi-layered, anisotropic, viscoelastic composites is complex, and mechanical tests often yield results that are difficult to interpret without some appreciation of the associated behavioural phenomena.[266] Here, relevant phenomena that have previously been observed in natural and man-made soft membranes in order to highlight their significance and gauge potential influence on the materials created for this study. Behavioural phenomena of organic soft tissues and synthetic surrogate materials are introduced here to provide a background for the chosen materials and test methods, as well as a rationale for the presentation and interpretation of the results. Detailed mathematical modelling and finite element analysis methods, often used to validate soft tissues are beyond the scope of this investigation. Results of empirical mechanical tests are used throughout this work to identify target specimen groups of significant interest for future exploration, where they occur.

In this section, behavioural traits that are unique to soft, multilayered elastomeric compounds are introduced and discussed. Examples of these traits include- anisotropic

non-linearity, viscoelasticity, stress/time/history dependant hysteresis, strain hardening and strain softening characteristics.[41, 45, 267] Behavioural phenomena such as the Payne effect and the Mullins effect are associated with these traits and have been observed in previous mechanical evaluations.[41, 47, 268] Other previously undocumented, uncharacteristic behaviour are also introduced in this chapter; in particular, the Piobert-Lüders (or Lüders) effect (banded, hierarchical extensibility), and the Portevin- Le Chatelier (PLC) effect (serrated stress/strain curves).[269, 270] These effects were observed during unreported, preliminary experimental testing of materials by the author, prior to this thesis. Discussing these effects is therefore necessary to provide the reader with a comprehensive understanding of the mechanical behaviours discussed in this work.

A review of key sources that describe phenomena such as the Payne Effect, the Mullins Effect, the Lüders effect and the PLC effect, respectively, are presented. Observations of these unique characteristics help deepen our understanding of synthetic membrane behaviour and strengthen the validation of physical models of soft tissue membranes used in this investigation.

2.16.1 Mechanical hysteresis

Mechanical hysteresis is the change in response to loading during cyclic tests that precondition the material being tested, to reveal viscoelastic, time dependent characteristics.[41] Preconditioning is a key factor in identifying the impact on anisotropy caused by fillers like fibres, yarns, and fabrics, as well as fluid fillers like oils. There is also a related international standard (designed for elasticated fabric) that could be adhered to when preparing, testing, and reporting data, which will be discussed in the next chapter in detail. Strangely, none of the consulted literature concerning the topic of multi-axial compression, mentions use of the standard.[264, 271, 272, 273, 274] As previously stated, lack of an agreed standard (adapted or otherwise) makes universal comparison almost impossible.[275]

For materials that have a multi-layered structure that also contain fillers, cumulative mechanical influences should be expected. Cyclic mechanical loading of filled elastomers in previous studies reported strain softening with hysteresis curves that usually start well-spaced from one another, but gradually move closer together.[276] The

principle effects caused by preconditioning of elastomers is shown in more detail in the final sections of this chapter. Cyclic test procedures are characterised (in the standard) by the multi-axial test (BS EN 20932-2), which will be discussed in the next chapter (Chapter 3). The current test standard specifies up to 10 cycles are enough to consider a specimen sufficiently 'preconditioned', which is in agreement with Fung's earlier work on preconditioning soft tissue membranes.[41, 275]

As loading history accumulates in the specimen with each additional cycle, the loading and unloading curves move closer together until, in some cases, they appear one on top of another, representative of a preconditioned specimen, at least for soft tissues.[41] Henceforth, readings can be confidently taken, assured there will be no further plastic deformation, so long as the load does not surpass the preconditioned threshold.[41] In some stiffer elastic materials where preconditioning could be thought of as a key feature of their organic function, like ligaments and tendon, the preconditioning phase can be considerable (ranging from 100 to 1000 cycles).[277] As there are no standards being adhered to, each research group usually chooses to precondition specimens however they see fit.[41, 277] Of course, varying the number of preconditioning cycles inevitably introduces additional variables in experimental tests, especially in force decay, relaxation, and permanent deformation (bagging). Bagging occurs when a fixed shape sags after being deformed and allow to return to its relaxed state, permanently deformed. Therefore, the number of cycles should be fixed at ten for all tests (five loading and five unloading cycles), which is consistent with the standard and other similar cyclic tests conducted on soft tissues.[275]

The physical characteristics, used to quantitatively measure soft membranes in the literature, can be reduced to simple tactility, or user perception of material behaviour, like hardness when pressed and slumping when held in the hand. Essentially, how it responds to deformation from human interaction, deformation and mechanical forces. Viscoelasticity is one of these key characteristics. How the material slumps in the hand when being handled is a good way to visualise viscoelasticity in the context of this work. Put into terms of biomechanical components, relaxation is smallest in elastin, larger in collagen, but largest in smooth muscle (found in connective tissues, hollow organs and some vasculature). Relaxation, viscoelasticity and the softening of elastomeric materials

during mechanical deformation, can be attributed to five important phenomena established by five key texts in the literature: Preconditioning[41], The Payne effect[46, 268] and the Mullins effect [47] and, to a lesser extent, the Lüders effect[269] and Portevin-le Chatelier effect.[270] These will all be discussed briefly in the following sections.

2.16.2 The Payne Effect

The Payne effect, also known as the Fletcher-Gent effect,[46] can be simplified as a softening effect that occurs in filled elastomers and fibrous soft tissues at small strain rates and so, is reversible. It has a significant effect on the behaviour of elastomers and should not be ignored when designing, testing, or validating specimens.[278] Usually it is accompanied by a loss of elastic modulus at increasing or constant strains and normally disappears with the absence of filler.[279] Researchers attribute the cause of the Payne effect and indeed, the Mullins effect (discussed in 2.16.3) to the non-uniform size, distribution, and quantity of fillers used. Since fillers are being used in this work too, both effects are introduced here. An increase in elastic modulus often accompanies the addition of fillers in elastomers, but it also causes a dislocation and reorientation, and sometimes the reformation, of bonds in the elastomeric matrix exhibited as a mechanical softening effect.[280, 281]

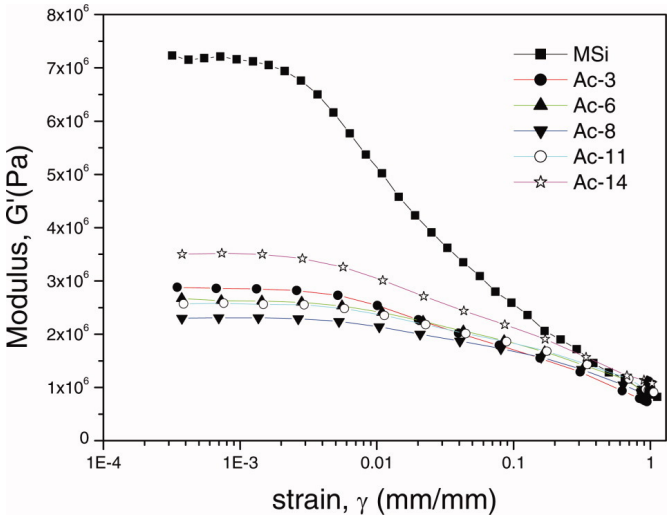

Figure 2.11 Strain softening traits of the Payne effect *[Ramier, J.].[282] Note the non-linear decrease in specimen stress as strain is increased at low strains <0.2. Reused under the Creative Commons Attribution-Non-Commercial- No Derivatives License (CC BY NC ND).*

Typically, the Payne effect is observed at small strains (under 20 %) and can be attributed

to the dislocation and reorientation of embedded fillers like powders, loose fibres, or fabrics.[151, 268] More recently, Morozov[283, 284] identified that the type of filler used and its composition or arrangement in the rubber influences the extent to which the Payne effect influences behaviour during deformation. In addition to filled synthetic elastomers, the presence of collagen and elastin fibres within soft tissues exhibits similar responses to deformation in multi-axial compression during cyclic testing and has previously been linked to the Payne effect.[285]

Human skin has been shown to be heavily influenced by the anisotropy caused by the directional fibres, leading to hardening at high strain rates and softening at low strain rates.[50, 172] Both biological soft tissues and filled synthetic elastomeric surrogates can exhibit anisotropic, viscoelastic properties attributed to the Payne effect, but also the Mullins effect, which is discussed in the following section.[41, 49, 267, 274]

2.16.3 The Mullins Effect

The Mullins effect is the progressive cyclic softening seen most often in filled rubber. More specifically, the Mullins effect describes the irreversible change at high strains in the mechanical properties of a soft, filled rubber that occurs during the first few deformations in cyclic tests, at higher strains.[46, 47, 153, 272]

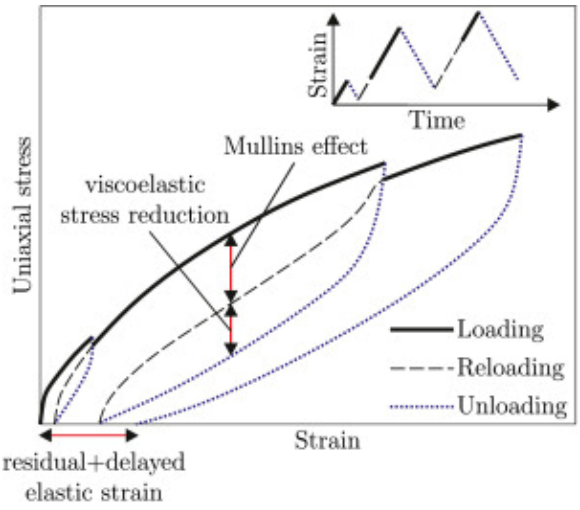

Figure 2.12 An example of the hysteresis curves affected by the Mullins effect.
The Mullins effect as seen during preconditioning/cyclic loading. The rate of recovery measured by force decay and degradation show how the Mullins effect influences membrane behaviour. [Fazekas, B.][286] Reused under the Creative Commons Attribution-Non-Commercial-No Derivatives License (CC BY NC ND).

The permanent aspect of the phenomena is caused by breakage of the bonds between filler particles and the surrounding matrix.[47] The softening effect increases as filler concentration increases, evidencing a strong relationship between filler amounts and the amount of strain softening.[287] Diani[287] and colleagues provide a comprehensive review of the literature concerning the Mullins effect, but they argue that its precise effects are still poorly understood and are often mistaken for the Payne effect. [287] Both phenomena describe softening of thermoplastic elastomers and filled elastomers, but are differentiated by the behaviour of, what Merabia[288] and colleagues call- 'glassy bridges' in their structure that occur during deformation, like extension.[288] The Mullins effect is used to describe the destruction of these 'glassy bridges', which progressively lessens the number of overall bridges as the material continues to be stretched putting further strain on the remaining bridges. As the material weakens, energy is lost and the softening effect is observed. The change is permanent.[288]

The Mullins effect was previously observed during uni-axial cyclic testing on porcine skin, where the investigators also found that the hysteresis loops, continually decayed and then stabilized, similar to the behaviour of human skin observed by Fung. [41, 264]

In contrast, skin from smaller mammals tends to respond quite differently to preconditioning deformation. Lanir[289] found that a preconditioned rabbit skin will return to its original size, but only after a large relaxation period, while living rat skin was found to fully recover after cyclic preconditioning, perhaps due to perfusion of living skin.[116]

2.16.4 The Lüders effect

The Lüders effect is a phenomenon that describes the progressive succession of loading across the test specimen starting at the grips and radiating to the centre of the specimen in waves or bands of increasing stress (in uni-axial tests).[269] Lüders bands, as they are known, are observable in stress strain tests on ductile metals and are often visible as serrations in the stress/strain curves prior to specimen yield and failure.[290, 291]

Of the three types of strain reliant Lüders banding, first described by Lüders, type 'C' bands are more likely to occur in softer materials as they are usually observed at lower strains in ductile materials.[269] In their study of the mechanical properties of styrene-based

thermoplastic elastomers, Torres and colleagues discovered the appearance of Lüders banding and related Portevin Le Chatelier effect apparent in results, during uni-axial tests.[292] Similar material behaviour was also observed in uni-axial extension tests on polycarbonate,[293] and polyurethanes.[294] Homogeneous polymeric materials like PDMS gels that have been dispersed in PDMS oil during preparation, might also exhibit a similar banded uni-axial extension.

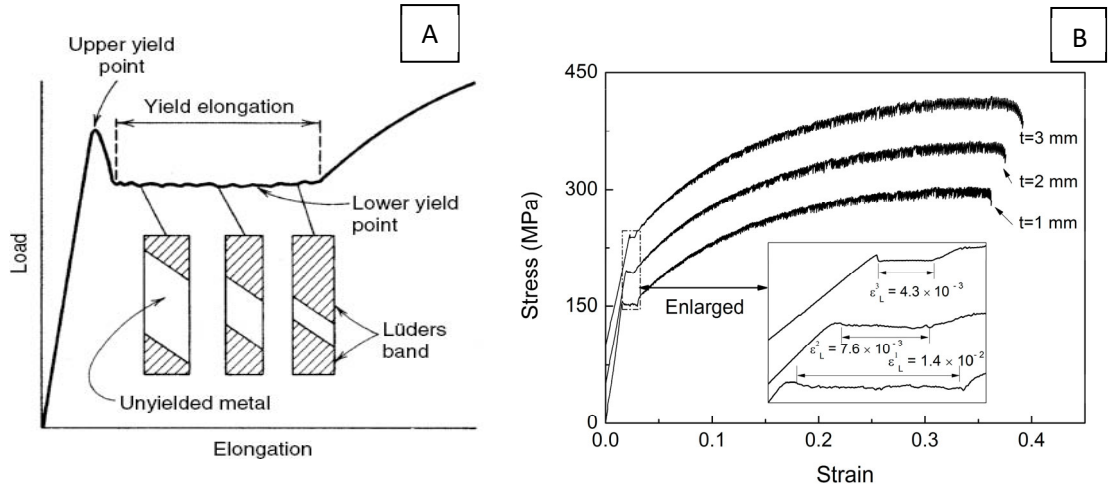

Figure 2.13 Schematic of Lüders effect in uni-axial extension.

Image 'A' shows how metallic specimens stretch to cause Luders banding in uni-axial extension tests.[209] Image 'B' show the Luders banding effect on three types of aluminium alloy each band type is known as band type A, B and C, influenced by thickness and stiffness of the specimen. The serrated flow patterns shown in both images is associated to the Portevin-le Chatelier (PLC) effect[296], described in 2.16.5. The serrations in the stress strain curves continue until the Lüders strain threshold is reached, at which point the curve may resume its uniformity until the ultimate tensile strength is met and the specimen ruptures at failure.

The presence of dangling polymer chains discussed earlier, may play a key role in Lüders banding formation due to the uneven molecular distribution of elastic response.[294] This shows that, although ductile metals like steel and soft polymers like polystyrene appear to be nothing alike, mechanically speaking, there may be some similarities that are not immediately apparent or previously reported in the literature.

From a pragmatic viewpoint of the prosthetist, presence of the Lüders banding may not have a great impact, but for broader applications like robotics and medical device design, it will be an important mechanical feature to be avoided.[111, 296, 297, 298, 299, 300]

2.16.5 The Portevin Le Chatelier effect

The PLC effect has been used to describe the serrated plastic flow and yield of ductile materials, like some metals such as steel[301] and aluminium, but has never been observed in elastomers.[302] It usually occurs when the test specimen weakens in one specific area (Lüders band formation) which propagates towards the centre of the specimen as extension proceeds. The phenomenon (seen in uni-axial extension to failure) is caused by instability in the microcrystalline structure and its subsequent progressive failure and recovery due to what Ren calls a "compartmental reorganisation of the molecular structure".[303] At a macroscopic level, the test specimen hardens, weakens, and yields in a cyclic fashion as strain is increased leading to the jerky, serrated vector seen in the stress strain trajectory.[304]

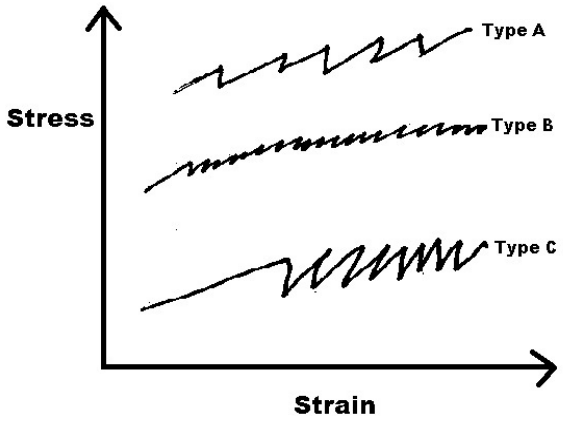

Figure 2.14 Serration types associated with the Lüders and PLC effect.
"Schematic illustration of the shape of the stress vs strain curves corresponding to the three different types of spatiotemporal arrangements of deformation bands associated with plastic instability".[304] Reused under the Creative Commons Attribution-Non Commercial-No Derivatives License (CC BY NC ND).

Again, this phenomenon may have a limited impact on the pragmatic side of prosthetics, but other related disciplines that make use of these findings may find it of great use, especially in robotics and medical device design.[297, 298, 299, 300] Extracting as many physical characteristics as possible from data sets will serve to deepen our understanding of synthetic membrane behaviour and strengthen future design and validation of soft tissue surrogates. In the next section the various test methods and equipment used to measure soft membranes that are reported in the literature, are presented.

2.17 Test methods for soft membranes and validation of results

The wide range of methods and equipment used to test the mechanical properties of soft tissues exists because of the requirements demanded by the discipline. For example, a plastic surgeon's need for data on the mechanical properties of skin[147] are very different to the needs of a dermatologist[305] or pharmaceutical company.[306] In other words, the focus, method, equipment and test site location understandably change in relation to the discourse. This discriminatory approach to testing is useful for the group leading the investigation but does little to advance the collective understanding of soft tissue and elastomer behaviour, when results cannot be reliably reproduced or compared. To replicate any soft tissue membrane, it is essential that characterisation methods are aligned to deliver reliable results. For example, a study exploring the hardness of the pancreas, compared it to PDMS-based alternatives.[307] In their investigation, indentation by durometer would have produced results that would be easily compariable and transferable. Instead a new tactile resonance sensor, was employed, with no standard referenced, again making comparison of results with other studies problematic.[308] As this study is concerned primarily with validation and replication of the tactility of *living* soft tissues, reports on *in vivo* methods, in humans, will be given preference where they exist. Despite the obvious inaccessibility of live human organs, some investigators have been able to successfully gather standardised data on mechanical properties of organs like the liver, during live surgery or immediately after the organ is removed from the body.[236, 309] Both investigations used contact-based, non-destructive methods like indentation by durometer, but examples like these are very rare in the literature. The mechanical properties of human skin, both *in vivo* and *ex vivo* (and *in vitro*) have been studied extensively in the literature, thanks to its accessibility. Research into the mechanical properties of soft tissue membranes like skin have, historically, been predominantly driven by dermatological research for the cosmetics industry. Decades of research by dermatologists has shown that the multi-layered structure of skin and its elastic response to stress, have been linked to many variables such as hydration,[51] age,[289, 310, 311, 312, 313, 314] site location on the body,[50, 315] sex,[188, 315] weight, lifestyle,[315] and other factors like temperature.[316, 317] During previous studies, data gathering methods, equipment and interpretation of results are rarely directly comparable due to the considerable variables that impact the results, with site location being arguably the most influential.[18, 50, 172, 173]

Soft tissue characterisation methods and equipment, that have no clear standard to follow for reporting results, are typically non-contact methods such as; vibro-acoustic spectrograph, harmonic motion imaging,[318] quasi-static compression and strain imaging, dynamic shear wave elastography, shear-wave propagation, sono-elastography and magnetic resonance transient elastography.[319] Other non-contact methods include, acoustic radiation force-based elasticity imaging,[320] and ultrasound elastography.[320] All of these techniques and related test devices are perfectly valid for limited research groups, with access to specific test equipment, but non-contact medical imaging methods cannot be reliably compared with contact methods for mechanical characterisation, partly because of the nature of these tests, but mainly due to the lack of suitably comparable test standards. Other methods that were not included in this investigation are; torsion,[188] and suction,[321] again, because of the lack of standardised equipment for testing. *In silico* modelling was also not used for the same reason, although it may be possible with some reverse engineering, this was not the focus of the current work. Although *ex vivo* studies and those carried out on non-human specimens such as pigs do have value, as porcine tissues are similar in appearance and function to human tissue (*in vivo* and *ex vivo*)[322] such data will be used sparingly, as some studies show porcine tissue to be stiffer and less extensible than human tissue.[103, 323, 324, 325] Other studies have shown current artificial skin models to be stiffer as well.[326] It has also previously been shown that, due to preservation methods and tissue morbidity, that cadaveric tissues lack some characteristics of living counterparts, but are still considered here, especially where no values exist for living (human) subjects, or the mechanical tests required to characterise the specimens are destructive by nature.[327]

2.18 Relevant data from the literature

In this section, relevant mechanical data describing biological soft tissues have been compiled to identify some transferable values that are in agreement with one another. In their review of the mechanical properties of human skin, Yazdi and colleagues provide a detailed account of mechanical characterisation results.[312] Literature on the mechanical properties of human adipose tissue are rare though.[234, 328, 329] More common are investigations of animal adipose tissues of the pig.[63, 231, 232, 233, 330]

2.18.1 Young's modulus data in the literature

Young's modulus is used primarily in engineering terms to describe measurements of stress (force) and strain in metals and crystalline structures, but only in the elastic range of a material.[19, 39, 50] Young's modulus (MPa) values reported in the literature have been compiled in Table 1.

Table 1. *The Young's modulus of human skin reported in the literature.*

Specimen site	Method	Modulus range (MPa)	Strength range (MPa)	Reference
Forearm skin	Indentation (Micro)	Modulus 0.35 - 0.5	-	331
Forearm skin	Indentation (Micro)	Modulus 0.04 - 0.08	-	18
Forearm skin	Indentation	Modulus 0.006 – 0.01	-	332
Back skin	Uni-axial (Tensile)	Modulus 4.6 - 20	-	39
Back skin	Uni-axial (Tensile)	Modulus 49 - 117	UTS (ultimate tensile strength) 13.2 – 30	50
Back skin	Uni-axial (Tensile)	Modulus (Parallel to Langers lines) 107.6 – 214 (Perpendicular to Langers lines) 11.1 – 130.1	UTS (Parallel to Langers lines) 22.3 – 33.7 (Perpendicular to Langers lines) 10.4 – 20.8	172
Maxillofacial skin	Uni-axial (Tensile)	Modulus 14 - 35	UTS 2 – 5	128
Maxillofacial skin	Uni-axial (Tensile)	Modulus 20	UTS 1.5 - 4.5	173
Abdominal skin	Uni-axial (Tensile)	Modulus 3 - 53	UTS 1 - 24	16
Abdominal skin	Uni-axial (Tensile)	Modulus 3 - 18	UTS 2 - 15	174
Abdominal subcutaneous adipose	Uni-axial (Tensile)	Modulus 0.001 – 0.004	-	175
Abdominal subcutaneous adipose	Uni-axial (Cauchy)	0.001 – 0.002	-	329

Table 1. The Young's modulus of human skin reported in the literature.
Indentation tests and uni-axial tests included in this table are also referenced in the related supporting literature.[19, 45, 212, 312, 333]

Young's modulus is the most commonly applied denominator for mechanical properties of soft tissues in the literature. The test methodologies used to gather data, included in

the table, recognised the standard (BS/ISO 37), or at least some aspects of it. Despite some test protocols being observed in most of the tests that were reported, the standard itself may not have been acknowledged specifically, perhaps because it was developed for rubbers and thermoplastic elastomers, rather than soft tissues. No equivalent standard exists specifically for soft tissues, despite the agreed similarities to elastomer behaviour already presented. So, results presented in Table 1, are given preference where test specimen shape, equipment, test speed or forces can be linked to the standard.

2.18.2 Hardness data in the literature

Hardness of soft tissues is easily measured with a device called a durometer using the standard (ASTM D2240). The Shore hardness readings given by the durometer ranges from 0-100 and will be discussed in more detail in the following chapter (Chapter 3). Soft tissue membranes like skin are usually measured in OO shore hardness. Because the orders of magnitude in Shore hardness overlap, the harder Shore hardness O (H O) and softer Shore hardness OO (H OO) are can be easily mistaken for one another.[338] The orders of magnitude actually overlap quite a lot, but are quite different, shown in Table 2 and discussed in detail in 3.2.1.

Table 2. *The Shore hardness scales (O, OO and OOO.*

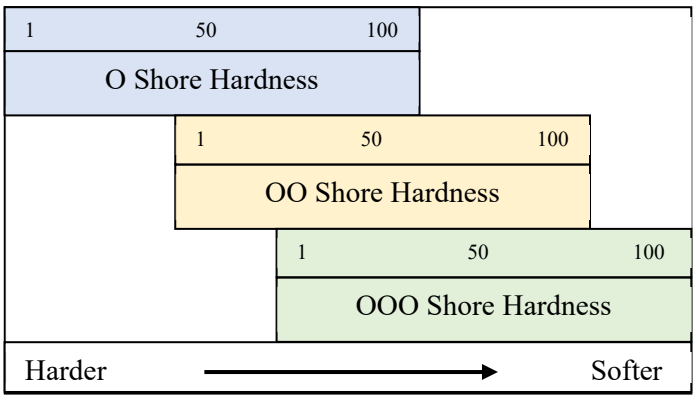

Table 2. Table of Shore hardness results from the literature.

This table shows three Shore hardness scales. Each scale is effective from 1 to 100. Each colour in the table represents a different hardness scale and shows its relationship with the other scales. Conversions are not exact and vary slightly with brand and location.

It should be noted that it was recently proposed that use of the durometer to measure living skin can be misleading when the underlying tissue thickness is not reported.[237] In

contrast, when gathering data on *surrogate* soft tissues, the thickness can be reliably measured.

Table 3. *The Shore hardness (OO) of human skin reported in the literature.*

Specimen site	Hardness range (Shore OO hardness)	Reference
Heel pad	39.9 – 46.4	334 *
Heel pad	50 - 60	237
Sole of foot	33.8 – 45.5	335
Forearm	28 - 50	336
Forearm	25	238
Upper arm	18	238
Hands	15	238
Leg	25	239
Fingertips, Forearm, thigh and forehead	25 - 58	17*
Sole of foot	20 - 37	337*
* assumes OO not O as stated		

Table 3. Table of Shore hardness results of human skin reported in the literature.

This table is a comparative table of hardness value of human skin reported in the literature. References allocated with a * were determined to be reporting errors that will be discussed at the end of this thesis in Chapter 7.

2.19 Discussion

This chapter provides an overview of our deepening understanding of soft tissue membranes, over the last few hundred years, mapping the growth of interest in soft membrane behaviour over the last 30 years, especially. It has also been shown how soft tissue surrogate materials like PDMS, have been employed in medical education and prosthesis development, thanks to their availability, affordability, and versatility, but the mechanical influence of PDMS additives have not been reliably measured. Literature has shown the changeable behaviour of natural and synthetic soft membranes, under load, are influenced by embedded textiles, fibre type, density, and arrangement. Fiber-

reinforced elastomeric composites, used in medical implants, for example, draw design inspiration from the functionality of natural fibres like collagen and elastin found in soft tissue membranes. Embedded fillers and textile structures control mechanical characteristics of synthetic soft tissue interfaces, like replacement arteries, prosthetic sleeves, and surgical simulations, but the variety of available additives have not been tested and assessed alongside one another before. A poor understanding of tunability in commercial PDMS gels, hampers development of more realistic soft tissue surrogates for use in clinical and theatrical prosthesis, surgical training aids and implants. The mechanical behaviour of softened or reinforced, multi-layered PDMS composites, that are familiar to clinical and theatrical prosthetists, have never been properly characterised using agreed standards. Unique traits exhibited by soft elastomeric membranes, such as anisotropic non-linearity, viscoelasticity, and stress, time or history dependent hysteresis, are well understood in soft tissue mechanics, but poorly understood in materials familiar to prosthetists. These behavioural traits, and the related phenomena, like strain hardening, strain softening and preconditioning, can be determined by standardised mechanical tests, seldom reported in the literature. The characteristic behaviour of soft tissues can be used to inform design practice and fabrication of new realistic, soft tissue surrogate membranes. An understanding of these principles is key to identifying adjustable material characteristics to simulate biological counterparts, such as human skin, fat and other soft tissues. The mechanical properties of soft tissues vary depending on the discipline, leading to a wide range of methods and equipment prevalent in the literature. This discriminatory approach to testing hinders understanding of soft tissue and elastomer behaviour. Non-contact methods like vibro-acoustic spectrograph, harmonic motion imaging, dynamic shear wave elastography, sono-elastography, magnetic resonance transient elastography, and ultrasound elastography are unsuitable for comparable mechanical characterisation due to the optical or molecular properties of PDMS substitutes. *In vivo* methods are preferred for validation and replication of soft tissue properties, but data on these methods are almost exclusively restricted to Shore hardness results, due to the destructive nature of other test methods. To help summarise the types of suitable data gathering methods figure 2.15 covers topics introduced in the next chapter. It shows two examples of typical uni-axial and multi-axial data gathering methods that help describe the behaviour of organic and synthetic soft membranes, and where data might be gathered, with standardised methods documented in Chapter 3.

Adapted from Shergold [103] and colleagues, graph 'A' shows a typical stress strain curves for soft membranes like pig skin and silicone rubber are shown in the graph. The coloured labels indicate approximate regions of interest where data is gathered, discussed in detail in 3.0. Graph content is not the focus here.

Adapted from Remache [315] and colleagues, graph 'B' shows a typical preconditioning/ hysteresis graph. Each curve shows loading and unloading cycle.
The labels indicate regions of interest. Graph content is not the focus here. Each region is given context in 3.0.

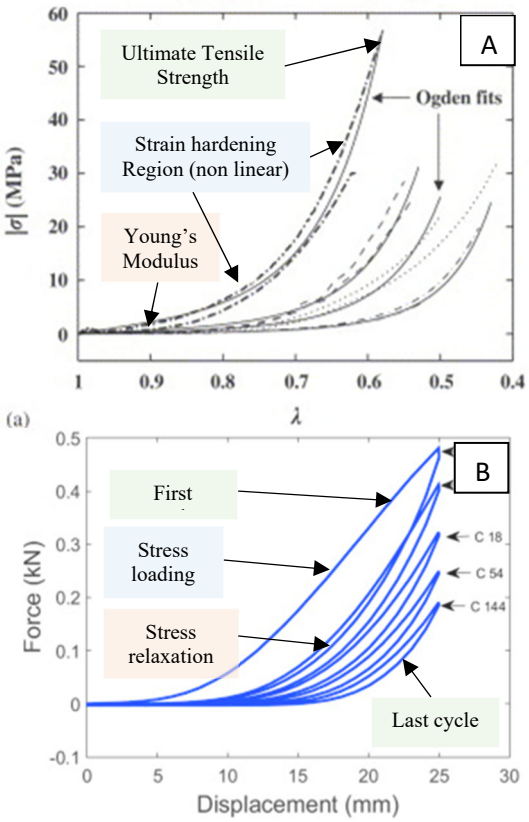

Figure 2.15 Mechanical data gathering regions reported in the literature. This table summarises the regions that are of interest to the communication and documentation of specific tests important to reliable and repeatable analysis of the results.

2.20 Conclusion

The gaps in the knowledge identified in the literature can be reduced to three key areas for investigation. Firstly, the mechanical impact of PDMS additives have not been reliably measured. Secondly, the variety of available additives have not previously been tested and comparatively assessed alongside one another using the same materials and standards. Thirdly, the mechanical behaviour of softened or reinforced, multi-layered PDMS composites, that are familiar to clinical and theatrical prosthetists, have never been properly characterised using agreed standards. Finally, bridging these gaps in knowledge will accelerate development of a wide range industries currently fuelled by prosthetist's tacit know-how. For the first time, prosthetists will be able to make informed design decisions about the mechanical performance of their creations, empowered with the ability to reliably predict behavioural outcomes relating to the additives they are so familiar with.

Chapter 3

Test Standards, Equipment and Methods

3.1 Introduction

This chapter aims to map out the test standards used to report experimental data and describe the methods and rationale for each test used. This chapter will not discuss universal test protocols published in the literature except where some options or equations help describe the method. For a comprehensive overview of each test procedure, readers are invited to visit the referenced standard instead.

International (ISO), British (BSI) and American (ASTM) standards, which are considered internationally acceptable and available globally, were used throughout this work to make results repeatable and accessible to others. Although each standard sets out specific instructions for reliable mechanical characterisation, they have options to suit different applications within each standard. So, this chapter also defines the specifics of each test by describing the particulars.

Data gathering methods that adhere to an agreed standard prevent confusion over test conditions, equipment, method, materials or analysis. Each test standard used here to define the behaviour of various PDMS composites, is based on similar examples in the literature conducted on skin or similar PDMS membranes. Because of the mechanical similarity of soft tissue and soft elastomers, studies on both subjects will be discussed and assessed for their transferability and merit.
Building on the knowledge generated by contributory fields, there are several suitable, agreed test standards that can bridge the gaps between disparate disciplines. Some tests are adapted from elasticated textile or rubber test standards, while others are specifically designed for soft tissues and elastomers. Whereas the previous chapter highlighted some mechanical similarities between these materials, this chapter discusses the standards capable of capturing their behavioural characteristics.

For most mechanical characterisation tests, particularly those used on soft tissue, test methods like uni-axial extension are regularly employed in the literature, but the standard that regulates equipment and result analysis is almost always ignored. Instead, the use of undisclosed, bespoke test equipment and test conditions make the prediction and replication of most results given in the literature a formidable task. So, to ensure others have the information they need to reproduce any test contained in this

thesis, all test parameters are detailed below on a topical basis.

3.1.1 Standards

A variety of industry standards were used to assess mechanical characteristics to ensure repeatability. The standards are given in the table below.

Table 4. *Suitable standards, purpose and measuring units.*

Standard (title/ code)	Purpose/data to be gathered	Units
Indentation by durometer ASTM D2240-21	Determine the hardness of specimens and resistance to indentation	Shore hardness (OO, OOO)
Determination of tensile stress-strain properties BS ISO 37:2017/ ASTM D412/ BS ISO 5893:2002	Determine the stress strain characteristics, including ultimate tensile strength and Young's modulus	Force at failure in Newtons (N), Elasticity in Young's modulus (MPa) and percentage of strain elongation/extension (%)
Multi-axial compression test ISO 20932-2:2018/ BS/ISO 14704-2:2007	Determine the hysteresis, unrecovered deformation, force decay and force decomposition	Force in Newtons (N), Millimetres of deformation, Newtons (N) over time (Seconds) and percentage of deformation (%)
BS/ISO23529: 2016	Preparation guidelines for all specimens	Temperature (C), humidity (%), time (days),

Table 4. An overview of standards used in all experiments.

Details of the purpose and units of measurement are provided in the table.

3.2.1 Indentation by durometer ASTM D2240-21

This standard is used to determine the hardness of a material and is measured in Shore hardness units. Shore hardness spans twelve orders of magnitude, each covering 0-100 units within their own respective ranges. The softest of these span five orders of magnitude that overlap one another. These are assigned to types; 'A', 'O', 'OO', 'OOO', and 'OOO-S', from hardest to softest, respectively. Each hardness range uses a different spring force and indenter shape specified in the standard.

Similar hardness tests, like the international hardness test standard (IHRD) D1415-18, have just one numerical range (0-100), equivalent to the type 'A' Shore hardness test. Although both IHRD and Shore hardness tests use similar test methodologies and protocols, but the Shore hardness test offers a greater range. [339]
Crucially, indentation by durometer is the only agreed standard that has been certified by the standard for the measurement of soft tissues and soft elastomers alike, which makes comparative studies particularly insightful.[94, 236, 237, 238, 239, 334, 335, 336, 337]

Hardness and spring force data are obtained from durometer readings and are recorded in the experimental chapters of this thesis, as per the standard. Indentation by durometer is a non-destructive test that uses a spring-loaded blunt cone, or hemispherical indenter, connected to a display (analogue dial or digital screen) to measure penetrative depth and related resistive force on the spring. Data values are expressed as Shore hardness units (e.g., SH OO or SH OOO). Reisfeld [340] determined that the OO calibrated durometer was best suited to measuring the hardness of skin.
Portability, ease of use, widespread availability and affordability have contributed to the durometer's popularity amongst investigators for over 100 years. Indentation by durometer has become a standard method for the characterisation of *in vivo* skin hardness by dermatologists in the diagnosis and assessment of diseases like scleroderma, psoriasis and diabetes.[17, 18, 238, 239, 309, 336, 341] The lack of acknowledgement of the standard and reported test protocols in most of these studies raises questions about result reliability, though. It is important to mention that many of these previous studies also used indentation to determine the elastic Young's modulus. However, according to Larsen[342], indentation of soft gels below 30 shore A hardness (like all OO/OOO hardness values) cannot be reliably converted, mathematically, to Young's modulus due to limitations within the formula. [342] Instead, Shore hardness and resistive spring force in Newtons have been used to describe spring force resistance in this thesis.[342] Other tests described in this chapter are conducted to attain Young's modulus values.
In addition, Chatzistergos[237] and colleagues argue that Shore hardness is more representative of bulk tissue hardness rather than the hardness of skin alone, claiming that a 7% reduction of Shore hardness was observed when specimen thickness increased by 25%. Therefore, the apparent hardness of the skin must consider

thickness and location as dependent factors in the result analysis. For example, the proximity of skin to deep fat, lean muscle or bone will undoubtedly influence results, especially where the skin is thinnest. So, location and thickness are important variables to consider in hardness tests on skin. Still, this investigation only concerns the measurement of composite polymeric elastomers rather than skin, so the thickness of membranes that are assessed here are controlled during fabrication and are reported for each specimen tested. Due to the softness of specimens created for this thesis, type OO durometer was used for most tests ('Checkline', Cedarhurst, NY, USA SN: 50168) (See figure 3.1) with the exception of membranes characterised in Chapter 6, where the resistive force on the OO durometer was too low to yield reliable results (<10SHOO). When the results of hardness tests are below 10, the more sensitive OOO-calibrated durometer was used instead of the OO-calibrated durometer.

Both durometer types used had an identical mass of 246 grams and were mounted to the same stand to reduce user error when collecting data.

The combined weight of the durometer and pneumatically controlled descending arm of the stand increased the total test mass exerted on the spring-loaded indenter to 403g. The stand conformed with ASTM D2240-03 (stand eligibility remained unchanged in the more recent ASTM D2240-21, too), type 2 stand-RX-OS-4H and controlled the rate of decent during tests, so each loading interaction was identical. The distance between the test surface and the specimen was 25mm for all tests.

Prior to test commencement, three specimens were plied to a total thickness of 6 mm,

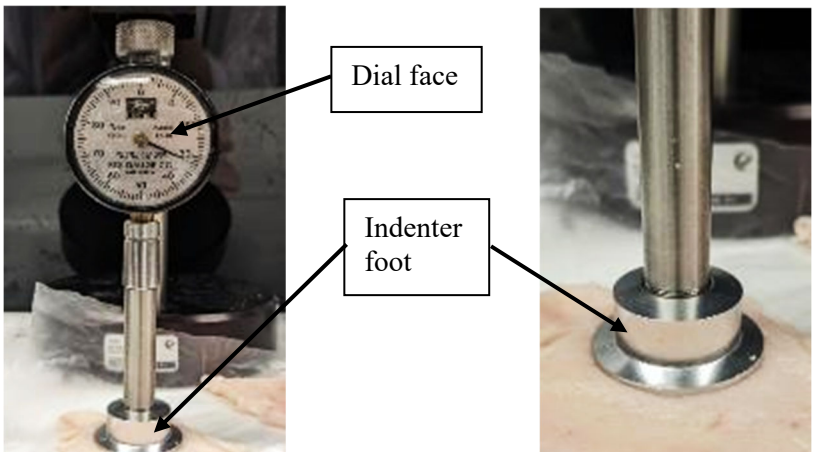

Figure 3.1 Stand mounted, standard OO calibrated durometer in use.

Gathering hardness data on porcine subcutaneous adipose tissue using a OOO calibrated durometer as per the standard.

using 3 x 2 mm thick disc specimens (as specified in ASTM D 2240-21). Each stack of specimens was measured five times in different, randomly selected locations. Each reading was only taken after full contact with the specimen for a duration of 3 seconds. Five measurements were taken 6 mm apart and 12 mm from any edge and recorded directly as a shore OO/OOO hardness value. The arithmetic mean was calculated and presented in the charts relative to each specimen group found throughout this work.

3.2.2 Spring force

Shore hardness values were converted to an indenter spring force value in Newton's as per the standard. Spring force is a useful tool for comparative purposes using the formula given in equation 3.1.

$$N = 0.203 + 0.00908\ HOO/HOOO \qquad Eq\ 3.1$$

Where N = the force in Newtons, H OO and H OOO equal the degree of hardness specified by the durometer

3.3 Determination of tensile stress-strain properties – BS ISO 37:2017/ ASTM D412/ BS ISO 5893:2002

Uni-axial extension to failure was performed on all specimens created for this thesis. Three test standards are required to gather legitimate data on fundamental material characteristics like ultimate tensile strength, Young's modulus and stress-strain data: BS ISO 37:2017, ASTM D412, and BS ISO 5893:2002.

The ZwickRoell Z2.5 tensile testing machine (ZwickRoell GmbH & Co. KG) was used to conduct tests as per the standards. Raw test data was captured using TestXpert II software (ZwickRoell GmbH & Co. KG), and results were processed using Matlab software (The Mathworks Inc, MA, USA) to determine Young's modulus. Graphs and charts were prepared using Microsoft Excel software (Microsoft, WA, USA). BS/ISO 37:2017 and ASTM D412 test standards were used to fix the test parameters to best suit the test specimen softness.

Test standard BS ISO 5893:2002 specifies three suitable methods of measuring

elongation (or 'deflection'); method A; grip to grip separation was selected to align results with similar publications in the literature.[103, 343]

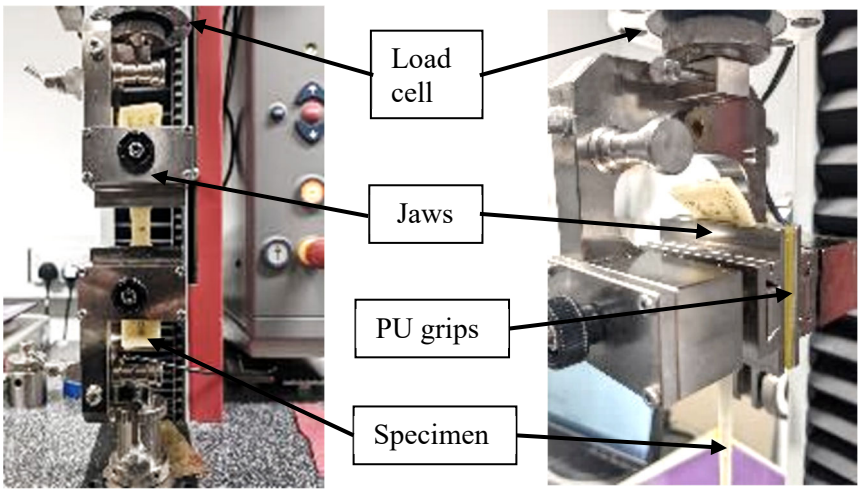

Figure 3.2 Uni-axial test specimens mounted on the Zwick tensile tester.

These images show the test rig set up that was the same for all tensile tests of all specimens. The pneumatic grips with hard elastomeric grips 'Vulkollan' (a hard polyurethane elastomer) prevented slip by applying constant pressure and surface friction, without damaging the specimens, even when the specimen began elongating and thinning at the grip. All tests were monitored for slippage both visually and digitally through the live recording of the stress-strain curves. If slippage occurred, the test was abandoned, and the specimen destroyed. The standard does not require the number of failed specimens to be recorded.

Pneumatic jaws with rubber (polyurethane) grips were used to prevent any slippage, as reported in the literature that can occur during the elongation of elastomeric membranes.[50, 173] The grips were mounted to a 200N load-cell with grip-to-grip separation set to 25 mm, preload of 0.05 N, and test speed of 50 mm/min.

Eleven test speed options are offered in the standards ranging from 1 mm/min to 500 mm/min. In contrast with other investigations of fibre filled PDMS that used 500 mm/min ,[165, 344] the present study and previous studies[11, 102] adopted 50 mm/min test speed to align it more closely with similar studies on human skin that used 55 mm/min. [165, 344] The main reason for slower test speeds on human skin is to allow the viscous and fibrous components time to respond to the deformation stresses. The same test speed was maintained for multi-axial examination for the same reason.

In contrast with other studies that focus on either high strain values (3-5%),[39] or low strain values (0-3%),[43] specific to their interests, this thesis explores all tensile properties of the materials tested by extending each specimen to failure. In this way, we obtain a comprehensive overview of the mechanical behaviour of the materials created and tested throughout this work. Data can be cropped to focus on specific regions of the graph, if required later.

There are three regions of uni-axial behaviour when testing soft tissue membranes like skin:

- Region one includes Young's modulus characteristics, usually determined at lower strains. This is the recoverable, elastic, linear region of extension.
- In region two, non-linear behaviour is first observed as the additives begin to have more influence.
- In region three, yield and failure of specimens occur. Specimens might begin to exhibit unusual behaviour in this region, especially depending on the presence and nature of the additives.

Each region described by this process is effectively a region of behavioural significance and has been evaluated using Young's modulus for region one, Stress/strain data for region two and UTS for region three.

3.3.1 Stress-strain

During tensile testing, the stress-strain curves that are generated describe each specimens' response to deformation, illustrating the initial loading and extension to yield and failure. Each curve allows visual appreciation of the linear elasticity (previously described) and non-linear elasticity at different strains with a constant speed, allowing a visual inspection of strain hardening and strain softening traits.[45]

Results are directly comparable because the same test speed was used for all specimens. Where possible, stress-strain results are shown at the same scale for instantaneous comparison amongst specimen groups. As the curve approaches the structural limit of each specimen, its failure characteristic trajectory is evident and is

given as UTS charts. Results are displayed in the experimental chapters as force (in Newtons) versus strain (%) for reasons previously described in Chapter 1. For reference 1 N/mm2 is equal to 1 MPa. So, results and curves are easily converted. In addition, Young's modulus is provided in each experimental chapter, as a chart.

3.3.2 Ultimate tensile strength

UTS maps the mechanical limitations of specimen groups. Strength is an indication of durability and is important, especially for reusable prosthetics like maxillofacial prostheses and surgical simulations where user interactions are not monitored or are sympathetic to appliance longevity. The UTS is identified by the sudden loss of stress during extension. Specimens do not have to rupture to be classified as failed; only significant, unrecovered, loss of resistance to stress is required to determine failure. Results are reported as MPa and are presented as a chart shown at the same scales where possible to improve comparison across specimen groups.

3.3.3 Young's modulus

Young's modulus was determined using the deformation slope's first rising, linear region. All readings were taken after the initial toe region of the curve as the specimen straightens under loading but before the non-linear part of the curve, as per the standard. Typically, the elastic region was under 1 N and under 100% extension in all the specimen groups tested. Young's modulus E, can be calculated by dividing the tensile stress (σ) by the extensional strain (ε) in the elastic (initial, linear) portion of the physical stress–strain curve. The calculation specified by the standard is given in equation 3.2:

$$E \equiv \frac{\sigma(\varepsilon)}{\varepsilon} = \frac{F/A}{\Delta L/L_0} = \frac{FL_0}{A\Delta L} \qquad \textit{Eq. 3.2}$$

Where E = Young's modulus (modulus of linear elasticity). F is the force exerted on an object under tension. A is the cross-sectional area, which equals the area of the cross-section perpendicular to the applied force. ΔL is the amount by which the length of the object changes. L_0 is the original length of the object.

Recent studies on the relationship between Youngs's modulus and Shore hardness by indentation have been conducted by Larson at silicone manufacturers, Dow Corning

Corporation (MI, USA).[342] Perhaps the most accurate and widely known correlation of durometer values to Young's modulus was first proposed by Gent[345] shown in equation 3.3:

$$E = \frac{0.0981(56+7.62336S)}{0.137505(254-2.54S)} \qquad \textit{Eq. 3.3}\ ^{34}$$

Where E = Young's modulus in MPa. *S* = ASTM D2240 Type A durometer hardness.

Other equations described a method of conversion from Shore A to Young's Modulus (in MPa) [342], shown in equation 3.4:

$$\log 10\ E = 0.0235S - 0.6403. \qquad \textit{Eq.3.4}$$

Where E = Young's modulus in MPa. *S* = durometer hardness (ASTM D2240 Type A)

A comparison of these conversions was also introduced by Larson.[342] However, it was concluded that although a conversion is possible, its accuracy is gradually lost as the materials become softer. Unfortunately, Larson doesn't mention the rate of this decay in the conversion model though.

3.4 Multi-axial compression test ISO 20932-2:2018

Data gathered from multi-axial tests provides useful information on the viscoelastic response to deformation, like hysteresis, force degradation, unrecovered deformation and force decay. The ZwickRoell Z2.5 tensile testing machine (ZwickRoell GmbH & Co. KG) was used to gather all multi-axial deformation data. All test results were collected using TestXpert II software (ZwickRoell GmbH & Co. KG), results were processed, and graphs and charts were prepared using Microsoft Excel (Microsoft, WA, USA).

The standard used herein, BS/ISO 14704-2:2007 and ISO 20932-2:2018, was adopted from the mechanical characterisation of elasticated fabrics, which share many mechanical properties with soft tissues and composite elastomers, especially the specimens containing textiles.

The Zwick Z2.5, tensile testing machine was configured according to the cyclic, compressive multi-axial testing standards, often referred to in the literature as preconditioning. Preconditioning, as previously discussed in Chapter 2, is a crucial part of determining the viscoelastic behaviour of non-linear materials like soft tissues and soft composite polymers, where mechanical behaviour is dependent on loading history.[41]

3.4.1 Multi-axial compression method

Specimens were secured using method 'A' - Dynamic test method; shown in figure 3.3, where a horizontally mounted, ring-clamp fixes the disc-shaped specimen in place whilst supported from underneath with a telescopic spacer block. The spacer block (not shown in figure 3.3) is used to mitigate the risk of the specimen weight distortion (sagging) due to unavoidable gravitational forces on the soft specimens prior to testing.

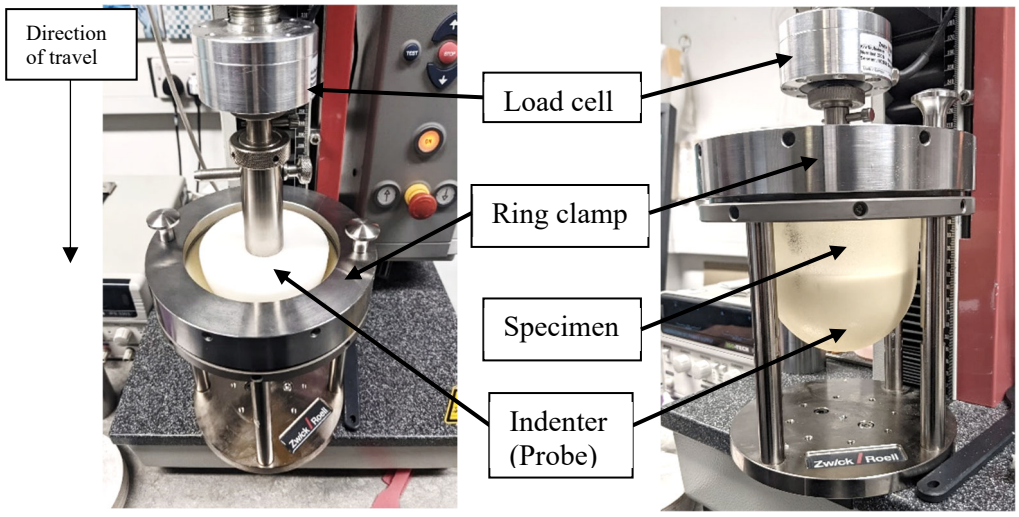

Figure 3.3 Multi-axial test specimens mounted on the Zwick tensile tester in compression. *The ZwickRoell Z2.5 tensile testing machine set up with the multi-axial ring clamp and hemispherical indenter (Probe). All specimens were tested in the same way, with the same setup.*

Once the specimen is fixed in place the block is removed before testing. During the test, the probe tip is pushed through the ring clamp measuring the resistance of the specimen as the load limit of 5 N is approached.

The hemispherical Teflon probe tip had a specific diameter of 100 mm, and the inside ring clamp diameter of the test area was 120 mm. The probe was fitted to a 200N

loadcell, and the speed was fixed for all Multi-axial tests at 50 mm/min. Each specimen was subjected to six cycles up to 5 N. 5 N is equivalent to the force exerted on soft tissues during palpation, handling or surgical procedures,[11, 346] although the gripping force with robot-assisted claspers was found to be slightly more at an average force of 7.5N, the contact area would be smaller and harder than force exerted by the surgeons hand, which is the focus here.[347]

The force-displacement curve for each specimen was collected throughout each cycle (loading and unloading). At the same time, the force decay was calculated by holding the sample at maximum force for a sixty-second period during the fifth cycle. During the sixth cycle (unloading at 0.2N), un-recovered deformation (bagging) was determined.

3.4.2 Hysteresis

Hysteresis is shown as a cyclic graph of elliptical curves showing the preconditioning profile of the sample, loading and unloading cycles during compressive deformation. Maximum deformation of specimens is given in equation 3.5.

$$S = E - L \qquad \textit{Eq. 3.5}$$

Where S = maximum deformation in mm, E is deformation on the fifth cycle at 5N in millimetres, and L is the original deformation at 0.2N in millimetres.

3.4.3 Force degradation

For the determination of force degradation, which indicates the loss of force in Newtons over time (60 seconds), samples were held at a maximum of 5N at the fifth cycle for sixty seconds, and force lost was recorded during this time. This helps to determine the extent and speed of relaxation. This experiment describes how the membrane will behave over time while relaxing, following repeated deformation.

3.4.4 Unrecovered deformation

After cyclic loading, the amount of permanent deformation measured in millimetres after loading cycles. After the force decay data has been gathered (in cycle 5) and the probe has returned to the starting position, the probe holds its position for a further 60 seconds. The probe then completes the final 6th cycle, recording the deformation (mm)

at 0.2N (unloading) to measure the amount of change between the first loading cycle and the final unloading cycle. The difference between these two figures can be used to measure the unrecovered deformation.

The vectors that form the characteristic hysteresis loop also offer an insight into the materials' behaviour under cyclic loading. Each specimen group will have quite different hysteresis formations reflective of their variable mechanical and chemical configurations. Permanent deformation is calculated using equation 3.6

$$C = Q - P \qquad \textit{Eq. 3.6}$$

Where C = the permanent deformation in mm, Q is the deformation at 0.2N after 60 seconds recovery period. P is the original deformation of the first cycle at 0.2N

3.4.5 Force decay (Stress relaxation)

Stress relaxation is the loss of stored elastic energy over time and is measured as a percentage. True, Hookean elastic materials do not lose their energy while held at extension over time, so long as the extension is within the elastic limit. Viscoelastic materials lose stored elastic energy quickly. The more 'viscoelastic' the material, the slower it responds to loading, causing it to lose or gain its stored energy slower.

Force decay is expressed in equation 3.7 and is a percentage measured over 60 seconds, expressed as A.

$$A = \frac{V - W}{V} \; X\,100 \qquad \textit{Eq. 3.7}$$

Where A= time in seconds, V is the maximum force (N) of the last cycle and W is the force (N) measured after 60 seconds.

3.5 Optical analysis

Visual inspection and appraisal were conducted on all specimens before and after tests. In most instances, physical changes in specimens can be seen with the naked eye after testing. Despite this, images of the specimens of each specimen group were also captured to document any microscopic changes in the specimens.

A digital microscope (Keyence VHX 5000, Milton Keynes, UK) with magnification of x200 was used in most instances to maintain consistency unless stated otherwise. Any significant changes in appearance or microscopic structure are noted in the

analysis of results for each experimental chapter wherever they occur.

3.6 Materials

Specific material composition for each specimen group is given in each related experimental chapter (Chapters 4, 5 and 6). Common to all specimens was the base ingredients, which are all commercially, available from *Polytek Development Corp' (PA, USA)*. Two types of addition cure silicones (PDMS) were used; Platsil® gel 10 and Platsil® gel OO-30.

Like most two-part PDMS's, one part is the base material made of silicon/ oxygen the other is a catalyst (platinum salt solution). All supplied as viscous fluids that require mixing in order to cure/crosslink.

Unlike many stiffer types of PDMS that use heat or light to cure, RTV2 silicones cure at room temperature through the cross-linking of molecules and eject no harmful molecules into the working environment during preparation, use or curing.

Care must be taken not to poison the PDMS with substances containing ammonia, sulphate, phosphate or tin-based materials. This leads to undesirable crosslinking inhibition and changes the final material properties, as does inaccurate measuring of the two equal parts. So extra care was taken to mitigate these risks throughout processing.

When mixed at the stoichiometric ratio (1:1) the viscous liquids form a gel with two native hardness's; Shore A 10 PDMS gel, called Platsil® gel 10, (equivalent to approximately Shore OO-50), and Shore OO-30 PDMS gel called Platsil® gel OO-30. Both materials have a softening agent (PEIE) added during preparation to reduce elasticity and improve tactility and viscous mobility. The influence of PEIE addition is given by the manufacturer (*Polytek*). A cross-linking retarder (Platsil® 71/73-part R) is also used for Platsil® gel 10 only due to its short pot-life.

The manufacturer (*Polytek*) states no changes in mechanical properties occur with its use other than delaying cure time.

In addition to these liquid additives, combinations of loose short-strand fibres, elasticated yarns and elasticated knitted fabrics are embedded to determine their influence of native material properties and behaviour. More details of these additives are given at the start of each related chapter.

3.7 General material preparation

All materials were prepared as per the standard -Preparation of test specimens (BS/ISO23529: 2016). To ensure the methods and results are widely accessible, materials were weighed, poured and mixed by hand in a plastic beaker using a clean wooden tongue depressor to mitigate contamination risk. Preparation, by hand, was given preference over available, automated mixing machines, because automated machines are primarily the domain of engineering applications and are rarely used by prosthetists. This is mainly due to cost and time implications associated with use of such equipment. Additionally, research also suggests that hand mixing by the experienced user yields superior results over a wider range of materials and fillers.[348] Each mixture was stirred for five minutes until thoroughly homogeneous before being degassed in a vacuum chamber for five minutes at -982 mbar (-736 mm Hg) to remove entrapped air from the mixture. After degassing, the mixture was removed from the vacuum chamber, poured into a levelled gauge mould that measured 500 mm x 500 mm x 2 mm and allowed to cure for 24 hrs.

Once cured, the membrane was powdered with talcum powder before being cut into test specimens, dumbbell and disc shapes for the uni-axial and Multi-axial tests respectively. Dumbbell cutting dye, type 1A, (shown in Figure 3.4) was selected for the tensile test shape because Annex C of the standard (ISO 37) confirmed that in multi-institute tests type 1A was least likely to break outside the test area. Specimens were cut prior to demoulding to mitigate the risk of sample distortion or warping prior to or during cutting. The back side of each specimen was also powdered with talcum powder during demoulding to prevent self-adhesion upon removal and storage. Completed specimens were stored according to the given standard (BS/ISO23529: 2016) until tested.

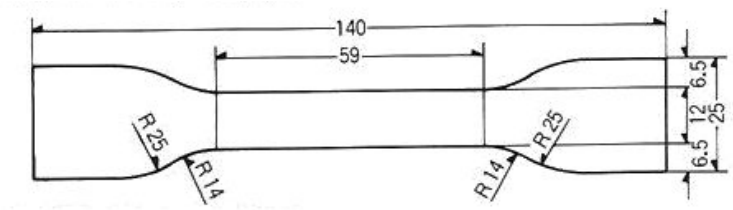

Figure 3.4 Uni-axial test specimen dimensions taken from the standard ISO37.

The dimensions for each uni-axial test specimen used throughout this work. It is the biggest dumbbell type, least likely to break outside the test area when testing very soft

3.8 Summary

A variety of tests were selected to best characterise material specimens with the most significant degree of accuracy and repeatability. The selected tests were Indentation by durometer, uni-axial tensile tests and Multi-axial tests. Results from these tests enabled the determination of hardness, spring force, uni-axial force versus extension, Young's modulus, ultimate tensile strength, hysteresis, force degradation, unrecovered deformation and force decay. Universal standards, techniques, equipment, and materials were adopted to ensure the comparability of test results across experimental chapters. Variables like additives, composition, amount of layers, embedded filler tension and filler orientations are all recorded in detail for each chapter, where they occur, to ensure repeatability and transparency.

The choice of material was informed by the literature reported by peers and the manufacturer's technical reports. Effective handling and processing of materials was informed by 20 years of experiential use in industry applications by the author. The choice of test equipment was informed by the standards and the literature in order to align this work with other similar investigations.

The following three chapters are the experimental chapters of this thesis. Their purpose is to document the design, fabrication, testing and characterisation of PDMS composites, previously unknown and undocumented in the literature.

Chapter 4

Mechanical behaviour of silicone membranes saturated with short strand, loose fibres

This chapter has been previously published-

Arm, R., Shahidi, A., Dias, T. (2019). 'Mechanical Behaviour of silicone membranes saturated with short-strand, loose polyester fibres for prosthetic and surrogate skin applications.' Materials. DOI 10.3390/ma12223647

Co-authors were supervisory team members (exDoS T.D). The complete first draft, design and conceptualisation, final edit and submission were all completed by the author (R.A)

4.1 Introduction

Elastomers saturated with embedded, loose, short-strand fibres (flock) are known in clinical and theatrical prosthesis appliance design for their ability to mimic the aesthetic qualities of skin. Fibres such as polyester, rayon or polyamide are produced in various lengths and colours and blended with a translucent liquid polydimethylsiloxane elastomeric gel (PDMS) to mimic the translucency, intrinsic pigmentation and texture of the living equivalent. Although well-known in the prosthesis industry for decades, currently, this knowledge is mainly tacit, embodied knowledge of the fabricators and technicians. Crucially, the impact these fibres have on the behavioural characteristics of soft PDMS elastomers remains almost unknown in the literature.

In this chapter, the influence that these loose, short-strand fibres have on the mechanical behaviour of PDMS gels will be explored. More specifically, PDMS gels, familiar to clinical and theatrical prosthetists, will be used to make the results relevant and repeatable. The agreed international test standards previously described in Chapter 3 will be used to capture data and record changes in mechanical hardness, stress strain characteristics, elasticity, hysteresis and viscosity (force decay/degradation) of specimens during indentation, uni-axial extension, cyclic and Multi-axial tests.

The main aim of this chapter is to quantify the mechanical influence of well-known fibre fillers used by clinical and theatrical prosthetists that are currently undefined and undocumented. To align this work with the scarce data in the literature, data on hardness and elastic Young's modulus are referenced and compared to the physical mechanical characteristics of (healthy) living skin. Predictive regression models are provided to enrich the results further, but mathematical, constitutive modelling of the physical specimens are beyond the scope of the current investigation.

Some known behavioural phenomena, (introduced in Chapter 2) that are associated with filled elastomers are expanded on where relevant in this chapter. The agreed mechanical test standards that have been used throughout this chapter are referenced, but not expanded upon, as these were described in detail in the previous Chapter 3.

4.2 Methods and materials

To gather the data necessary for the characterisation of the presented composites, changes in mechanical response was measured in two different PDMS gel composite groups. For destructive tests, 50 individual specimens were tested in uni-axial tests and 10 specimens were tested in Multi-axial tests. Each specimen group was split into five sub-groups, including the control group, with each group relating to an increasing fibre content (between 0 % and 4 %). Each group was prepared as single-layered membranes (2 mm in thickness), cut into two different shapes for testing (dumbbells and discs).

4.2.1 PDMS preparation

Using two different colourless PMDS base components mixed according to the manufacturer's specification, two PDMS liquid composite blends were prepared as per figure 4.1 below. All the materials used in this study are commercially available from Mouldlife, Suffolk UK, but are produced in the USA by *Polytek* Dev' Corp'.

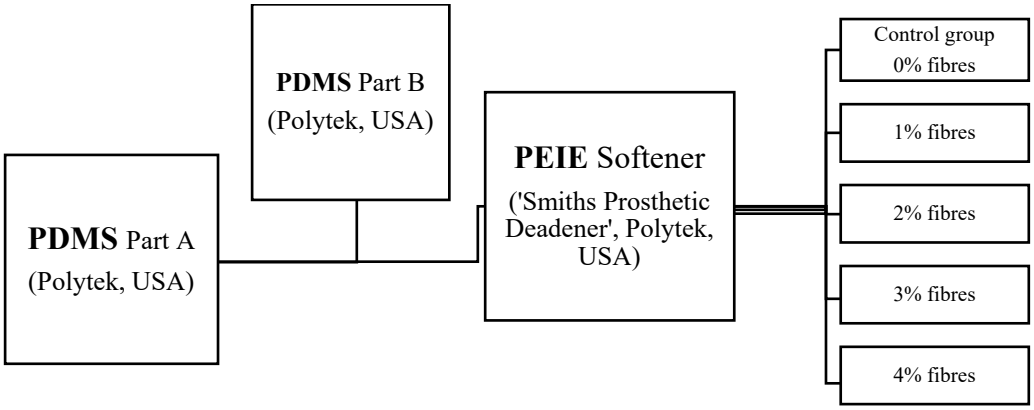

Figure 4.1 Flow diagram of the method for PDMS preparation in different fibre percentages. *The same method but with different ratios were used in all of the material sheet preparations.*

4.2.2 Additives

Softening component (Smiths' Theatrical Prosthetic Deadener) was added in different ratios to each PDMS. This softening agent is known to modify PDMS gels to behave more like skin and soft tissue by reducing typical elastic 'snap' while increasing viscoelastic behaviour.[103] The ratio for each ingredient is given in Table 5.

Table 5. *Mixing ratios and materials used to prepare the membranes.*

Base material: OO-30 PDMS (PlatSil® gel OO-30)	**Base material: A-10 PDMS** (PlatSil® gel 10)
Recipe	Recipe
1 part A + 1 part B + 1 part PEIE + Retarder (3%)	2 parts A + 2 parts B + 3 parts PEIE + Retarder (3%)
2:1 ratio (mixed PDMS: PEIE)	4:3 ratio (mixed PDMS: PEIE)
Fibre saturation 0%, +1%, +2%, +3%, +4%	Fibre saturation 0%, +1%, +2%, +3%, +4%

Table 5. Mixing ratios and materials used to prepare the membranes.

Materials are available from a variety of Polytek (MA, USA) distributors, worldwide.

4.2.3 Fibres

PDMS A-10 (blue) was prepared with blue flocking fibres, and PDMS OO-30 (pink) was prepared using pink flocking fibres. The choice of fibre pigmentation was for easy visual distinction amongst the sample groups. The length and average diameter of both fibre colours used (blue and pink) were found to be identical (19.4 μm).

4.2.4 Fibre analysis

Commercially available, short-strand, flocking fibres were also included in facial soft tissue simulants created for a previous investigation in ballistics at Cranfield Defence Academy.[104] While their high absorbency, strength and flexibility were suitable for this earlier application, they remained uncharacterised for theatrical and maxillofacial prostheses. A Keyence VHX5000 digital microscope (Buckinghamshire, UK) was used to measure the length and width of these fibres was measured at x800 magnification. (Figure 4.2A) Five measurements of diameter along the length of each fibre shaft and one measurement of length were recorded for each of the ten randomly selected fibres. The average diameter and length for these fibres were 19.4 +/- 0.2 μm and 807.5 +/- 3.7 μm, respectively. Fibres were added to the PDMS gel elastomer during the liquid phase of preparation in varying concentrations as a percentage of the batch specimen weight. A magnified view (x100) of the cured specimen membrane with 2 % fibre content in shown in Figure 4.2B.

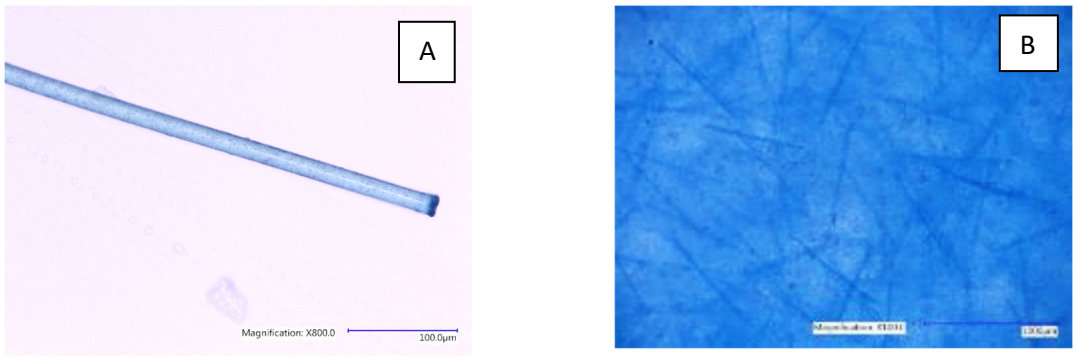

Figure 4.2 The fibre type used in all tests.

Image 'A' shows an individual fibre at ×800 magnification. The burred, cut-edge visible in the image suggested that the fibres were cut with a hot blade during manufacture. Image 'B' shows PDMS A-10 with 2% fibre saturation at ×100 magnification, notice the heterogeneous scattering of fibres in specimen samples.

4.2.5 Sample sheet preparation

Two different PDMS composite base liquids were blended for all of the mechanical testing: A-10 PDMS (Platsil® gel 10, *Polytek*, USA) and OO-30 PDMS (Platsil® gel OO-30, *Polytek*, USA). Skin simulants used in multiple investigations by Mahoney[104] and colleagues were developed by the author (RA) as a two-layered PDMS-based composite membrane (described in this investigation as separate layers) that agreed with the hardness values of human skin and pig skin reported in the literature.[128]

Liquid ingredients and ratios for both blends are given in Table 5, but both materials similarly contained a PDMS base material (A), PDMS catalyst (B), PEIE (S) and cross-link retarder (R). While the base elastomer ratios remained the same for all of the test specimens in both groups, for comparative analysis, the percentage of used fibres within the compound was modified with increments of 1 % from 1 % to 4 %. A control specimen group, absent of embedded fibres, was also included to assess the impact of the fibre introduction.

4.2.6 Preparation method

Each composite blend was mixed by hand using a plastic beaker and wooden tongue depressor for five minutes. The mixture was poured into a second, clean plastic beaker and mixed again for a further three minutes before being degassed at -982.052 mbar of vacuum for five minutes to remove residual air content, that might have been

introduced during homogenisation. The prepared liquid compound was poured into a levelled, 500 mm x 500 mm x 2 mm plastic gauge mould and left to cure for 48 hours. All specimen groups were cut from the sample sheet using the British standard recommended for the preparation of rubber compounds (BS/ISO 23529:2016). They were powdered with talc prior storage for two weeks at a constant 22 °C and 50 to 60 % humidity, prior to testing.

4.2.7 Tensile test specimen preparation

An ASTM D412 Type 1A dog bone (dumbbell) shaped stamp was used to cut 50 specimens for uni-axial tensile testing. This die is the largest size in either the BS/ISO 37:2011 or the ASTM D412 equivalent standard and was also used in similar previous studies on pig skin and rubber.[45, 346] Smaller dies present problems with very soft specimens due to the nature of this destructive test, but more importantly, annex C of the standard states that type 1A dye is least likely to break outside the test area during tensile tests.

4.2.8 Durometric and Multi-axial sample preparation

A steel disc template with a 145 mm diameter was used to cut specimens for Multi-axial and indentation tests using a surgical scalpel. A new surgical scalpel blade was used to cut each specimen group.

4.2.9 Mechanical tests

Indentation by durometer measured the hardness (H OO), uni-axial tension testing measured the elastic modulus and ultimate tensile strength (UTS) at break and Multi-axial compression testing measured hysteresis, force decay and relaxation. Three mechanical tests were performed using two standard compliant pieces of test equipment specified in detail in Chapter 3.

4.2.10 Specimen specification

Throughout this study, the composite made from Platsil® Gel 10 and additional components is termed simply as *'PDMS A-10'* (available from Mouldlife, Suffolk UK). In addition, the composite made from Platsil® Gel OO-30 and additional components is termed as *'PDMS OO-30'* (available from Mouldlife, Suffolk UK).

The names ascribed to the two material groups throughout this study (A-10 and OO-30) refer to the initial elastomeric hardness of the starting materials for each blend prepared. As a softening agent was added at a consistent amount the initial hardness of both materials is lower than the native hardness implied by the brand name. For example, Platsil® Gel 10 does not have a Shore A value of 10. The elastomeric hardness will change dependant on the additives used, in particular the amount of fibres added during preparation of the materials in their liquid state.

4.3 Results

The results of mechanical testing on A-10 and OO-30 are presented here separately to help delineate the relationships between the PDMS and the fibre contents, starting with a comparison of hardness among all ten groups tested.

4.3.1 PDMS A-10 and PDMS OO-30 Durometric hardness

The hardness of the PDMS membranes used in this study were evaluated using an AMST standard (D 2240-21) OO calibrated durometer, as previously used to measure human skin hardness.[255] The applied force for each result has been calculated using the equation (Eq. 4.1) as specified in the standard.

$$F\ (N) = 0.203 + 0.00908\ H\ OO \qquad Eq.\ 4.1$$

Where F = the force in Newtons and H OO is the Shore hardness (OO)

Hardness characteristics are described by the H OO average hardness and equivalent force measured by the indenter spring in Newton's. As can be seen in figure 4.3, the control specimen group for PDMS A-10 had the lowest initial hardness value after the addition of the softening agent of 10.76 H OO, (exerting an average spring force resistance of 0.3 N); This is because the ratio of PDMS-to-softener was higher for the A-10 than it was for OO-30 (4:3 and 2:1 respectively) making A-10 initially softer. The hardness of both OO-30 and A-10 specimens increased when adding fibres.

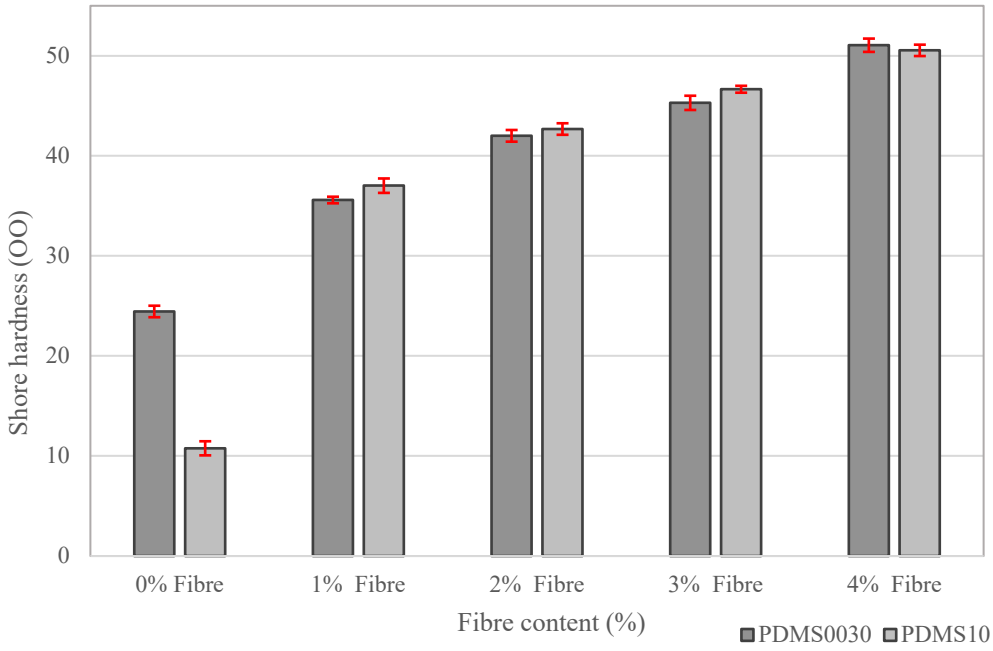

Figure 4.3 Shore hardness values (OO)- indentation by durometer.

The influence of incremental fibre addition for two different PDMS gels (OO-30 and A-10). Each bar indicates a mean Shore hardness value between 0 and 50 H OO. The dark coloured bars show the OO-30 gel with and without fibres, while the lighter coloured bars show A-10 gel with and without fibres. Each bar represents the mean average of five separate specimen tests. Each pair of bars represents the changing amounts of added fibres to a fixed amount of PDMS gel (OO-30 and A-10). Error bars shown, in red, for each group represent the standard deviation.

4.3.1.1 Hardness changes in group A-10 fibre filled membranes

There was a sudden and significant increase in hardness as fibres were introduced to group A10, increasing from approximately 10 H OO to 37 H OO.

Fibre saturation of 2 %, 3 % and 4 % further elevated hardness, albeit more gradually, to 42.68 H OO, 46.66 H OO and 50.54 H OO respectively, with the calculated spring force resistance of 0.59 N, 0.63 N and 0.66 N.

4.3.1.2 Hardness changes in group OO-30 fibre filled membranes

The effect of incremental fibre addition on hardness was somewhat less dramatic in the PDMS OO-30 group. The control specimen for this group had a hardness value of 24.44 H OO. By increasing the fibre saturation from 1 % to 4 %, specimen hardness

increased from 35.58 H OO to 51.06 H OO, and the average spring force resistance increased from 0.53 N to 0.67 N.

4.3.2.1 Linear regression for group A-10 fibre filled membranes

Analysis of the group A-10 specimens, containing only fibres (without the control group, lacking fibres), revealed that the presence of fibres had a proportional influence on the hardness of the PDMS membranes. A strong relationship between fibre content and hardness was found ($R^2 = 0.9908$) when using the equation shown in equation 4.2.

$$y = 4.454x + 33.09 \qquad \textit{Eq. 4.2}$$

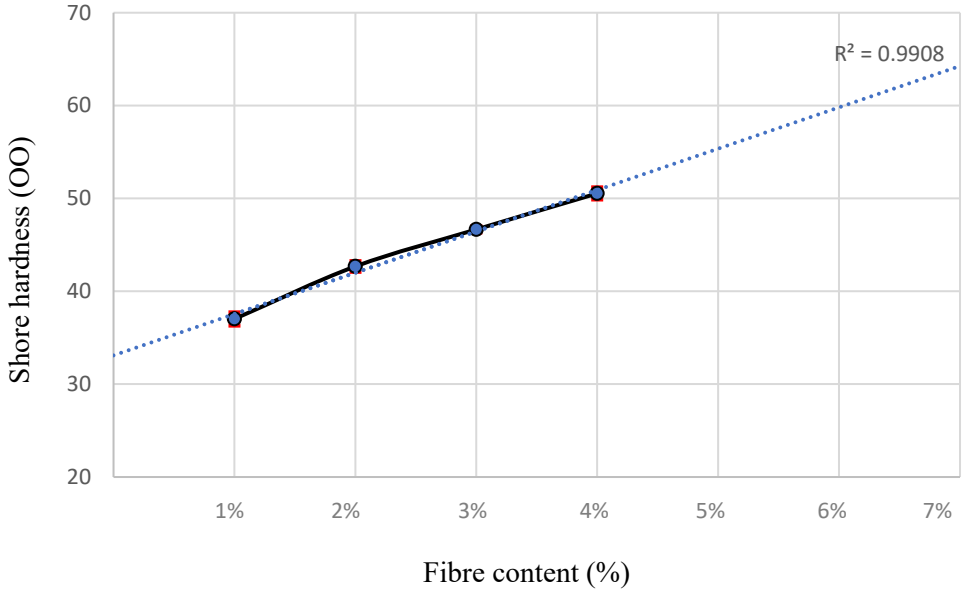

Figure 4.4 Linear regression of Shore hardness values (OO) for group A-10 plotting the influence of increasing loose fibre content. *Each large dot represents a data point based on fibre percentage. The dotted line shows the potential predicted trajectory of hardness based on the data provided by 125 data points. Error bars are shown in red for each group and represent the standard deviation.*

4.3.2.2 Linear regression for group OO-30 fibre filled membranes

A strong relationship between hardness and fibre content was observed in group OO-30, exhibiting a strong positive linear coefficient of $R^2 = 0.9867$. Equation 4.4 was used to calculate the R^2 value.

$$y = 4.974x + 31.05 \qquad \text{Eq. 4.4}$$

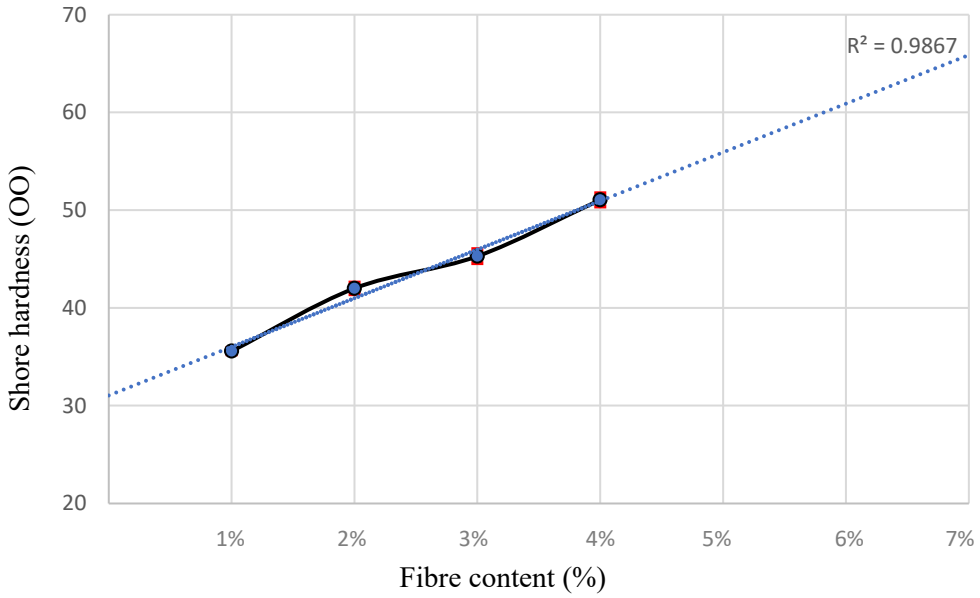

Figure 4.5 Shore hardness values (OO) for group OO-30 - The influence of increasing loose fibre content. *The hardness is displayed in Shore hardness to illustrate increasing hardness. Each large dot represents a data point taken from the mean average of hardness values in each group based on fibre percentage. The dotted line shows the linear regression based on the data provided by 125 individual readings. Error bars are shown in red for each group's standard deviation.*

The linear regression demonstrated a strong correlation with the data plotted as a solid line, but the small variation amongst the specimens made it difficult to see error bars for all groups. For a clearer view of the error bars see figure 4.3.
In the next section, tensile tests results are presented.

4.3.3 Tensile test results PDMS A-10 fibre filled membranes

During uni-axial tensile testing on specimens made with PDMS A10, specimens lacking fibres could be seen to be almost linear in their behaviour, albeit with a slight strain hardening phase between 300 % and 500 %, prior to entering a secondary phase of isotropic extension until failure. When fibres were introduced to the specimen preparation (1 %), an increase in elastic modulus was most noticeable at low strains, while strain hardening was seen at higher strains. At around 200 % strain (for

specimens with added fibres), the internal fibre matrix appeared to absorb the loading stress, (as can be seen in figure 4.6) shown by the sharp yield 'heel' of the curve before entering a long curve, forming a long and exaggerated plastic phase of permanent deformation prior to failure. While this behaviour was recognised in all the specimens with more than 1% fibre saturation, the yield profile became more exaggerated as the fibre content was increased, (as can be seen in figure 4.6) and the membranes became stiffer and more extensible.

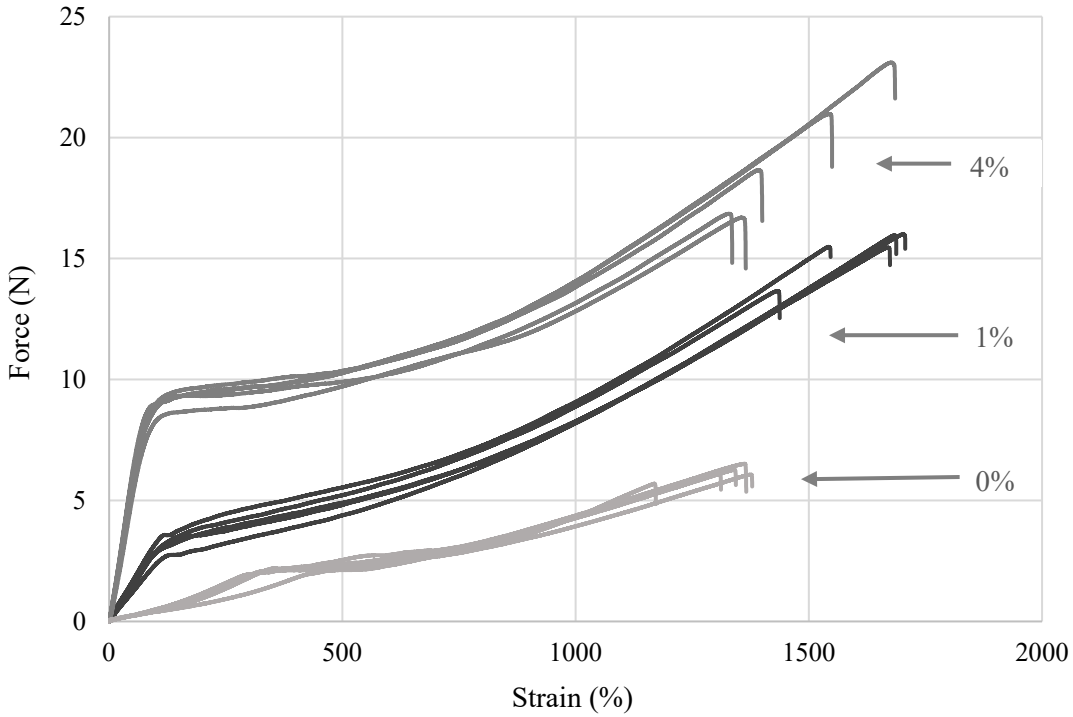

Figure 4.6 Uni-axial force vs strain (%) comparison of fibre percentage in PDMS A10. *Each curve in the graph represents one uni-axial test specimen with either 0 %, 1 % or 4 % added fibres. The three different groups (each group is shown as a different grey scale tone) are shown here together to demonstrate the influence of added fibres on the mechanical characteristics of the PDMS membranes. Groups with 2 % and 3 % added fibres have been excluded in the comparative graph in the interest of clarity, although they were tested and are consistent with the presented data. All results are available to view in the appendices.*

4.3.4 Ultimate tensile strength of fibre filled membranes

The UTS of test specimens was also affected by the presence of fibres. As shown in figure 4.7, the UTS increased as more fibres were added. The most significant rise in the maximum force occurred from 0 % to 1 % fibre saturation (6.14N to 15.31N). A

smaller but significant increase was seen in each subsequent group as the percentage of fibre saturation was increased. Generally, the UTS increased in specimens saturated with an incremental percentage of fibre inclusion from 1 % to 4 %.

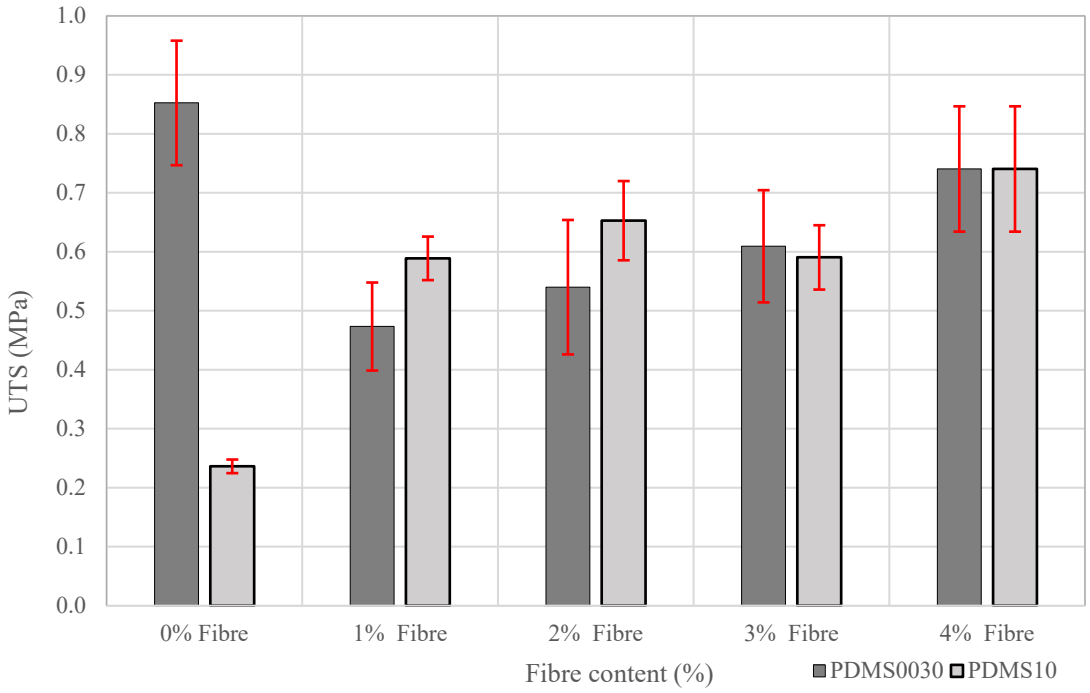

Figure 4.7 Ultimate tensile strength (UTS) – The influence of increasing fibre content. *UTS tests show the effect of fibre addition on mechanical strength. Each bar represents the mean average of five separate specimen tests. The darker bars are the PDMS OO-30 samples, and the lighter bars are the PDMS A-10 samples with 0% - 4% added fibres, indicated by the axis. Error bars are shown in red.*

Polytek development Corp®, specifies a UTS of 1.57 MPa for unmodified Platsil® gel 10. The modified blend used in this study with added softener gave a UTS of 0.236 MPa at 1311 % strain and exhibited an average elastic Young's modulus of 0.029 MPa, which can be seen in figure 4.8. While the Ultimate Tensile Strength and Young's modulus increased by adding more fibres to the compound, the strain percentage reduced from 1521 % at 2 % fibre saturation to 1460 % at 4 % fibre saturation.

4.3.5 Young's modulus of fibre saturated PDMS composites

The test specimens from the A-10 group with 1 % fibre saturation exhibited a mean Young's modulus of 0.11 MPa, whereas the specimen group with 4 % fibres exhibited

a mean Young's modulus of 0.43 MPa, roughly a 0.1 MPa increase in modulus for each percentage of added fibres (Figure 4.8).

A comparison of the changes that occurred in Young's modulus can be seen in figure 4.8. Data shows that the presence of fibres influences changes in elasticity.

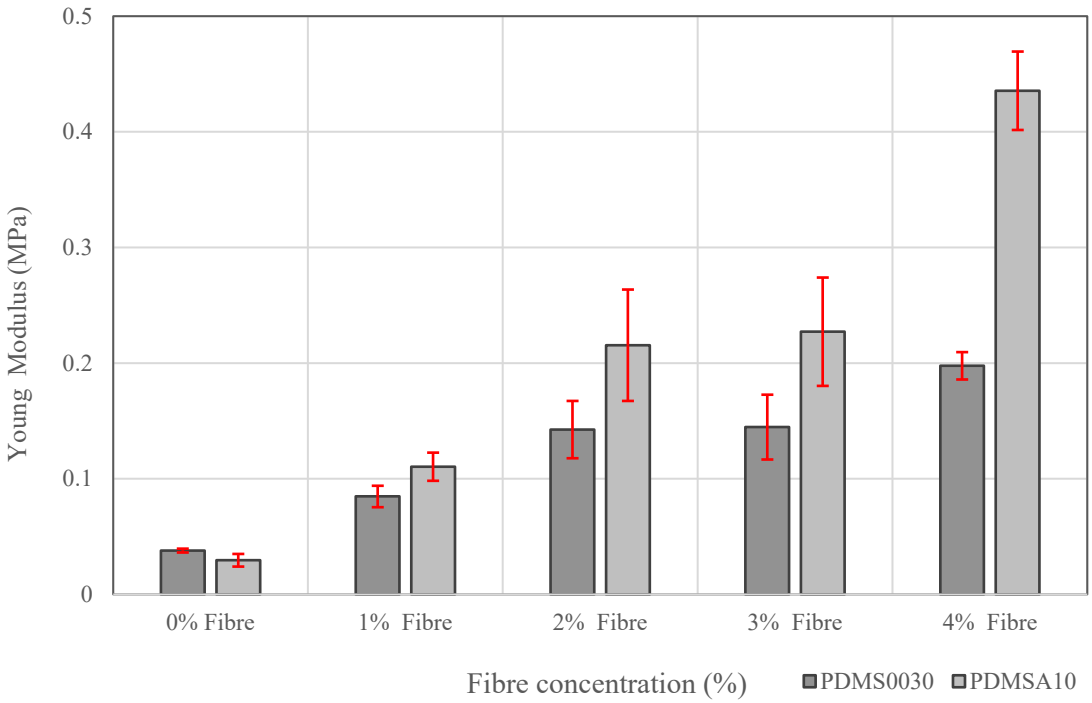

Figure 4.8 Young's modulus comparison of fibre saturated PDMS composites.
Each bar represents the mean average of five separate specimen tests. The darker bars are the PDMS OO-30 samples, and the lighter bars are the PDMS A-10 samples with 0 % - 4 % fibres, indicated by the axis. Error bars are shown in red.

The most noticeable change in modulus occurred in specimens made from PDMS A10 Modulus increased from 0.02 MPa without fibres to 0.11 MPa with just 1 % fibre saturation. The modulus further increased to 0.21 MPa at 2 % saturation but did not appear to increase significantly between 2 % and 3 %. Another significant gain in modulus was observed at 4 % fibre saturation, where the modulus increased again between 3% and 4% from 0.22 MPa to 0.43 MPa. Less significant changes occurred in specimens that contained PDMS OO-30, but the relationship between an increase in fibres and the modulus was still apparent. The relationship between incremental fibre content and Young's modulus was also recorded. A weak linear regression

plotted using the equation 4.5 revealed $R^2 = 0.9102$.

$$y = 0.0341x + 0.0572 \qquad Eq.\ 4.5$$

For specimens containing OO-30 PDMS and incremental fiber addition. A linear regression using equation 4.6 revealed a weaker relationship between specimens containing A10 PDMS and incremental fiber addition, with $R^2 = 0.8764$.

$$y = 0.0987x + 0.0005 \qquad Eq.\ 4.6$$

4.3.6 Tensile test results PDMS OO-30

Increasing fibre content in test specimens caused significant mechanical changes in modulus and extensibility clearly shown in Figure 4.9.

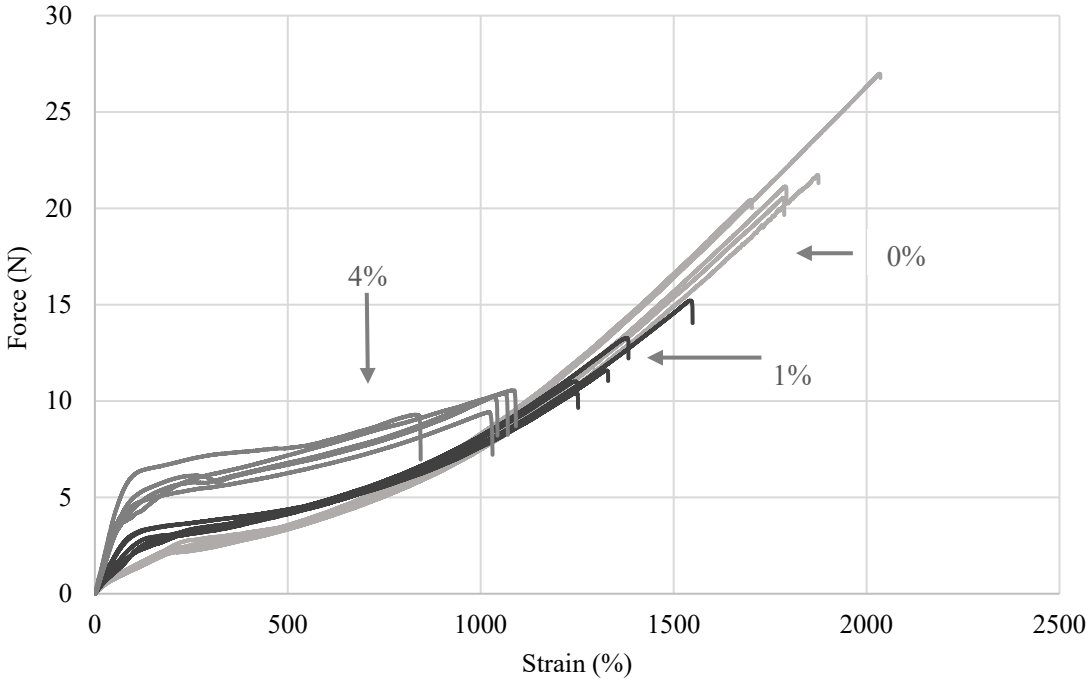

Figure 4.9 Uni-axial force against strain (%) comparison of properties influenced by fibre percentage in PDMS OO-30.

Each vector in the graph represents one uni-axial test specimen with either 0 %, 1 % or 4 % added fibres as labelled. Each tone represents one test group (dark grey, mid grey and light grey). Groups with 2 % and 3 % added fibres have been excluded in the comparative graph in the interest of clarity.

Most notable was the immediate reduction in extensibility by above 1000 % with the presence of just 1 % added fibres at high strains. Further reductions in extensibility continued with each additional percentage of added fibres. The increase in strength and elasticity at low strains at the higher fibre concentrations was also notable.

The manufacturer of PDMS OO-30, *Polytek development Corp*®, specifies a UTS of 0.81 MPa for unmodified *Platsil*® gel OO-30. The modified blend with added softener, but without fibres, used in this study gave a UTS of 0.852 MPa at 1836 % strain and presented an average elastic Young's modulus of 0.037 MPa. The maximum force recorded at the point of rupture was 22.16 N. The introduction of fibres caused an initial, significant drop in the force required to break the specimens at 1 % fibre content, before gradually increasing again with the incremental addition of fibres up to 4 %. The test specimen group with 1 % fibre saturation exhibited an average UTS of 0.473 MPa at 1347 % strain with an average Young's modulus of 0.084 MPa. The required force to rupture the specimens with 1 % fibre was recorded as 12.3 N increasing to 19.25 N with 4 % fibre saturation.

4.3.7 Image analysis of fibre saturated PDMS composites

Visual analysis of the samples showed permanent deformations after testing to failure, in all groups above 1 % fibre saturation, shown in figures 4.10A and 4.10B.

The previously random arrangement of fibres appeared to orient themselves in the direction of the applied force within the PDMS structure when stretched to failure (figure 4.10C). This is consistent with the typical response of skin at high strain rates.[64, 103] When the specimen samples ruptured, fibres were seen to emerge in the direction of applied force on the distal end of the specimen (figure 4.10D).

Interestingly, the increase in elastic modulus also caused an increase in visible, permanent deformation of specimens once the elastic limit was exceeded. As can be seen in figures 4.10A and B, an increase of fibre concentration from 1 % to 2 % caused a dislocation of fibres due to extension prior to failure.

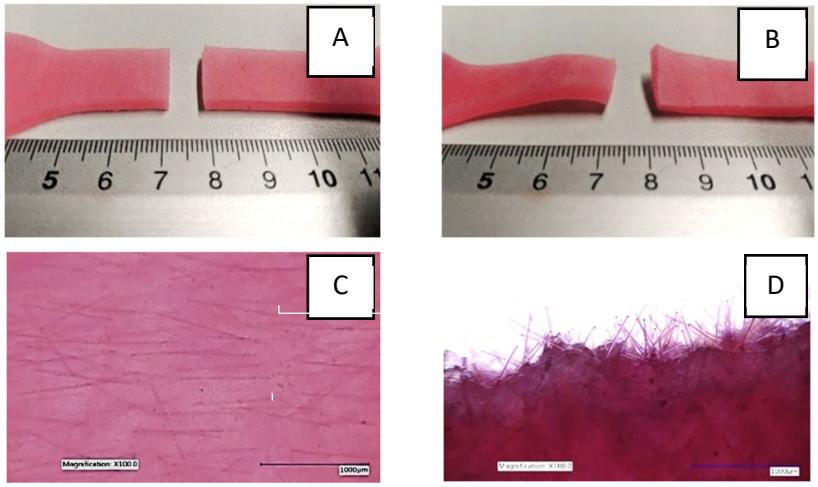

Figure 4.10 Images of the tensile test specimens after failure.

Image 'A' shows a clean break with no visual signs of permanent deformation at 1 % fibre saturation while image 'B' exhibits signs of permanent deformation at 2 % fibre saturation. Image 'C' shows fibres aligned in the direction of load after specimen failure at 3 % fibre addition. Image 'C' shows exposed fibres on the broken edge of PDMS OO-30 with 4 % fibre addition. Images 'C' and 'D' are ×1OO magnification.

4.3.8 Multi-axial test results of fibre saturated PDMS composites

The Multi-axial cyclic test (six cycles) was performed on all of the disc specimens up to 5 N, conforming to the force threshold of 4.4 N to 8.8 N given in the literature, reproducing the force exerted on the living tissue during surgery by the surgeons' hand tools.[104, 349] Force decay was calculated while the sample was held at maximum force (5 N) for 60 seconds at the fifth cycle.

Evaluation of the unrecovered deformation, shown in figure 4.11, revealed little difference between groups with added fibres, even as fibre saturation was increased from 1 % to 4 %. The largest deformation was seen in specimens without added fibres with the highest unrecovered deformation (3.32 mm) being observed in group A-10 with 0 % fibre saturation. As can be seen in figure 4.12, force decay rose gradually as more fibres were added to both PDMS groups, with the exception of PDMS A-10 at 4 % fibre saturation, which exhibited a small drop.

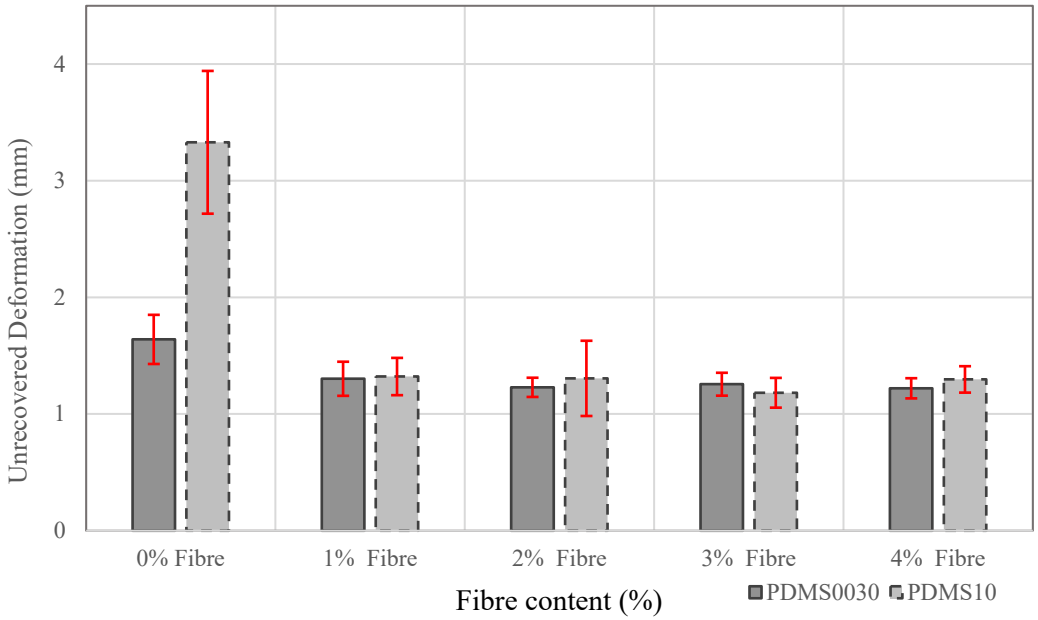

Figure 4.11 Unrecovered deformation of fibre saturated PDMS composites.

The arithmetic mean for each specimen sample group observed in all specimens after 60 seconds at 5 N. The darker bars show the PDMS OO-30 samples, and the lighter bars show the PDMS A-10 samples with 0 % - 4 % fibres, indicated by the axis. Error bars representing the standard deviation amongst specimens are shown in red.

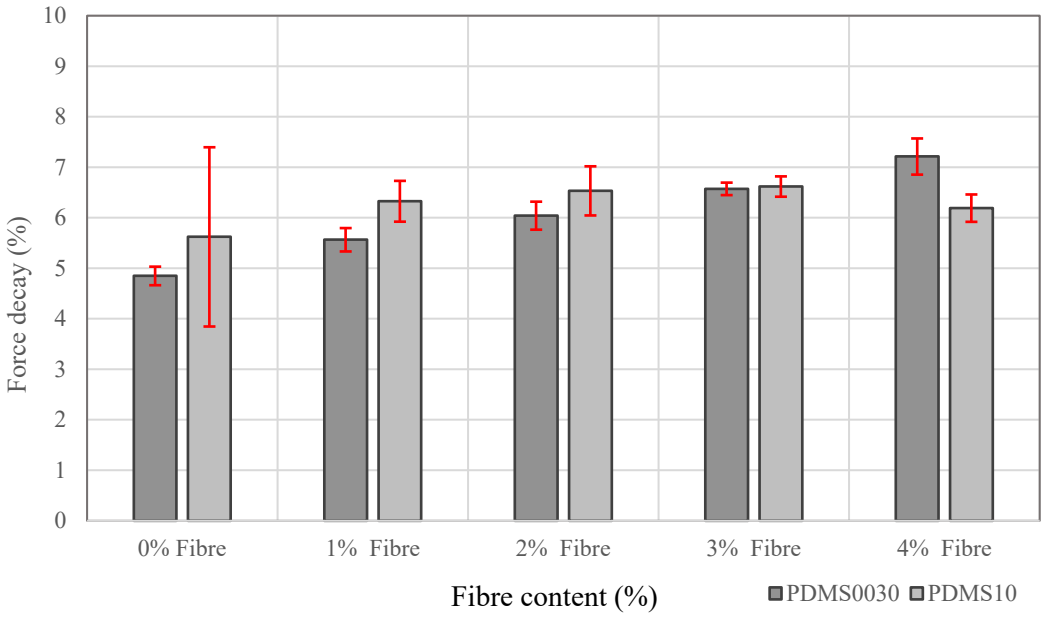

Figure 4.12 Force decay comparison of fibre saturated PDMS composites.

The arithmetic mean for each specimen sample group measured after 60 seconds on the 5th loading cycle are shown. The darker bars show the PDMS OO-30 samples, and the lighter bars show the PDMS A-10 samples with 0 % - 4 % fibres, indicated by the axis. Error bars representing the standard deviation amongst specimens are shown in red.

more significant change was observed in PDMS OO-30 specimens during the incremental addition of fibres, continuing the increasing trend of around +0.5 % force decay/energy loss for each additional percent of fibres added.

4.4 Discussion

Mechanical characterisation of the test specimens conducted using standards created for the testing of elastomers and elasticated fabrics were used to help verify the influence of fibre content on PDMS membranes. The principle focus of this work was to quantify the precise mechanical impact of incremental amounts of loose, short strand fibre dispersal in ten groups of test specimens using two different PDMS composites. Data was gathered and analysed to measure the change in mechanical response to deformation. The test standards used to characterise material responses were chosen primarily to improve interdisciplinary comprehension, repeatability and dissemination amongst peers.

The following discussion is broken into three sections related to the nature of each test method; indentation, uni-axial extension and multi axial compression.

4.4.1 Hardness characteristics of fibre saturated PDMS composites

Since indentation is the only standardised test method suitable for live subjects, due to its non-destructive nature, it enables comparative analysis of results between living skin and fibre saturated PDMS. Reported hardness values for living human skin (and animal blood vessels) gathered using a durometer have been given as 20 H OO to 58 H OO. [17, 94, 337, 334] The values achieved with the addition of fibres is capable of covering most of the reported values without altering the stoichiometric ratio of the PDMS gel.[17, 94, 337, 334] The predictive hardness graphs for given group A-10 (R^2 = 0.9908) and group OO-30 (R^2 = 0.9867), can be used reliably to predict hardness gains, using only fibres without other additives. With the addition of 6 % fibres a hardness of around 60 H OO should be achievable for both base PDMS gels. However, when increasing fibre saturation values above 5 %, the PDMS/fibre composite begins to exhibit considerable thixotropic behaviour making the PDMS composite too viscous to pour or control layer thicknesses reliably. With such a viscous medium, it would be difficult to avoid air entrapment (such as bubbles and empty voids) during use, especially whilst degassing or applying material into moulds.

In this study, it has been shown that the presence of loose fibres increased the hardness value proportional to the fibre percentage added in both PDMS blends. For every additional percentage of fibres added, hardness increased by 5 degrees of hardness (± 1 H OO), showing that the stiffness of PDMS can be altered using the addition of fibres as opposed to adding or altering the chemical composition. This is important because varying the chemistry of the PDMS can have additional, undesirable repercussions such as unpredictable curing time and changes in the mechanical properties of the composite.[103]

4.4.2 Uni-axial characteristics of fibre saturated PDMS composites

It has been shown that the modulus of soft membranes like human skin, is highly variable and is dependent on many factors such as age, sample site, orientation of Langer lines, hydration, temperature, test conditions and equipment. For this reason, considerable literature produced over the past six decades have reported very different uni-axial test results for elastic modulus comparison (discussed in Chapter 2)

The elastic modulus of specimens in all of the groups tested during this study was in good agreement with the literature and was found to be within the lower range of modulus threshold values ranging from 0.0296 MPa to 0.435 MPa (± 0.033 MPa) where the literature discloses a slightly wider range of 0.014 MPa to 0.6 MPa.[16, 349, 350]

The stiffest membrane containing 4 % fibre saturation gave a maximum stress of 0.74 MPa for PDMS A-10 and 0.197 MPa for PDMS OO-30, which was within the Young's modulus threshold given in the literature (0.0045 MPa to 221.9 MPa).[45] Whereas this threshold value, was more widely regarded in the literature to be within 2.5MPa - 30MPa.[173-177] This may be due to the hyper-elastic nature of soft PDMS gels, but can also be attributed to the lack of internal structures found in nature and random arrangement of loose fibres embedded in the PDMS specimens. These results are in agreement with test results of tear strength of identical PDMS blends that had been bonded together prior to testing as part of a forensic reconstruction of cranial ballistic injury patterns at 2 % fibre saturation.[346] Although both membranes were tested together and not independently as in this study, the hardness was, again in good agreement with the literature, but the extensibility was found to be too high when compared to data given in the literature.

Additionally, during the tensile test, the fibre orientation changes to align with the force axis. Above 1 % fibre saturation, the elastomeric content of the specimens is no longer high enough to deter permanent deformations. At higher concentrations of 2 % fibres and above the fibres slide out of their surrounding matrix while aligning themselves in the direction of applied force, bending the fibre outside of its initial position upon relaxation, meaning that they are unable to return to their original position, permanently distorting the surrounding gel matrix.
The force required to permanently deform specimens was highest in groups with higher fibre saturation, but all specimens that contained fibres behaved uncharacteristically for isotropic elastomers.
The change in fibre organisation can be attributed to the short linear phase of the graph below 100 % extension, where the fibres are being rearranged and aligned in the direction of applied force, but not yet absorbing load, allowing the PDMS to exhibit a typically Hookean elastic, linear slope with a shorter and steeper trajectory than the following, much longer strain-hardening phase. (Figure 4.9)

Ultimately the presence of fibres affects the results of all uni-axial tests by introducing short-term strength to the elastic phase. As presented in this study, the viscoelastic anisotropic behaviour of the PDMS specimens with <1 % fibre saturation had no permanent deformation as the fibre concentration was low enough not to affect the viscoelastic profile. In contrast, specimens with more than 2 % fibre saturation had variable stress versus strain relationship, which is strongly related to fibre saturation. Overall, the modulus was able to be increased by 0.1 MPa per 1 % percentage of fibres added.

The tensile characteristics of living skin may be mimicked more accurately by altering the extensibility and architecture of embedded fibre/fabric components to reproduce the progressive alignment of fibres in the direction of applied force and the straightening of the coiled collagen and elastin fibres in the skin during extension.[41]

4.4.3 Multi-axial characteristics of fibre saturated PDMS composites

Three-dimensional forces exerted by surgeons' tools during surgery is quite high (4.4 N – 8.8 N)[104] while a quantitative study of the forces exerted by the surgeons gloved

hand when manipulating live organs is much lower.[349] Therefore, the cyclic specimens tested during Multi-axial compression were subject to a maximum of 5 N force during cyclic tests and the relaxation of the specimens was measured. In PDMS A-10 blend, which included a softening agent (Smiths Theatrical Prosthetic Deadener), as previously characterised in the literature,[16] it was found that the addition of fibres helped to stabilise the specimen's physical behaviour and reduced permanent deformation at low strain percentages. Unrecovered deformation decreased with the increment of additional fibres in both groups between 0 % and 1 % while the most significant drop was recorded for PDMS A-10 in this region. It was clear that by increasing the fibre concentration above 1 % the unrecoverable deformation was unaffected.

By increasing the fibre saturation, the force decay percentage gradually increased in both groups, with a slight decrease at 4% for PDMS A10.

The presence of fibres was found to correlate with the strength of the composite membrane structure. Added strength appears to be caused by the presence of fibres as they take up a portion of the load during alignment with the direction of loading forces, especially at higher strain-rates and during cyclic tests, while increasing the fibre saturation gradually increased the force decay but not the permanent deformation.

4.5 Summary

This study presents a non-clinical look at the design, fabrication and validation of potential prosthetic soft tissue surrogates, whose mechanical behaviour can be tuned to meet similar characteristics to those observed in soft membranes like human skin. Prior to this investigation, the precise influence of fibre addition on PDMS gel properties was unknown in the literature.

Importantly, this work has shown, for the first time, how fibre presence affects the behaviour of PDMS gels used in clinical and theatrical prosthesis. It was observed that by varying the concentration of fibres, one can manipulate key mechanical characteristics that would be very useful in everyday practice.

Fibre concentration has a profound and variable effect on the hardness, strength, viscoelasticity, and recovery of human skin.[41, 61, 62 161] Just as fibres play a role in the fundamental behaviour of human skin, synthetic fibres have been shown to have a

direct impact on the mechanical properties of elastomeric membranes.[160, 161, 162]

Unique to this study, it has been shown how fibre fillers can be used, with some degree of accuracy, to control specific mechanical properties like hardness, modulus, and permanent deformation in PDMS membranes. A strong linear coefficient was discovered, albeit, with only four data points, that suggests hardness in fibre filled PDMS membranes may be predictable. In contrast, increasing fibre content had almost no effect on the permanent deformation of specimens in cyclic Multi-axial tests, suggesting that some mechanical properties can be altered independently.

Typical of filled PDMS elastomers, all of the specimens exhibited exaggerated plastic deformation, but the effect was much more noticeable in specimen groups with added fibres. Additionally, relaxation occurred more slowly in specimens with higher fibre saturations, showing that increasing the fibre content slowed the atomic dislocation of PDMS crystalline structures, probably due to the reorienting fibres absorbing the stress during the loading process. Reverse hysteresis phenomena was attributed to the loss of energy caused by the dislocation of fibres within the PDMS structure, because energy loss was reduced when the fibre saturation was increased. Finally, viscoelastic creep was seen in all of the specimens during Multi-axial deformation and was most significant in specimens with less added fibres. It was presumed that this was because the crystalline structure was reinforced by the presence of the fibres. More work needs to be done to expand on these findings.

The fibre length, orientation and architecture offer an alternative method for controlling the exaggerated extensibility seen in the current results. Use of more organised embedded fabric structures may offer an additional opportunity to manipulate the mechanical performance of PDMS elastomeric membranes in addition to loose, short-strand fibres used to control hardness: This will be explored further in Chapter 5.

To accommodate higher percentages of fibres, a much lower native viscosity PDMS could be used to aid mixing and dispensing. PDMS oil has previously been shown to reduce PDMS viscosity, albeit at the expense of many other mechanical properties, including reducing the hardness, tear-resistance, and tensile strength.[16, 349] This will be discussed further in Chapter 6.

To conclude, it has been shown that embedded, loose, short-strand fibres have a

measurable effect on the mechanical properties of PDMS composites and that they are able to be used to vary the mechanical properties of PDMS membranes to reflect the hardness of living human skin. However, the extensibility of fibre filled PDMS membranes remains too great and does not reflect the extensibility of human skin. To address this, in the next chapter, the investigation will focus on the impact of interconnected/continuous, longer fibres, like yarns or elastic textiles that can be embedded in PDMS liquid elastomeric composites.

Chapter 5

Mechanical behaviour of multi-layered, reinforced silicone membranes for clinical and theatrical prosthesis

5.1 Introduction

Where the previous chapter focused on characterisation of the two separate, fibre filled, PDMS gel membranes, this chapter focuses on characterisation of a multi-layered membrane made up of the two previous membranes with the addition of a third layer of embedded textiles. In particular, uni-directional elasticated yarns and knitted fabric. The directionally biased textile elements are also tested at different tensions and orientations that were inspired by tests conducted on fibrous soft tissue membranes, like skin, found in the literature.[16, 50, 172, 351, 352, 353] Firstly, two different, previously characterised PDMS composites with known mechanical behaviours, are prepared. The base PDMS layer will be a softened Shore OO-30 with 1% (short-strand, loose) fibre saturation, the upper layer will be a softened Shore A-10 with 4% fibre saturation, as per the previous chapter (4). Such a multi-layered composition offers a softer, more extensible lower layer and a harder, less extensible upper layer. Secondly, the multi-layer lamination method allows for a precise placement of the fibre architecture (yarn or fabric) to be embedded between the two layers. Only the fibre architecture, orientation and tension will change during this investigation. The PDMS membrane composition remains constant. The resulting reinforced, multi-layer, composite membranes are then mechanically characterised using the same standards as discussed in the previous chapters (3 and 4).

The aim of this chapter is to understand the mechanical influence of embedded yarns and fabrics within a known multi-layered PDMS composite membrane. More specifically, how fibre architecture, orientation, and tension, can be used to influence and control the mechanical behaviour of multi-layered PDMS membranes. PDMS membrane behaviour will be compared to some of the known mechanical traits of soft tissue membranes such as skin.

This chapter begins with a brief overview of key literary sources that focus on mechanical characteristics of natural and synthetic, fibre reinforced soft membranes.

5.1.1 Rationale

To measure the effect of tension on the yarn and fabric, specimen groups are created while held under varying amounts of controlled tension, referred to henceforth as ‘pretensioning’. The amount of pretension exerted on yarns and fabrics during the embedding process was informed, firstly, by the extensibility of the elastane yarn and

secondly, by the extensibility of skin. Preliminary tests on the yarn revealed its changing appearance under strain, using a digital microscope, specified in Chapter 3 (at x200 magnification). As the yarn was stretched the nylon wrapper was almost completely straight at 100% pretension, (twice its original length). This is shown in more detail, later in figure 5.2. Secondly, the extensibility of skin, was found to be 50%,[30] while others found it to be 100%.[31, 32, 174, 189, 190] Changes in the pretensioning of the embedded yarn and fabric offered a measurable control over the variable extensibility of each membrane without changing the technical textile specifications under investigation. Elastane was chosen because it represents a fine gauge textile that can be stretched to measure the influence of orientation as well as stretch (pretension) simultaneously. There are many possible candidates for this purpose, but elastane was preferred because it has previously been used to limit the extensibility of fibre-filled, multi-layered PDMS membranes in forensic studies and surgical training models to limit extensibility of PDMS gels.[104, 214] Use of known PDMS membrane characteristics (in Chapter 4) are expanded in this chapter, while the use of test standards, detailed in Chapter 3, help mitigate any disparity of results and conveys the transferability of the applied methods. Knitted, nylon-based elastane (*Lycra)* also easily conforms to three-dimensional shapes and is readily available in most countries as stockings and tights. Finally, most relevant to the current investigation, Rothman[30] and colleagues found the extensibility of juvenile skin to be 50%, while others found it to be 100% in a wider age range.[31, 32, 174, 189, 190] So, for this study, a pretensioned extension on the PDMS membranes with embedded knitted elasticated fabric was tested at 0%, 50% and 100%. In this way, a tuneable membrane can be created with repeatable, predictable mechanical properties, enabling prosthetic fabricators to mimic different membrane characteristics to meet a variety of industry needs as discussed in Chapter 1.

5.2 Methods and material

A summary of the test standards and equipment used in this investigation are discussed in detail in Chapter 3. Variations specific to this chapter are described below.

5.2.1 Methods

In total this chapter includes results of 175 uni-axial tests, 70 Multi-axial tests, 325

indentation tests and 350 microscopic images of specimens before and after testing where changes or destruction of specimens were observed (uni-axial tests). Tests were categorised into 16 specimen groups based on changes in the preparation method involved for each group. Each group contained a minimum of five specimens and two spares in case of defects or equipment malfunction. The methods, standards and materials used in this investigation are identical to those used in the previous Chapter (4) and are discussed at length in Chapter 3. In this chapter, the standards applied to testing are particularly relevant because indentation by durometer testing is a measure of hardness in elastomers and soft tissue, uni-axial tests were developed for testing the modulus, UTS and extensibility of rubbers, and the Multi-axial tests were designed for testing force/time dependence in elasticated fabrics. These tests give mechanical data on the ultimate tensile strength, Young's modulus, force decay, force relaxation, and shore hardness. Additional data on the force at failure, maximum extension and yield characteristics are also discussed.

5.2.2 Hardness tests

Indentation by durometer was used to measure the hardness of 13 specimen groups. The first three of the 16 groups were textiles, so cannot be measured with the hardness test. Measurements were obtained from five specimens per group. Each specimen was measured in five separate places as per the standard and the mean for each group was calculated and presented in the results for comparison. Shore hardness test data was gathered from the unused, excess material, after tensile test dumbbells and Multi-axial discs were cut from the specimen sheet. Ample excess material was available for hardness testing due to the shape of mechanical test specimens and specimen arrangement (described in more detail in 5.3.7).

5.2.3 Tensile tests

Each of the 13 groups that contained embedded textiles were prepared as per the standards described in Chapter 3. A total of 16 groups are prepared and tested. Groups one, two and three lacked any PDMS. Group one was a single yarn and group two consisted of 6 strands on a weft, so these two groups were not cut into a standard dumbbell shape as the remaining 14 groups were. To maintain consistency in tensile tests, the neck of the dumbbell (or *dog bone*)- shaped die (type A) was measured

against the width of the weft and the distance between yarns determined. Six yarns, including the intervals between the yarns, equalled the width of the dumbbell die, so a weft that held exactly 6 parallel yarns was selected for group 2 testing. In group 3, dumbbells could be cut directly from the knitted fabric for tensile testing. The remaining 13 groups all containing PDMS, were all cut with the same die prior to testing. The sheet preparation temperature was 21 degrees C +/-2 degrees and humidity were between 40-60%. Prepared test sheets were stored for at least 2 weeks after crosslinking at the preparation temperature and humidity prior to testing.

5.2.4 Multi-axial tests

A steel template measuring 145mm in diameter was used to cut each of the 70 discs for testing from each sheet of material using a surgical scalpel and cutting mat. Each specimen was cut with at least 2mm gap between. All specimens and were stored alongside the tensile test specimens described in 5.2.3.

5.3 Specimen preparation

In this section, all materials and methods involved in production of the PDMS membranes are described.

5.3.1 PDMS composites membranes selected for layering

Two suitable base elastomers were selected for this study. Both were identical to the membranes characterised in Chapter 4 and were similar to those used in a forensic study of soft tissues.[104] In this study, one layer of PDMS featured a composition ratio of 1A:1B:1S with 1% (red) loose short-strand fibres. A second layer of PDMS featured ratio of 2A:2B:3S with 4% (beige). (Figures 4.1 and 5.1)

These percentages were chosen because they have both been previously tested and were shown to exhibit properties analogous to human skin as previously described in Chapter 4. For this study, to mimic the subcutaneous layer, a 1% (by weight) fibre content was added to a soft, Shore 00-30 PDMS composite that was 2mm thick. For the stiffer epidermal layer, 4% fibre content was added to a harder Shore A10 PDMS composite membrane, which was <1mm thick.[196]

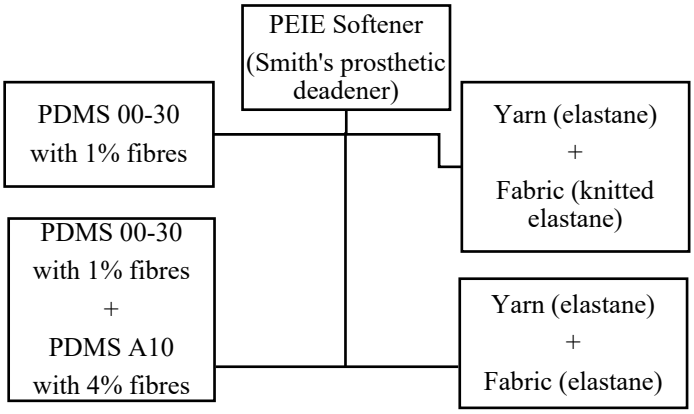

Figure 5.1 Schematic of PDMS composite specimens ingredients.

Simplified flow chart showing each component tested and its relationship to other components. While PDMS A10 is used as a substitute epidermis, the OO-30 is used as a substitute subcutaneous layer. These were independently characterised in Chapter 4.

5.3.2 Elastane yarn

Single cover 16/SC ('S' twist direction, single cover)/090 Cr:22/1/60 (elastane size)/60 (twists per meter) n66 (Nylon type) was used to prepare all textile specimens. (Fig 5. 2)

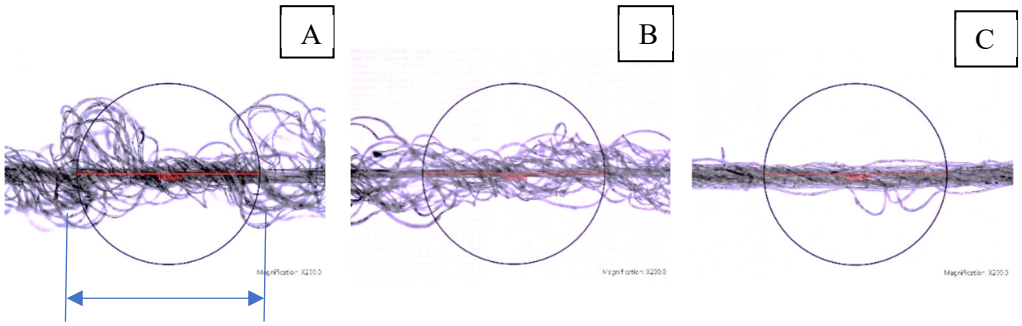

Figure 5.2 The effect of tension on the profile of elastane yarn.

A single lycra yarn is shown here at three stages of extension. 'A' shows the yarn in its relaxed state at 0% extension (25mm) and how the nylon wrapping fibres are loosely twisted around the central PU core. 'B' shows the yarn at 50% extension as the fibre cover starts to align and the core yarn becomes most visible. Image 'C' shows the yarn at 100% extension where the cover fibres mostly lay flat against the surface of the core yarn. The black circle featured in all the images represents 1mm diameter. All images were taken at x200 magnification.

First, single elasticated yarns were tested under uni-axial extension to identify individual strand behaviour. Then an array of single yarns was produced on knitted float (or weft) with a uni-directional, parallel yarn arrangement, which will be discussed in 5.4. Each yarn was set at 1mm increments along the float. The length of each yarn was

500mm long and was linked to a second identical float at its proximal end. Both single and multiple yarns were tested in uni-axial extension only.

5.3.3 Knitted elastane fabric

The knitted jersey elastic fabric was created specifically for this experiment using a flatbed knitting machine (Stoll CMS ADF-3, H. Stoll, GmbH & Co KG. Stollweg 1, d-72760 Reutlingen, Germany). The yarn used for the fabric were identical to the yarn shown in 5.3.2. Knitting was performed using 18-gauge needles in a single jersey, half gauge pattern. (Fig 5.3)

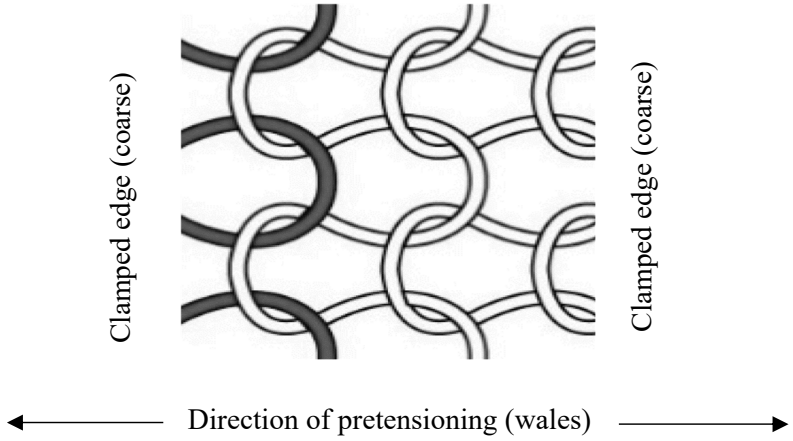

Figure 5.3 Diagram of the knit structure used in all test specimens with embedded fabric content. *The single jersey knit offered good extensibility and permeability. Slack was removed from the fabric as it was clamped along the coarse direction. All specimens were stretched in the wales direction only.* [*Adapted from*; *Jansen, K. M. (2020). Performance evaluation of knitted and stitched textile strain sensors. Sensors, 20(24), 7236.]*

Each piece of knitted fabric measured 800mm in length (wales) and 600mm in width (course) enough to comfortably cover the 500mm^2 gauge mould and leave room for the clamping plates which measured 600mm long and 100mm wide. To reliably determine the mechanical influence of the multi-layered composite membrane it was important to isolate the fabric to one layer. So, the fabric was embedded in the softer, less viscous OO-30 gel composite. To delineate each materials' mechanical behaviour, the fabric was tested independently first using the test regime as specified in Chapter 3 (excluding hardness).

5.3.4 Embedding the textiles in PDMS gel composite

Yarns and fabrics were held at three different pretensions during the embedding process. (Fig 5.4) Both textile types were embedded in the PDMS OO-30 composite (previously characterised in Chapter 4). The prescribed method of production for all specimens is described below in 5.3.5 and visualised in Figures 5.5 to 5.9 below.

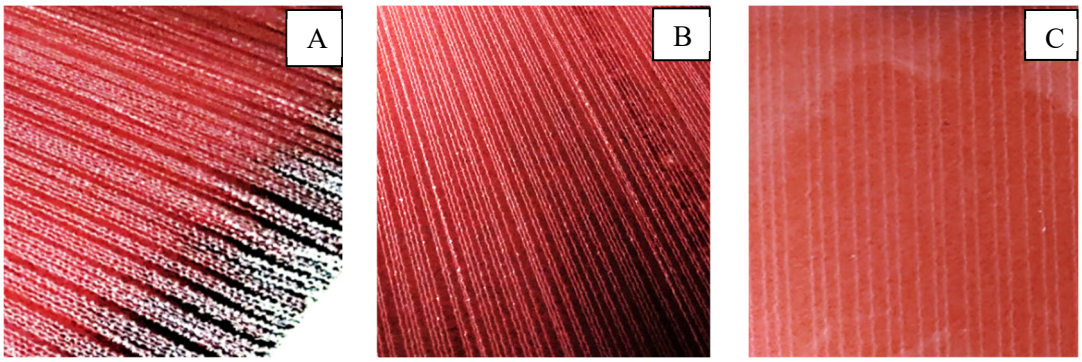

Figure 5.4 Alignment and tensioning of the uni-directional yarns on the weft. *Images 'A', 'B' and 'C' were taken using a digital camera during fabrication of membranes with varying applied tensions. Image 'A' shows the uni-directional yarns held in their relaxed state (0% pretension) during the embedding process in the gauge mould. Note the crimped appearance of the parallel yarns are most visible at the edge of the specimen adjacent to the weft (included in the bottom right of image 'A'). Image 'B' shows the membrane during fabrication while held at 50% pretension. Note how the yarns began to straighten and spacing becomes more uniform. Images 'C' shows the membrane at 100% pretension, just after curing. Note how the yarns appear finer with more regular spacings and are straighter than the previous membrane specimens. The rule is provided in image 'C' to illustrate scale of the yarn spacing.*

5.3.5 Membrane production method

This same method of production was used to make all membranes, that contained PDMS gel, are described in figures 5.5 – 5.9.

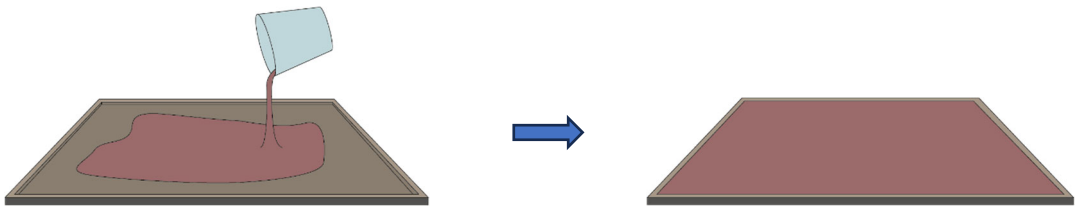

Figure 5.5 Pouring the OO-30 PDMS composite into the gauge mould.
To make all specimens (single and multi-layered), the gauge mould was filled with OO-30 PDMS composite and allowed to settle flat. The same amount was mixed and poured for each specimen to ensure consistent thickness in each group.

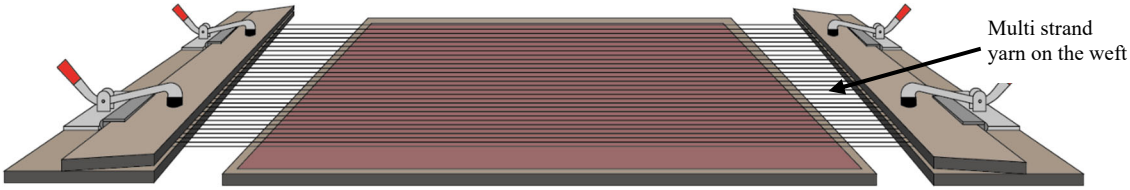

Figure 5.6 Embedding the uni-directional yarns on the weft using clamping jaws.

For membranes with uni-directional yarns, the yarn weft was clamped at either end then tensioned to the appropriate amount before being laid on top of the liquid OO-30 PDMS composite. The composite soaked into the yarns, fixing them in their pretensioned state as the PDMS cured. Clamps were held in position by screwing them to the worktop.

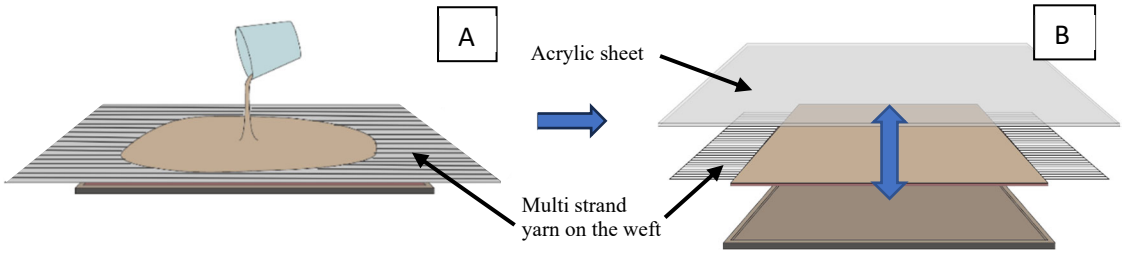

Figure 5.7 Multi-layering of the uni-directional yarns on the weft.

For multi-layered membranes with uni-directional yarns; The clamps were removed with the yarns fixed in place by the cured PDMS. The upper layer of PDMS A10 composite was poured onto the fixed yarns (shown in image 'A') and allowed to self-level and vent any trapped air caused by pouring. Once levelled, a sheet of transparent, rigid polymethylmethacrylate (acrylic) plastic (shown top in image 'B'), was placed on top and pressed into place by hand to maintain an even surface topology. An exploded view of this process in shown in image 'B'. This step was necessary because the material had a higher viscosity due to initial viscosity and high fibre content. Thickness was managed by use of a consistent weight of material for each batch.

Figure 5.8 Embedding the fabric in PDMS using the clamping jaws.

For membranes with embedded fabric, either end of the fabric was clamped then tensioned to the appropriate amount before being laid on top of the liquid OO-30 PDMS composite. The composite soaked into the fabric, fixing it in the pretensioned state as the PDMS cured. The clamps were held in position by screwing them to the worktop.

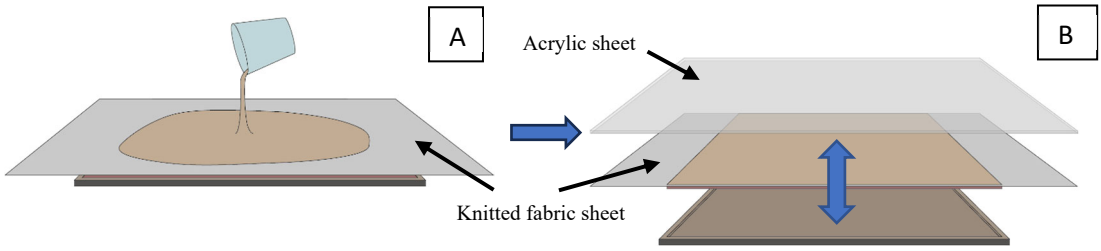

Figure 5.9 Multi-layered membranes containing fabric.

To add the second layer of PDMS, the clamps were removed with the fabric fixed in place by the OO-30 PDMS composite. Shown in image 'A', the upper layer of PDMS A10 composite was added and allowed to self-level and vent any trapped air caused by pouring. Once levelled, a sheet of rigid acrylic plastic sheet, or polymethylmethacrylate (PMMA) was placed on top and pressed into place by hand to maintain an even surface topology. An exploded view of this process in shown in image 'B'.

5.3.6 Pretensioning of embedded textiles

All specimens containing textile elements were subject to pretensioning. The uni-directional yarns and knitted fabric were pretensioned using a pair of clamping, flat jaws, fitted with lever clasps to secure the textiles at a fixed distance. The distances were marked squarely on the test bench and fixed in place via four pre-drilled holes used to secure the clamps and attached textile elements in the precise location until the PDMS composite was fully cured. The amount of pretension was determined as a percentage of 500mm (being the yarn and fabrics original length). The final distances for each group were 0% (500mm), 50% (750mm) and 100% (1000mm) of original yarn/fabric test length (500mm). Distances were selected for two reasons. Firstly, the same distances were used in similar, previous studies on human skin. [31, 32, 174, 189, 190]

Secondly, these percentages were chosen because, at 0% the wrapper strands of the elastane yarn were relaxed and loosely coiled around the core yarn and without tension, while at 100% the wrapping was laid flat against the core yarn (shown in fig. 5.2)

In the interest of gathering comparative data, the fabric was clamped along the course direction in a relaxed but flattened state, then stretched in the wales direction for all six specimen groups containing the fabric (as previously shown in figure 5.3).

In total, 13 PDMS composite membranes were created for this investigation. Six test

membranes with single-layered of OO-30 PDMS gel (2.0+/-0.5mm thick), and seven test membranes with multi-layered OO-30/A10 PDMS gels (3.0+/-0.5mm thick).
Each of the three sheets in both groups were prepared with the yarn and fabric held at different pretensions, relaxed (0%), 50% and 100% relative to their original length. A further three sheets were prepared with embedded yarn and three sheets were prepared with embedded fabric. Both groups were prepared using the multi-layered PDMS composite (00-30/ A10). Each group was also prepared with the yarn and fabric held at three different pretensions (relaxed, 50% and 100%).
One final sheet was prepared with the multi-layered composition, without fabric, to serve as a baseline specimen to measure the influence of yarn and fabric addition. One sheet, measuring 500mm × 500mm was created for each group. (Sheet membranes and final uni-axial specimens are shown in figure 5.10A and 5.10B)

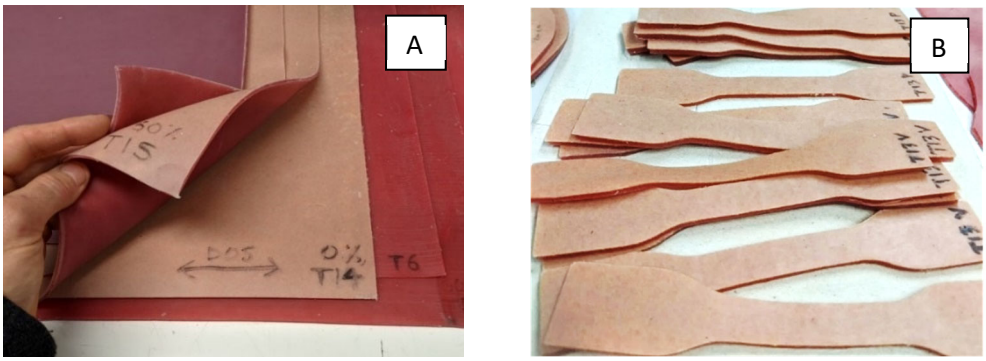

Figure 5.10 Group sheets preparation for mechanical testing.

Image 'A' shows the variety of the finished single and multi-layered membrane sheets prepared and ready for die-cutting into dumbbells and discs for mechanical testing. Notice the direction of stretch (pretension) was marked on each sheet to mitigate risk of mixing up the specimen yarn orientation relative the test direction.

Image 'B' shows some dumbbell shaped, multi-layered test specimens cut and ready for tensile testing. Each specimen was marked with yarn orientation prior to cutting to avoid mislabelling and a black dot was added to the centre of each specimen prior to loading on the tensile tester to ensure that the specimens were mounted centrally in the clamping jaws.

After 48 hours cure-time, the wales direction (of the pretensioning) was marked on each sheet with a permanent black marker and all sheets were dusted with talc to remove surface static, friction, and tackiness and to prevent debris (that might cause

damage) from sticking to the surface during handling and storage. All specimens for mechanical testing were cut from the same sheet, specific to each group.

5.3.7 Orientation of specimens

Specimens were cut using the standard approved (type A) die in 3 different directions; 0°, 45° and 90°, informed by the literature.[50, 172] To mitigate the risk of variation all specimens were harvested from a single continuous membrane. The longest side of the tensile test cutting die was aligned with the required test direction. At least six specimens were cut with the die positioned in three alignments, shown in figure 5.11.

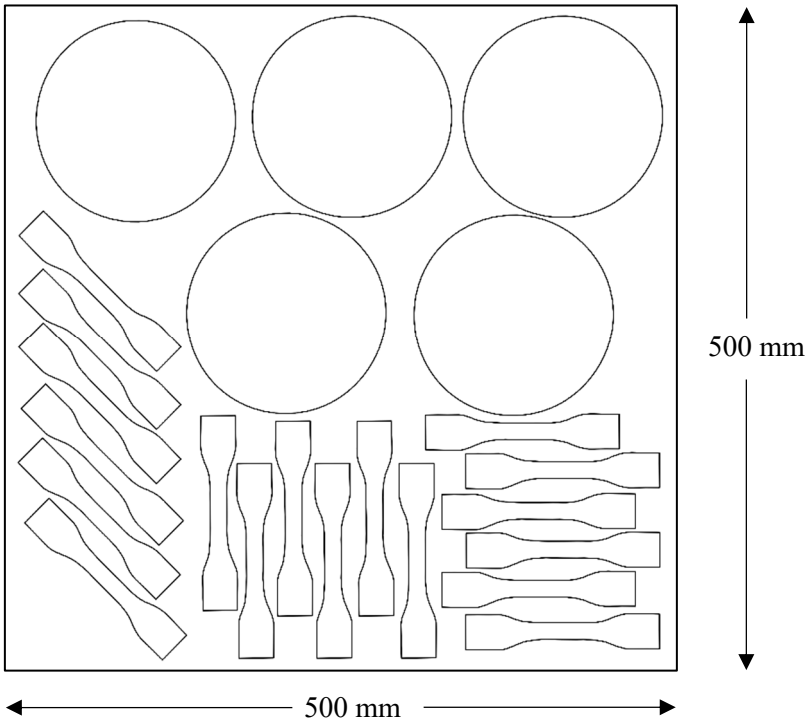

Figure 5.11 Cutting pattern for specimen preparation

All specimens were cut from a single sheet of 500mm x 500mm. Only the orientation of the die stamp was changed to assess influence of yarn and fabric orientation.

Each group designation was assigned a letter (V, P or D) according to the direction of stretch from which the die was oriented and the specimen cut. Vertical (0°) refers to the direction of pretension matched the direction of extension (V). Diagonally (45°) refers to pretension direction being bias in relation to the direction extension (D). Perpendicular (90°) refers to the direction pretension being at a right angle to the direction of extension (P). (Fig 5.12)

Figure 5.12 Test specimens cut and ready for uni-axial testing

All specimens were marked with an alphanumerical label relating to the group and direction of pretensioning. Multi-axial test specimens are the circular shapes visible beneath the dumbbell-shaped test specimens.

5.4 Results

The following is an account of results recorded during mechanical testing on specimens created and tested using the same standards and equipment as previously described in Chapter 3. Predictive modelling is only used where a clear relationship was observed in the data. Results are presented as two main sections; Firstly, results from tests conducted on yarn embedded PDMS membranes are presented in section 5.4. Secondly, results of experiments on PDMS membranes with embedded fabric, follow, in section 5.5.

5.4.1 Hardness results of membranes embedded with unidirectional yarn

The hardness for each specimen (Figure 5.13) show that changes in the amount of pretension exerted on specimens with embedded yarns did not significantly affect the hardness of the PDMS membranes. Almost no perceivable change occurred among all specimens, even when comparing relaxed yarns to those held at twice their original length. As detailed in Chapter 4, the hardness of OO-30 PDMS with 1% loose fibre addition, and A-10 PDMS with 4% loose fibre addition, was 35 H OO and 50 H OO respectively. The mean hardness of multi-layered membrane (without textiles) was 49 H OO. No significant change (+2 H OO) was observed in specimen groups containing the uni-directional yarns embedded in the OO-30 composite, when the pretension of yarns was increased. Shown in Figure 5.13, specimen hardness ranged from 46 H OO to 48 H OO. A small, increase from 47 H OO to 51 H OO (+4 H OO) occured when the second, harder layer, was added (with no pretensioning of the yarns).

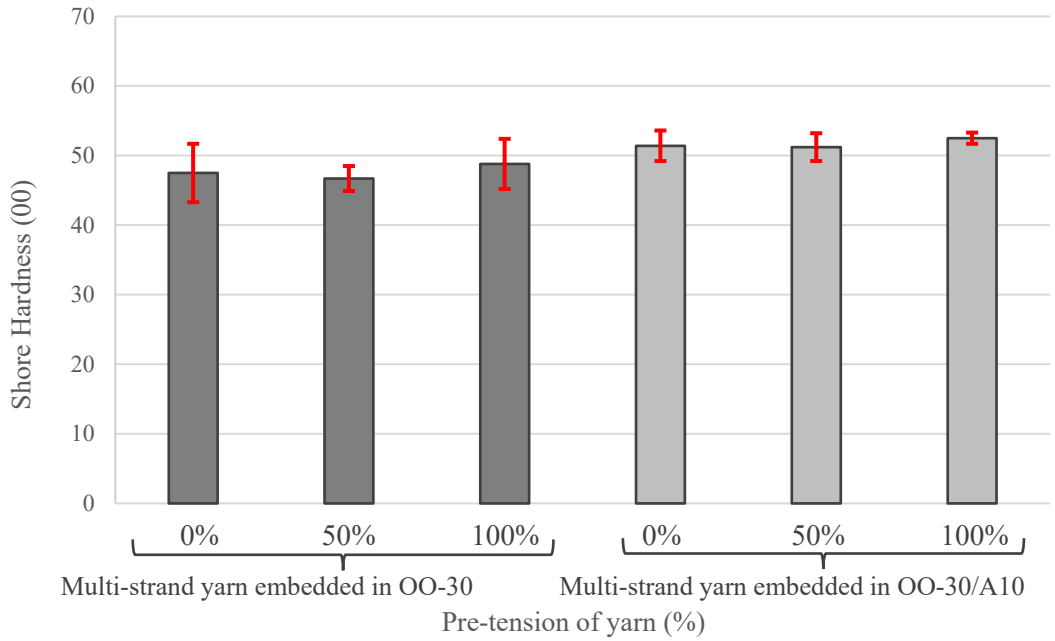

Figure 5.13 Shore hardness values (OO) of PDMS membranes with embedded yarn.

The figure shows hardness values recorded during Shore hardness tests by indentation with a OO calibrated durometer. Each bar represents the mean hardness for each group tested. The darker bars indicate the mean hardness values for OO-30 gel composite embedded with the uni-directional yarns, while the lighter bars indicate the multi-layered composite consisting of OO-30 with embedded yarn and the secondary stiffer A10 composite membrane. Error bars, shown in red for each group, represent the standard deviation.

5.4.2 Uni-axial tensile tests

Tests conducted on specimens that were multi-layered with embedded uni-directional yarns were tested at 0° and 90° because there was almost no difference in the results of tests conducted on the uni-directional yarns when embedded in OO-30 membranes at 45° and 90°.

5.4.3 Uni-axial characteristics of the yarns and embedded uni-directional yarns

It was not possible to reliably determine the original cross-sectional area of yarn or fabric specimens, because of the air gaps between the yarns of the fabric as well as the air gaps between the yarn core and wrapping fibres, so calculating the UTS with accuracy was not feasible (because UTS = Maximum force divided by the original cross-sectional area).

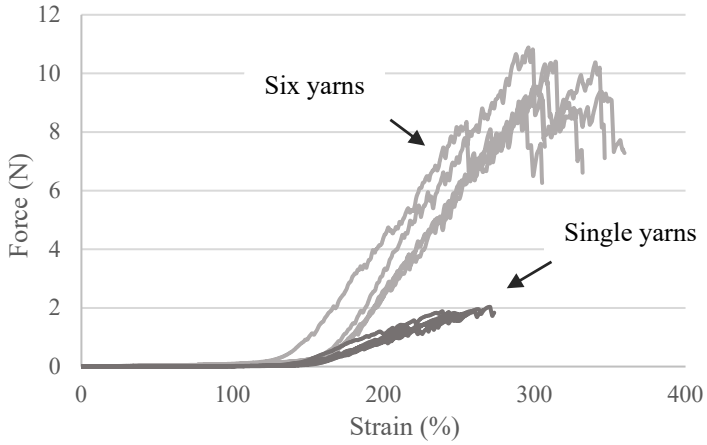

Figure 5.14 The mechanical characteristics of the yarn in uni-axial extension to failure. *The lighter grey lines on the graph represent the individual yarns while the darker grey lines represent the multi-yarn specimens (six parallel yarns).*

The mean maximum force (F_{max}) of the single yarn was 1.88 N, while the mean F_{max} of the multi-strand specimens was 10.08 N. (Fig. 5.14)

Both groups of specimens exhibited a smooth elastic response for the first half of their extension as the crimped nylon wrapper of the elastane yarn straightened, followed by progressive decreases due to the individual nylon filaments rupturing, up to yield at 300% strain.

The linear elastic region for the single and uni-directional yarns was the same, at approximately 125% strain, but the mean force required to reach the strain hardening region, after the heel, for individual yarns was just 0.03 N, whereas the mean force required to reach the same strain percentage for the multi-yarn specimens (consisting of six individual yarns) was slightly higher at 0.1 N.

5.4.4 Uni-axial stress strain results for embedded uni-directional yarns

Data collected during uni-axial extension to failure of single-layered specimens containing embedded yarn indicated that the amount of pretensioned and orientation influences the behaviour of specimens. The graphs below (Figures 5.15A-D) offer a comparison of this influence and clearly show the relationships between membranes made of OO-30. Results from the uni-directional yarns without PDMS (Fig 5.15A) are also given alongside the results at the same scale, to offer a comparative view. Data gathered on the uni-directional yarns without PDMS and multi-layered specimens without yarns are also shown together in Fig 5.16A.

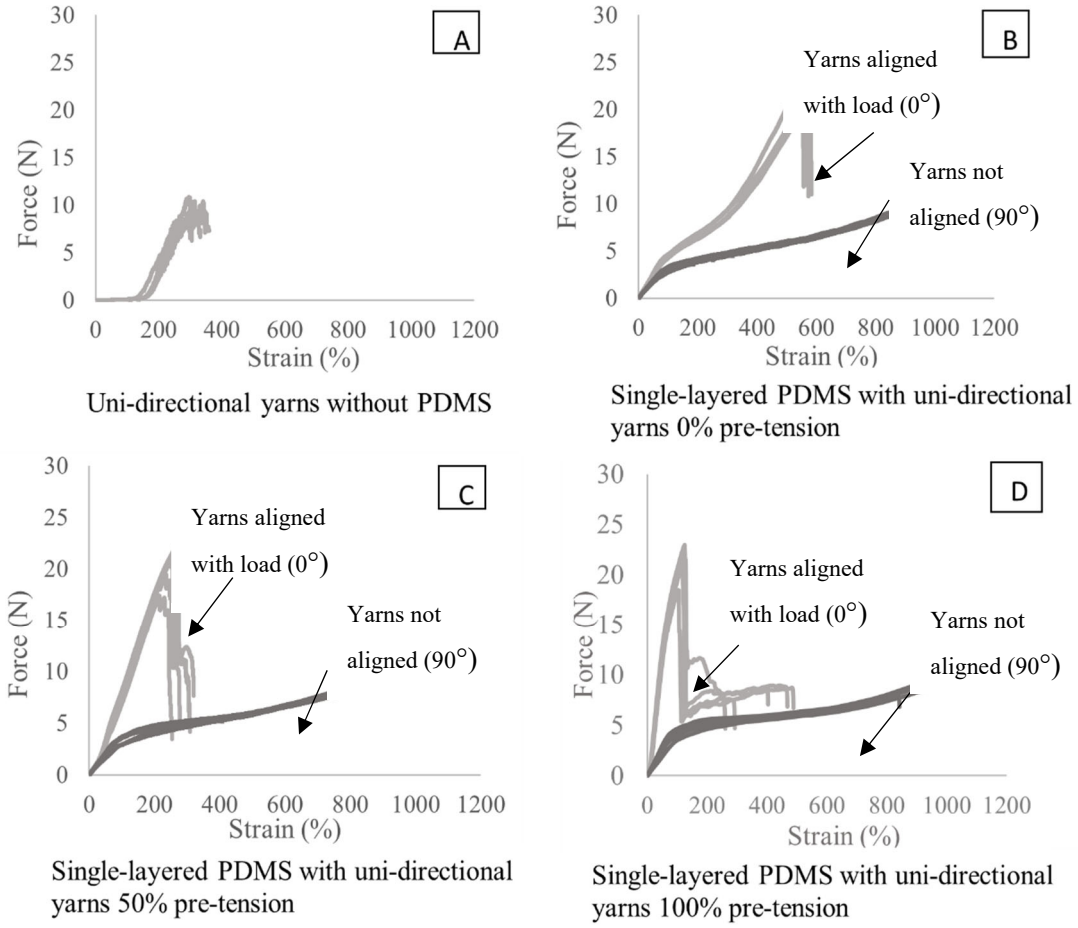

Figure 5.15 Uni-axial force vs strain (%) comparison of uni-directional yarns embedded in a single-layered membrane.

Graph 'A' shows the data for tests on the yarn prior to embedding. Graphs 'B', 'C' and 'D' shows the increasing amount of pretension exerted on the embedded yarns during the embedding process from 0% to 100% respectively. All light grey vectors show the composite membrane behaviour when aligned with the direction of extension. The dark grey vectors show the behaviour of the composite membranes containing yarns that were not aligned with the direction of extension (90° angle).

All other results for multi-layered PDMS specimens with embedded yarns. All graphs (figures 5.16A-D) are displayed at the same scale for easy comparison.

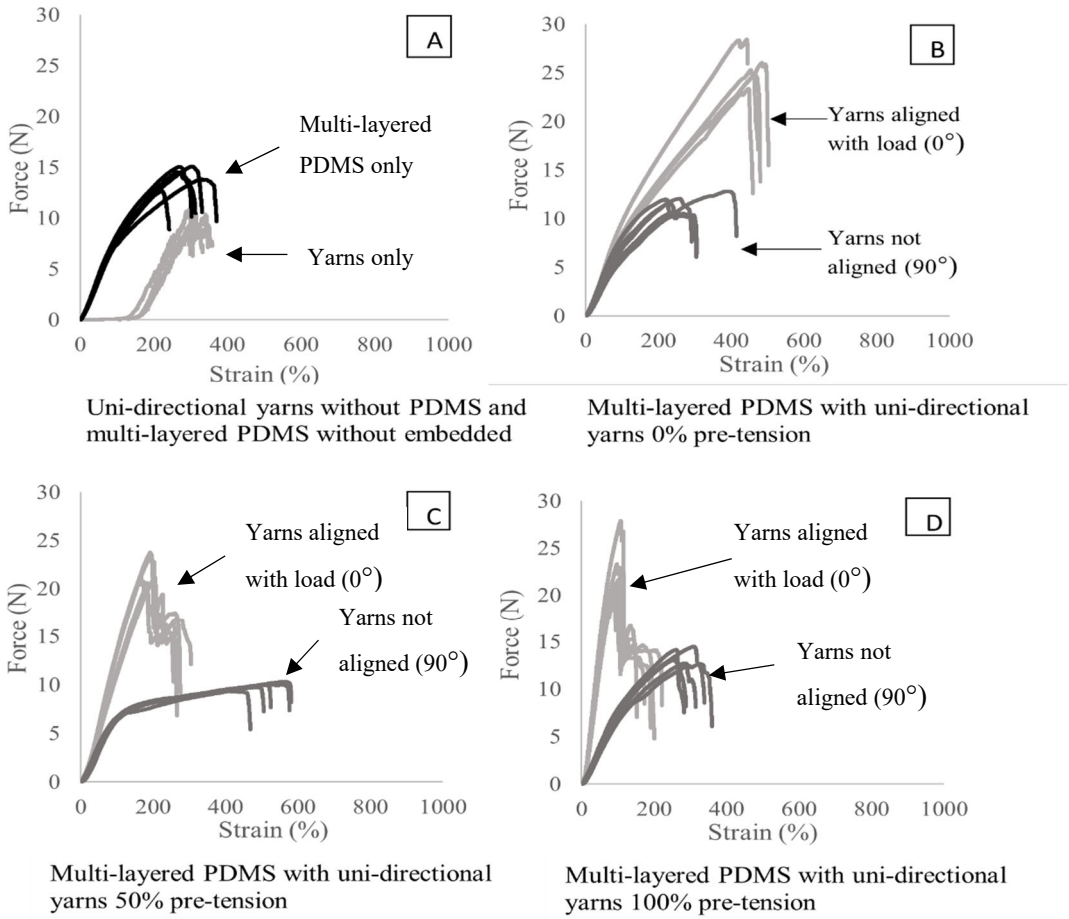

Figure 5.16 Uni-axial force vs strain (%) comparison relating to directional, uni-directional yarns embedded in multi-layered PDMS composite membrane.

Graph 'A' shows the data for tests on the yarn prior to embedding shown in light grey and data for tests on multi-layered PDMS specimens without embedded yarn are shown in black. Graphs 'B', 'C' and 'D' shows the increasing amount of pretension exerted on the embedded yarns during the embedding process from 0% to 100% respectively. All light grey vectors show the composite membrane behaviour when aligned with the direction of extension. The dark grey vectors show the behaviour of the composite membranes containing yarns that were not aligned with the direction of extension (90° angle).

It can be seen in the graphs presented (figures 5.16A-D) that introduction of embedded yarns immediately increased the strength of specimens that contained yarns that were aligned with the direction of extension by 40% compared to specimens that lacked yarns. In contrast, specimens that had embedded yarns at 90° angle, relative to extension, were weakened by the presence of yarns by 20%, but only in the groups that contained yarns with pretension of 0% and 50% (figures 5.16B and 5.16C). Interestingly, specimens with 100% pretensioned yarns (fig. 5.16D) had no effect on

the overall strength of the membrane at a 90° angle to the direction of loading but had a significant effect on strength when the yarns were aligned with the direction of loading (at 0°). The strengthening effect of the yarns can also be seen in graphs (figures 5.16B and 5.16C) Increasing the pretension exerted on embedded yarns reduced extensibility from an initial 460% strain seen in relaxed yarns to 115% strain in specimens that contain yarns embedded at 100% pretension.

5.4.5 UTS of uni-directional yarns embedded in OO-30 PDMS composite

When embedded in the OO-30 PDMS composite, the uni-directional yarns showed some changes in behaviour at differing pretensions, shown in figure 5.17.

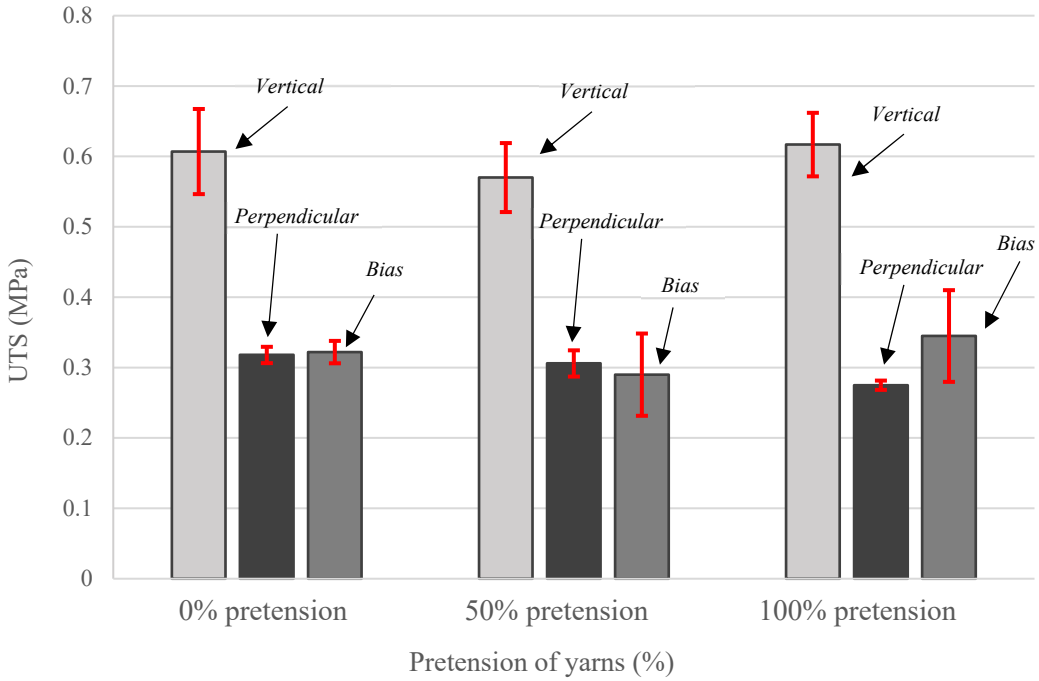

Figure 5.17 Ultimate tensile strength - The influence of increasing pretension of embedded uni-directional yarns in OO-30 PDMS composite membrane.

UTS results show the effect of yarn orientation and pretension. The light grey bars show specimens with yarns that were aligned in the direction of loading (0°). The dark grey bars indicate specimens with yarns perpendicular to loading direction (90°) and the mid-grey bars show specimens with yarns oriented in the bias direction (45°). Error bars represent the standard deviation in each group and are shown in red.

When the yarns were oriented with the direction of loading, there was a small decrease in tensile strength, but large increased in extensibility, by approximately 250%. Similar increases in extensibility were seen in the other groups too, when compared

to tests on uni-directional yarns without PDMS. However, when compared to tests on identical membranes without yarns (described in Chapter 4), a decrease in extensibility up to 500% was seen in specimens with embedded yarns aligned at 45° and 90°, relative to the direction of extension. Also, the elastic region of specimens with embedded yarns reduced by half, compared to specimens without PDMS.

Shown in figure 5.17, the orientation of yarn had a greater effect than the pretension on the tensile strength. While the yarns were oriented in the loading direction, the UTS was between 0.57 MPa and 0.617 MPa. When the yarns were not oriented with loading direction the UTS of the remaining two groups was between 0.275 MPa and 0.345 MPa. Because no significant differences were found between 45° and 90° orientation, only 0° and 90° are shown multi-layered specimens in figure 5.18

5.4.6 UTS of uni-directional yarns embedded in multi-layered PDMS membranes

When aligned with the direction of load extension (at 0°), the multi-layered composite membrane was not significantly affected by the amount of pretension. (Fig. 5.18)

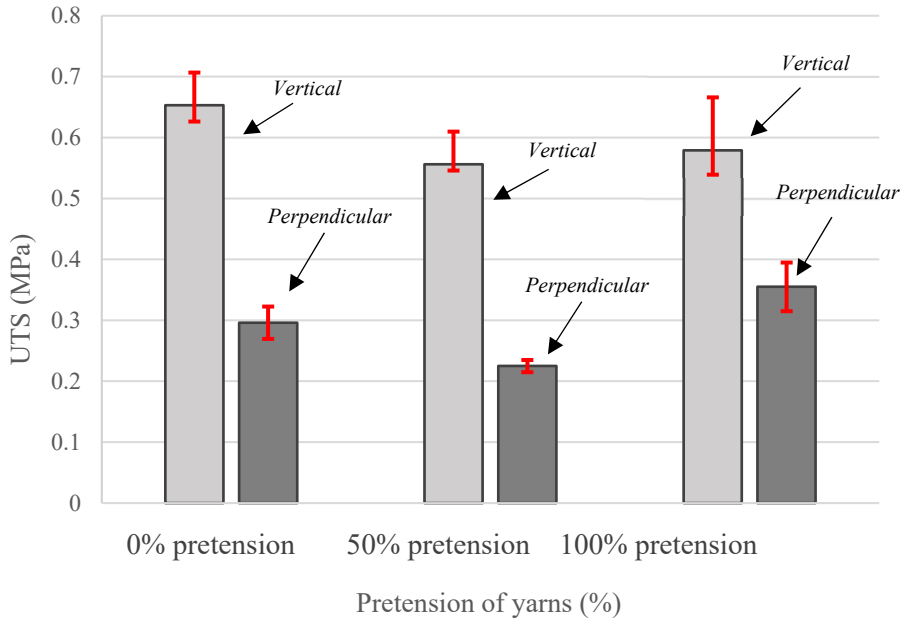

Figure 5.18 Ultimate tensile strength - The influence of increasing pretension of embedded uni-directional yarns in multi-layered composite membrane.

UTS results show the effect of yarn orientation and pretension. The light grey bars show yarns that were aligned with the direction of loading (at 0°), the darker bars indicate specimens with embedded yarns that were at 90°. Error bars show the standard deviation in each group and are shown in red.

Interestingly, the UTS of aligned specimens fell slightly as the amount of pretension was increased, from 0.653 MPa in a relaxed state, to 0.579 MPa at 100% pretension. In contrast, the UTS increased slightly as the amount of pretension was increased in specimens that were not aligned with the direction of extension (90°), from 0.296 MPa in its relaxed state, to 0.355 MPa at 100% pretension.

5.4.7 Young's modulus of single layered PDMS composite with embedded yarns

All unidirectional yarns specimens that were embedded in OO-30 PDMS composite exhibited a small variation in Young's modulus when tested in uni-axial extension. Shown in figure 5.19, almost all specimens were found to have an elastic Young's modulus between 0.091 MPa and 0.159 MPa. (Fig 5.19)

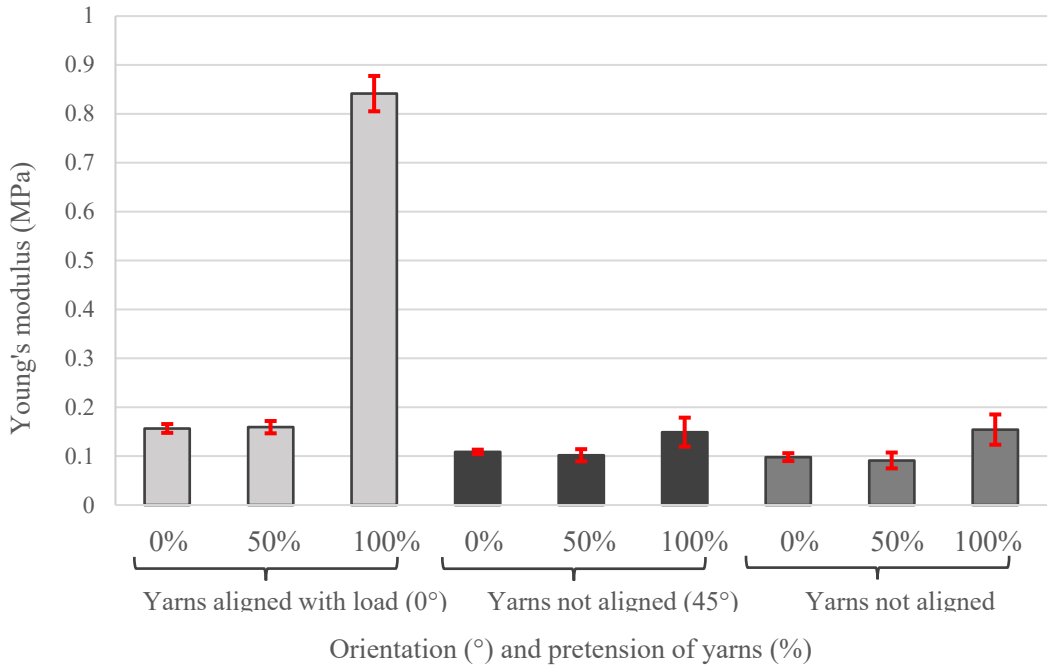

Figure 5.19 Young's modulus – The influence of specimen orientation and pretension of uni-directional yarns embedded in OO-30 PDMS composite.

Bar chart shows the change in Young's modulus of specimens when segregated by yarn alignment angle. The light grey bars represent changes in Young's modulus among specimens that were aligned with the direction of loading at different pretensioned values as indicated. ALL darker coloured bars represent changes in Young's modulus among specimens that were not aligned with the direction of loading at different pretensioned values. Error bars show the standard deviation in each group and are shown in red.

5.4.8 Young's modulus of multi-layered PDMS composite with embedded yarns

An increase in Young's modulus between 0.04 MPa and 0.1 MPa was observed in almost all groups with the multi-layered composition when compared to previous groups with only one layer of PDMS composite. Multi-layered specimens that lacked embedded yarns exhibited a Young's modulus of 0.22 MPa, which was in the same region as most other groups that contained embedded yarn (0.17 MPa to 0.25 MPa).

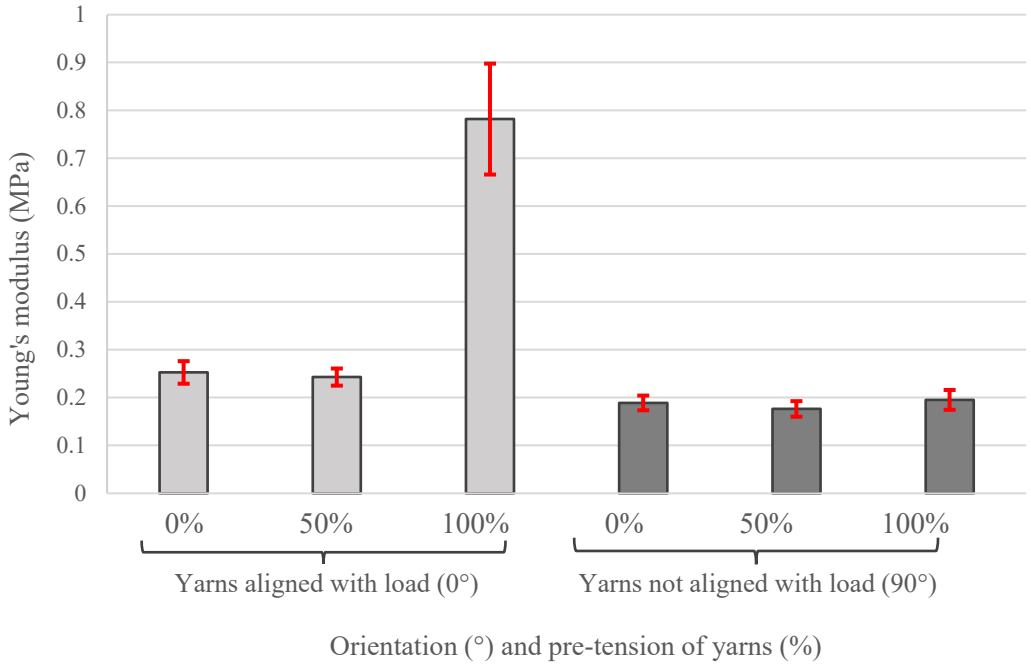

Figure 5.20 Young's modulus – The influence of specimen orientation and pretension of uni-directional yarns embedded in multi-layered PDMS composites.

Shows the change in Young's modulus of specimens when segregated by yarn alignment angle. The light grey bars represent changes in Young's modulus among specimens that were aligned with the direction of loading at different pretensioned values as indicated. The darker coloured bars represent changes in Young's modulus among specimens that were not aligned with the direction of loading at different pretensioned values. Error bars show the standard deviation in each group and are shown in red.

The Young's modulus fell slightly from 0.841 MPa to 0.781 MPa when comparing single-layered specimens to multi-layered specimens with load-aligned yarns at a pretension of 100%. (See fig. 5.20) Similar to the previous group (fig. 5.19) with only one layer of PDMS, this group still exhibited a far higher modulus than any other group with a four-fold increase in elasticity. Young's modulus was affected the least by specimens that were not aligned with the direction of loading (at 90°), with a

pretension of 100%.

5.4.9 Hysteresis of membranes embedded uni-directional yarns

Multi-axial tests were performed on all disc-shaped specimens with a large hemispherical indenter to determine the viscoelastic response to deformation. Multi-axial test details for preconditioning are discussed in detail in Chapter 3.

Cyclic preconditioning was conducted on all specimens that contained uni-directional yarns embedded in the OO-30 PDMS composite and the multi-layered PDMS composite, the results are shown in figure 5.21 A-D. Each curve is a loading and unloading cycle. Summarily, each graph contains all cycles for one group, each group contains five specimens and each specimen was cycled five times.

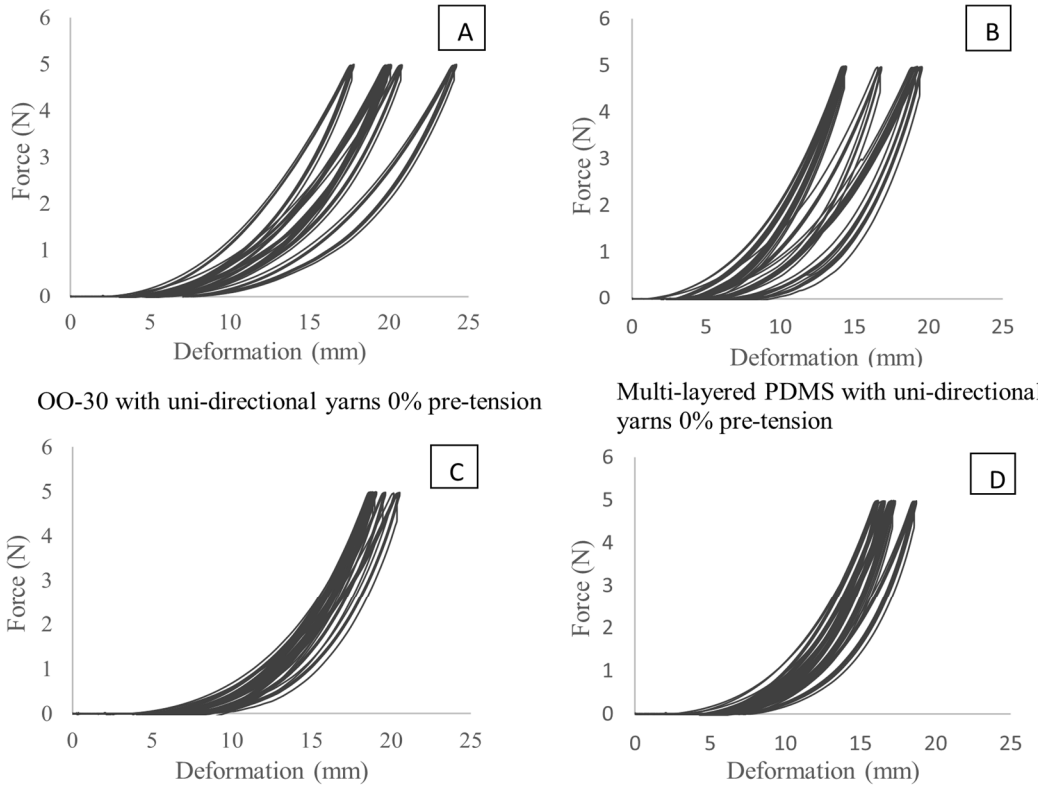

OO-30 with uni-directional yarns 0% pre-tension

Multi-layered PDMS with uni-directional yarns 0% pre-tension

OO-30 with uni-directional yarns 100% pre-tension

Multi-layered PDMS with uni-directional yarns 100% pre-tension

Figure 5.21 Hysteresis (force vs deformation) - The influence of yarn tension.

Multi-axial cyclical tests measuring the characteristic hysteresis loops exhibited by each group. Each specimen preconditioning is shown in the graph. Five loading cycles and five unloading cycles were conducted for each specimen. The first loading cycle is seen on the extreme left in every group, while the final unloading cycle can be seen on the extreme right of each group.

The most significant changes occurred in the repeatability and consistency of deformation.

As shown in figure 5.21A, specimens that contained relaxed yarns in a single layer of PDMS had the largest variation in deformation amongst specimens between the first and the last loading cycles, with a range of 6.5mm, while specimens that had a multi-layered composition had a smaller range of 5mm (figure 5.21B).

In contrast, specimens that contained 100% pretensioned yarns had much less variation in the deformation results, with just a 1mm variation in cyclic deformation in single layer specimens and 2mm variation observed in multi-layered specimens (shown in figure 5.21C and 5.21D respectively). Almost all specimens exhibited between 15mm and 20mm of deformation that did not appear to correlate well with any changes in pretension or number of PDMS layers.

5.4.10 Force degradation of membranes embedded uni-directional yarns

During multi-axial tests performed on all specimens with embedded yarns, the rate of force degradation was measured for 60 seconds. The results from tests on relaxed yarns and 100% pretensioned yarns, embedded in single and multi-layered PDMS membranes are presented in figure 5.22A-D.

Overall, results showed a viscoelastic, time-dependent response to constant loading of 5 N, although no specimens exhibited more than 0.7 N force degradation during the 60 seconds. Specimens that contained a single layer of PDMS, with relaxed embedded yarns, degraded the least amount during the test period, suggesting a better elastic response and recovery when compared to other groups. Specimens that contained a multi-layered PDMS with 100% pretensioned yarns showed the steepest rate of force degradation. Relaxation in this group continued a declining trend until the end of the test period, evidence of greater time-dependent viscoelasticity in multi-layered specimens with 100% pretensioned embedded yarns. (Fig 5.22)

Most relaxation of specimens occurred in the first 20 seconds of the test period for specimens that had a single layer of PDMS, while in contrast, specimens that had a multi-layered composition continued to relax throughout the test period.

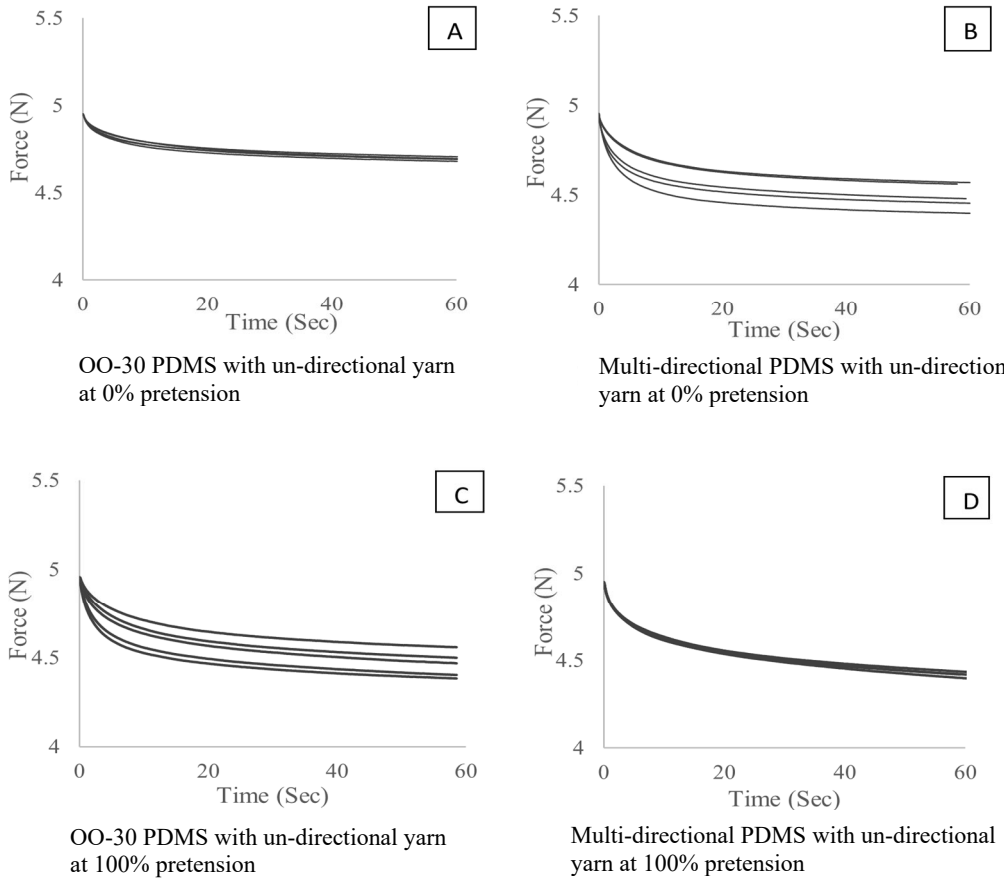

OO-30 PDMS with un-directional yarn at 0% pretension

Multi-directional PDMS with un-directional yarn at 0% pretension

OO-30 PDMS with un-directional yarn at 100% pretension

Multi-directional PDMS with un-directional yarn at 100% pretension

Figure 5.22 Force degradation (stress relaxation)- The influence of yarn tension and the number of layers.

Specimens were measured over 60 seconds while held at 5 N, as per the standard. Image 'A' shows single layered PDMS with relaxed embedded yarns. Image 'B' shows multi-layered PDMS with relaxed embedded yarns. Image 'C' shows single layered PDMS with embedded yarns held at 100% pretension. Image 'D' shows multi-layered PDMS with embedded yarns at 100% pretension. Each graph axis is labelled accordingly.

Interestingly, the two groups that exhibited the least variation amongst test specimens were the single layered PDMS with relaxed embedded yarns and multi-layered PDMS with 100% pretensioned embedded yarns; Indicating no clear relationship between result variation and yarn tension or number of layers added.

5.4.11 Unrecovered deformation of membranes embedded uni-directional yarns

The amount of permanent (unrecovered) deformation was measured after the Multi-axial tests on all specimens and helped describe the plasticity of specimens, shown in figure 5.23. As can be seen in the graphs (Figure 5.23), all specimens tested exhibited

permanent change between 1.5mm and 3.4mm, as a result of cyclic deformation up to 5 N. Specimens with a single layer of PDMS showed the least amount of permanent deformation.

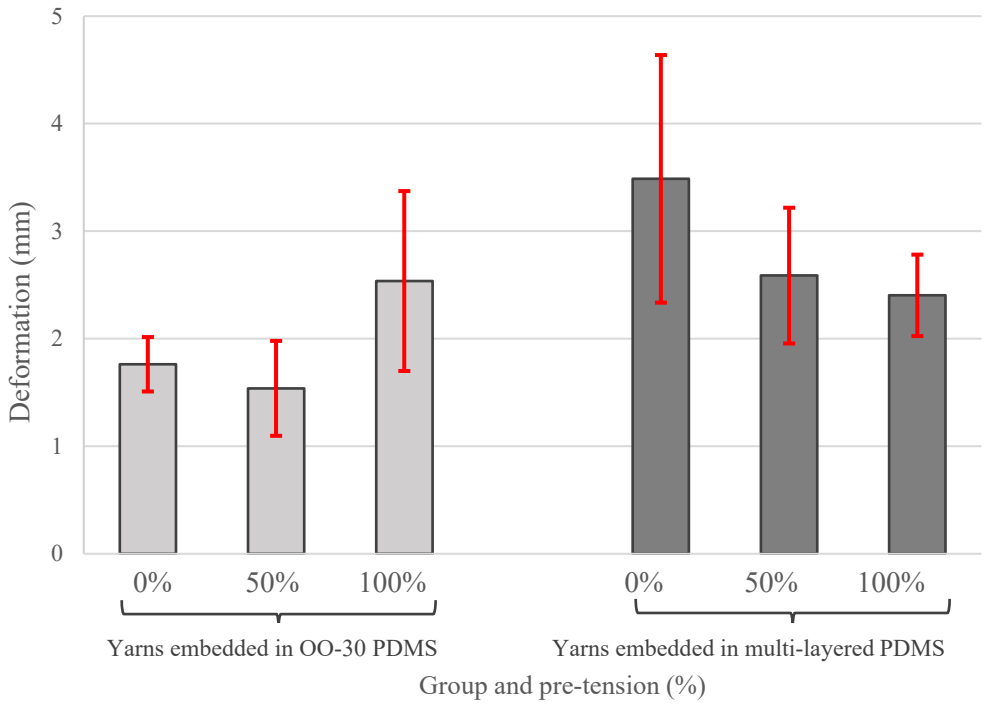

Figure 5.23 Unrecovered deformation of PDMS with embedded yarns- The influence of increasing yarn tension and number of layers.

The chart shows a comparison between single layered specimens and multi-layered specimens that were embedded with uni-directional yarns held at various pretensioned amounts (0%, 50% and 100%). The light grey bars show the specimens that contained yarns embedded in a single layer of PDMS (OO-30) while the darker grey bars show the multi-layered PDMS specimens with embedded yarns. Each bar represents the mean of five test specimens. Error bars represent the standard deviation for each group of specimens and are shown in red.

While there was a small difference between the single and multi-layered specimens, there appeared to be no correlation between the amount of deformation and the amount of pretension exerted on embedded yarns during specimen preparation. The multilayered membranes exhibited greater unrecovered deformation than the membranes with only a single layer. As discussed in the previous chapter, membranes with more fibres (4%) experienced greater permanent deformation. Membranes with a single layer varied a little, but not consistently.

5.4.12 Force decay of membranes embedded uni-directional yarns

During the multi-axial investigations, the amount of force decay was recorded as a percentage of lost energy after a 60 second holding period at 5 N, shown in figure 5.24. Increasing embedded yarn pretension appeared to affect the amount of force decay observed most significantly in single-layered specimens. As shown in figure 5.24, a substantial decay in force of almost 10% was found in single layered specimens at 100% pretension, which correlates with the increase in Young's modulus seen only in this group during uni-axial tests.

Specifically, this particular group saw a sharp increase in decay from 5.8% to 9.9% when comparing the single-layered specimens with 50% pretension and the single-layered specimens with 100% pretension, respectively.

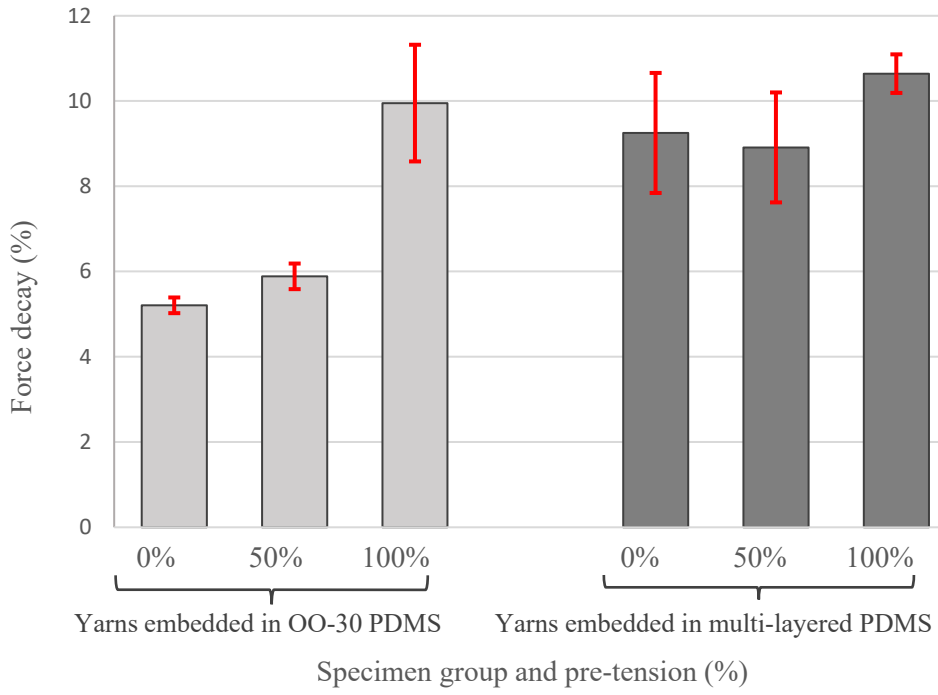

Figure 5.24 Force decay- The influence of increasing yarn tension and layering.

Bar chart showing the relationship between embedded uni-directional yarn pretension and the percentage of force decay. The light grey bars represent specimens made from a single layer of PDMS while the dark grey bars represent specimens made from the multi-layered PDMS. Each bar represents the mean of five test specimens. Error bars represent the standard deviation for each group of specimens and are shown in red.

5.5 Results regarding PDMS composite membranes with embedded fabric

This section focuses on the behaviour of PDMS composite membranes that have been embedded with fabric using the same standards and equipment as previously used on all PDMS composite membranes. The fabric created for these experiments was produced using yarn obtained from the same batch of yarn, as experiments conducted on specimens containing the uni-directional yarns, to mitigate the risk of variation in yarn production. This approach offers directly comparable results to help define and delineate the influence of key mechano-structural changes in PDMS membranes.

5.5.1 Hardness of fabric embedded in PDMS composites

Specimens made with OO-30 embedded with fabric were found to have a hardness ranging from 47 H OO with relaxed embedded fabric, to 52 H OO with 100% pretensioned embedded fabric. The results are shown in Figure 5.25.

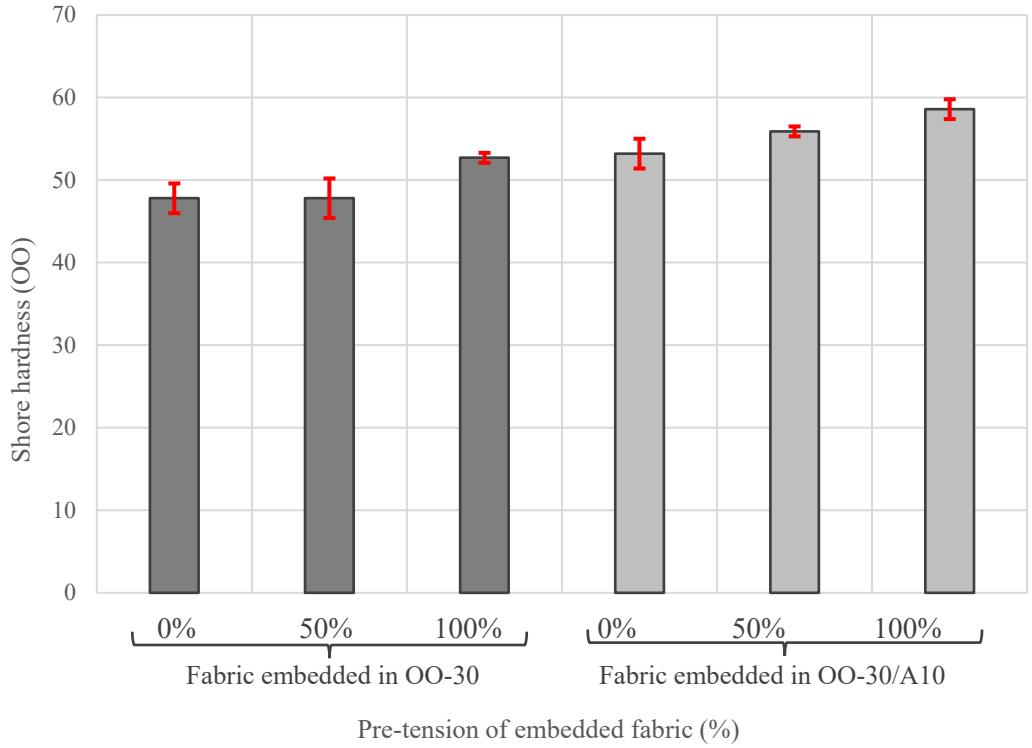

Figure 5.25 The hardness of PDMS membranes with embedded fabric

The figure shows hardness values recorded with a OO calibrated durometer. Each bar represents the mean hardness for each group tested. The darker bars indicate values for OO-30 gel composite embedded with the fabric, while the lighter bars indicate the multi-layered composite membrane. Error bars, shown in red, represent the standard deviation.

Specimens made with the multi-layered PDMS composite (with the added A-10 layer) saw the most noticable change in hardness from 49 H OO without fabric to 53 H OO with the introduction of relaxed embedded fabric, to 58 H OO with the 100% pretensioned embedded fabric. (Fig 5.25)

Linear regression of the data revealed a fairly weak correlation ($R^2 = 0.75$) between hardness and pretension of embedded fabric in specimens that were made from the single layered OO-30 PDMS composite. Conversly, there was a good linear correlation ($R^2 = 1.00$) between the hardness and fabric tension when embedded in the multi-layered PDMS. A predictive model describing the relationship between hardness and embedded fabric tension has been given in figure 5.26. It was also found that a small but gradual hardening occurred in the multi-layered PDMS, as the pretension of the embedded fabric was increased. Specifically, it was found that, 3.2 H OO increments occurred per 50% increase in pretensioning of the fabric.
However, this data needs further work with additional data points to be used reliably.

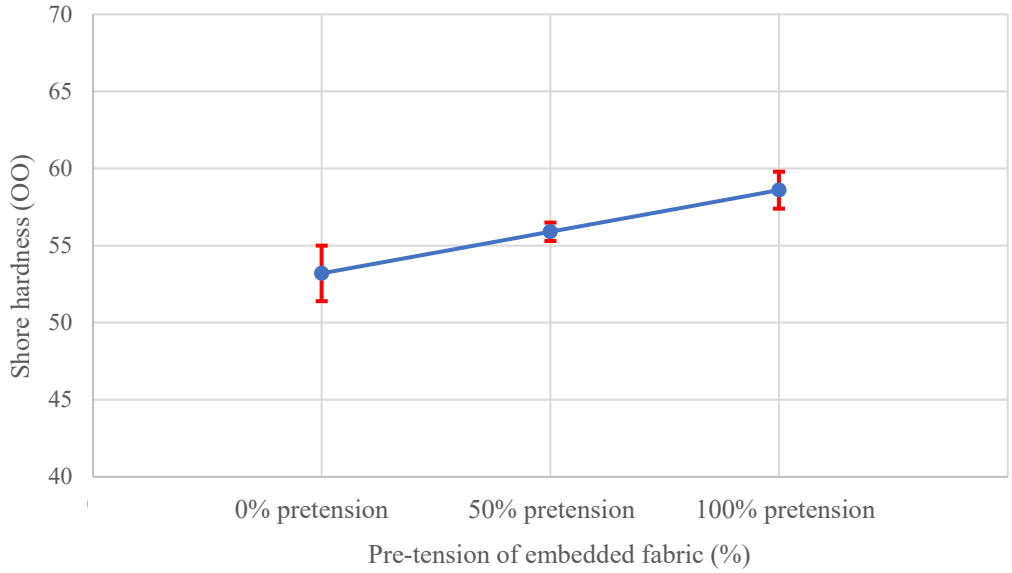

Figure 5.26 Linear regression of Shore hardness of membranes with fabric embedded in multi-layered PDMS, versus, increasing pretension on embedded fabric.
The mean hardness of all specimens in the same group are marked by the coloured dots. Linear regression is shown by the solid line. The model predicted hardness to increase by 3.2± 0.5 degrees of hardness per 50% increase in fabric pretension. Error bars are shown in red for each group representing the data set's standard deviation.

The strong linear coefficient was calculated using equation 5.1.

$$y = 2.7x + 50.5 \qquad \textit{Eq. 5.1}$$

5.5.2 Uni-axial tensile tests of fabric embedded in PDMS composites

Before mechanical tests on the PDMS composites were performed, the fabric was tested without any PDMS in uni-axial extension, to gather baseline data on fabric behaviour. The fabric was tested in three orientations (0°, 45° and 90°) relative to the direction of stretch that would later be applied to the composites.
The fabric was tested first, then the PDMS specimens that contained embedded fabric. Uni-axial stress strain relationships, UTS and Young's modulus results are all presented in turn.

5.5.3 Characteristics of the fabric

Testing the fabric prior to embedding it within the PDMS allows for direct comparative analysis between the groups and helped determine the most resilient orientation to use for pretensioning during the embedding process.
The maximum force prior to uni-axial failure of the knitted fabric was 26 +/- 0.9 N in the wales direction, a little less in the coarse direction at 20.7 +/- 1.6 N, but was much less in the bias, at just 7.3 +/- 3.7 N.
All three groups behaved similarly in the elastic range, at lower strains under 125% extension, but the two groups with the greatest extensibility (wales and coarse) exhibited strain hardening characteristics at higher strains. All fabric test specimens exhibited progressive failure of individual yarns at higher strains above 300% extension. The greatest tensile strength was seen in wale direction, so it was determined that this would be the direction of pretension when embedding the fabric in PDMS. Clamping would occur along the coarse direction in the next phase.
Additionally, specimens extended in the bias direction were included in this investigation due to their weaker, but stiffer, mechanical properties that contrasted with the wales and coarse directional properties. Specimens extended in the bias can be seen during extension in Fig 5.27.

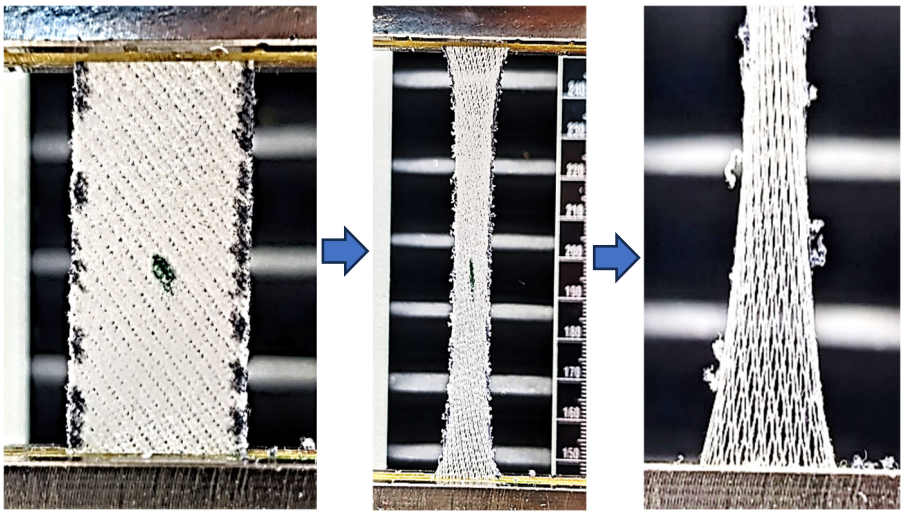

Figure 5.27 Uni-axial tests being conducted on fabric specimens.

The image shows fabric specimens during extension. All specimens in the images were cut on the bias and marked with a central dot for alignment when clamping. During extension specimens begin to fray at the edges prior to failure. This may explain the serrated stress strain vectors exhibited by all the fabric specimens as shown in figure 5.28A

5.5.4 Uni-axial stress strain results for single-layered PDMS composites with embedded fabric

When testing fabric only specimens, elasticity in all three orientations was found to be similar, but the extensibility was reduced by more than half when extended to failure in the bias direction, seen in figure 5.28A. When the relaxed fabric was embedded in the PDMS gel, (Figure 5.28B) extensibility and strength of the fabric was significantly improved in the bias direction but did not appear to have much influence on the wales or coarse oriented specimens.

The elastic yield of all specimens containing fabric and PDMS remained relatively stable <100% strain in all orientations (shown in figure 5.28B, 5.28C and 5.28D). After the elastic yield, specimens that contained fabric with >50% pretension, showed the most significant changes in behaviour as illustrated in Figure 5.28B and 5.28C. Acute strain hardening until failure was observed in the bias direction when the fabric was relaxed in the PDMS composite. A similar strain hardening effect was also observed in the wales direction when pretension was present in specimens. Specimens

with relaxed fabric, oriented in the wales and the coarse direction during tests, exhibited similar linear behaviour at first, but with three distinct yield indicators, typical of fabric/polymer composites. The first observable yield occurred at low strains <100% strain as the elastic limit was reached, which was the same as the other specimen groups.

The second yield indicator occurred at high strains >1250% strain and was revealed by distinctive undulations in the otherwise smooth curve, shown in figure 5.28B.

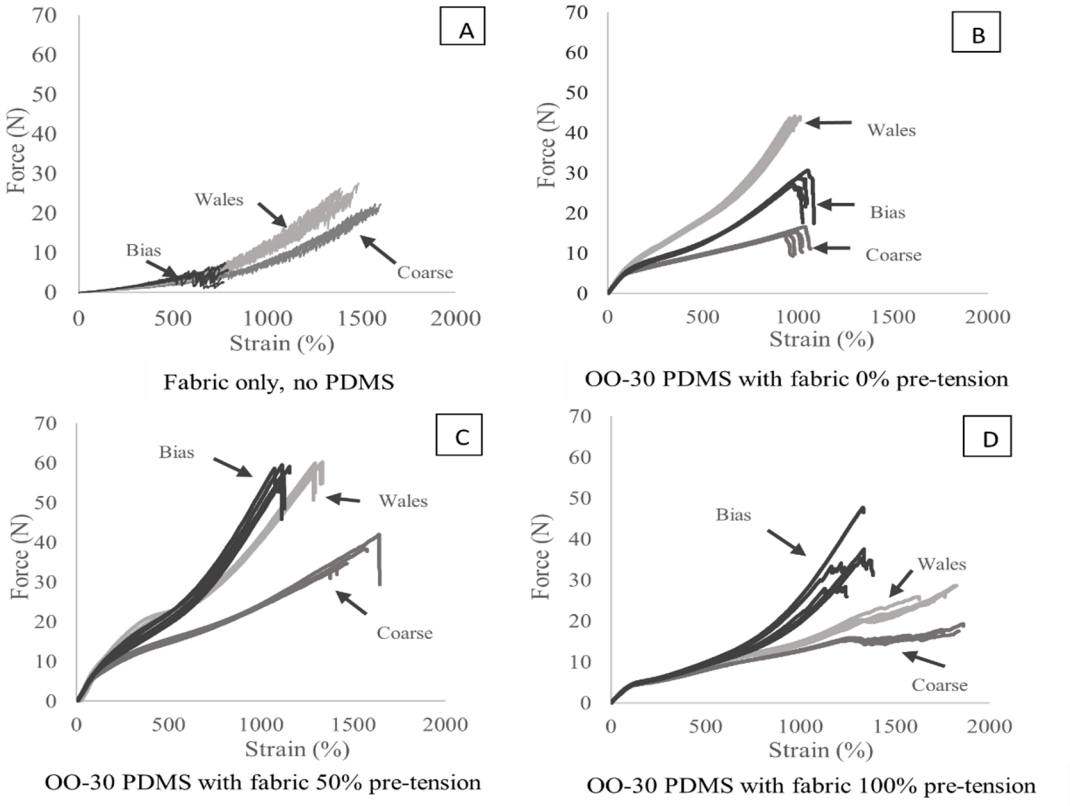

Figure 5.28 Uni-axial extension to failure showing influence of fabric orientation on PDMS OO-30 composite behaviour.

Each group is labelled with its respective fabric orientation. In this figure, all specimen vectors are given in the graph to describe each group's unique behaviour at different orientations and to demonstrate the membrane's mechanical consistency. Graph 'A' shows the mechanical behaviour of fabric specimens without PDMS. Graph 'B' shows relaxed fabric embedded in PDMS OO-30 composite. Graph 'C' shows pretensioned (50%) fabric embedded in PDMS OO-30 composite. Graph 'D' shows pretensioned (100%) fabric embedded in PDMS OO-30 composite.

As can be seen in Figure 5.28A, the breaking strain of the fabric was in the same strain (%) range for wales and coarse orientation as the undulations in figure 5.28B (>1250%), whereupon it is presumed the fabric gradually failed and PDMS content was recruited to absorb loading in the failure region, until full specimen failure at around 1800%. Specimens containing embedded fabric that was pretensioned at 50% all exhibited a significant increase in overall strength, but a reduction in extensibility.

Along with the reduced extensibility, in coarse and wales orientations, the serrations seen in 5.28A disappeared with the introduction of PDMS to the fabric and were replaced with a smooth vectors exhibiting strain hardening trajectories, seen in Figure 5.28B, C and D.

Specimens oriented in the coarse direction were still the weakest though, typically failing at <50 N, but they were the most extensible, reaching up to 1600% strain.

When oriented in the wales direction membranes almost doubled in overall strength, but extensibility was reduced significantly by around 500%. The most significant changes were observed when testing membranes with embedded fabric that were pretensioned by 100% (fig. 5.28D). Extensibility was reduced in all specimen orientations, in this group, by approximately 400%.

Specimens oriented in the bias exhibited the most significant change when compared to the other groups with less pretension, reducing in overall strength by half but retained almost all of its extensibility. All specimens with 100% pretensioned embedded fabric failed at <1080% strain.

5.5.5 Uni-axial results for multi-layered PDMS composites with embedded fabric

When fabric was embedded in a relaxed state with 0% pretension applied, the membranes in the wales and coarse orientation behaved almost identically. Meanwhile, in the bias orientation, there was a distinct strain hardening effect seen at 800% extension that continued to increase until failure at 1300% extension. When a

pretension was applied to the embedded fabric, the characteristics of specimens oriented in the wales direction exhibited significant strain hardening at 1000% extension through to failure. Specimens aligned in the coarse and bias directions remained almost unchanged.

Specimens in all multi-layered groups behaved similarly to the previous groups with only one layer (fig. 5.29).

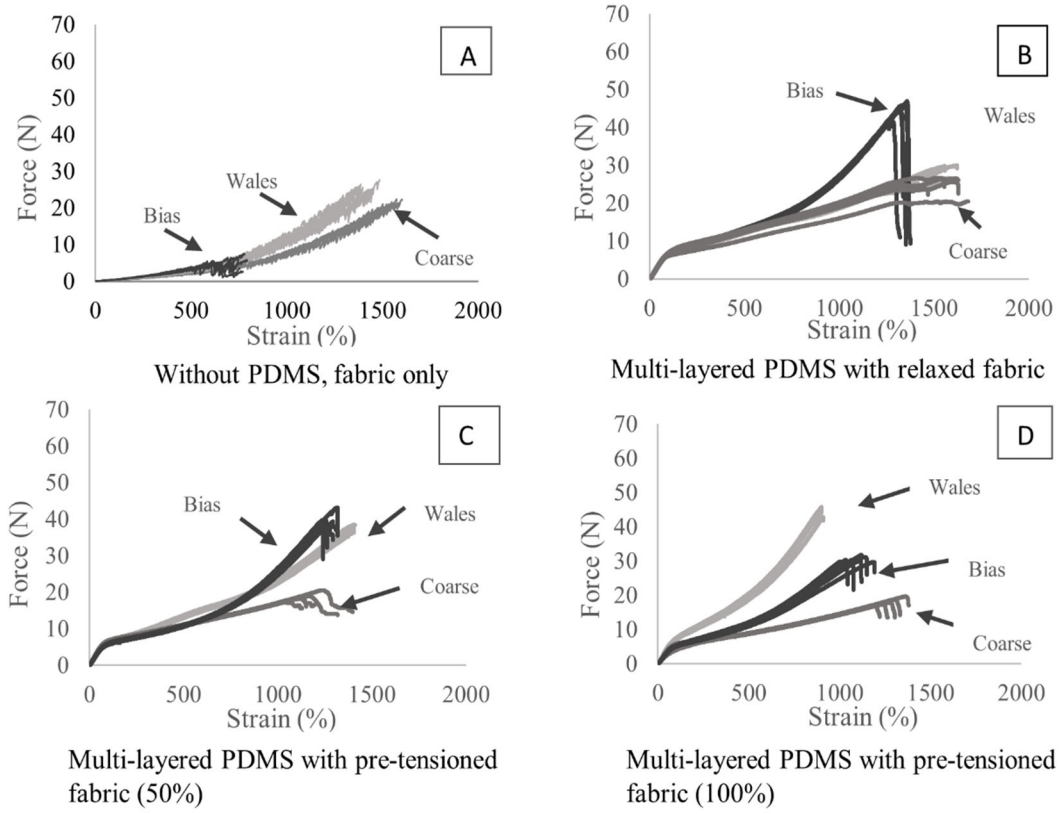

Figure 5.29 Comparison of knitted lycra fabric orientation and multi-layer PDMS composite behaviour - Uni-axial extension to failure.

Each group is labelled with fabric orientation. Each vector describes the unique behaviour at different orientations, they are shown here to evidence consistent performance. Graph 'A' shows the behaviour of fabric specimens without PDMS (reproduced from figure 5.28A) for comparative purposes. Graph 'B' shows relaxed fabric embedded in the multi-layered PDMS composite. Graph 'C' shows pretensioned (50%) fabric embedded in the multi-layered PDMS composite. Graph 'D' shows pretensioned (100%) fabric embedded in the multi-layered PDMS composite. Although clearly labelled, specimens containing 0% pretensioned fabric behaved so similarly in the wales and coarse direction, that it is difficult to separate them in graph 'B', but the results are shown more clearly in the UTS and Young's modulus results in the proceeding sections.

At 100% pretension, however, the behaviour of specimens aligned in the wales and bias showed significant change, while specimens aligned in the coarse direction remained almost unchanged. Specimens aligned in the bias exhibited a decrease in strength by around 25%, meanwhile, the specimens aligned in the wales direction exhibited a small increase in strength but a large decrease in extensibility. In comparison, multi-layered PDMS specimens that lacked embedded fabric began to yield at a mean force of 14.22 N of stress and 311.3% strain.

5.5.6 UTS comparison of all specimens embedded with fabric

The UTS results for all specimens that contained fabric are shown in the chart below for easy comparison. (Fig 5.30)

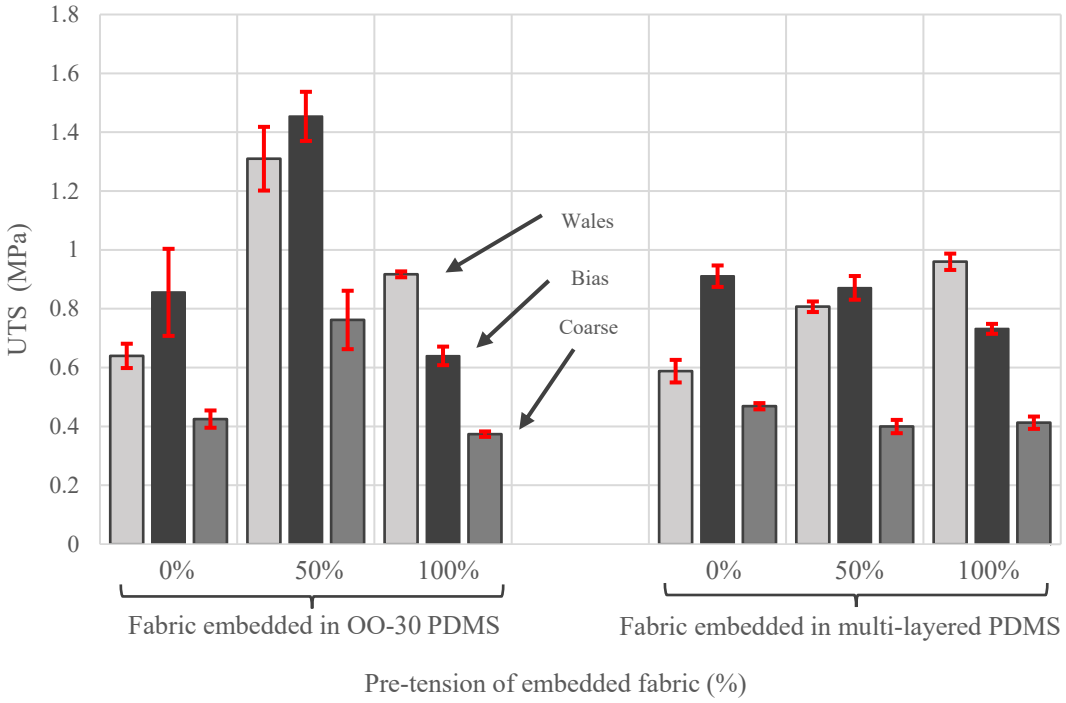

Figure 5.30 Ultimate tensile strength – Comparison of knitted lycra fabric orientation and multi-layer PDMS composite pretension.

Results show the effect of fabric direction and pretension on strength. Light grey bars show the specimens aligned in the wales direction during loading at different pretensioned values, the darkest bars indicate specimens with bias alignment relative to the direction of loading, the mid-grey bars represent specimens that were aligned in the coarse direction during loading. Error bars represent standard deviation and are shown in red.

Results visualise changes in the UTS of all 90 uni-axial tests conducted on specimens containing embedded fabric. Each bar represents the mean value of identical five specimens. Since each specimens' cross-sectional area of each specimen is considered when determining the UTS, results are directly comparable. All specimens showed a fluctuating change in behaviour at differing pretensions and orientations.

Results show the group with fabric (at 50% pretension) embedded in a single layer of (OO-30) PDMS, were strongest, and were almost twice as strong, in all orientations, as specimens that contained relaxed fabric. Specimens in the wales orientation increased from 0.64 MPa to 1.31 +/-0.1 MPa, while specimens in the wales orientation increased from 0.85 MPa to 1.45 +/-0.08 MPa, in the coarse orientation specimen strength increased from 0.42 MPa to 0.76 +/-0.09 MPa.

The weakest specimens, in all groups tested, contained embedded fabric oriented in the coarse direction, with little change in the UTS observed between specimens groups, even when the relaxed fabric was embedded or an additional PMDS layer was added.

As fabric pretension was increased from 0% to 100% for specimens that were multi-layered, the UTS decreased slightly by 0.17 +/- 0.01 MPa in specimens oriented in the bias direction. Meanwhile multi-layered specimens with fabric oriented in the wales direction increased gradually by a total of 0.37 +/- 0.03 MPa as the pretension was increased from 0% to 100%, with good predictability ($R^2 = 0.9896$) using the linear regression given in equation 5.2. By comparison, specimens that lacked embedded fabric had a mean UTS of 0.39 +/-0.02 MPa.

$$y = 0.186x + 0.413 \qquad \textit{Eq. 5.2}$$

5.5.7 Young's modulus of fabric embedded in multi-layered PDMS composite

The Young's modulus for all specimens that contained fabric embedded in either a single or multi-layer PDMS membrane, are shown below in figure 5.31. Each bar in the figure represents the mean value of five identical specimens. Results show that all specimens with a single layer of PDMS had a significant change in behaviour at differing pretensions and orientations, while the specimens with a multi-layered composition changed little.

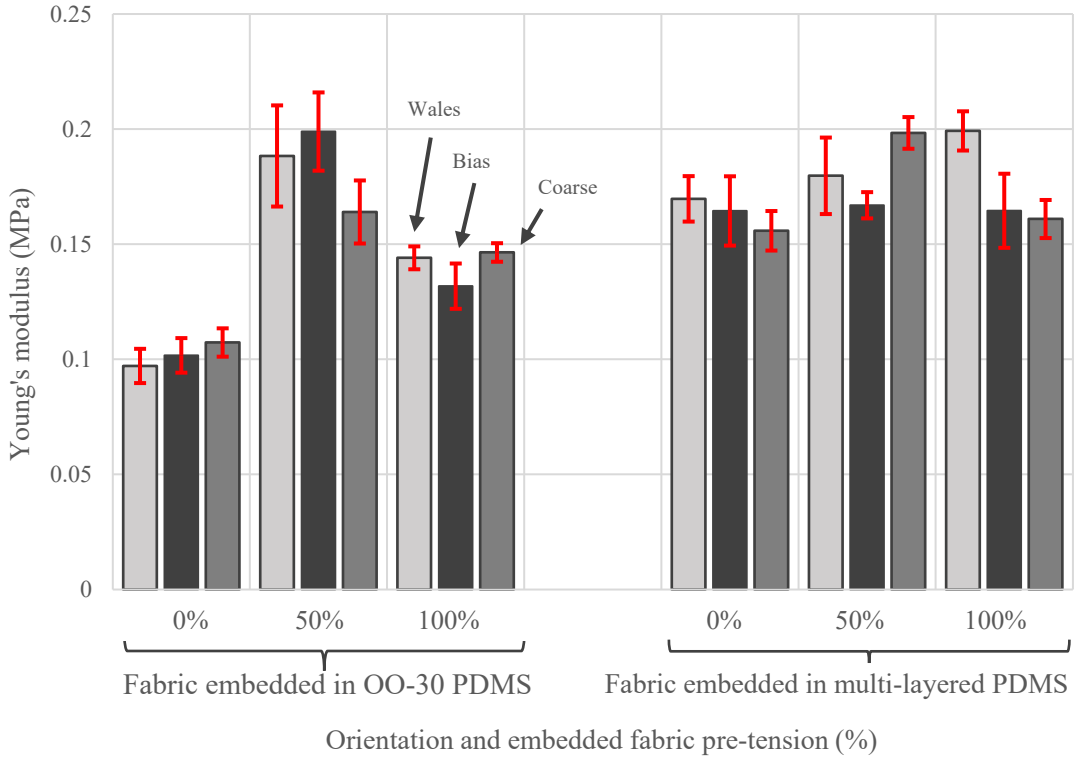

Figure 5.31 Young's modulus – The influence of specimen orientation and pretension of fabric embedded in PDMS composite.

The figure shows the change in Young's modulus due to orientation. As labelled, the light grey bars show specimens aligned in the wales direction at different pretensions, all of the darkest bars indicate specimens with bias alignment relative to the direction of loading, all the mid-grey bars represent specimens that were aligned in the coarse direction relative to loading. Error bars represent the standard deviation in each group and are shown in red.

Overall, results showed a poor relationship between the orientation and amount of pretension in all specimens. However, a significant change was observed in the group comprised of a single layer of PDMS and where fabric was pretensioned to 50%, particularly in specimens oriented on the bias and wales, both of which saw the largest increase in Young's modulus of all specimens tested, doubling in elasticity from 0.1 MPa to 0.198 MPa and 0.09MPa to 0.18 MPa, bias to wales, respectively.

Specimens oriented in the coarse direction, increasing from 0.1MPa to 0.16MPa. Only multi-layered specimens oriented in the wales direction showed any predictable gain in elasticity ($R^2 = 0.967$) using the formula provided in equation 5.3.

$$y = 0.0147x + 0.1534 \qquad \textit{Eq. 5.3}$$

By way of comparison, the Young's modulus for specimens lacking embedded fabric was 0.22 MPa (+/-0.017 MPa). No other significant relationships were observed.

5.5.8 Multi-axial - Hysteresis of fabric embedded in PDMS composites

Cyclic loading during dynamic multi-axial compression is shown in figure 5.32.

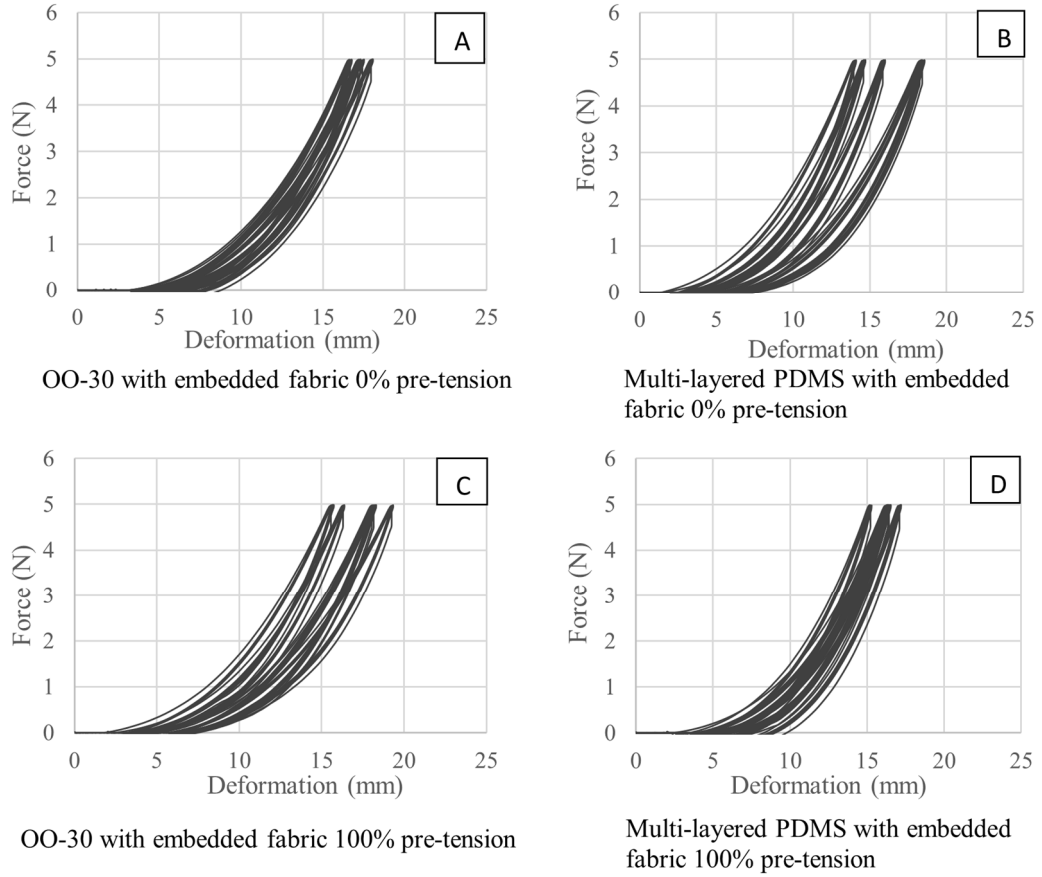

OO-30 with embedded fabric 0% pre-tension

Multi-layered PDMS with embedded fabric 0% pre-tension

OO-30 with embedded fabric 100% pre-tension

Multi-layered PDMS with embedded fabric 100% pre-tension

Figure 5.32 The influence of increasing fabric tension- Hysteresis (force vs deformation). *Multi-axial cyclical tests measuring the characteristic hysteresis loops exhibited by each group. Each specimen preconditioning is shown in the graph. Five loading cycles and five unloading cycles were conducted for each specimen. The first loading cycle for each group is seen on the extreme left in every group, while the final unloading cycle can be seen on the extreme right of each group.*

During multi-axial compression investigation of test specimens, it was found that the group comprised of single-layered PDMS specimens with 100% pretensioned embedded fabric and the group that comprised of multi-layered PDMS specimens with relaxed embedded fabric, were the most time dependent in their viscoelastic response to cyclic loading. This can be seen in the provided graphs as preconditioning hysteresis cycles that exhibited more widely spaced curves (fig. 5.32).

The remaining groups were less time-dependent, with the group composed of single-layered PDMS and relaxed embedded fabric being the least viscoelastic in pre-conditioning cyclic tests. All groups performed similarly in multi-axial deformation at 5 N, rarely achieving under 15mm of deformation, largely staying within the 15mm to 20mm threshold for deformation, even when the groups that exhibited the most viscoelastic change during pre-conditioning are considered.

Other characteristics such as force degradation and unrecovered deformation and force decay reveal a more detailed picture of the mechanical response of specimens to multi-axial examination. Lastly, there was no significant difference in results of identical tests conducted on specimens that lacked fabric.

5.5.9 Force degradation of fabric embedded in PDMS composites

No noticeable difference was observed in the rate of force degradation when measured over 60 seconds at 5 N of constant loading. Most force degradation occurred within the first 20 seconds of all of the tests, regardless of the group being investigated. Not more than 0.5 N of force was lost during this period of the tests. (Fig 5.33)

All of the groups also continued to relax until the end of the 60 seconds, albeit very slowly. Typically, this was less than 0.03 N over the final 20 seconds of most tests. The similarity amongst test group results are shown in figure 5.33. Even specimens that lacked the embedded fabric, offered comparable results regarding the profile of force degradation spanning 0.5 N over 60 seconds.

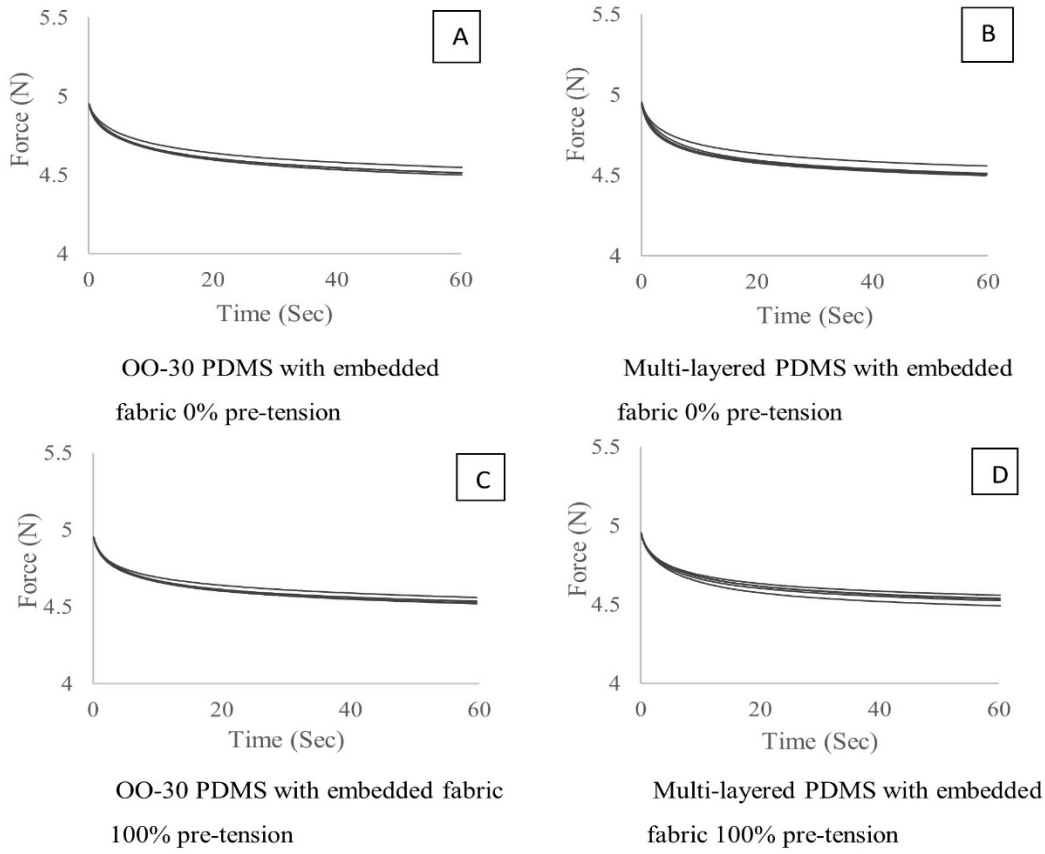

Figure 5.33 Force degradation- The influence of increasing yarn tension.

Force degradation measured over 60 seconds while held at 5 N. Results are the mean averages of experiments on each group. The graph describes the relationship between the change in force degradation and the amount of pretension of embedded yarns. Each vector represents an average of each group's rate of force decay. Each group is labelled according to the amount of pretension used in its preparation.

5.5.10 Unrecovered deformation of fabric embedded in PDMS composites

The amount of permanent deformation was measured for all specimens (fig 5.34). Results indicate that all specimens show significant plasticity in their behaviour.

Groups varied by an average of just 1mm across all specimens. The greatest amount of unrecovered deformation (and error) occurred in specimens that contained 50% pretensioned fabric for both single-layered and multi-layered specimens, but only by a small amount (> 0.5mm). Specimens that lacked fabric did not differ from these results either, with a mean of 2.3mm +/- 0.08mm of unrecovered deformation.

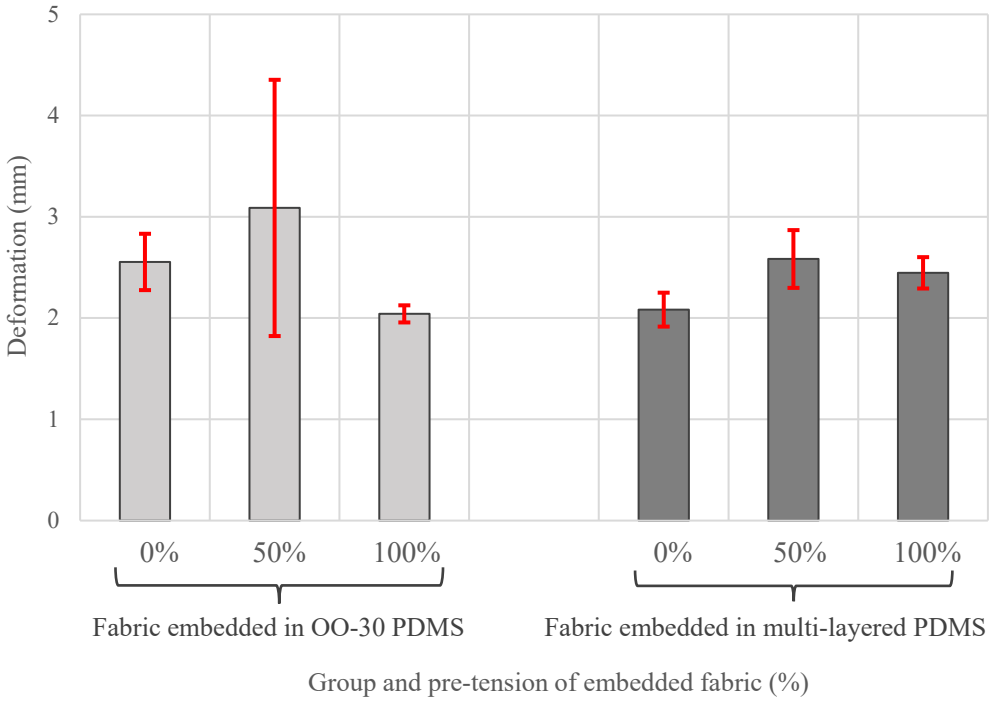

Figure 5.34 Unrecovered deformation PDMS with embedded fabric.

Single layered specimens and multi-layered specimens embedded with fabric with pretensions (0%, 50% and 100%). The light grey bars show the specimens that contained fabric embedded in a single layer of PDMS (OO-30), the darker grey bars show the multi-layered PDMS specimens with embedded fabric. Each bar represents the mean of five test specimens. Error bars represent standard deviation for each group of specimens and are shown in red.

5.5.11 Force decay of fabric embedded in PDMS composites

The percentage of force decay measured for each specimen group after a 60 second holding period at 5 N, during multi-axial investigations. As shown in the chart provided in figure 5.35, all specimens show a significant amount of viscoelastic behaviour.

Changes occurred in the amount force decay, but no perceivable relationships were observed between the amount of pretension exerted on embedded fabric or number of PDMS layers. Once again, the groups with 50% pretensioned fabric in both, single and multi-layered specimens, were shown to be slightly less viscoelastic than other groups tested, (< 2%), especially considering the standard deviation in each group.

Multi-layered PDMS specimens, that lacked embedded fabric, exhibited a mean of force decay of 7.6 % compared to 8.1 % for all other groups.

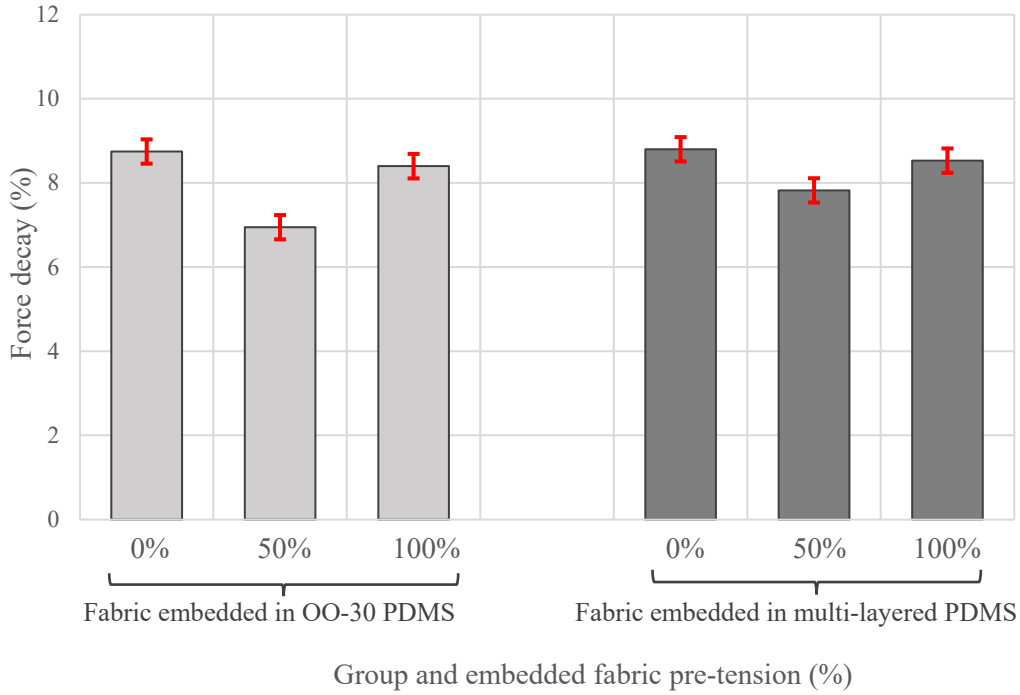

Figure 5.3 Force decay- The influence of increasing fabric tension.

Bar chart showing the relationship between embedded fabric pretension and the percentage of force decay. The light grey bars represent specimens made from a single layer of PDMS while the dark grey bars represent specimens made from the multi-layered PDMS. Each bar represents the mean of five test specimens. Error bars represent the standard deviation for each group of specimens and are shown in red.

5.6 Discussion on the behaviour of PDMS membranes with textiles

The principle focus of this chapter was to determine the precise influence of textiles used to reinforced PDMS composite membranes. Materials familiar to prosthetists, that might be used to reproduce some of the unique, anisotropic qualities of human, soft tissue membranes, like skin. Reliability of results and repeatability of tests was ensured by using agreed international standards and equipment, designed for mechanical characterisation of elastomers and elasticated fabrics, specimens. This discussion is presented in two main sections; Section 5.6 discusses membranes with embedded yarns, section 5.7 discusses membranes with embedded fabric.

This discussion focuses on identifying and delineating the precise changes in mechanical behaviour, due to the influence of embedded textiles. Both sections include separate discussions for each mechanical characteristic observed- Shore hardness, UTS and Young's modulus, hysteresis, force degradation, unrecovered deformation, and force decay. The amount of pretension and angle of orientation were informed by literature on the behaviour of human skin.[30, 31, 50, 172, 174, 189, 190]

5.6.1 Hardness characteristics of PDMS membranes with embedded yarns

The introduction of yarns embedded in the PDMS composite caused a perceivable 12 H OO increase in hardness of the single layered composite from (35 H OO to 47 H OO) when comparing single layered specimens with embedded yarns to single layered specimens lacking yarns, that were previously discussed in chapter (4). The hardness of multi-layered specimens without yarns was 49 H OO, so the presence of yarns caused a greater increase in hardness, than the addition of a second layer. It is possible that the spacing of the yarns may have contributed to the increase in hardness that was observed, as the yarns would have increased overall density of the membrane due to their incompressibility and close proximity to one another. Changing the spacing of the yarns may have an influence on the overall observable hardness. Interestingly though, changing the amount of pretension exerted on embedded yarns during specimen fabrication had no significant effect on the overall hardness of any specimen. When a second (thinner and stiffer) layer was added to create the multi-layered PDMS composite, a small, increase in hardness was noticed, as might be expected, since a layer of slightly stiffer material was being added, but the small increase, of 4 H OO, that was observed, would be difficult to recognise with palpation alone.

5.6.2 Uni-axial characteristics of PDMS membranes with embedded yarns

Uni-axial characterisation of the yarns without the PDMS layer was important to fully understand their role in composite membrane behaviour and how they might be employed to influence the uni-axial behaviour of PDMS composites. Equally important was the characterisation of the baseline, multi-layered PDMS composite absent of yarns. Uni-axial stress strain graphs are important because it allowed for a detailed view of the changeable mechanical properties throughout extension. It also

helps quantify key mechanical traits like, non-linearity, Young's modulus and UTS; especially useful when comparing data from this study with the data from the literature. Because most of the existing data in the literature refers to experiments conducted without use of the available standards, references to existing data are given where relevant, but in general, results presented in this work are intended as a baseline for comparative studies and development of more realistic materials and repeatable simulations and surrogates.

When aligned with the direction of loading, the unidirectional yarns that were not embedded in PDMS exhibited yield at around 10 N, while the yield of the multi-layered specimens lacking yarns was 14 N. Embedding the yarns in the single layered PDMS composite offered more than twice the strength of the yarns alone, helping the membranes achieve 22 N before yielding, proving that the yield strength of the single-layered composite (OO-30) was directly influenced by the presence of the yarns.
Embedding of the yarns into a known, single-layered PDMS composite also produced other interesting mechanical effects. Firstly, extensibility decreased as the amount of pretension was increased showing that the pretension of yarns was a reliable method of reducing PDMS extensibility in a controlled manner. Secondly, all specimens in the group with pretensioned yarns (100%), that were aligned in the direction of extension, exhibited similar failure strain percentages as the values given in the literature for excised human skin, between 100% and 150%.[16, 116] All other specimens with load-aligned yarns also exhibited similar gains in yield strength characteristics regardless of the amount of pretension on the embedded yarns, (around 22 N), but with differing failure strain percentages, between 100% (at 100% pretension) and 575% (with no pretension). Furthermore, specimens with aligned relaxed yarns had a higher failure strain percentage >500%) and exhibited strain hardening traits that are characteristic of soft tissues in extension.[50, 172]
Meanwhile, the specimens with 50% and 100% pretension had an almost linear extensibility with only a slight strain softening prior to failure. Specimens with yarns embedded at a 45° and 90° that were tested, both exhibited almost identical mechanical behaviour; strain softening before strain hardening, a recently identified mechanical feature associated with the mechanical behaviour of skin.[45] The cause of this change in behaviour lays in the way the yarns corrupt the homogeneity of the

PDMS, effectively creating tracks of thinned, weakened PDMS along their course. Once the heel of the curve is exceeded the yarns separate from the surrounding matrix, the PDMS component takes up the strain causing the strain softening region seen in the data. As the PDMS composite absorbs the load, the loose fibres in the composite are recruited to absorb increasing amounts of the strain causing the strain hardening effect. This characteristic was absent in the specimens with aligned yarns because the yarns absorbed the load throughout extension, until failure, which was in agreement with the literature.[21] The results from the UTS tests support this hypothesis as all specimens (single and multi-layered PDMS) with aligned yarns (0°) exhibited twice the amount of strength seen in the other specimen groups. The presence of a second layer of PDMS did almost nothing to the overall strength of any specimen either, proving that the yarns had a greater influence on mechanical strength and extensibility than the PDMS.

Interestingly, however, the elastic modulus of all specimens was between 0.1 MPa and 1.5 MPa, except for all specimens that contained aligned yarns with 100% pretension that were 7 to 8 times the modulus of all other specimens. It is assumed that this was caused by the yarns being recruited to absorb loading almost instantly during extension, as the elasticity of the yarns was impacted by the pretension procedure. Other groups were more reliant on the elasticity of the PDMS composite. Further evidence supporting this theory was found in the multi-layered group. Here, the addition of a second layer of PDMS composite had a small effect on membrane elasticity, raising the modulus threshold of all specimens by 0.21 MPa +/- 0.04 MPa, with one exception; The group containing yarns aligned in the direct of extension at 100% pretension, which exhibited similar elastic modulus as the single layered group, with an equally distinctive increase in modulus to 0.78 MPa.

Finally, in all specimens that had a multi-layered composition and embedded yarns, that were not aligned in the direction of extension, saw a significant reduction in extensibility (-50%), compared to specimens with only a single layer of PDMS composite, revealing that the presence of a second stiffer layer of PDMS has a greater influence on the extensibility of the membranes with embedded yarns.

5.6.3 Multi-axial characteristics of PDMS membranes with embedded yarns

Multi-axial cyclic compression was conducted >5 N, as previously specified and the relaxation of the specimens was measured to determine the viscoelastic behaviour of specimens. Preconditioning is a process that allows for the loading history of specimens to be considered when assessing the mechanical response to deformation. Loading history, is a well-known influential factor in the characterisation of anisotropic, viscoelastic membranes,[41] only the multi-axial test standard offers specific guidelines on recording and presenting this trait.

Specimens with 100% pretensioned yarns that were embedded in a multi-layered PDMS lost their stored energy more slowly than all other test specimens. This indicated that this particular group was more viscoelastic than other groups but results of the force degradation also showed that this group had the least variation amongst individual specimens within the group, suggesting a greater predictability and reliability in mechanical response to loading. In addition, when compared to the groups with only a single layer of PDMS, the presence of a second layer of PDMS appeared to stabilise the amount of force decay in all specimens, regardless of the amount of pretension exerted on embedded yarns.

5.6.4 Summary of PDMS membranes with embedded yarns

Changing the amount of pretension exerted on embedded yarns during specimen fabrication had no significant effect on the overall hardness of any specimen, but adding a second layer of PDMS did slightly increase hardness. Embedding the yarns in the PDMS composite doubled the strength of the structure, compared to the yarns alone. Extensibility decreased as the amount of yarn pretension was increased. All of the specimens in the group with 100% pretensioned embedded yarns, that were aligned with the direction of loading, showed similar failure strain percentage as excised human skin. Changing the pretension percentage affected the failure strain percentages, but not the yield force. Specimens with yarns embedded at a 45° and 90° exhibited strain softening before strain hardening, known features associated with the mechanical behaviour of skin. The yarns aligned with loading had a greater influence on the mechanical strength of the specimens, while the multi-layered composition had

a greater effect on extensibility in all other groups that were not aligned with the direction of loading. The elastic modulus of specimens that contained load-aligned yarns with 100% pretension exhibited a modulus seven to eight times higher than that of all other groups. Specimens with 100% pretensioned yarns that were embedded in a multi-layered PDMS lost their stored energy more slowly than all other test specimens. The presence of a second layer of PDMS appeared to stabilise the amount of force decay.

5.7 Discussion regarding PDMS membranes embedded with fabric

The effects of embedding fabric in PDMS with different amounts of tension was investigated to assess their suitability for use as analogous soft tissue membranes for clinical and theatrical prosthetic applications.

Results were presented in a visually digestible manner best suited to the interdisciplinary audience for which it was intended, amongst clinical prosthetic research communities and practicing theatrical prosthetists.

5.7.1 Hardness characteristics of PDMS membranes embedded with fabric

The introduction of embedded fabric caused an increase in hardness that was proportional to the increase in pretension exerted on the fabric during the embedding process, especially among the groups comprised of the multi-layered PDMS composites. Despite the limited number of data points, emerging data revealed a strong linear relationship (R^2 =1.00) between the fabric tension and hardness, but only in the multi-layered configuration. Although the predictability of the linear regression model was good, the range of hardness values was quite small from a tactility viewpoint of the prosthetist (increase of 3.2 H OO +/- 0.5, per 50% increase in fabric pretension). Interestingly, a similar increase in hardness (3.4 H OO) was also observed with the introduction of embedded fabric, so a perceivable increase in hardness of almost 10 H OO can be anticipated when comparing multi-layered specimens without fabric, to equivalent specimens with fabric, at 100% pretension.

Since the proximity of the fabric layer to the test surface was less in the specimens

with multiple layers, it can be assumed that the fabric tension had more effect on hardness than the addition of a second layer of PDMS. Data that showed single-layered specimens with 100% pretensioned fabric, was harder than multi-layered specimens without fabric, which adds weight to this theory.
Considering all of the data, the fabrics influence on hardness was minimal compared to other influencing factors such as loose fibre content as seen in Chapter 4. Nevertheless, it is an influential, and predictable factor to be considered when preparing reinforced soft tissue prosthesis that need to convey a precise hardness value.

5.7.2 Uni-axial characteristics of PDMS membranes embedded with fabric

The knitted fabric that was tested without a supporting PDMS matrix was weaker and less extensible, than specimens containing relaxed fabrics that were embedded in the PDMS, but only in the bias direction during extension, breaking earlier and extending less than the other orientations tested. More specifically, fabrics tested in the bias, were four times weaker but three times stiffer than specimens extended in the coarse and wales direction. Multi-layered specimens that lacked embedded fabric were similarly weak compared to all specimens with embedded fabric, except specimens that contained embedded fabric tested in the coarse orientation, where the UTS was similar to specimens without fabric (around 0.4 MPa in all cases) but the elongation was very different. For example, specimens oriented in the coarse direction exhibited elongation between 1000% and 1600%, which was the same as the fabric tested by itself (without PDMS), whereas specimens that lacked fabric, only extended to around 300%. It can be assumed that this was due to the elasticated fabric being recruited to absorb the strain throughout elongation, with the PDMS having almost no influence on extensibility, when the fabric was oriented in the coarse direction, because the extensibility of the fabric outperformed that of the PDMS.

When relaxed fabric was embedded in the single-layered PDMS composite, all three directions had similar stiffness, but different strengths. Specimens tested in the bias doubled in strength, while specimens in the coarse and wales weakened by a third. As the amount of embedded fabric pretension was increased, the strength of the

specimens in the bias continued to increase. When comparing fabric without PDMS to specimens with 100% pretensioned embedded fabric, both cut on the bias, specimens were ten times stronger and three times more extensible.

Interestingly, specimens containing fabric, extended in the coarse and wales orientation, strengthened first, before weakening at 100% pretension, while all specimens containing fabric with 50% pretension were more resilient in overall strength and extensibility.

All specimens that were tested in the bias orientation, exhibited a distinct 'deckchair' – shaped curve, resulting from strain softening before strain hardening, shown in figure 5.36. Like soft tissues, this characteristic 'deckchair' shaped curve was previously reported as having three distinct phases of deformation.[45] These phases are shown together in the graph provided in figure 5.36.

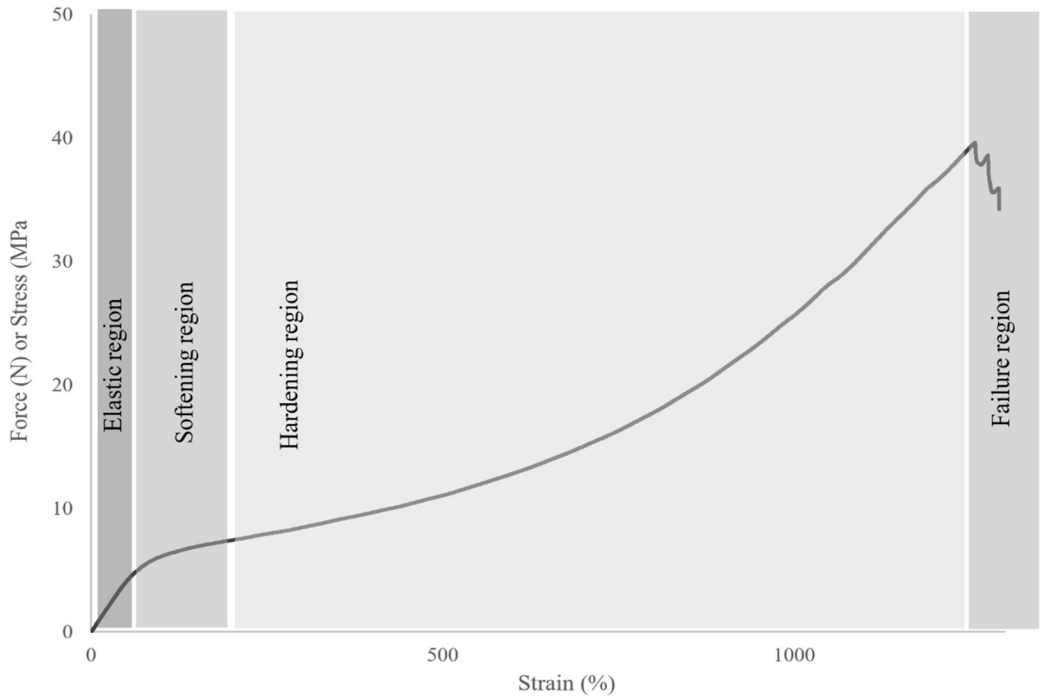

Figure 5.36 Non-linear characteristics of membranes embedded with reinforcing fabrics. *Graph shows the typical example of 'deckchair' shaped curve of the mechanical response to uni-axial loading as per the agreed standard. Regional changes of one test specimen are highlighted and labelled to describe each phase of deformation up to failure.*

First, the linear part of the vector describes the 'toe' region of deformation, known to be the elastic response of collagen fibres that are gradually realigning with the direction of strain, slowly straightening.[103] This can be likened to the straightening of

the elastane yarns that are aligned diagonally to the direction of strain when extended in the bias. Once they are aligned with the direction of loading, the second phase begins. This is illustrated by the 'heel' of the vector trajectory, evident in the results of soft tissues in extension and the PDMS composites presented in this study.[39, 50] In soft tissues, this phase is understood to be caused by the aligned collagen fibres stretching.

Now, because collagen fibres are known to have a higher elastic modulus than elastin fibres, collagen fibres progressively bear the load of strain until they reach their elastic limit.[354] This response is partly due to their three-dimensional arrangement in the ground substance, so the fibres cannot all be recruited to take up the strain simultaneously, rather-gradually, resulting in the strain-softening effect. In rubbers, this is also known as the Mullins effect, which occurs during the first elongation phase of uni-axial testing. In the composites tested here, this is influenced by the elasticity of the fibre filled PDMS substrate, which responds to strain in a similar way to the ground substance found in soft tissue membranes like skin.

In the final phase of the 'deckchair' curve,[45] the collagen fibres enter their plastic phase of deformation while the elastin fibres are recruited to bear the remaining load supported by the highly extensible viscoelastic ground substance.[41] In agreement with the literature, this phase is represented by the recruitment of the PU filament at the core of each elastane yarn, strengthened by the PDMS matrix surrounding the knitted yarn architectural sub-structure. This characteristic manifests as a gradual strain hardening of the specimens in extension prior to failure.

The failure characteristic of the PDMS composites support this theory too and can be seen as a 'tail' of serrated strain, immediately prior to test secession, that was due to the final few threads of yarn failing after rupture of the PDMS matrix at true specimen failure (shown in figure 5.37).

Figure 5.37 Uni-axial specimen, after extension to failure.
The image shows a detailed view of a tensile test specimen comprised of multi-layered PDMS composite with 50% pretensioned fabric, cut in the bias. Notice the permanent deformation, and how the top layer is more deformed than the lower layer, evidence of its heterogenic anisotropy. The crimped broken ends of the elastane yarns are also visible, protruding out of the distal end of the specimen, along with the short strand fibres.

Not all specimens tested during this investigation exhibited the same 'deckchair' shaped curves during uni-axial extension though. Almost all specimens that were oriented in the coarse direction exhibited an almost linear behaviour in extension to failure after the initial 'heel' yield at the start of the softening phase, common to all test specimens. This indicated that pretensioning the fabric had a significant influence on the anisotropic characteristics. In fact, all specimens with a single layer of PDMS exhibited different strength and extensibility when the embedded fabric pretension was increased as previously mentioned, but all the specimens with embedded fabric and a multi-layered composition, behaved almost identically in the coarse orientation. This suggested that the act of multi-layering the PDMS stabilised the behaviour of the embedded fabric somehow, especially in the coarse orientation, that was unchanged during the embedding process. Results from the UTS and Young's modulus examination support these observations too.

Furthermore, visual inspection of the specimens after testing revealed that the second, stiffer layer ruptured only at failure, usually in the same region as the fabric, whereas the softer OO-30 composite had multiple fractures or splits along its length as seen in figure 5.38. This behaviour only appeared in multi-layered specimens with embedded fabric though.

Figure 5.38 Uni-axial specimen, after extension to failure.

The image shows a detailed view of a tensile test specimen comprised of multi-layered PDMS composite with 50% pretensioned fabric, cut in the bias. Notice the multiple failure fractures in the layer with embedded fabric and the intact upper layer, as well as the permanent deformation.

While no apparent relationship was observed between orientation, pretension and UTS in single-layered specimens in any orientation, or multi-layered specimens in coarse or bias orientations, specimens oriented in the wales direction during extension increased in UTS, and a strong linear relationship between UTS and pretension of embedded fabric was observed ($R^2 = 0.9896$). Again, these predictive models had only three data points, so should be used with this in mind.

Similar results were observed when analysing Young's modulus results too, where no relationships were seen in any other group except in the multi-layered specimens containing fabric oriented in the wales direction during extension. Despite the limited number of data points a strong linear relationship began to emerge between Young's modulus and pretension of the embedded fabric was observed ($R^2 = 0.967$).

5.7.3 Multi-axial characteristics of PDMS membranes embedded with fabric

Multi-axial characterisation is an important, but often overlooked, aspect of the mechanical behaviour of elastomers and soft tissues. Despite there being only a handful of studies using the standardised multi-axial compression characteristics of soft materials, it is agreed that the behaviour of soft tissues and elastomers are comparable in many ways.[355] However, it should also be noted that the

characterisation of soft tissues or soft elastomers have never been tested using the agreed standards, until this investigation was conducted. It has been determined that most specimens tested during this investigation exhibited anisotropic, viscoelastic characteristics. Some specimen groups were found to be slightly more time-dependent than others, but generally, there was little significant difference between groups, regardless of the number of layers or the amount of pretension exerted on embedded fabric.

Even when compared to specimens without fabric, no significant difference in multi-axial deformation was observed.

5.7.4 Summary of PDMS membranes embedded with fabric

It has been revealed that the introduction of fabric produces a small, initial increase in membrane hardness, and that there was a strong linear relationship between the amount of tension exerted on the fabric during the embedding process and the increase in hardness (R^2=1.00).

Notably, it was found that the presence of embedded fabric limited the overall strength and extensibility of PDMS membranes especially when oriented in the wales and bias directions. The pretension of the fabric in the bias, in particular, had the largest effect on the anisotropic behaviour of PDMS membranes, that was characteristic of soft tissue membrane behaviour in many ways, except in UTS. Specimens tested in the bias doubled in strength, while specimens in the coarse and wales weakened by a third. When oriented in the bias, PDMS with embedded fabric at 100% pretension, was ten times stronger and three times more extensible than the fabric alone. While specimens containing fabric with 50% pretension were more resilient in overall strength and extensibility.

A strong linear relationship was also found between UTS and the pretension of embedded fabric (R^2 = 0.9896), while the multi-layered specimens containing fabric oriented in the wales direction during extension were found to have a strong linear relationship between Young's modulus and pretension of the embedded fabric (R^2 = 0.967).

During multi-axial characterisation, specimens exhibited an anisotropic, time-dependent viscoelastic response to loading.

5.8 Conclusion of PDMS membranes with embedded yarns

The mechanical influence of PDMS composites with embedded elastane yarns was investigated. The fabrication, test methods and results have been presented with a specific focus on creating new knowledge for the interdisciplinary researcher and prosthetists with an interest in improving clinical or theatrical prosthetic design practice.

Prior to this investigation, the precise influence that continuous, unidirectional, elasticated yarns had on PDMS composites was unknown in the literature. Previous investigations have used cast PDMS filaments with differing hardness's in an attempt to mimic the non-linearity of soft tissue membranes like human skin with some success.[210, 211, 212] Multi-material PDMS-based isotropic materials were blended and layered in various ways to achieve elastic modulus close to that of skin, but the lack of adjustable fibres and fibre architecture in previous strategies, limited the mechanical control over known behavioural characteristics of soft tissue membranes such as hardness, strength and extensibility.[50] Moreover, the lack of explicit test standards used in the published experiments made repeatability amongst peers problematic, especially for uni-axial tensile tests.

In contrast, the multi-material composites explored and characterised in this work, have shown how the lamination of multi-material PDMS composites and adjustability in direction of embedded yarns can reduce extensibility in mechanically weakened membranes. In particular, this work has revealed how embedding of elastane yarns, and manipulation of the embedded yarn tension and orientation were in agreement with the literature on human skin. The influential changes that have been presented here can be used to control aspects of anisotropy and viscoelasticity that were not previously achievable.

Most importantly, adoption of previously undocumented fabrication materials and methods, that are familiar to clinical and theatrical prosthetists, such as layering and embedding of reinforcing textiles, are crucial to wider audience uptake and engagement with the findings of this work.

5.8.1 Conclusions of PDMS membranes embedded with fabric

The purpose of this explorative work was to identify influential additives able to alter the mechanical characteristics of PDMS gels and elastomers. Achieving mechanical properties like hardness and tensile strength similar to soft tissue membranes can be achieved by procuring suitable, commercially available PDMS and additives. Using the information documented here, variations from 10 H OO to 50 H A and from 10kPa to 10MPa respectively are acheivable.[356, 357] However, engineering PDMS composites that yield more complex biomechanical traits such as anisotropic viscoelasticity and adjustable elongation is far more involved than choosing the right base material. Experienced prosthetists have been embedding fabrics in PDMS membranes for decades, with a deep understanding of its benefits, mainly that it increases the native strength of commercial PDMS elastomers, but this technical know-how has remained the embodied, tacit knowledge of the prosthetists domain, remaining unpublished and unquantified, until now.

Finally, this work has revealed conclusive data-based evidence that proves the orientation and tension of embedded fabric has a direct, measurable influence on a range of mechanical characteristics, beyond simply adding strength. Moreover, this work explicitly contributes new knowledge to the field of functional prosthetics by describing the mechanisms for control over key behavioural traits linked to the performance of organic counterparts such as; extensibility, elasticity, anisotropy, and viscoelasticity.

Chapter 6

Mechanical Effects of Oil Dispersal on Silicone Gel Membrane Behaviour

6.1 Introduction

In this chapter, changes in the mechanical properties of silicone gel when incremental amounts of oil were added was investigated. More specifically, the mechanical influence of PDMS (polydimethylsiloxane) oil dispersion in a two-part, room temperature vulcanising (RTV2) PDMS gel has been characterised using a variety of repeatable standards to support the development of very soft, simulated oily tissues, like human subcutaneous adipose tissue (fat).

An overview of previous PDMS gel use, as a soft tissue simulant material in clinical and theatrical prosthesis, was provided as a background to this work in Chapter 2. In particular, the behaviour of adipose tissues and synthetic surrogate properties were discussed to help frame unique characteristic traits. Here, their suitability as adipose tissue simulants are produced and assessed. To do this a series of PDMS gel membranes were prepared with varying amounts of added oil and were subjected to rigorous testing. Before any surrogate tissues could be formulated, a series of indentation tests by durometer, on warmed porcine adipose tissue were conducted to establish a benchmark data set. A series of PDMS composite membranes were then produced and subjected to identical tests to determine changes in hardness as the amount of oil was increased. The gathered data on hardness was compared to data on human adipose tissue given in the literature. Next, the effect of oil dispersal on PDMS gel cure-time was ascertained and documented. Uni-axial tensile tests on oil saturated PDMS membranes established the elastic modulus, strength and stress/strain behaviour as the amount of added oil was increased, while also allowing for the identification of any unexpected behavioural phenomena evident in the stress/strain characteristics. Finally, multi-axial tests were conducted to identify the effect of preconditioning on the viscoelastic, time-dependent properties of the PDMS membranes at specific hardness intervals.

The overarching objective of this chapter was to create new knowledge concerning materials that were familiar to clinical and theatrical prosthetists, presenting results in a way that was accessible to researchers, designers and modellers as well as prosthetists from various disciplinary backgrounds. Providing results using

standardised methods may enable user groups to recreate mechanical characteristics of materials presented in the current study for a variety of subject specific uses including, but not limited to, clinical and theatrical prosthetics as well as soft tissue simulation for surgical training.

6.2 Methods and materials

PDMS gel with Shore A hardness of 10 was combined with pure PDMS oil to identify its influence on behaviour. Internationally agreed test standards used in this study, allow direct comparative analysis with the literature.

6.2.1 Test standards and equipment

A summary of the test standards and equipment used in this investigation are discussed in detail in Chapter 3. Variations specific to this chapter are described below.

6.2.2 Specimen grouping and storage

Five test groups were created for this experiment. Each of the five test groups contained different amounts of oil, and each group consisted of five test specimens (not including three spare specimens in case of defects). All specimens were created in one week from the same batch of ingredients and materials and stored together at room temperature for four weeks until testing commenced. All tests were conducted within two weeks, and the temperature and humidity were recorded before and after each test.

6.2.3 Material selection

As discussed in previous chapters, a commercially available PDMS gel (*Polytek*, PlatSil® gel 10, Neills Materials, Bury St Edmunds, UK) with Shore A hardness of 10 was used; it is referred to as the 'PDMS gel' herein.[177] More specifically it consists of a two-part, viscous fluids that need to be combined in equal parts in order to cure into an elastomer. The short cross-linking time (cure-time) of the chosen PDMS gel was important because the addition of PDMS oil in the gel (prior to curing) causes an increasing delay in cross-linking, slowing the cure-time gradually as more oil is added. The PDMS oil was dispersed in PDMS gel during preparation to ensure homogeneity. The amount of oil added to each group was increased in 50% increments from 0% to

200%, by weight. Here, the mechanical influence on the cured materials was examined with respect to agreed standards.

Both PDMS gel and oil are widely available in the UK and internationally via '*Polytek* Development Corp' (MA, USA), 'Smooth-on Inc', (PA, USA), 'Wacker Chemie AG', (Munich, Germany) and many other global distributors and has been used in similar previous studies by the author and others.[6, 11, 104, 358, 359]

6.2.4 Porcine fat preparation

Porcine adipose tissue was harvested from the belly fat of an 18-month-old bacon pig slaughtered for consumption, purchased commercially from a licensed local butcher (Michael Carter fresh foods, Mapperley, Nottingham), 24 hours after slaughter and stored in a chilled cabinet. The outer skin and underlying flesh were debrided from the fat to a uniform thickness of 6 mm using a surgical scalpel whilst chilled. The fat specimens were allowed to warm up to room temperature, then further warmed to 37°C in saline solution before testing. Testing was conducted using a OOO calibrated Shore hardness durometer (Rex gauge LLC, IL, USA) mounted onto a RX-OS-4H stand (Rex gauge LLC, IL, USA) to eliminate operator error. Twenty-five readings were taken from three separate specimens from the same region of the same animal and recorded as per the standard previously mentioned.

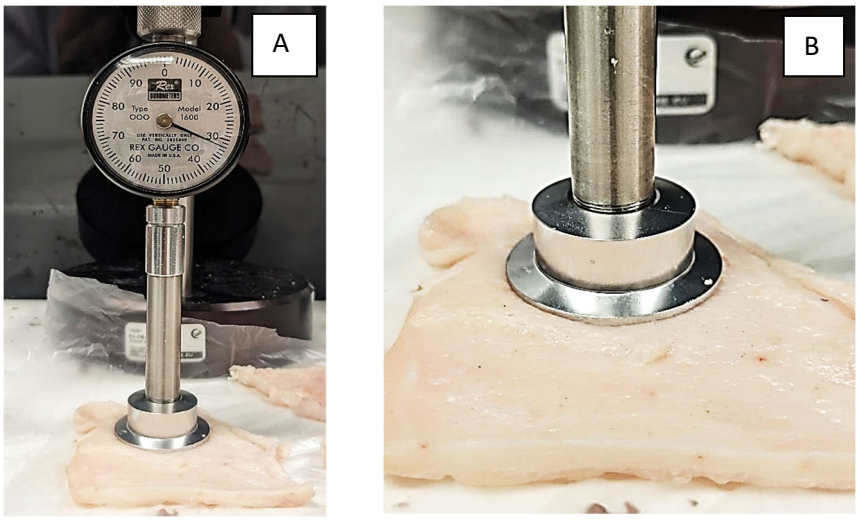

Figure 6.1 Hardness testing on porcine subcutaneous adipose tissue. *Data gathering using a OOO calibrated Shore hardness durometer. Image 'A' shows the durometer mounted to the test stand to minimise user error. Image 'B' shows a close-up contact with the specimen during the test.*

6.2.5 PDMS gel and oil preparation

All of the synthetic, elastomeric materials were prepared as per the standard (BS/ISO23529: 2016). To ensure the methods and results are widely accessible, materials were weighed, poured and mixed by hand in a plastic beaker using a clean wooden tongue depressor to mitigate contamination risk. There are known contaminants that may cause PDMS cross-link inhibition (sulphur, tin and tin-based alloys or compounds) or equipment bonding (glass/silica chemical bonding). The gel was thicker and more opaque than the oil, so visual and tactile queues were used to ensure oil dispersion in the gel. While mixing, a yellow colour was also added to aid mixing and ensure homogeneity. This method of material preparation, by hand, was given preference over available, automated mixing machines, because automated machines are the primarily the domain of engineering applications and are rarely used by clinical prosthetists and never used by theatrical prosthetists due to cost and time implications. More-over, research also suggests that hand mixing (by an experienced user) offer better mixing results over a wider range of materials and fillers.[348]

Each mixture was stirred for five minutes until thoroughly homogeneous before being degassed in a vacuum chamber for five minutes at -982 mbar (-736 mm Hg) to remove entrapped air from the mixture. After degassing, the mixture was removed from the vacuum chamber, poured into a levelled gauge mould that measured 500 mm x 500 mm x 2 mm and allowed to cure for 24 hrs. Once cured, the membrane was powdered with talcum powder before being cut into test specimens, dumbbell and disc shapes for the uni-axial and multi-axial tests respectively.

Figure 6.2 Multi-axial test specimens after testing*. All of the specimens were prepared, stored and tested over consecutive days to mitigate variable changes in specimen condition or test environment. After testing, specimens were stacked and stored as pictured above, for future reference.*

Specimens were cut prior to demoulding to mitigate the risk of sample distortion or warping prior to or during cutting. The back side of each specimen was also powdered with talcum powder during demoulding to prevent self-adhesion upon removal and storage. Completed specimens were stored according to the given standard above until tested.

6.3 Results

All individual datasets are reported in the appendix (see content). The results that are presented only describe the characteristics of the test specimens from a tactile perspective. The optical and visual analysis via digital image correlation are excluded from this study.

6.3.1 The effect of oil dispersal in PDMS gel cure-time

A total of 25 specimens were prepared for this experiment, five groups of five, each group with varying oil content (0%, 50%, 100%, 150% and 200% oil).

Adding PDMS oil is known to slow cross-linking in all PDMS gels, but no values have been given in the literature. Hence, for this study, it was useful to document the precise impact of oil addition on the cure time. The full cure time is defined here as the demoulding time, not the working time. Full cure occurs where the material was no longer tacky and could be removed from the mould without leaving a residue. Working time is the period the gel stays in its fluid state.

It was found that when blended with the PDMS gel, PDMS oil slowed reaction time by 63% (15 minutes) with the introduction of just 50% oil. For each additional 50% of oil, reaction time was delayed by an additional 31% +/- 13% (average of 7.5 minutes +/-3mins). Ambient test conditions were 23.7°C and 15% RH (relative humidity). Cure time is not affected by volume as PDMS is a room temperature vulcanising elastomer so is only affected by ambient temperature, not volume.

6.3.2 Hardness

All hardness data was gathered and prepared using the guidelines given in the standard. Results are reported using three characterisation perspectives, as specified by the standard: Shore hardness, spring force and linear regression.

6.3.2.1 Shore hardness of porcine SAT and PDMS gel with dispersed oil

Results of the indentation tests using a Shore OOO calibrated durometer on warmed (porcine) subcutaneous adipose tissue showed an average of 31.7 H OOO with a standard deviation of 6.91 H OOO. Only porcine hardness by indentation is reported to offer a context to indentation results on surrogate specimens, because it is the only standard where both materials lay within the remit of the standard.

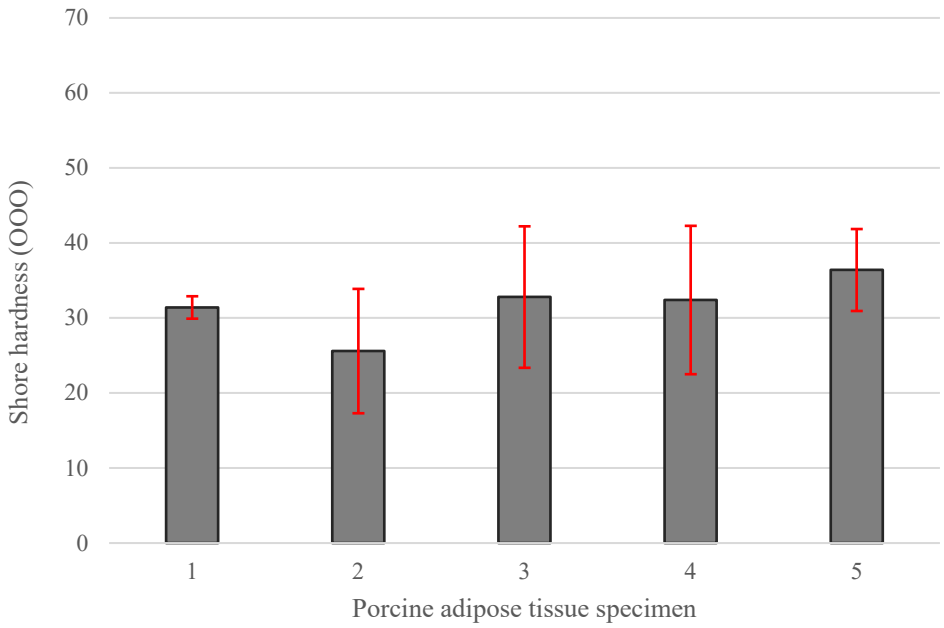

Figure 6.3 Shore hardness values (000) - The hardness of porcine adipose fat

The results of shore hardness tests conducted on porcine adipose fat taken from the belly fat of an 18-month-old bacon pig, measured with a OOO calibrated durometer. The error bars represent the standard deviation of the data sets and are shown in red.

In identical hardness tests on PDMS specimens, it was found that, as the amount of oil was increased, the hardness of the material significantly softened, steadily becoming softer as the added oil was increased. After a slightly larger initial drop in hardness of 16 H OOO between the control group with no added oil and the group with the least amount of added oil (50%), hardness gradually depleted as more oil was added. The average reduction in hardness across the remaining three groups (O3, O4 and O5) was 9 H OOO for every 50% of added oil.

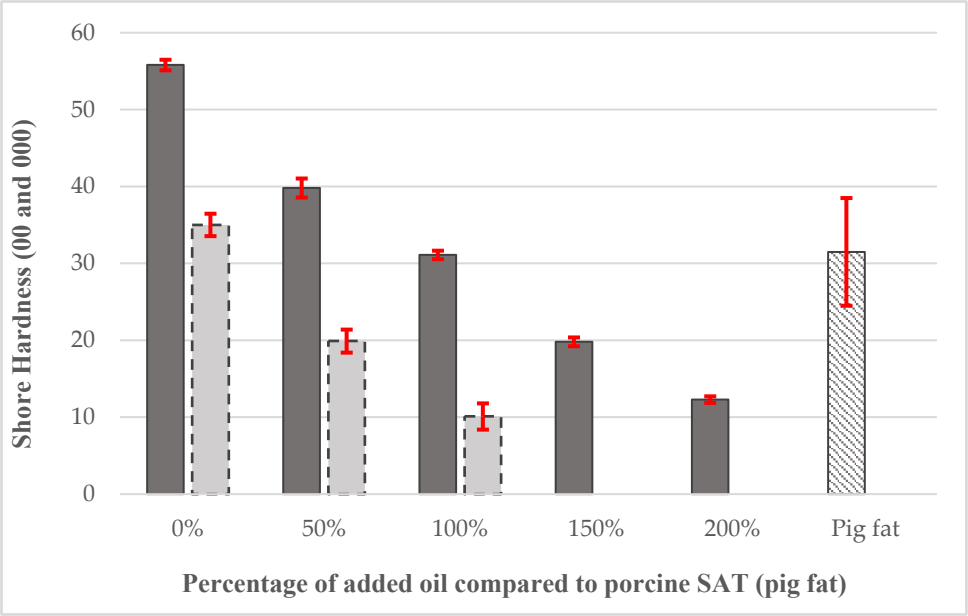

Figure 6.4 Shore hardness values (OO and OOO) - *The influence of increasing oil content. Each bar represents shore hardness between 0 and 60. The dark coloured bars show the 000 hardness while the lighter coloured bars show 00 hardness for each group. The cross-hatched bar represents the mean hardness of porcine SAT. Error bars shown in red for each group represent the standard deviation.*

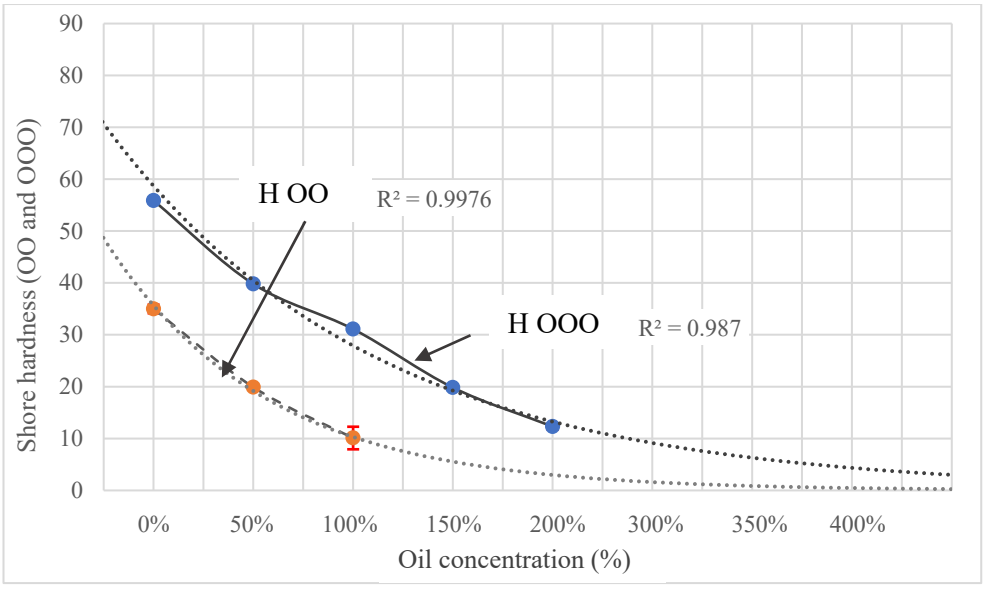

Figure 6.5 Shore hardness values (OO and OOO) influence of increasing oil content. *Results shows two shore hardness scales for direct comparison. The data line is marked by solid line (labelled) H OO and H OOO Shore hardness. A predictive negative exponential trend is shown by the dotted line. Error bars are present in red for each group representing the data set's standard deviation, but the small deviation in results makes seeing the error bars difficult. To see the error bars more clearly, see figure 6.4.*

6.3.3 Linear regression of PDMS gel membranes with dispersed oil

The negative exponential trend regression for both hardness scales (H OO and H OOO) used to measure specimens are shown in figure 6.5 for comparison. As can be seen in the graph (fig 6.5) only OOO hardness range was able to span the range achieved with oil saturated specimens and should be considered the most reliable data set. Data gathered at OOO Shore hardness had a negative exponential trend value of $R^2 = 0.9875$, and the equation for the relationship shown below (equation 6.1)

$$y = 85.184e^{-0.372x} \qquad Eq.\ 6.1$$

For OO Shore hardness readings, the linear regression was found to be similarly strong, at $R^2 = 0.9976$. The formula for a linear relationship has been provided below (equation 6.2)

$$y = 66.311e^{-0.62x} \qquad Eq.\ 6.2$$

6.3.4 Spring force

The force required to overcome the calibrated spring force at 55 H OOO was 0.7 N, while at 40 H OOO the force was 0.56 N. Spring resistance continued a downwards trend to just 0.29 N at 10 H OOO. The spring calibration tolerance in all indentation tests by durometer was 0.00908 +/- 0.0182 N. The resistive spring force in Newtons was calculated using the formula given below in equation 6.3 as per the standard.

$$N = 0.203 + 0.00908\ H\ OOO \qquad Eq.\ 6.3$$

6.3.5 Uni-axial tensile testing of PDMS gel membranes with dispersed oil

All PDMS specimens underwent uni-axial testing as per the standard. Analysis of uni-axial data has been presented using the standard format. In uni-axial examination specimens were securely fastened with pneumatic clamps, to prevent slippage, to a tensile testing machine and extended to failure to determine the ultimate tensile strength, elastic modulus. The stress strain curves also offer an insight into the mechanical characteristics of each specimen during extension.

Results are reported with a focus on three characteristic specimen traits, as specified by the standard; Ultimate tensile strength at high strain rates, elasticity at low strain rates, expressed as Young's modulus, and force versus strain (as this is more accessible than stress against strain).

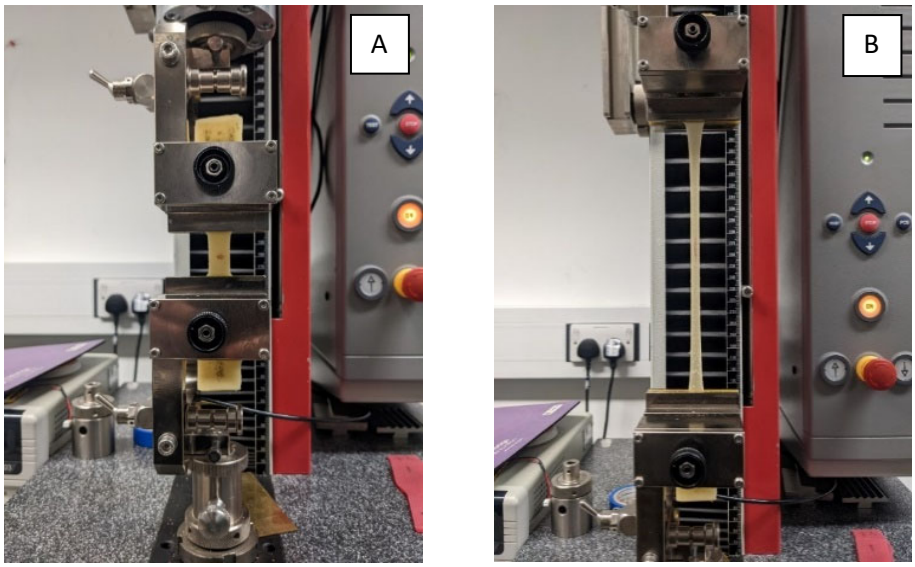

Figure 6.6 Tensile test specimen mounted to the tensiometer.

Image 'A' shows the specimen at a low strains. Image 'B' shows the specimen during testing at a high strain prior to failure. The use of pneumatic clamping jaws seen in the images was effective at preventing specimen slippage seen in other studies because the jaws tightened on the specimen as thinning occurred during extension.

6.3.6 Ultimate tensile strength of PDMS gel membranes with dispersed oil

During uni-axial testing, UTS data was gathered as per the standard. A comparison of the UTS for all PDMS test specimens are shown in Figure 6.7. Porcine SAT was not tested because a uniform membrane, demanded by the standard, was not feasible without freezing the tissue, which changes the mechanical properties of soft tissues. The load cell used in all tests remained the same to enable reliable comparison among groups with different compositions. Despite an initially steep loss of strength with the introduction of oil, strength was lost at a much slower rate as the amount of oil was increased beyond 50%. The addition of just 50% added oil weakened the PDMS gel by 73%. The force required to rupture the specimens can also be seen in figure 6.7, demonstrating that changes in UTS are dependent on oil content.

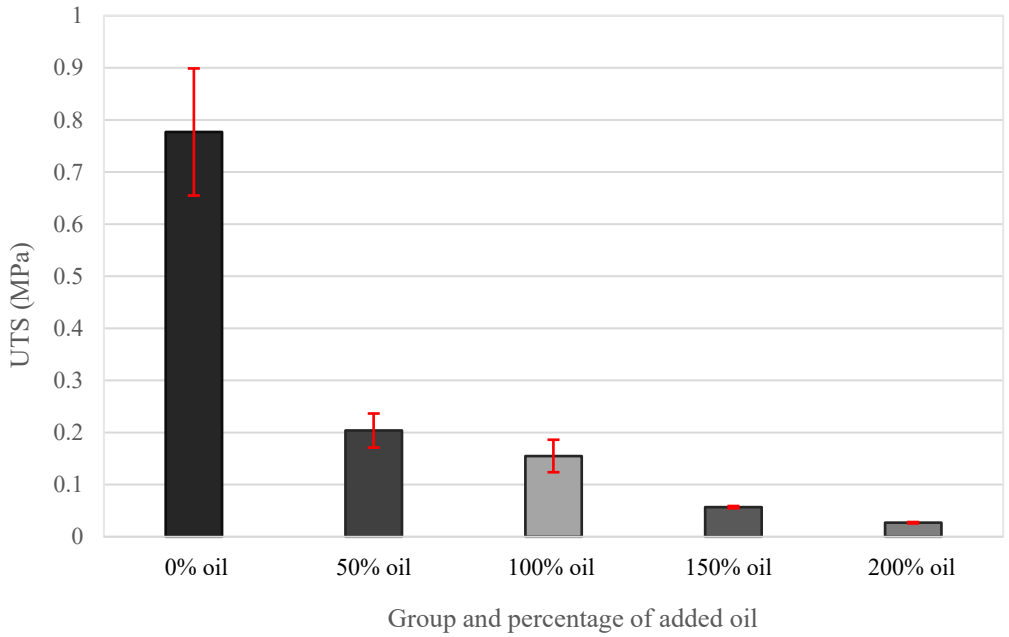

Figure 6.7 Ultimate tensile strength (UTS) - The influence of increasing oil content. *Ultimate tensile strength tests show the effect of adding oil on the mechanical strength of PDMS. Error bars (shown in red) indicate the standard deviation. The predictive model for this data has been presented in figure 6.8.*

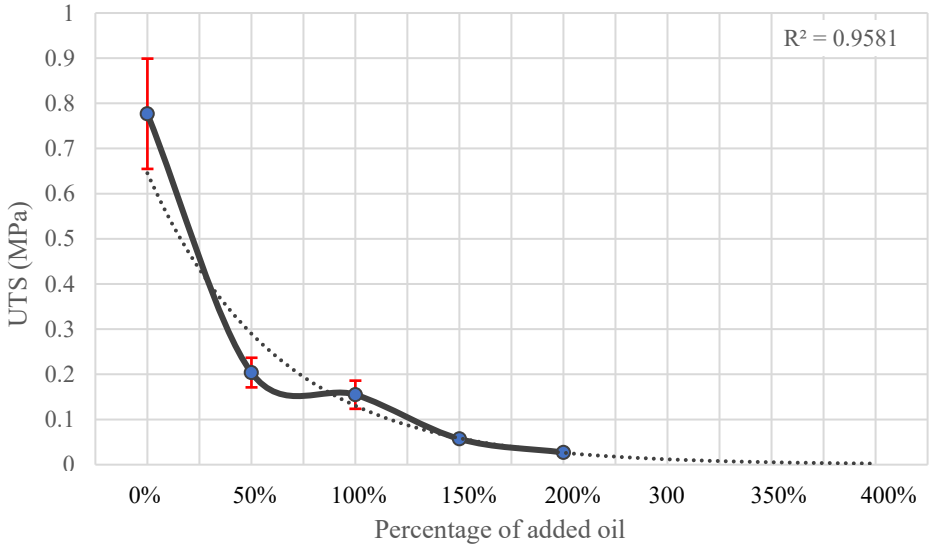

Figure 6.8 Ultimate tensile strength (UTS) predictive model- The influence of increasing oil content. *A clear negative exponential relationship can be seen between the decrease in UTS and the increase in oil content in all specimens tested. The negative exponential trendline was chosen here as the best fitting model and is shown by the dotted line that was predicts the strength to dimmish to less than 0.01 MPa at 350% added oil. Error bars are shown in red.*

The R^2 value for the UTS was calculated to be R^2= 0.9581 and the equation used to calculate this given in equation 6.4.

$$y = 1.4358e^{-0.799x} \qquad Eq.\ 6.4$$

The error value (standard deviation) declined among specimens in each group as the added oil percentage was increased, diminishing to 0.001 in specimens with 200% added oil. A regression model of data without the control group (0% oil) offered better linearity R^2 = 0.9623 using the equation given in equation 6.5.

$$y = -0.0629x + 0.268 \qquad Eq.\ 6.5$$

6.3.7 Young's modulus of PDMS gel membranes with dispersed oil

Elastic modulus was calculated using the deformation slope's first, rising, linear part. All readings were taken after the initial toe region of the curve as the specimen straightens under loading but before the anisotropic area of the curve.

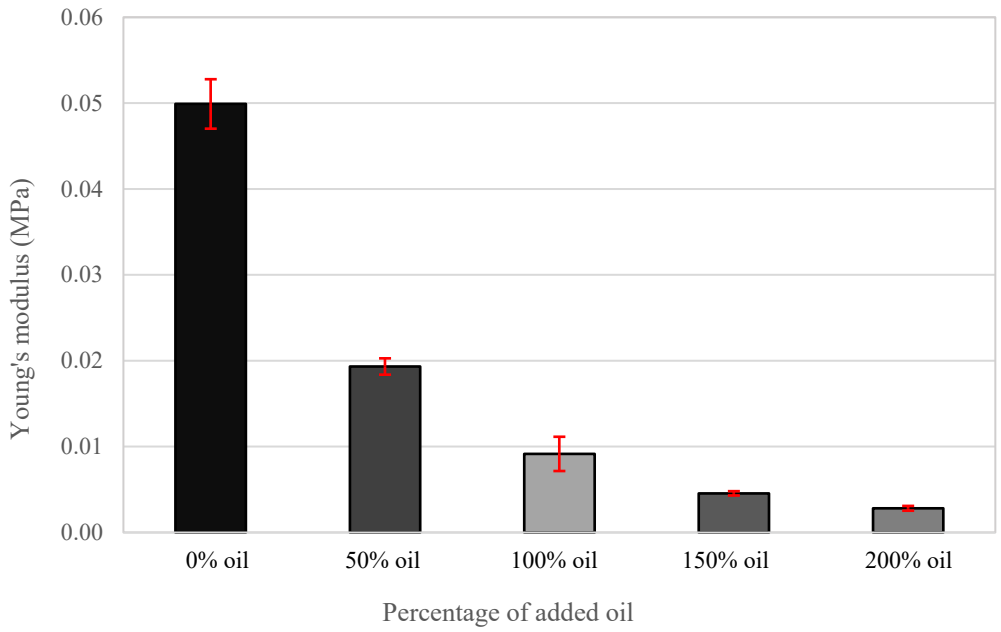

Figure 6.9 Young's modulus - The influence of increasing oil content.

Bar chart showing the change in moduli with increasing amounts of PDMS oil. Error bars indicate the standard deviation in each group of 5 specimens. Each bar represents the arithmetic mean average deformation (mm) observed in each group tested. The linear regression value is presented along with the derivative equation used to calculate the value in figure 6.10.

For Young's modulus, the elastic region was under 1 N and under 100% extension in all the specimen groups tested with oil and the control group without added oil.

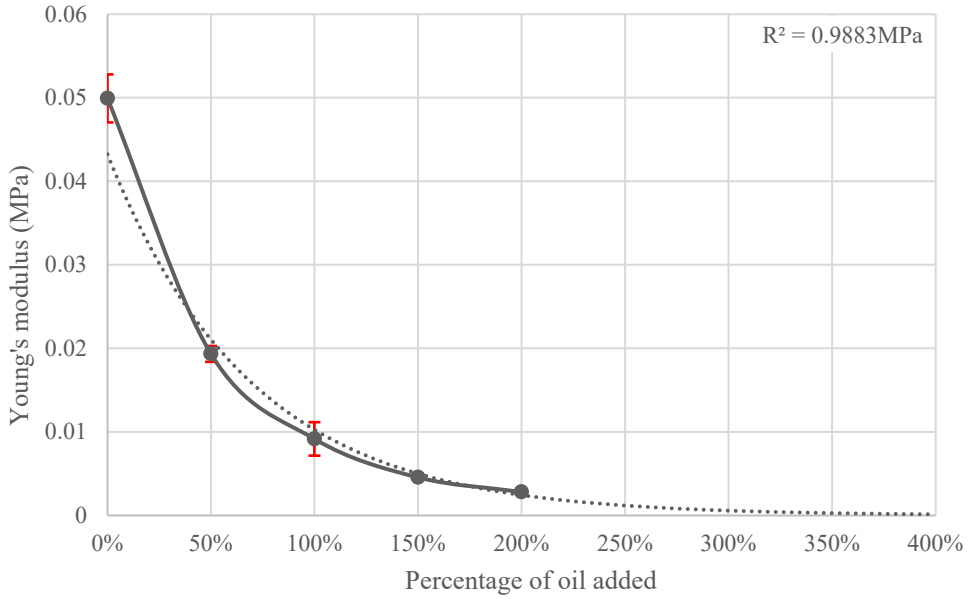

Figure 6.10 Young's modulus predictive model - The influence of increasing oil content. *A clear negative exponential relationship can be seen between the decrease in Young's modulus and the increase in oil content in all specimens tested. The negative exponential trendline was chosen here as the best fitting model and is shown by the dotted line that was predicted to diminish to less than 0.001MPa at 350% added oil.*

Evaluation of the linear regression revealed a value of $R^2 = 0.9883$, suggesting a strong relationship between the amount of oil added and Young's modulus. Equation 6.6 was used to calculate the R^2 value of the modulus.

$$y = 0.0432e^{-1.438x} \qquad \textit{Eq. 6.6}$$

With the addition of just 50% oil, the elasticity of the PDMS fell by >60% to 0.019 MPa. With the addition of 100% oil (equal parts PDMS gel and oil) elasticity fell by >80% to 0.009 MPa. This trend in decreasing elastic modulus continued throughout the test specimen groups as the amount of added oil was increased. At the maximum amount of added oil (200%), the modulus was just 0.002 MPa (or 2 kPa).

6.3.8 Force versus extension results of PDMS gel membranes with dispersed oil

Uni-axial results are displayed in standard force (N) against strain (%), as per the standard. Figure 6.11) shows all of the groups together for comparison, while Figure 6.12 offers a closer look at the results with a specific focus on the graph vectors of specimens that contained oil.

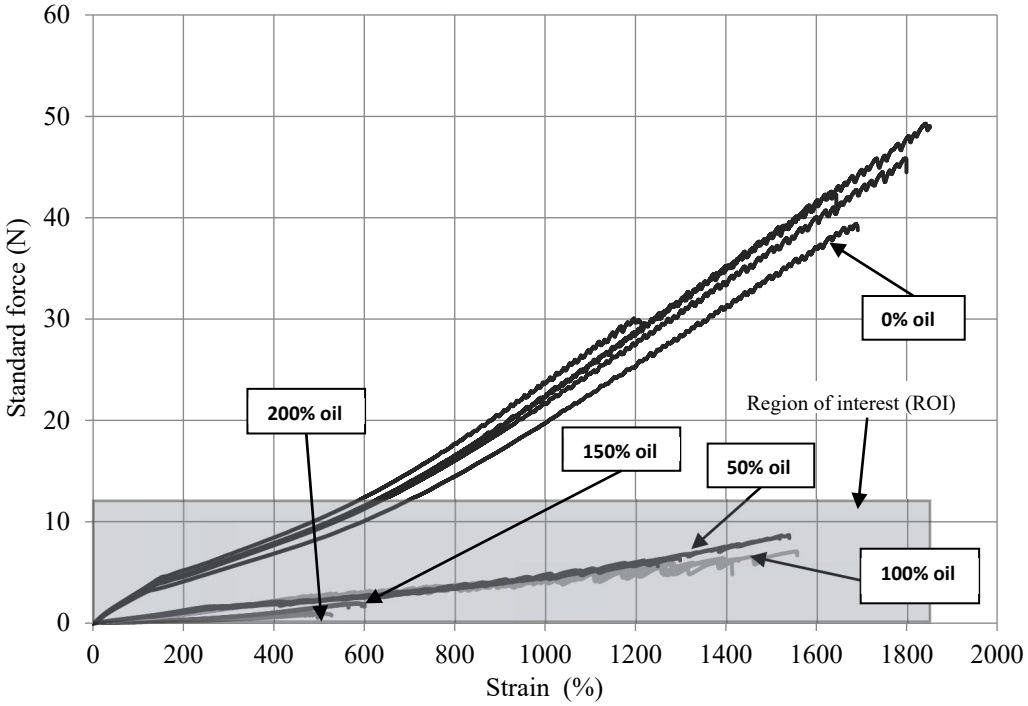

Figure 6.11 The influence of increasing oil content - Uni-axial extension to failure.
Each group is labelled with its respective oil content. In this figure, all specimen groups are shown to reveal the comparative changes in mechanical properties, with and without added oil. Data from specimens containing oil appear on this graph to have a linear, Hookean vector at this scale. To clarify the influence of oil addition, the reader is invited to see the graph below that shows the region of interest presented in more detail. Figure 6.12 provides a zoomed in view of the region of interest.

In Figure 6.11, it can be seen that the two groups containing the most added oil exhibited a decrease in overall extensibility of >1000% when compared to the three remaining groups with no oil and less oil added. These results are more clearly revealed in Figure 6.12, which allows a closer inspection of the region of interest highlighted by the selected area above.

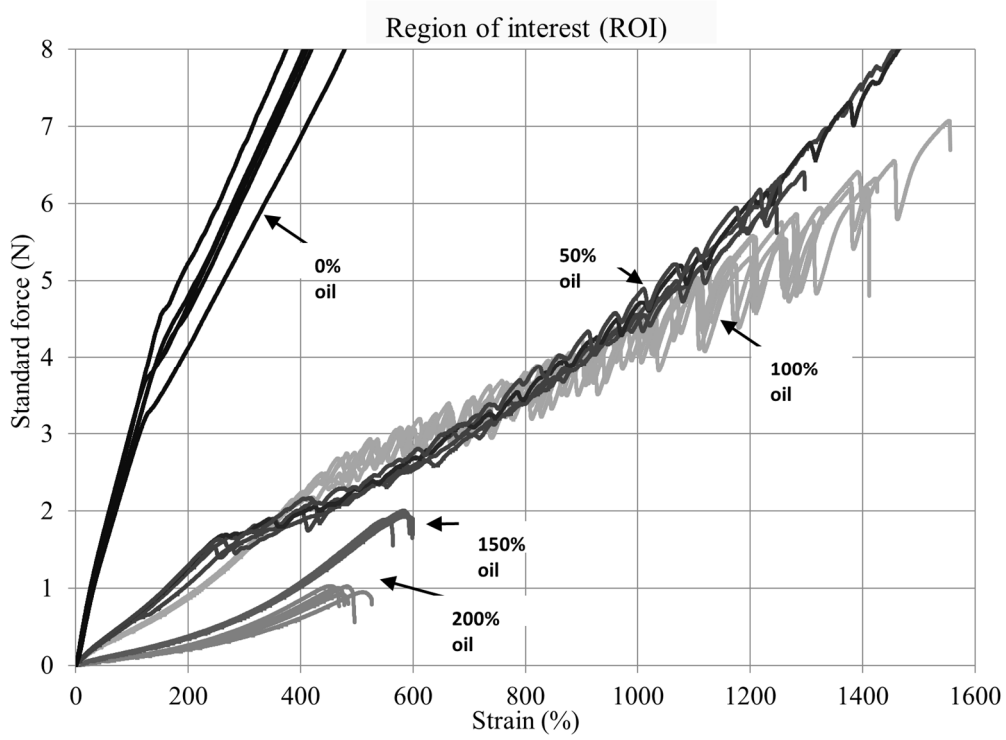

Figure 6.12 Uni-axial extension to failure (force versus strain %) - Magnified view of region of interest, showing the influence of increasing oil content more clearly.

An enhanced view of the ROI indicated by the highlighted box in Figure 6.11. After a closer inspection of stress strain curve characteristics, it can be seen that all specimen groups exhibit a strain hardening quality, with a relatively short linear elastic region followed by a gradually steepening vector.

The two groups with the most added oil showed the lowest ultimate tensile strength, yield, and breaking point, all occurring in short succession. This is suggestive of a very weak, hyperelastic gel with non-linear, characteristics.

Robust, and highly elastic at low strains up to 100 % elongation, the PDMS without added oil also had a very long, non-linear, hardening trajectory up to around 1000 % elongation; this non-linear region is the viscoelastic strain hardening region where the atomic crystalline structure begins to fracture and reorganise, hardening in the process. At very high strain rates, between 1000 % and 1800 %, all specimens in the group with no oil group began to exhibit signs of permanent deformation. Specimens with the least amount of added oil (50% -100%) exhibited an inclined serrated vector at high strain rates during extension, evidence of Luders banding propagation and the subsequent Portevin La Chatelier effect.

All specimens in the two groups with the least amount of added oil also behaved this way, exhibiting three very different behavioural zones. One group (without oil) had high elastic modulus and high extensibility, another group had lower elastic modulus but equally high extensibility (50% - 100% added oil), and finally, a third group (150% - 200% added oil) had low elastic modulus and very low extensibility.

6.3.9 Multi-axial test result of PDMS gel membranes with dispersed oil

Multi-axial data analysis has been presented using the standard adopted from elastic fabric test standard procedures, as described in Chapter 3. The influence of oil content on deformability and time-dependent loss of elasticity was observed, which was expected given the results from the uni-axial tests. Exaggerated extensibility was immediately noticeable as shown in figure 6.13. Hysteresis, force degradation, unrecovered deformation and force decay were measured, and the results are presented forthwith.

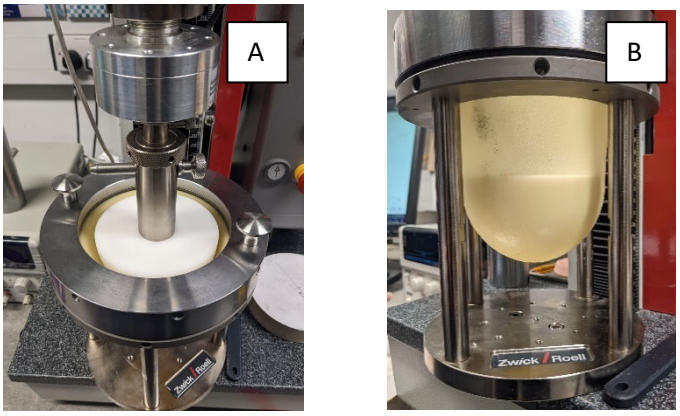

Figure 6.13 Specimens mounted to Zwick Roell ring clamp during multi-axial testing.
Image 'A' shows the test apparatus during dynamic multi-axial testing. Image 'B' shows specimens with 200% exhibiting extreme extensibility (>70mm at 5 N) due to added oil.

6.3.10 Hysteresis of PDMS gel membranes with dispersed oil

The mechanism for the preconditioning effect is discussed in more detail in Chapter 2. During preconditioning of the control specimen group, that was lacking added oil, only slight changes were seen in loading and unloading vectors, typical of a pseudoelastic material behaviour.[54] As the oil content increased, the elastic response gradually slowed, demonstrating increased viscoelastic strain softening at and above 100% oil saturation (shown in figure 6.14). Greater change during preconditioning was observed in all groups with added oil. The loading and unloading curves for all

specimens are shown comparatively, below, in figure 6.14.

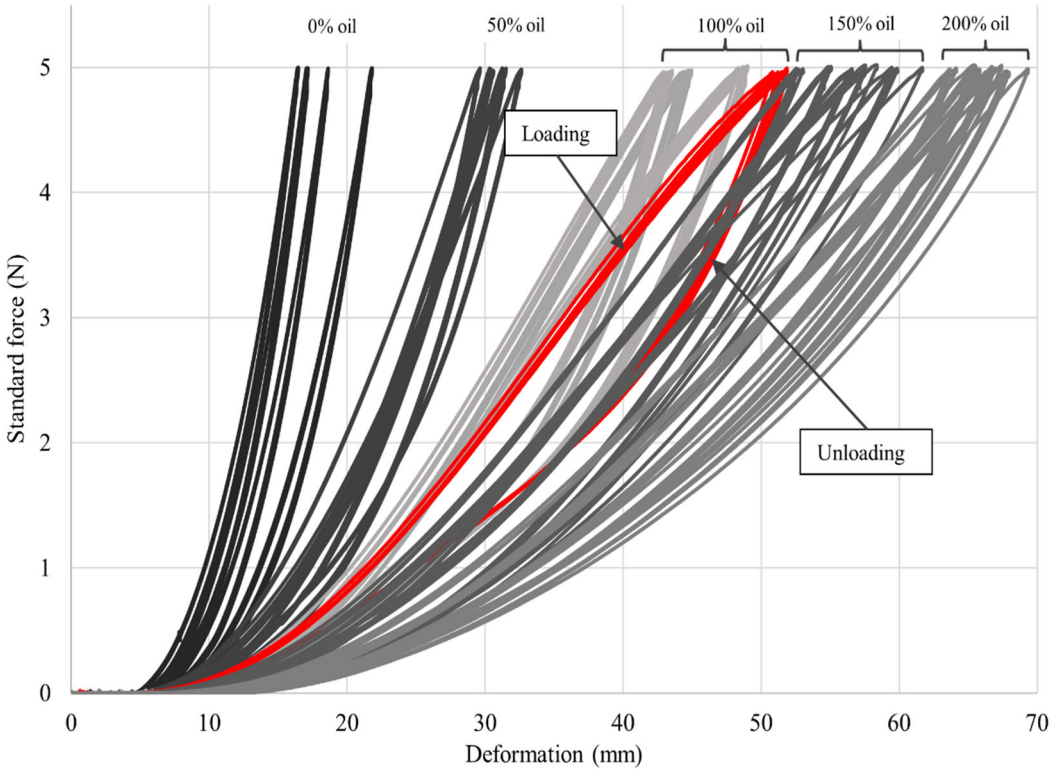

Figure 6.14 The influence of increasing oil content: Hysteresis (force vs deformation). *Multi-axial cyclical tests measuring the characteristic hysteresis loops exhibited by each group. Each specimen preconditioning is shown in the graph rather than an average of the group. Five loading cycles and five unloading cycles were conducted for each specimen. The first loading cycle for each group is seen on the extreme left in every group, while the final unloading cycle can be seen on the extreme right of each group. In the interest of clarity, one specimen cycling (with 100% oil) has been highlighted in red to demonstrate the loading and unloading cycle. All specimens are labelled and sectioned with brackets to clarify where the specimen groups begin to overlap at any point on the loading or unloading curves.*

6.3.12 Force degradation of PDMS gel membranes with dispersed oil

To examine the amount of force degradation, 5N of force was applied to each specimen and the loss of energy calculated to help determine the extent and speed of relaxation. This experiment helps describe how materials will behave over time while relaxing, following repeated deformation. It was found that relaxation was still slightly declining by the end of all tests, in all groups, but not significantly.

As can be seen in Figure 6.15, there appears to be no clear relationship between the

amount of added oil and the rate of energy loss in all specimens when held at 5 N for 60 seconds.

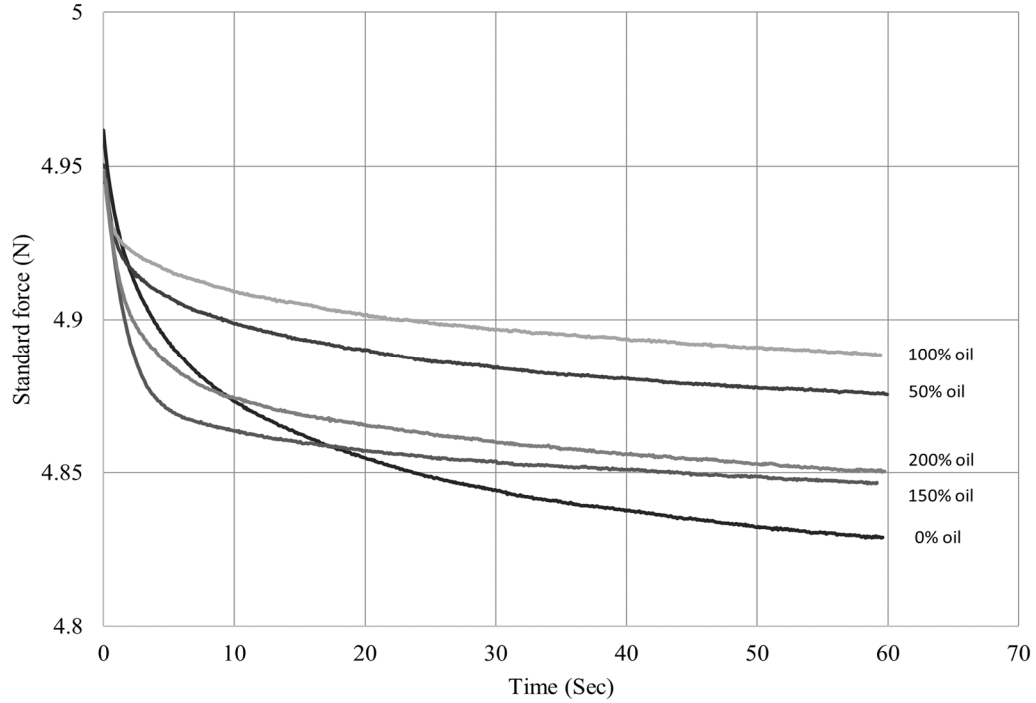

Figure 6.15 The influence of increasing oil content - Force degradation measured over 60 seconds while held at 5 N.

Presented results are the mean averages of experiments on each group. The graph shows the poor relationship between change in force degradation and the amount of added oil. Each vector represents an average of each group's rate of force decay. Each group is labelled according to the amount of oil used in its preparation.

However, the group with 150% oil content behaved slightly differently than the rest of the groups, exhibiting greater energy loss than the other specimens during the first five seconds of the tests.

Conversely, less energy was lost for the remainder of the 60-second test period compared to the other groups tested. All of the groups with added oil lost most of their stored energy within the first two to three seconds proceeding to relax more slowly for the duration of the test, whereas, in contrast, the PDMS without oil had a much more gradual loss of energy over the 60-second test period. Although some differences were apparent in the graph, the loss of force is relatively small in all cases (<0.05 N) and therefore was not significant. Deviation among specimens was also insignificant (<0.1 N).

6.3.13 Unrecovered deformation of PDMS gel membranes with dispersed oil

Unrecovered deformation or 'bagging' results record the rate of permanent change influenced by holding each specimen at 5N for 60 seconds. Analysis of the unrecovered deformation data revealed that each group exhibited gradual incremental plasticity or permanent deformation, except for the group with 150% added oil, where the amount of permanent deformation was approximately twice what one might assume when compared to other specimen groups. This group also had a significant deviation of almost 5 mm between specimens, indicating an unexpected anomaly in all specimens with 150% added oil content. Results demonstrate the material's permanent deformation rate increased as more oil was added. The graph helps illustrate the disproportionate increase in permanent deformation at 150% oil content compared to the other groups tested. The sharp increase in plastic deformation at 150% distorts the otherwise steady incremental plastic deformation rate observed in all the remaining specimen groups, upsetting the initially strong predictive model and giving a low overall predictive R^2 value = 0.654 using the formula shown below in equation 6.6. Interestingly with group containing 150% oil removed from the chart, the predictive model is significantly improved and the $R^2 = 0.9881$ ($y = 0.5185x + 0.1181$).

$$y = 0.7137x - 0.0771 \qquad Eq.6.6$$

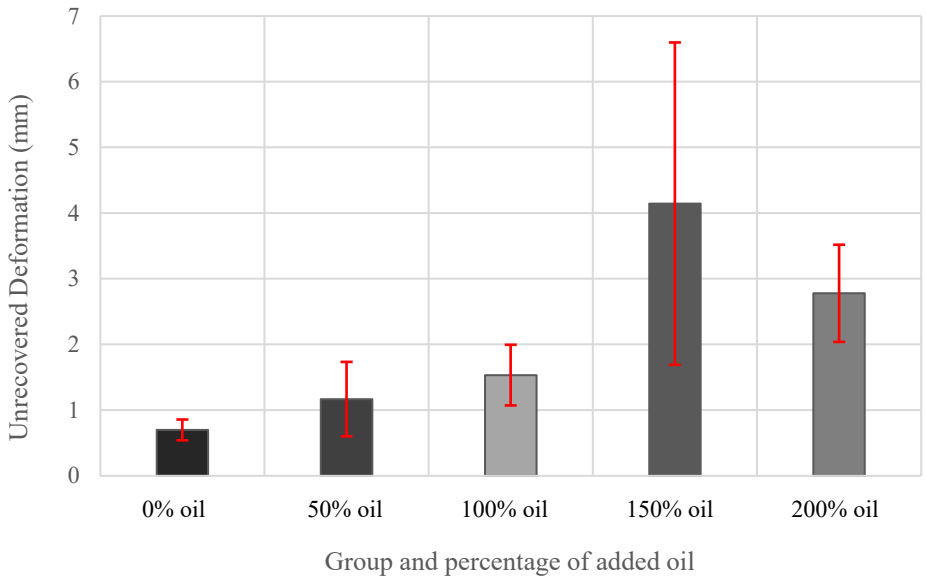

Figure 6.16 The influence of increasing oil content - Unrecovered deformation (mm).

Results show permanent deformation. Error bars indicate standard deviation.

6.3.14 Force decay of PDMS gel membranes with dispersed oil

Force decay results are shown in the chart (Figure 6.17).

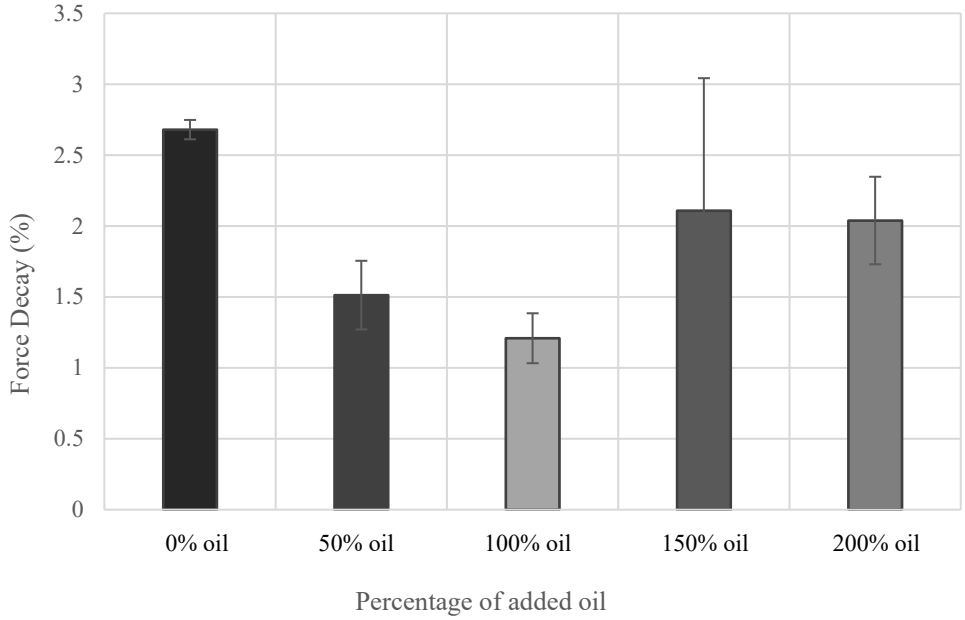

Figure 6.17 Force decay over 60 seconds - comparison of oil addition in PDMS gels. *Results demonstrate the poor relationship between oil content and the relaxation characteristics of the PDMS, with all specimen groups containing oil relaxing less than PDMS without oil.*

A force decay study was subsequently conducted where it was seen that there was a poor correlation between the amount of added oil and the rate of force decay over 60 seconds, with a difference of <1.5% among all specimen groups. This was supported by the low linear regression value of 0.363.

6.4 Discussion of results for PDMS gel membranes with dispersed oil

Characterisation of the specimens using standards for the testing of elastomers and elasticated fabrics were used to help verify the influence of oil dispersal and enrich the sparse data in the literature. More specifically, the principle focus of this work was to quantify the precise mechanical impact of incremental amounts of oil dispersal in five groups of test specimens. Data was gathered and analysed to measure the change in mechanical response to deformation. The test standards used to characterise material responses were chosen primarily to improve interdisciplinary comprehension, repeatability and dissemination amongst peers.

Previous mechanical characterisation of adipose fatty tissues has shown that the hardness, elasticity and strength are all quite low compared to other soft tissues and is beyond the reach of most commercially available synthetic gels. A priority for this work was to report measurable methods and predictive models for the softening of PDMS gels well below the mechanical values offered by commercially available materials.

It has been recognised that, despite its widespread use, porcine tissues, such as the skin, the liver and kidneys, can be up to twice as hard and less elastic than human equivalents.[11, 103, 110, 114, 236] This is especially true of the skin, where there are many differences between human and porcine skin, most notably- thickness and hardness, due partly to its different structure and surface topography.[236, 323, 361] Despite this, porcine fat has not explicitly been measured or compared to human fat, so it has been used sparingly in this study to offer a benchmark for comparison whilst considering the potential differences. In addition, the effects of temperature are rarely discussed in the literature, even though it is known to have a large influence on hardness and extensibility, which adds another layer of complexity to comparison between studies in the literature. In contrast, this study has been rigorous with all information necessary to repeat these experiments adding value to any future work in this area. In-depth analysis of animal or human tissue is beyond the scope of this investigation although it is envisioned that the data provided here will aid such comparative studies in the future.

6.4.1 Hardness of PDMS gel membranes with dispersed oil

Porcine adipose tissue test results were given here to provide baseline data at the same scale to aid in a visual comparison with synthetic mediums. As the OO calibrated durometer was unable to measure the softest of the five synthetic specimen groups created for this investigation (150% and 200% added oil), a OOO hardness calibrated durometer (H OOO) was used in addition to OO hardness results to broaden the comparison with other studies that may have used the OO calibrated durometer. Only Shore hardness by indentation is reported to provide context to indentation results on surrogate specimens, because these test methods remain the only agreed test certified

for the characterisation of soft tissues and soft, synthetic gels alike.

The results show the average hardness of warmed porcine adipose tissue to be 31.7 H OOO, equivalent to PDMS gel with 100% added oil, whereas the hardness of PDMS gel without oil was equivalent to 55.8 H OOO.

6.4.2 Uni-axial of PDMS gel membranes with dispersed oil

The manufacturer of PDMS A10 (*Platsil gel*® 10, *Polytek Development Corp*.®) gives data on additional mechanical properties of their supplied material, presumably taken from uni-axial tests. However, no standards are mentioned in the manufacturer's literature, nor are the test protocols specified. To quantify the mechanical impact of oil addition, it was necessary to first characterise a control group with both uni-axial and multi-axial standards. The results on *Platsil gel*® 10, reported here, show that, when using the standard, extensibility was far more significant than previously reported by the manufacturer (970 %), with an average 1634 % strain percentage at an average of 41 N. In addition, the ultimate tensile strength of the control group specified by the manufacturer was 1.57 MPa, but the results reported using the standard, found it to be significantly weaker, at only 0.77 MPa.

Such considerable differences in the control group's characteristics do not present a problem for analysis or transferability of the data here though, since the new control values are reported and used comparatively in place of the given values in the manufacturers literature.
As has been shown in previous chapters, Young's modulus has been the focus for many previous biomechanical investigators using uni-axial tests, but a Young's modulus only reveals the Hookean, character of the mechanical profile, exclusively at low-strains. However, the Young's modulus for human adipose tissue was previously found to be 0.011 +/- 0.006 MPa. Interestingly, PDMS membranes with 100% added oil were found to have 0.009 +/- 0.004MPa.

Extension to failure helped to provide a more comprehensive mechanical profile, where at high-strains, strain softening and hardening was seen. Extension to failure

tests revealed several behavioural phenomena; the Lüders effect, the PLC effect and the Mullins effect (as previously discussed in Chapter 2). Interestingly, the PLC effect[270] and associated Lüders effect,[269] both appear in the literature, albeit exclusively in tensile testing on hard materials, especially alloys like aluminium and steel.[301, 302] This study is the first time both effects have been observed in soft elastomeric gels. The precise mechanism of the serration was likely initiated by strain softening at low strains (the Mullin's effect) and has been previously described as the 'flow region' of the material. Serrations at low strains are classified as type 'C' Lüders bands on the linear vector of the graphs (figures 6.11 and 6.12).[291] Type C bands are recognisable by their large serrations (amplitude) of banded stress propagating randomly along the specimen length in diagonal waves.[303] As seen most clearly, in figure 6.12, the specimens group containing 50% oil exhibited a short Lüders plateau at around 300% extension, providing supporting evidence of the Lüders effect in action. In metals, this usually occurs *before* strain hardening, not afterwards, as was observed in the current investigation. Similar to ductile metal behaviour, the flow region seen here, manifests when the specimens are deformed beyond the elastic limit and can no longer return to the original length, eventually resulting in each specimen's rupture (failure).

Further test methods were adopted from elasticated fabric test standards used for hyperelastic and viscoelastic properties similar to the behaviour of soft elastomeric gels. Such standards were adopted mainly because no such standards exist for testing elastomers, which is likely the root cause of such disparity in the literature. Instead, here the standard has been used to provide clarity and guidance on test protocols for future investigations.

6.4.3 Multi-axial of PDMS gel membranes with dispersed oil

During multi-axial testing, a gradual increase in viscoelasticity was noticed across all groups, consistent with the increasing amount of oil. Groups with more oil were affected the most by preconditioning, evident in the intervals between loading and unloading. The graphs presented in the results help illustrate a clear relationship between the amount of added oil and the increase in deformability, loss of elasticity over time, and permanent deformation.

Interestingly, it was noticed that specimens with 150% oil content behaved differently than the rest of the groups during all multi-axial tests, except when investigating hysteresis. In particular, the group with 150% oil exhibited a greater energy loss (relaxation) than the other specimens during the first 5 seconds. It could be argued that, on its own, this was not significant (<0.05 N). Further, all specimens with 150 % oil exhibited a large deviation in force decay results and significant plastic deformation (bagging)- almost double the amount seen in other specimens, even when compared to the group with the most added oil. Results from the group with 150% added oil were so different from all other specimens that it disrupted the otherwise good predictive model for unrecovered deformation, instead giving a poor correlation between oil content and bagging amount (R^2 value = 0.654). One would be forgiven for thinking that this group was defective in some way, and that perhaps its fabrication or storage had affected its behaviour somehow, but this was not the case. All specimens were produced and stored together. More importantly, analysis of cyclic hysteresis showed the group conforming to the expected softening pattern due to incremental oil addition, as seen in other tests like uni-axial and hardness. It is not understood why this particular group behaved more like a plastic than a viscoelastic solid, and it has been identified as a candidate for future investigations.

6.5 Summary

This work aimed to investigate the effect of oil dispersion in PDMS gel for use as a surrogate fatty tissue of the hypodermis. The dearth of mechanical data on human fat, in the literature, made this task difficult, so limited data was gathered on porcine equivalent to demonstrate transferability and provide a benchmark for surrogate behaviour.

Utilisation of popular materials, that are well-known in the arts, have been examined in this study, making results especially useful to multidisciplinary researchers and fabricators of clinical and theatrical prosthetics. This study has identified several, previously unknown, quantitative, behavioural changes relating to the use of oil addition in PDMS that will be particularly useful to prosthetists such as predictive changes in cure-time, hardness, modulus and extensibility.

Test standards, used throughout this study, expedited the development of a robust test regime that exploits a variety of accessible test methods and machines, inviting other investigators to add their own transferable data, observations and analysis. In this way, it is possible that this work will create a foundation for all future development of both physical and constitutive models of very soft tissues like adipose tissues.

Key findings of this work were:

1. Large differences were observed in all tests when comparing specimens with and without oil, except in force decay and force degradation experiments.
2. A strong correlation was found between increasing oil content and decreasing hardness, UTS and elastic modulus.
3. A strong correlation was found between increasing oil content and increasing extensibility and cure-time.
4. A weak relationship was found between increasing oil content relaxation and elastic recoverability.
5. Evidence of the Lüders effects were observed, for the very first time, in soft PDMS gel membranes with 50% and 100% added oil. Related PLC effect was also suspected.
6. PDMS gel (Shore A-10) membranes with 100% added oil was best at mimicking subcutaneous adipose tissue. It exhibited the same hardness observed in identical tests on warmed porcine fat and the Young's modulus of human fat given in the literature.

Future work should focus on further investigating the behaviour of PDMS gel with 100%-150% added oil because the most unusual mechanical behaviour was observed in these groups, as well as being most similar to human fat and warmed porcine fat. Although not necessarily of interest to prosthetists, digital image correlation would enhance the study with visual cues on material characteristics, especially at rupture, and finite element analysis of human fat measured alongside these materials would further enrich the findings presented here.

6.6 Conclusion

This work provided clear test methods and results that are accessible to a broad

audience, especially to prosthetists who may have a limited a understanding of biomechanics and material science, cogently detailing the mechanical influence of oil dispersal in silicone-based materials like PDMS gel.

Most importantly, this work enables prosthetists to create more scientifically accurate soft tissue models with tuneable and predictable mechanical properties.

Chapter 7
Conclusion

7.1 Executive summary of the thesis

In this chapter, the contributions to knowledge are contextualised with regards to the original aims, objectives and research questions, that were introduced in Chapter one. Overall, this work has shown how silicone-based elastomeric gels were modified to form synthetic membranes that could mimic aspects of soft tissue behaviour. Target characteristics were informed by biomechanical studies of human anatomy. Each synthetic membrane's method of fabrication was documented to ensure transparency and reproducibility of the characteristics revealed in the results. All the ingredients used to produce the membranes are well known by prosthetists and widely available, but the mechanical influence of their employment was poorly documented until now. Mechanical characterisation is important because it helps researchers and prosthesis fabricators, measure and compare results, pooling knowledge to support informed design decisions about material performance.

PDMS gels and fillers, used in this work, are often used by prosthetists to produce visual and tactile effects, but the influence of fillers on gel behaviour had not previously been measured in a way that would allow comparison with data on soft tissues that could be easily accessed and understood by multiple disciplines, where practitioners have varying disciplinary backgrounds. In the interest of widening participation among interdisciplinary peers and beneficiaries, complex mechanical behaviour was simplified with a universal language and the use of standards, while constitutive mathematical modelling was largely avoided.

Clinical prosthetists, medical modellers, designers of implantable devices, and soft roboticists, will benefit from the results of tests as well as the mechanical test regime established in this thesis, improving the reliability of the data and repeatability of the results among peer groups. Maxillofacial and theatrical prosthetists, in particular, will benefit from reported manipulation of characteristics that are important to them, such as softening, strengthening, and hardening of PDMS gels, without altering their stoichiometric ratios.

Findings from this work establish a solid foundation of mechanical data gathering protocols for prosthetic-grade materials. The results presented will help accelerate development of other more realistic soft tissue surrogates in the future.

7.2 Contribution to knowledge

An overview of the discoveries demonstrating a contribution to knowledge in the mechanical behaviour of PDMS membranes, previously unknown in the literature, are summarised below.

- Embedded loose fibres harden PDMS membranes in a significant and predictable way. They also increase strength and plasticity but reduce elasticity.
- Embedded uni-directional yarns offer controllable anisotropy and strength in PDMS membranes without effecting hardness.
- Embedded fabrics induce multi-directional anisotropy in PDMS membranes, measurably increase hardness, elasticity, plasticity and strength, and significantly reduce extensibility.
- The dispersal of oil in PDMS gel drastically reduce membrane hardness, strength, and elasticity, but increase cure-time, extensibility, creep, and viscoelasticity.

In the next section, a final detailed overview of all the findings relating to the research questions are provided.

7.3 Addressing the research questions

This section includes a summary of conclusive results that are specific to the research questions outlined in Chapter 1 and are in agreement with the literature.
Each subsection is structured to answer each of the three original research questions. Sections 7.3.1, 7.3.2 and 7.3.3 answer questions 1, 2 and 3 respectively.

7.3.1 What are the mechanical characteristics of PDMS membranes saturated with loose, short-strand fibres?

A strong linear relationship was discovered between fibre content and Shore hardness- $R^2 = 0.9908$ (A10) and $R^2 = 0.9867$ (OO-30). More specifically, for every 1% of added loose fibres, hardness increased significantly, by 5 degrees of hardness (+/- 1 H OO). It was found that the hardness of PDMS composites that were investigated could range from 10.7 H OO to 51 H OO simply using fibre addition as shown. Living skin hardness of the foot, leg, arm, hand and head, was reported to be between 15 H OO and 50 HOO.[17, 94, 334, 337]

The UTS of PDMS A10 without additives was 0.77 MPa (around half the amount

specified by the manufacturer) when tested with the standard. The addition of the softener, reduced UTS to 0.23 MPa, but the addition of 4% loose fibres restored the UTS to 0.74 MPa in both OO-30 and A10 PDMS.

'Deckchair-shaped' stress strain curves featured in all specimens containing fibres, characteristic of soft tissues in extension.

Young's modulus for the softened PDMS A10 lacking fibres was 0.02 MPa. Increasing fibre content by 1% increased elasticity by 0.1 MPa and reduced extensibility at failure by 500% strain. The addition of 4% fibre content increased the modulus to 0.43 MPa, but reduced extensibility by 1000 % strain compared to PDMS lacking fibres. A PDMS fibre saturation of 3 % had a modulus of 0.22 MPa which was within the region of bladder membrane tissue modulus, specified in the literature (0.25 MPa).[362]

The viscoelastic properties of the PDMS membranes appeared almost unaffected by the presence of loose fibre fillers, except for a slight increase in force decay, signalling that the membranes became more easily fatigued as the fibre content increased.

7.3.2 What are the mechanical characteristics of multi-layered PDMS gel membranes embedded with textiles?

A strong linear relationship was found between fabric tension and increasing membrane hardness (R^2 =1). Hardness gains, increasing fabric tension, caused an increase of 3.2 H OO per 50% increase in tension.

Uni-directional yarns aligned in the direction of the extension embedded in multi-layered PDMS, tripled UTS compared to PDMS without yarns. Embedded fabrics increased UTS of single layered PDMS by six times when pretensioned at 50% of its original length, which is the same as facial and abdominal soft tissues reported in the literature (1.45 MPa).[16, 173]

Multi-layered PDMS membranes exhibited similarly high modulus when yarns were aligned with loading. The same group ruptured at 27.5 N and 100% strain, similar to human skin reported in the literature[16] The modulus was much less than specified in the literature though.[50] Specimens with embedded fabric all had a similar modulus.

Only multi-layered membranes that contained embedded uni-directional yarns with 100 % pretension responded differently than the other membranes. They appeared to store more energy and lose it more slowly during relaxation as the second layer

stabilised the membrane's behaviour. All membranes reinforced with textiles exhibited time-dependent viscoelasticity, but pretension, orientation, and layering made little difference to the membrane behaviour.

7.3.3 What is the mechanical influence of oil dispersal in PDMS gel membranes?

A strong relationship was discovered between the amount of added oil and the reduction in PDMS hardness. When measured using a OOO calibrated durometer the coefficient was found to be $R^2 = 0.9875$. With a less sensitive OO calibrated durometer, the coefficient relationship was $R^2 = 0.9976$. Results confirmed that PDMS A10 with 100% (1:1) added oil was best at mimicking pig fat hardness although human fat is known to be softer. The first 50% (2:1 PDMS to oil) of added oil caused reduction of 16 H OOO (15.1 H OO). Every additional 50% of added oil reduced hardness by 9 H OOO (9.7 H OO). The addition of 50% oil extended cure-time by 63% and for each additional 50% cure-time was extended a further 31%.

The initial introduction of oil caused the biggest loss in membrane strength. Dispersal of just 50% oil in PDMS A10 caused a significant reduction in UTS by 73%. The UTS of PDMS A10 without oil was 0.77 MPa, but with 50% added oil (2:1, PDMS to oil), the membrane had lost almost three-quarters of its strength. At 200% added oil (1:2, PDMS to oil) UTS was reduced to 0.027 MPa ($R^2 = 0.9623$.)

A strong exponential relationship ($R^2 = 0.9883$) was discovered between the Young's modulus and the amount of oil dispersed in the PDMS A10. Moduli ranged from 0.019 MPa to 0.0028 MPa were achieved by increasing the amount of added oil.

Elastic Young's modulus of very soft tissues like the human liver and fat was reported in the literature as 0.012 MPa and 0.001 MPa respectively, confirming the suitability of PDMS/oil dispersal as an ideal surrogate capable of covering the entire modulus range given in the literature.[175, 329, 363, 364]

Increasing the amount of oil content in the PDMS membranes had a significant effect on deformability, permanent deformation, and time dependent viscoelasticity: All increasing as the oil content was increased. Membranes containing 150 % oil lost stored energy more quickly and exhibited plastic deformation at higher strain rates, almost double the rate of all of the other groups, even the group with a higher percentage of oil content. It was not understood why this group behaved so differently

from the rest, perhaps due to the PLC effect and specific oil ratio.

7.4 Challenges to the research

The main challenge with this research was identifying erroneous literature. Some examples are still being referenced by peer group studies and published, carrying forward errors unwittingly. Some errors in reporting, base their data on historic errors in reported data, spanning 30 years of publications. The seven errors identified all relate to either a lack of standardised testing, or a lack of experience with PDMS. Errors that were detected and noted have not been referenced here out of professional curtesy. Identifying erroneous literature had a significant impact on research time.

In one example, authors reported on the Young's moduli of fat, and other soft tissues, based on results reused from other papers. The original authors being cited, did not report the source of their data. In another example, incorrect documentation of the test equipment was suspected due to the published results. Fortunately, the original report also featured an image of the investigator using the correct equipment. In a third example, the authors cite use of 'silicone oil' but describe it as a well-known softening agent, which in fact, contains no silicone oil.

7.4.1 The impact of the Covid19 pandemic

Finally, the Covid19 pandemic has an impact on two separate aspects of this work. Firstly, access to laboratories and technicians was lost for 12 months. Secondly, university closure happened during specimen preparation for the work presented in Chapter 5. So, all the pre-Covid19 specimens (60 specimens in total) had to be discarded and remade because the test window had expired (as per the standard) by the time the university was reopened.

7.5 Future work

In the course of this work, lessons were learned about PDMS elastomer behaviour patterns that gave glimpses into other fascinating behaviour not documented in the literature. This has laid the pathway for potential areas of future work.

- The self-adhesive properties of PDMS gel with softeners (PEIE) over 100% should be investigated in more detail, for potential as a self-adhesive, reusable

maxillofacial and mastectomy prosthetics.

- The Lüders and PLC effect were observed in soft gel behaviour during this study, and a deeper investigation into its causes is required. Plastic behaviour, more commonly associated with rigid materials like metal and plastic, was found to occur in soft PDMS membranes, but only between 50% and 100% added oil. Accumulated strain mapping and digital image correlation during extension would build a more detailed picture of the behaviour.
- Other future investigations will include layering all of the membranes that were found to mimic the properties of skin to determine its usefulness as a surrogate skin for learning suturing techniques and surgical simulations.
- The mechanical characteristics of the material compositions presented throughout this work have the potential to inform the development of many other soft tissues like organs and vasculature.

References

1. McDonald, C. L., Kartin, D., & Morgan, S. J. (2020). A systematic review in prosthetics and orthotics education research. *Prosthetics and Orthotics International*, *44*(3), 116-132.

2. Wolfaardt, J. F., Tam, V., Faulkner, M. G., & Prasad, N. (1992). Mechanical behavior of three maxillofacial prosthetic adhesive systems: a pilot project. The Journal of prosthetic dentistry, 68(6), 943-949.

3. Debreceni, T. (2013). *Special Makeup Effects for Stage and Screen: Making and Applying Prosthetics*. Taylor & Francis.

4. Bibb, R., Eggbeer, D., & Paterson, A. (2014). *Medical modelling: the application of advanced design and rapid prototyping techniques in medicine*. Woodhead Publishing.

5. Gaddum, N., Dillon-Murphy, D., Arm, R., Rafiq, I., Chabiniok, R., Morgan, G., ... & Hussain, T. (2022). In Silico Modelling of Aortic Strain and Strain Rate in Aortic Coarctation Treated with Stent Angioplasty with Comparison to Clinical Cohorts. *Applications in Engineering Science*, *12*, 100123.

6. Abeywardena, C. L., Vanheusden, F. J., Walker, K. F., Arm, R., & Zhang, Q. (2020). Fetal movement counting using optical fibre sensors. *Sensors*, *21*(1), 48.

7. Mahoney, P., Carr, D., Arm, R., Gibb, I., Hunt, N., & Delaney, R. J. (2018). Ballistic impacts on an anatomically correct synthetic skull with a surrogate skin/soft tissue layer. *International Journal of Legal Medicine*, *132*, 519-530.

8. Naumann, D. N., Bowley, D. M., Midwinter, M. J., Walker, A., & Pallister, I. (2016). High-Fidelity simulation model of pelvic hemorrhagic trauma: the future for military surgical skills training?. *Military medicine*, *181*(11-12), 1407-1409.

9. Harris, J. R., & Thompson, D. M. (2021). Modelling and Simulation Technologies for Training Medical/Healthcare Professionals.

10. McCreesh, S. (2021). In a simulated adult trauma patient, can pelvic binders be applied accurately by paramedics and HEMS paramedics? A pilot observational study. *British Paramedic Journal*, *6*(1), 23-29.

11. Arm, R., Shahidi, A., Clarke, C., & Alabraba, E. (2022). Synthesis and characterisation of a cancerous liver for presurgical planning and training applications. *BMJ Open Gastroenterology*, *9*(1), e000909.

12. Anon 2022. Markets and markets, Healthcare Simulation Market report. Available at: https://www.marketsandmarkets.com/Market-Reports/healthcare-medical-simulation-market-1156.html

13. Bholat, O. S., Haluck, R. S., Murray, W. B., Gorman, P. J., & Krummel, T. M. (1999).

Tactile feedback is present during minimally invasive surgery. *Journal of the American College of Surgeons*, *189*(4), 349-355.

14. Basdogan, C., De, S., Kim, J., Muniyandi, M., Kim, H., & Srinivasan, M. A. (2004). Haptics in minimally invasive surgical simulation and training. *IEEE computer graphics and applications*, *24*(2), 56-64.

15. Holzmann, H., Korting, G. W., Kobelt, D., & Vogel, H. G. (1971). Studies on mechanical properties of human skin in relation to age and sex. *Archiv für klinische und experimentelle Dermatologie*, *239*, 355-367.

16. Jansen, L. H., & Rottier, P. B. (1958). Some Mechanical Properties of Human Abdominal Skin Measured on Excised StripsA Study of their Dependence on Age and how they are Influenced by the Presence of Striae. *Dermatology*, *117*(2), 65-83.

17. Falanga, V., & Bucalo, B. (1993). Use of a durometer to assess skin hardness. *Journal of the American Academy of Dermatology*, *29*(1), 47-51.

18. Pailler-Mattei, C., Bec, S., & Zahouani, H. (2008). In vivo measurements of the elastic mechanical properties of human skin by indentation tests. *Medical engineering & physics*, *30*(5), 599-606.

19. McKee, C. T., Last, J. A., Russell, P., & Murphy, C. J. (2011). Indentation versus tensile measurements of Young's modulus for soft biological tissues. *Tissue Engineering Part B: Reviews*, *17*(3), 155-164.

20. Aziz, T., Waters, M., & Jagger, R. (2003). Analysis of the properties of silicone rubber maxillofacial prosthetic materials. *Journal of dentistry*, *31*(1), 67-74

21. Zhang, Y., Karasu, F., Rocco, C., Van Der Ven, L. G. J., Van Benthem, R. A. T. M., Allonas, X., ... & De With, G. (2016). PDMS-Based Self-Replenishing Coatings. Polymer, 107, 249-262.

22. Clayton, M., & Philo, R. (2010). *Leonardo da Vinci: the mechanics of man*. Getty Publications.

23. Gordon, J. (1815). *A System Of Human Anatomy* (Vol. 1). Blackwood. 223-225

24. Struthers, J. (1848). Inaugural dissertation on the anatomy and physiology of the human skin. *Annexe Thesis Digitisation Project 2017 Block 14*.

25. Gray, H., & Carter, H. V. (1858). *Gray's anatomy: a facsimile*. Grange Books.

26. Langer, K. (1861). Zur Anatomie Und Physiologie Der Haut. Über Die Spaltbarkeit Der Cutis S. B. Akad. Wiss. Wien, 44.

27. Cleland, J. (1874). *Animal Physiology, the Structure and Functions of the Human Body*. Collins.

28. Hitchcock, E. (1873). *Elementary Anatomy and Physiology...* Ivison, Blakeman, Taylor & Company.

29. Schade, H. (1912). Untersuchungen Zur Organfunction Des Bindegewebes: I. Mittheilung: Die Elasticitätsfunction Des Bindegewebes Und Die Intravitale Messung Ihrer Störungen. *Zeitschrift Für Experimentelle Pathologie Und Therapie*, *11*, 369-399.

30. Rothman, S. (1954). Physiology and Biochemistry of the Skin. *(No Title)*.

31. Ridge, M. D., & Wright, V. (1966). Mechanical properties of skin: a bioengineering study of skin structure. *Journal of applied physiology*, *21*(5), 1602-1606.

32. Ridge, M. D. (1964). *The rheology of skin: A bio-engineering study of the mechanical properties of human skin in relation to its structure* (Doctoral dissertation, University of Leeds).

33. Sodeman, W. A., & Burch, G. E. (1938). A direct method for the estimation of skin distensibility with its application to the study of vascular states. *The Journal of Clinical Investigation*, *17*(6), 785-793.

34. Kirk, E., & Kvorning, S. A. (1949). Quantitative measurements of the elastic properties of the skin and subcutaneous tissue in young and old individuals. *Journal of Gerontology*, *4*(4), 273-284.

35. Burton, A. C. (1954). Relation of structure to function of the tissues of the wall of blood vessels. *Physiological reviews*, *34*(4), 619-642.

36. Meredith, R. (1975). The structures and properties of fibres. *Textile Progress*, *7*(4), 1-74.

37. Mitton, R. G. (1945). Mechanical properties of leather fibres. *J. Soc. Leather Trades' Chem*, *29*, 169-194.

38. Highberger, J. H. (1947). The structural stability of the collagen fiber in relation to the mechanism of tanning. *American Leather Chemists' Association. Journal*, *42*, 493-511.

39. Manschot, J. F. M., & Brakkee, A. J. M. (1986). The Measurement And Modelling Of The Mechanical Properties Of Human Skin In Vivo—II. The Model. *Journal Of Biomechanics*, *19*(7), 517-521.

40. Samani, A., & Plewes, D. (2004). A method to measure the hyperelastic parameters of ex vivo breast tissue samples. *Physics in medicine & biology*, *49*(18), 4395.

41. Fung, Y. C. (1993). Biomechanics: Mechanical Properties Of Living Tissues. Behaviour Of Soft Tissues Under Uni-axial Loading. 2nd Edition. New York: Springer, 7.5, 269–71.

42. Lee, J. M., & Boughner, D. R. (1985). Mechanical properties of human pericardium. Differences in viscoelastic response when compared with canine pericardium. *Circulation research*, *57*(3), 475-481.

43. Wijn, P. F. (1980). *The alinear viscoelastic properties of human skin in vivo for small deformations* (Doctoral dissertation, [Sl: sn]).

44. Kalra, A., Lowe, A., & Al-Jumaily, A. M. (2016). Mechanical behaviour of skin: a

review. *J. Mater. Sci. Eng*, *5*(4), 1000254.

45. Nicolle S, Decorps J, Fromy B, Palierne JF. New Regime In The Mechanical Behavior Of Skin: Strain-Softening Occurring Before Strain-Hardening. J Mech Behav Biomed Mater. 2017 May;69:98-106. Doi: 10.1016/J.Jmbbm.2016.12.021. Epub 2016 Dec 27. PMID: 28049090.

46. Fletcher, W. P., & Gent, A. N. (1953). Apparatus For The Measurement Of The Dynamic Shear Modulus And Hysteresis Of Rubber At Low Frequencies. Rubber Chemistry And Technology, 26(1), 181-187.

47. Mullins L (1948) Effect Of Stretching On The Properties Of Rubber. Rubber Chem Technol 21:281–300

48. Sreeja, T. D., & Kutty, S. K. N. (2001). Cure Characteristics and Mechanical Properties of Natural Rubber—Short Nylon Fiber Composites. *Journal of Elastomers & Plastics*, *33*(3), 225-238.

49. Groves, R. B., Coulman, S. A., Birchall, J. C., & Evans, S. L. (2013). An Anisotropic, Hyperelastic Model For Skin: Experimental Measurements, Finite Element Modelling And Identification Of Parameters For Human And Murine Skin. Journal Of The Mechanical Behavior Of Biomedical Materials, 18, 167-180.

50. Ni Annaidh, A. N., Bruyère, K., Destrade, M., Gilchrist, M. D., & Otténio, M. (2012). Characterization of the anisotropic mechanical properties of excised human skin. *Journal of the mechanical behavior of biomedical materials*, *5*(1), 139-148.

51. Hendriks, F. M., Brokken, D., Oomens, C. W. J., & Baaijens, F. P. T. (2004). Influence Of Hydration And Experimental Length Scale On The Mechanical Response Of Human Skin In Vivo, Using Optical Coherence Tomography. *Skin Research And Technology*, *10*(4), 231-241.

52. Holzapfel, G. A. (2001). Biomechanics of soft tissue. *The handbook of materials behavior models*, *3*(1), 1049-1063.

53. Rivlin, R. S., & Saunders, D. (1951). Large elastic deformations of isotropic materials VII. Experiments on the deformation of rubber. *Philosophical Transactions of the Royal Society of London. Series A, Mathematical and Physical Sciences*, *243*(865), 251-288.

54. Ogden, R. W. (1972). Large deformation isotropic elasticity–on the correlation of theory and experiment for incompressible rubberlike solids. *Proceedings of the Royal Society of London. A. Mathematical and Physical Sciences*, *326*(1567), 565-584.

55. Yeoh, O. H. (1993). Some forms of the strain energy function for rubber. *Rubber Chemistry and technology*, *66*(5), 754-771.

56. Arruda, E. M., Boyce, M. C., & Quintus-Bosz, H. (1993). Effects of initial anisotropy on the finite strain deformation behavior of glassy polymers. *International Journal of Plasticity*, *9*(7), 783-811.

57. Gent, A. N. (1996). A new constitutive relation for rubber. *Rubber chemistry and*

technology, *69*(1), 59-61.

58. Nickell, S., Hermann, M., Essenpreis, M., Farrell, T. J., Krämer, U., & Patterson, M. S. (2000). Anisotropy of light propagation in human skin. *Physics in Medicine & Biology*, *45*(10), 2873.

59. Niknejad, H., Peirovi, H., Jorjani, M., Ahmadiani, A., Ghanavi, J., & Seifalian, A. M. (2008). Properties of the amniotic membrane for potential use in tissue engineering. *Eur Cells Mater*, *15*, 88-99.

60. Park, S., Chien, A. L., Brown, I. D., & Chen, J. (2023). Characterizing viscoelastic properties of human melanoma tissue using Prony series. *Frontiers in Bioengineering and Biotechnology*, *11*, 1162880.

61. Freinkel, R. K., & Woodley, D. T. (Eds.). (2001). *The biology of the skin*. CRC Press.

62. Haake, A., Scott, G. A., & Holbrook, K. A. (2001). Structure and function of the skin: overview of the epidermis and dermis. *The biology of the skin*, *2001*, 19-45.

63. Gefen, A., & Dilmoney, B. (2007). Mechanics of the normal woman's breast. *Technology and Health Care*, *15*(4), 259-271.

64. Gallagher, A. J., Ní Annaidh, A., Bruyère, K., Otténio, M., Xie, H., & Gilchrist, M. D. (2012, September). Dynamic tensile properties of human skin. In *IRCOBI conference* (Vol. 59, pp. 494-502). Dublin (Ireland: International Research Council on the Biomechanics of Injury.

65. Goodyear, C. (1839). Specification Of A Patent For An Improvement In The Manufacture Of Gum Elastic Shoes. Granted To CHARLES GOODYEAR, Roxbury, Norfolk County, Massachusetts July 24th, 1838. *Journal Of The Franklin Institute, Of The State Of Pennsylvania, For The Promotion Of The Mechanic Arts; (1828-1851)*, *24*(1), 24.

66. Coran, A. Y. (1994). Vulcanization. In *Science And Technology Of Rubber* (Pp. 339-385). Academic Press.

67. Goldberg, A. J., Craig, R. G., & Filisko, F. E. (1980). Tear energy of elastomers for maxillofacial applications. *Journal of Oral Rehabilitation*, *7*(6), 445-451.

68. Joseph, J., Patel, R. M., Wenham, A., & Smith, J. R. (2018). Biomedical applications of polyurethane materials and coatings. *Transactions of the IMF*, *96*(3), 121-129.

69. Challenger, F. (1949). Prof. FS Kipping, FRS. *Nature*, *164*(4159), 93-94.

70. Kipping, F. S. (1927). XVII.—Organic derivatives of silicon. Part XXXII. The carbon–silicon binding. *Journal of the Chemical Society (Resumed)*, 104-107.

71. Kipping, F. S. (1937). The bakerian lecture organic derivatives of silicon. *Proceedings of the Royal Society of London. Series A-Mathematical and Physical Sciences*, *159*(896), 139-148.

72. Hyde, J. F. (1965). Chemical Background of Silicones: The siloxane linkage as a structure-

building device gives variety and versatility to the silicones. *Science*, *147*(3660), 829-836.

73. Noll, W. (2012). *Chemistry and technology of silicones*. Elsevier.

74. Mazurek, P., Vudayagiri, S., & Skov, A. L. (2019). How to tailor flexible silicone elastomers with mechanical integrity: a tutorial review. *Chemical Society Reviews*, *48*(6), 1448-1464.

75. Rochow, E. G. (1946). Introduction to silicone chemistry. *Transactions of The Electrochemical Society*, *90*(1), 303.

76. Kipping, F. S. (1904, January). Organic derivative of silicon. Preparation of alkylsilicon chlorides. In *Proc. Chem. Soc* (Vol. 20, p. 15).

77. Crabtree, J., & Kemp, A. R. (1946). Weathering of Soft Vulcanized Rubber. *Industrial & Engineering Chemistry*, *38*(3), 278-296.

78. Leonard, M., Wang, N., Lopez-Pamies, O., & Nakamura, T. (2020). The nonlinear elastic response of filled elastomers: Experiments vs. theory for the basic case of particulate fillers of micrometer size. *Journal of the Mechanics and Physics of Solids*, *135*, 103781.

79. Mark, J. E. (1985). Molecular aspects of rubberlike elasticity. *Accounts of Chemical Research*, *18*(7), 202-206.

80. Bokobza, L. (2004). The reinforcement of elastomeric networks by fillers. *Macromolecular Materials and Engineering*, *289*(7), 607-621.

81. Seyferth, D. (2001). Dimethyldichlorosilane and the direct synthesis of methylchlorosilanes. The key to the silicones industry. *Organometallics*, *20*(24), 4978-4992.

82. Ring, M. E. (1991). The history of maxillofacial prosthetics. *Plastic and reconstructive surgery*, *87*(1), 174-184.

83. Bulbulian, A. H. (1965). Maxillofacial Prosthetics: Evolution And Practical Application In Patient Rehabilitation. *The Journal Of Prosthetic Dentistry*, *15*(3), 554-569.

84. Destruhaut, F. (2019). International Journal of Maxillofacial Prosthetics (iJMP). *Int J Maxillofac Prosthetics*, *4*, 2-8.

85. Jones, K. P. (1997). Natural Versus Synthetic Rubber Uptake In Tyres. *Journal Of Natural Rubber Research*, *12*, 186-198.

86. Ackerman, A. J. (1953). Maxillofacial prosthesis. *Oral Surgery, Oral Medicine, Oral Pathology*, *6*(1), 176-200.

87. Barnhart, G. W. (1960). A new material and technic in the art of somato-prosthesis. *Journal of Dental Research*, *39*(4), 836-844.

88. Chao, A. H., Garza III, R., & Povoski, S. P. (2016). A review of the use of silicone implants in breast surgery. *Expert Review of Medical Devices*, *13*(2), 143-156.

89. Grenvik, A., & Schaefer, J. (2004). From Resusci-Anne To Sim-Man: The Evolution Of Simulators In Medicine. *Critical Care Medicine*, *32*(2), S56-S57.

90. Sullivan, D. A. (2001). *Cosmetic Surgery: The Cutting Edge Of Commercial Medicine In America*. Rutgers University Press.

91. Gearhart, D. F. (1970). Polyvinyl Chloride (Cordo) Facial And Body Prostheses. *Bull. Prosthet. Res*, *10*, 214-218.

92. Lewis, D. H., & Castleberry, D. J. (1980). An assessment of recent advances in external maxillofacial materials. *The Journal of prosthetic dentistry*, *43*(4), 426-432.

93. Lewis, C. M. (1980). Inflammatory carcinoma of the breast following silicone injections. *Plastic and Reconstructive Surgery*, *66*(1), 134-136.

94. Maclean, C., Brodie, R., & Nash, D. H. (2019). Shore OO hardness measurement of bovine aorta and mock vessel materials for endovascular device design.

95. Nair, K. (2021). Unfinished Bodies: The Sticky Materiality Of Prosthetic Effects. *JCMS: Journal Of Cinema And Media Studies*, *60*(3), 104-128.

96. Hatamleh, M., Polyzois, G., Nuseir, A., *Et Al* (2016). Mechanical Properties And Simulated Aging Of Silicone Maxillofacial Elastomers: Advancements In The Past 45 Years. Journal Of Prosthodontics, 25(5), 418-426.

97. Ariani, N., Visser, A., Van Oort, R. *Et Al* (2013). Current State Of Craniofacial Prosthetic Rehabilitation. Int J Prosthodont, 26(1), 57-67.

98. Payne, C. (2020). Applying Pre-Made Prosthetics. In Makeup Artistry For Film And Television (Pp. 238-247). Routledge.

99. Barhate, A. R., Gangadhar, S. A., Bhandari, A. J., & Joshi, A. D. (2015). Materials Used In Maxillofacial Prosthesis: A Review. Pravara Medical Review, 7(1).

100. Boyce, M. C., & Arruda, E. M. (2000). Constitutive Models Of Rubber Elasticity: A Review. Rubber Chemistry And Technology, 73(3), 504-523.

101. Palchesko, R. N., Zhang, L., Sun, Y., & Feinberg, A. W. (2012). Development Of Polydimethylsiloxane Substrates With Tuneable Elastic Modulus To Study Cell Mechanobiology In Muscle And Nerve. Plos One, 7(12), E51499.

102. Arm, R., Shahidi, A., & Dias, T. (2019). Mechanical Behaviour Of Silicone Membranes Saturated With Short Strand, Loose Polyester Fibres For Prosthetic And Rehabilitative Surrogate Skin Applications. Materials, 12(22), 3647.

103. Shergold, O. A., Fleck, N. A., & Radford, D. (2006). The Uni-axial Stress Versus Strain Response Of Pig Skin And Silicone Rubber At Low And High Strain Rates. International Journal Of Impact Engineering, 32(9), 1384-1402.

104. Mahoney, P., Carr, D., Harrison, K., *Et Al* (2019). Forensic Reconstruction Of Two Military

Combat Related Shooting Incidents Using An Anatomically Correct Synthetic Skull With A Surrogate Skin/Soft Tissue Layer. International Journal Of Legal Medicine, 133, 151-162.

105. Lu, Y., Biswas, M. C., Guo, Z., Jeon, J. W., & Wujcik, E. K. (2019). Recent Developments In Bio-Monitoring Via Advanced Polymer Nanocomposite-Based Wearable Strain Sensors. Biosensors And Bioelectronics, 123, 167-177.

106. Nguyen, T., & Khine, M. (2020). Advances In Materials For Soft Stretchable Conductors And Their Behaviour Under Mechanical Deformation. Polymers, 12(7), 1454.

107. Payne, T., Mitchell, S., Bibb, R., & Waters, M. (2015). Development Of Novel Synthetic Muscle Tissues For Sports Impact Surrogates. Journal Of The Mechanical Behaviour Of Biomedical Materials, 41, 357-374.

108. Sparks, J., Vavalle, N., Kasting, K., *Et Al* (2015). Use Of Silicone Materials To Simulate Tissue Biomechanics As Related To Deep Tissue Injury. Advances In Skin & Wound Care, 28(2), 59-68.

109. Engelhardt, S., Sauerzapf, S., Preim, B., *Et Al* (2019). Flexible And Comprehensive Patient-Specific Mitral Valve Silicone Models With Chordae Tendineae Made From 3D-Printable Molds. International Journal Of Computer Assisted Radiology And Surgery, 14, 1177-1186.

110. Estermann, S. J., Pahr, D. H., & Reisinger, A. (2020). Quantifying Tactile Properties Of Liver Tissue, Silicone Elastomers, And A 3D Printed Polymer For Manufacturing Realistic Organ Models. Journal Of The Mechanical Behaviour Of Biomedical Materials, 104, 103630.

111. Wehner, M., Truby, R. L., Fitzgerald, D. J., Mosadegh, B., Whitesides, G. M., Lewis, J. A., & Wood, R. J. (2016). An integrated design and fabrication strategy for entirely soft, autonomous robots. *nature*, *536*(7617), 451-455.

112. Dimaggio, P. J., Waer, A. L., Desmarais, T. J., *Et Al* 2010). The Use Of A Lightly Preserved Cadaver And Full Thickness Pig Skin To Teach Technical Skills On The Surgery Clerkship—A Response To The Economic Pressures Facing Academic Medicine Today. The American Journal Of Surgery, 200(1), 162-166.

113. Ghirelli, M., Mattioli, F., Federici, G., Ferri, G., Malagoli, A., Trebbi, M., & Presutti, L. (2020). Ex Vivo Porcine Larynx Model For Microlaryngoscopy Laryngeal Surgery: Proposal For A Structured Surgical Training. Journal Of Voice, 34(4), 629-635.

114. Ramphal, P. S., Coore, D. N., Craven, M. P., *Et Al* (2005). A High Fidelity Tissue-Based Cardiac Surgical Simulator. European Journal Of Cardio-Thoracic Surgery, 27(5), 910-916.

115. Sappenfield, E. C., & Tunitsky-Bitton, E. (2021). Beef Tongue Surgical Simulation Model For Posterior Vaginal Repair. Obstetrics & Gynecology, 137(5), 837-842.

116. Vogel, H. G., & Denkel, K. (1985). In Vivo Recovery Of Mechanical Properties In Rat Skin After Repeated Strain. Archives Of Dermatological Research, 277, 484-488.

117. Schachner, T., Bonaros, N., Ruttmann, E., *Et Al* (2007, January). Training Models For Coronary Surgery. In Heart Surgery Forum (Vol. 10, No. 4, P. 215). Forum Multimedia Publishing.

118. Feins, R., Burkhart, H., Conte, J., (2017). Simulation-Based Training In Cardiac Surgery. The Annals Of Thoracic Surgery, 103(1), 312-321.

119. Demasi, S. C., Katsuta, E., & Takabe, K. (2016). Live Animals For Preclinical Medical Student Surgical Training. Erodium Journal Of Surgery, 3(2), 24.

120. Anders, K. H., Goldstein, B. G., Lesher, J. L., *Et Al* (1989). The Use Of Live Pigs In The Surgical Training Of Dermatology Residents. The Journal Of Dermatologic Surgery And Oncology, 15(7), 734-736.

121. De La Garza-Castro, O., Sánchez-González, S. G., Delagarza-Pineda, O., *Et Al* (2018). Dermatology Surgery Training In A Live Animal Model. *Journal Of Morphological Sciences*, *35*(03), 187-190.

122. Bowling, J., & Botting, J. (2005). Porcine Sebaceous Cyst Model: An Inexpensive, Reproducible Skin Surgery Simulator. Dermatologic Surgery, 31(8), 953-956.

123. Cosman, P., Hemli, J. M., Ellis, A. M., & Hugh, T. J. (2007). Learning The Surgical Craft: A Review Of Skills Training Options. ANZ Journal Of Surgery, 77(10), 838-845.

124. Niebuhr, N. I., Johnen, W., Güldaglar, T., *Et Al* (2016). Radiological Properties Of Tissue Surrogates Used In A Multimodality Deformable Pelvic Phantom For MR-Guided Radiotherapy. Medical Physics, 43(2), 908-916.

125. Appleby-Thomas, G. J., Hazell, P. J., Wilgeroth, J. M., *Et Al.* (2011). On The Dynamic Behaviour Of Three Readily Available Soft Tissue Simulants. Journal Of Applied Physics, 109(8).

126. Liney, G. P., Tozer, D. J., & Turnbull, L. W. (1999). A Simple And Realistic Tissue-Equivalent Breast Phantom For MRI. Journal Of Magnetic Resonance Imaging: An Official Journal Of The International Society For Magnetic Resonance In Medicine, 10(6), 968-971.

127. Antoniou, A., & Damianou, C. (2022). MR Relaxation Properties Of Tissue-Mimicking Phantoms. Ultrasonics, 119, 106600.

128. Falland-Cheung, L., Piccione, N., Zhao, T., Lazarjan, M. S., Hanlin, S., Jermy, M., & Waddell, J. N. (2016). Investigation Of Dental Alginate And Agar Impression Materials As A Brain Simulant For Ballistic Testing. Forensic Science International, 263, 169-175.

129. Navarro-Lozoya, M., Kennedy, M. S., Dean, D., & Rodriguez-Devora, J. I. (2019). Development Of Phantom Material That Resembles Compression Properties Of Human Brain Tissue For Training Models. Materialia, 8, 100438.

130. Milano, E. G., Capelli, C., Wray, J., Biffi, B., Layton, S., Lee, M., ... & Biglino, G. (2019). Current And Future Applications Of 3D Printing In Congenital Cardiology And Cardiac

Surgery. *The British Journal Of Radiology*, *92*(1094), 20180389.

131. Batteux, C., Haidar, M. A., & Bonnet, D. (2019). 3D-Printed Models For Surgical Planning In Complex Congenital Heart Diseases: A Systematic Review. *Frontiers In Pediatrics*, *7*, 23.

132. Galliotto, F. (2021) Congenital Trainheart: Development Of A Fully 3D Printed Simulator For Hands-On Surgical Training.

133. Hussein, N., Kasdi, R., Coles, J. G., & Yoo, S. J. (2020). Use Of 3-Dimensionally Printed Heart Models In The Planning And Simulation Of Surgery In Patients With Raghib Syndrome (Coronary Sinus Defect With Left Superior Vena Cava). *JTCVS Techniques*, *2*, 135-138.

134. Herzberger, J., Sirrine, J. M., Williams, C. B., & Long, T. E. (2019). Polymer Design For 3D Printing Elastomers: Recent Advances In Structure, Properties, And Printing. *Progress In Polymer Science*, *97*, 101144.

135. Durban, M. M., Lenhardt, J. M., Wu, A. S., et al (2018). Custom 3D Printable Silicones With Tunable Stiffness. *Macromolecular Rapid Communications*, *39*(4), 1700563.

136. Seo, E., Choi, J., Lee, B., Son, Y. A., & Lee, K. J. (2019). Dye Clicked Thermoplastic Polyurethane As A Generic Platform Toward Chromic-Polymer Applications. *Scientific Reports*, *9*(1), 18648.

137. Ozbolat, V., Dey, M., Ayan, B., Povilianskas, A., Demirel, M. C., & Ozbolat, I. T. (2018). 3D Printing Of PDMS Improves Its Mechanical And Cell Adhesion Properties. *ACS Biomaterials Science & Engineering*, *4*(2), 682-693.

138. Yirmibesoglu, O. D., Morrow, J., Walker, S., *Et Al.* (2018). Direct 3D Printing Of Silicone Elastomer Soft Robots And Their Performance Comparison With Molded Counterparts. In *2018 IEEE International Conference On Soft Robotics (Robosoft)* (Pp. 295-302). IEEE.

139. Kim, Y., Yuk, H., Zhao, R., Chester, S. A., & Zhao, X. (2018). Printing Ferromagnetic Domains For Untethered Fast-Transforming Soft Materials. *Nature*, *558*(7709), 274-279.

140. Laferrier, J. Z., & Gailey, R. (2010). Advances In Lower-Limb Prosthetic Technology. *Physical Medicine And Rehabilitation Clinics*, *21*(1), 87-110.

141. Cruz, R. L., Ross, M. T., Powell, S. K., & Woodruff, M. A. (2020). Advancements In Soft-Tissue Prosthetics Part A: The Art Of Imitating Life. *Frontiers In Bioengineering And Biotechnology*, *8*, 121.

142. Cruz, R. L., Ross, M. T., Powell, S. K., & Woodruff, M. A. (2020). Advancements In Soft-Tissue Prosthetics Part B: The Chemistry Of Imitating Life. *Frontiers In Bioengineering And Biotechnology*, *8*, 147.

143. Cruz, R. L., Ross, M. T., Skewes, J., Allenby, M. C., Powell, S. K., & Woodruff, M. A. (2020). An Advanced Prosthetic Manufacturing Framework For Economic Personalised Ear Prostheses. *Scientific Reports*, *10*(1), 11453.

144. Fell, C. A. (2021). *Soft Robotic Devices For Emulating Vascular Mechanobiology* (Doctoral Dissertation, Queensland University Of Technology).

145. Larrabee Jr, W. F. (1986). A Finite Element Model Of Skin Deformation. I. Biomechanics Of Skin And Soft Tissue: A Review. *The Laryngoscope*, *96*(4), 399-405.

146. Podlesnij, S., Hrushko, O., Kovalenko, A., & Stashkevych, I. (2021). Mechanical Tests And Properties Of Living Tissues And Biomaterials In A Biomechanics Course. *Teaching And Subjects On Bio-Medical Engineering*, 317.

147. Griffin, M., Premakumar, Y., Seifalian, A., Butler, P. E., & Szarko, M. (2016). Biomechanical Characterization Of Human Soft Tissues Using Indentation And Tensile Testing. *Jove (Journal Of Visualized Experiments)*, (118), E54872.

148. Olson, S. A., Marsh, J. L., Anderson, D. D., & Latta, L. L. (2012). Designing A Biomechanics Investigation: Choosing The Right Model. *Journal Of Orthopaedic Trauma*, *26*(12), 672-677.

149. Huda, Z., & Huda, Z. (2022). Elasticity And Viscoelasticity. *Mechanical Behavior Of Materials: Fundamentals, Analysis, And Calculations*, 119-142.

150. Hilton, H. H. (2017). Elastic And Viscoelastic Poisson's Ratios: The Theoretical Mechanics Perspective. *Materials Sciences And Applications*, *8*(4), 291-332.

151. Holt WL (1931) Behavior Of Rubber Under Repeated Stresses. Journal Of Industrial Engineering Chemicals 23:1471–1475

152. Yasenchuk, Y. F., Marchenko, E. S., Gunter, S. V., Baigonakova, G. A., Kokorev, O. V., Volinsky, A. A., & Topolnitsky, E. B. (2021). Softening Effects In Biological Tissues And Niti Knitwear During Cyclic Loading. Materials, 14(21), 6256.

153. Peña, E., Peña, J. A., & Doblaré, M. (2009). On The Mullins Effect And Hysteresis Of Fibered Biological Materials: A Comparison Between Continuous And Discontinuous Damage Models. International Journal Of Solids And Structures, 46(7-8), 1727-1735.

154. Ehret, A. E., & Itskov, M. (2009). Modelling Of Anisotropic Softening Phenomena: Application To Soft Biological Tissues. International Journal Of Plasticity, 25(5), 901-919.

155. Yi, J. Y. S., Dierks, E. J., Over, L. M., & Hauck, M. J. (2012). Prosthetic Reconstruction Of The Orbit/Globe. *Oral And Maxillofacial Surgery Clinics*, *24*(4), 697-712.

156. Over, L. M., & Dierks, E. (2022). Interdisciplinary Prosthetic Rehabilitation Following Bilateral Maxillectomy With Total Upper Lip And Unilateral Zygoma Resection: A Clinical Report. *The Journal Of Prosthetic Dentistry*.

157. Montgomery, P. C., & Kiat-Amnuay, S. (2010). Survey Of Currently Used Materials For Fabrication Of Extraoral Maxillofacial Prostheses In North America, Europe, Asia, And Australia. *Journal Of Prosthodontics: Implant, Esthetic And Reconstructive Dentistry*, *19*(6), 482-490.

158. Abdullah, H. A., & Abdul-Ameer, F. M. (2018). Evaluation Of Some Mechanical

Properties Of A New Silicone Elastomer For Maxillofacial Prostheses After Addition Of Intrinsic Pigments. The Saudi Dental Journal, 30(4), 330-336.

159. Haug, S. P., Andres, C. J., & Moore, B. K. (1999). Colour Stability And Colorant Effect On Maxillofacial Elastomers. Part III: Weathering Effect On Color. The Journal Of Prosthetic Dentistry, 81(4), 431-438.

160. Sreeja, T.; Narayanankutty, S. Studies on Short Nylon Fibre-Reclaimed Rubber/ Elastomer Composites. Ph.D. Thesis, Cochin University of Science and Technology, Kerala, India, January 2001; pp. 19–21

161. Cacciola, G., Peters, G. W. M., & Schreurs, P. J. G. (2000). A three-dimensional mechanical analysis of a stentless fibre-reinforced aortic valve prosthesis. *Journal of Biomechanics*, *33*(5), 521-530.

162. Heim, F., & Gupta, B. S. (2009). Textile heart valve prosthesis: the effect of fabric construction parameters on long-term durability. *Textile Research Journal*, *79*(11), 1001-1013.

163. Wu, W., & Zuo, H. (2018). Silicone rubber composites modified by chopped basalt fibers treated with coupling agent. *Silicon*, *10*, 2555-2559.

164. Setua, D. K., & De, S. K. (1984). Short silk fibre reinforced nitrile rubber composites. *Journal of materials science*, *19*, 983-999.

165. Ziraki, S., Zebarjad, S. M., & Hadianfard, M. J. (2016). A study on the tensile properties of silicone rubber/polypropylene fibers/silica hybrid nanocomposites. *Journal of the Mechanical Behavior of Biomedical Materials*, *57*, 289-296.

166. Pissarenko, A., & Meyers, M. A. (2020). The Materials Science Of Skin: Analysis, Characterization, And Modeling. *Progress In Materials Science*, *110*, 100634.

167. Humphrey, J. D. (1995). Mechanics Of The Arterial Wall: Review And Directions. *Critical Reviews™ In Biomedical Engineering*, *23*(1-2).

168. Footner, E., Firipis, K., Liu, E., et al (2023). Layer-By-Layer Analysis Of In Vitro Skin Models. *ACS Biomaterials Science & Engineering*.

169. Delalleau, A., Josse, G., Lagarde, J. M., Zahouani, H., & Bergheau, J. M. (2006). Characterization of the mechanical properties of skin by inverse analysis combined with the indentation test. *Journal of biomechanics*, *39*(9), 1603-1610.

170. Pailler-Mattei, C., & Zahouani, H. (2004). Study of adhesion forces and mechanical properties of human skin in vivo. *Journal of adhesion science and technology*, *18*(15-16), 1739-1758.

171. Zahouani, H., Pailler-Mattei, C., Sohm, B., Vargiolu, R., Cenizo, V., & Debret, R. (2009). Characterization of the mechanical properties of a dermal equivalent compared with human skin in vivo by indentation and static friction tests. *Skin research and technology*, *15*(1), 68-76.

172. Ottenio, M., Tran, D., Annaidh, A. N., Gilchrist, M. D., & Bruyère, K. (2015). Strain Rate And Anisotropy Effects On The Tensile Failure Characteristics Of Human Skin. Journal Of The Mechanical Behavior Of Biomedical Materials, 41, 241-250.

173. Jacquemoud, C.; Bruyere, K.; Coret, M. Methodology To Determine Failure Characteristics Of Planar Soft Tissues Using A Dynamic Tensile Test. J. Biomech. 2007, 2, 468–475.

174. Dunn, M. G., & Silver, F. H. (1983). Viscoelastic behavior of human connective tissues: relative contribution of viscous and elastic components. *Connective tissue research*, *12*(1), 59-70.

175. Alkhouli, N., Mansfield, J., Green, E., Bell, J., Knight, B., Liversedge, N., ... & Winlove, C. P. (2013). The mechanical properties of human adipose tissues and their relationships to the structure and composition of the extracellular matrix. *American Journal of Physiology-Endocrinology and Metabolism*, *305*(12), E1427-E1435.

176. Fenton, L. A., Horsfall, I., & Carr, D. J. (2020). Skin and skin simulants. *Australian Journal of Forensic Sciences*, *52*(1), 96-106.

177. *Polytek* Dev' Corp®. PlatSil® Gel-OO & Gel-10 Soft, Translucent, RTV Liquid Silicone Rubbers for Theatrical Prosthetics, Lifecasting & Mold Making Applications. Technical Bulletin. Available online: https://*Polytek*.com/content/pdf/technicalbulletin/*Polytek*_TB_PlatSilGels_5-5-2021.pdf

178. Oikarinen, A. (1994). Aging of the skin connective tissue: how to measure the biochemical and mechanical properties of aging dermis. *Photodermatology, photoimmunology & photomedicine*, *10*(2), 47-52.

179. Weinstein, G. D., & Boucek, R. J. (1960). Collagen and elastin of human dermis. *Journal of Investigative Dermatology*, *35*(4), 227-229.

180. El-Domyati, M., Attia, S., Saleh, F., et al (2002). Intrinsic aging vs. photoaging: a comparative histopathological, immunohistochemical, and ultrastructural study of skin. *Experimental dermatology*, *11*(5), 398-405.

181. Zhalmuratova, D., La, T, Yu, K., Szojka, A., Andrews, S, Adesida, A., ... & Chung, H. J. (2019). Mimicking "J-Shaped" And Anisotropic Stress–Strain Behavior Of Human And Porcine Aorta By Fabric-Reinforced Elastomer Composites. ACS Applied Materials & Interfaces, 11(36), 33323-33335.

182. Zhalmuratova, D., & Chung, H. J. (2020). Reinforced Gels And Elastomers For Biomedical And Soft Robotics Applications. ACS Applied Polymer Materials, 2(3), 1073-1091.

183. Edsberg, L., Maier, R. E., Mates, R. E., & Lauren, M. (1999). Mechanical properties of human skin subjected to cyclical normal pressure. *J Rehab Res Dev*, *36*, 133-41.

184. Flynn, C., Taberner, A., & Nielsen, P. (2011). Modeling the mechanical response of in vivo human skin under a rich set of deformations. *Annals of biomedical engineering*, *39*, 1935-1946.

185. Lim, K. H., Chew, C. M., Chen, P. C. Y., Jeyapalina, S., Ho, H. N., Rappel, J. K., & Lim, B. H. (2008). New extensometer to measure in vivo uni-axial mechanical properties of human skin. *Journal of biomechanics*, *41*(5), 931-936.

186. Sherman, V. R., Tang, Y., Zhao, S., Yang, W., & Meyers, M. A. (2017). Structural characterization and viscoelastic constitutive modeling of skin. *Acta biomaterialia*, *53*, 460-469.

187. Edwards, C., & Marks, R. (1995). Evaluation of biomechanical properties of human skin. *Clinics in dermatology*, *13*(4), 375-380.

188. Agache, P. G., Monneur, C., Leveque, J. L., & De Rigal, J. (1980). Mechanical properties and Young's modulus of human skin in vivo. *Archives of dermatological research*, *269*, 221-232.

189. Wöhlische, E. , Grunin, W. (1943). Pflugers Archive. 246, 469.

190. Bailly, L., Toungara, M., Orgéas, L., Bertrand, E., Deplano, V., & Geindreau, C. (2014). In-plane mechanics of soft architectured fibre-reinforced silicone rubber membranes. *Journal of the mechanical behavior of biomedical materials*, *40*, 339-353.

191. Nigmatova, F., Maksudov, N., Kasimova, A., & Shin, E. (2018). Compression Clothes For Sports-Critical. *International Journal Of Advanced Research In Science, Engineering And Technology*, *5*(12).

192. Venkatraman, P., & Tyler, D. (2015). Applications Of Compression Sportswear. *Materials And Technology For Sportswear And Performance Apparel*, *195*.

193. Manshahia, M., & Das, A. (2014). Effect Of Fiber And Fabric Constructional Parameters On Dynamic Behavior Of Compression Athletic Wear. *Fibers And Polymers*, *15*, 414-421.

194. Tan, Y. Y., Chia, P. Z., Quek, Y. H., Tracy, K. J., & Yogiaman, C. (2022). Multimaterial Knit Skins: A Design-to-Fabrication Workflow for Mass Customized Freeform Membrane Panels. *Technology| Architecture+ Design*, *6*(2), 184-199.

195. Mishra, R., & Petru, M. (2022). Application of knitted fabrics in textile structural composites. In *Advanced Knitting Technology* (pp. 411-470). Woodhead Publishing.

196. Silver, F. H., Jaffe, M., & Shah, R. G. (2018). Structure and behavior of collagen fibers. In *Handbook of properties of textile and technical fibres* (pp. 345-365). Woodhead Publishing.

197. Teegarden, D. M. (2004). *Polymer Chemistry: Introduction To An Indispensable Science*. NSTA Press.

198. Winkler, J. K. (2019). *The Du Pont Dynasty*. Pickle Partners Publishing.

199. Zhang, G., Yin, T., Nian, G., & Suo, Z. (2021). Fatigue-resistant polyurethane elastomer composites. *Extreme Mechanics Letters*, *48*, 101434.

200. Tremblay, D. (2010). Mechanical and structural characterization of ascending aortic tissues and graft materials used in the aortic arch reconstruction.

201. O'Rourke, M., Farnsworth, A., & O'Rourke, J. (2008). Aortic dimensions and stiffness in normal adults. *JACC: Cardiovascular Imaging*, *1*(6), 749-751.

202. Larena-Avellaneda, A., Dittmann, G., Haacke, C., Graunke, F., Siegel, R., Dietz, U. A., & Debus, E. S. (2008). Silicone-based vascular prosthesis: assessment of the mechanical properties. *Annals of vascular surgery*, *22*(1), 106-114.

203. Rajeev, R. S. (2008). 12 Fiber-Reinforced Elastomers. *Current Topics in Elastomers Research*, 351.

204. Fay, J. 2001. Prosthetic Liner Having Longitudinal Inelasticity. US6231617B1;WO02091960A1. Available At: Https://Worldwide.Espacenet.Com/Patent/Search/Family/026680586/Publication/US6231617B1?Q=Prosthetic%20silicone%20liner&Querylang=En%3Ade%3Afr

205. Hilmar, J., Freygarour, T., Sigurour, A., Palmi, E. 2001. Composite Elastic Material. US2001039159A1·2001-11-08. Available At: Https://Worldwide.Espacenet.Com/Patent/Search/Family/028675050/Publication/US2001039159A1?Q=Prosthetic%20silicone%20liner&Querylang=En%3Ade%3Afr

206. Shoichiro, G., Tadanori, F., Shinya, S. 2011. Socket Liner For Artificial Limb And Method For Manufacturing The Same. JP2013043032A. Available At: Https://Worldwide.Espacenet.Com/Patent/Search/Family/048007402/Publication/JP2013043032A?Q=Prosthetic%20silicone%20liner&Querylang=En%3Ade%3Afr

207. Bache, A., Valois, C., Oddsson, M. 2019. Knitted Interface. US11723782B2·2023-08-15. Available At: Https://Worldwide.Espacenet.Com/Patent/Search/Family/056609962/Publication/US11723782B2?Q=Prosthetic%20silicone%20liner&Querylang=En%3Ade%3Afr

208. Dias, T., Cork, C., Oliveira, C., Arm, R., Hurley, W. 2017. Prosthetic Sleeve. US2017216058A1·2017-08-03. Available At: Https://Worldwide.Espacenet.Com/Patent/Search/Family/051629547/Publication/US2017216058A1?Q=20170216058&Querylang=En%3Ade%3Afr

209. Yasenchuk, Y. F., Marchenko, E. S., Gunter, S. V., et al (2021). Softening Effects In Biological Tissues And Niti Knitwear During Cyclic Loading. Materials, 14(21), 6256

210. Chanda, A., & Mcclain, S. (2019). Mechanical Modelling Of Healthy And Diseased Calcaneal Fat Pad Surrogates. Biomimetics, 4(1), 1.

211. Gupta, V., Singla, R., Singh, G., & Chanda, A. (2023). Development Of Soft Composite Based Anisotropic Synthetic Skin For Biomechanical Testing. Fibers, 11(6), 55.

212. Makode, S., Singh, G., & Chanda, A. (2021). Development Of Novel Anisotropic Skin Simulants. Physica Scripta, 96(12), 125019.

213. Wang, Y., Gregory, C., & Minor, M. A. (2018). Improving mechanical properties of molded silicone rubber for soft robotics through fabric compositing. *Soft robotics*, *5*(3), 272-290.

214. Chamberlain, E. R. (2004). *U.S. Patent No. 6,685,481*. Washington, DC: U.S. Patent And Trademark Office. Available at: https://patents.google.com/patent/US6685481B2/en?oq=Chamberlain%2c+E.+R.+(2004).+U.S.+Patent+No.+6%2c685%2c481.+Washington%2c+DC:+U.S.+Patent+And+Trademark+Office.

215. Pfeil, S., Katzer, K., Kanan, A., Mersch, J., Zimmermann, M., Kaliske, M., & Gerlach, G. (2020). A Biomimetic Fish Fin-Like Robot Based On Textile Reinforced Silicone. Micromachines, 11(3), 298.

216. Eduok, U., Faye, O., & Szpunar, J. (2017). Recent Developments And Applications Of Protective Silicone Coatings: A Review Of PDMS Functional Materials. Progress In Organic Coatings, 111, 124-163.

217. Esteves, A. C. C., Brokken-Zijp, J., Laven, J., Huinink, H. P., Reuvers, N. J. W., Van, M. P., & De With, G. (2009). Influence Of Cross-Linker Concentration On The Cross-Linking Of PDMS And The Network Structures Formed. Polymer, 50(16), 3955-3966.

218. Ni Annaidh, A. N., Destrade, M., Ottenio, M., Bruyere, K., & Gilchrist, M. D. (2014, May). Strain rate effects on the failure characteristics of excised human skin. In *Proceedings of the 9th international conference on the mechanics of time dependent materials (MTL), Montréal, QC, Canada* (pp. 27-30).

219. Sherratt, M. J. (2009). Tissue elasticity and the ageing elastic fibre. *Age*, *31*(4), 305-325.

220. Chang, S. L., Howard, P. S., Koo, H. P., & Macarak, E. J. (1998). Role of type III collagen in bladder filling. *Neurourology and Urodynamics: Official Journal of the International Continence Society*, *17*(2), 135-145.

221. Lillie, M. A., & Gosline, J. M. (2002). The viscoelastic basis for the tensile strength of elastin. *International journal of biological macromolecules*, *30*(2), 119-127.

222. Matera, D. L., Dilillo, K. M., Smith, M. R., Davidson, C. D., Parikh, R., Said, M., ... & Baker, B. M. (2020). Microengineered 3D Pulmonary Interstitial Mimetics Highlight A Critical Role For Matrix Degradation In Myofibroblast Differentiation. *Science Advances*, *6*(37), Eabb5069.

223. Rising, A., & Harrington, M. J. (2022). Biological Materials Processing: Time-Tested Tricks For Sustainable Fiber Fabrication. *Chemical Reviews*, *123*(5), 2155-2199.

224. Shiffman, M. A., & Di Giuseppe, A. (2006). *Liposuction*. Berlin, Heidelberg: Springer.

225. Berry, M. G., & Davies, D. (2011). Liposuction: A Review Of Principles And Techniques. *Journal Of Plastic, Reconstructive & Aesthetic Surgery*, *64*(8), 985-992.

226. Chowdhry, S., Davis, J., Boyd, T., Choo, J., Brooks, R. M., Kelishadi, S. S., ... & Wilhelmi, B. J. (2015). Safe Tummy Tuck: Anatomy And Strategy To Avoid Injury To The Lateral Femoral Cutaneous Nerve During Abdominoplasty. *Eplasty*, *15*.

227. Masson, J. K. (1962). Lipectomy: The Surgical Removal Of Excess Fat. *Postgraduate Medicine*, *32*(5), 481-488.

228. Karastergiou, K., & Fried, S. K. (2017). Cellular mechanisms driving sex differences in adipose tissue biology and body shape in humans and mouse models. Sex and gender factors affecting metabolic homeostasis, diabetes and obesity, 29-51.

229. Klein, J. 2000. Tumescent Technique: Tumescent Anesthesia and Microcannular Liposuction. Mosby, St. Louis, Mo., 2000. 5, pp213.

230. Williams, W. R. (1880). Anatomy of the Knee Joint. Journal of anatomy and physiology, 14(Pt 2), 178.

231. Comley, K., & Fleck, N. (2012). The compressive response of porcine adipose tissue from low to high strain rate. International Journal of Impact Engineering, 46, 1-10.

232. Comley, K., & Fleck, N. A. (2010). A micromechanical model for the Young's modulus of adipose tissue. International Journal of Solids and Structures, 47(21), 2982-2990.

233. Comley, K., & Fleck, N. A. (2010). The toughness of adipose tissue: measurements and physical basis. Journal of biomechanics, 43(9), 1823-1826.

234. Fontanella, C. G., Toniolo, I., Foletto, M., Prevedello, L., & Carniel, E. L. (2022). Mechanical Behavior of Subcutaneous and Visceral Abdominal Adipose Tissue in Patients with Obesity. Processes, 10(9), 1798.

235. Kerdok, A. E., Ottensmeyer, M. P., & Howe, R. D. (2006). Effects of perfusion on the viscoelastic characteristics of liver. Journal of Biomechanics, 39(12), 2221-2231.

236. Yoon, Y. C., Lee, J. S., Park, S. U., Kwon, J. H., Hong, T. H., & Kim, D. G. (2017). Quantitative assessment of liver fibrosis using shore durometer. Annals of surgical treatment and research, 93(6), 300-304.

237. Chatzistergos, P. E., Allan, D., Chockalingam, N., & Naemi, R. (2022). Shore hardness is a more representative measurement of bulk tissue biomechanics than of skin biomechanics. Medical Engineering & Physics, 105, 103816.

238. Kissin, E. Y., Schiller, A. M., Gelbard, R. B., Anderson, J. J., Falanga, V., Simms, R. W., ... & Merkel, P. A. (2006). Durometry For The Assessment Of Skin Disease In Systemic Sclerosis. *Arthritis Care & Research: Official Journal Of The American College Of Rheumatology*, *55*(4), 603-609.

239. Romanelli, M., & Falanga, V. (1995). Use Of A Durometer To Measure The Degree Of Skin Induration In Lipodermatosclerosis. *Journal Of The American Academy Of Dermatology*, *32*(2), 188-191.

240. Tong, J., Lim, C. S., & Goh, O. L. (2003). Technique To Study The Biomechanical Properties Of The Human Calcaneal Heel Pad. The Foot, 13(2), 83-91.

241. Andriot, M., Chao, S. H., Colas, A., *Et Al* (2007). Silicones In Industrial Applications. Inorganic Polymers, 61-161.

242. Henderer, J. D., Budenz, D. L., Flynn, H. W., Schiffman, J. C., Feuer, W. J., & Murray, T. G. (1999). Elevated Intraocular Pressure And Hypotony Following Silicone Oil Retinal Tamponade For Complex Retinal Detachment: Incidence And Risk Factors. *Archives Of Ophthalmology*, *117*(2), 189-195.

243. Miller, J. B., Papakostas, T. D., & Vavvas, D. G. (2014, September). Complications Of Emulsified Silicone Oil After Retinal Detachment Repair. In *Seminars In Ophthalmology* (Vol. 29, No. 5-6, Pp. 312-318). Taylor & Francis.

244. Krzystolik, M. G., & D'Amico, D. J. (2000). Complications Of Intraocular Tamponade: Silicone Oil Versus Intraocular Gas. *International Ophthalmology Clinics*, *40*(1), 187-200.

245. Venczel, M., Bognár, G., & Veress, Á. (2021). Temperature-Dependent Viscosity Model For Silicone Oil And Its Application In Viscous Dampers. Processes, 9(2), 331.

246. Li, X., Li, J., & Dong, G. (2020). Bioinspired Topological Surface For Directional Oil Lubrication. ACS Applied Materials & Interfaces, 12(4), 5113-5119.

247. Howell, C., Vu, T. L., Lin, J. J., Kolle, S., Juthani, N., Watson, E., ... & Aizenberg, J. (2014). Self-Replenishing Vascularized Fouling-Release Surfaces. ACS Applied Materials & Interfaces, 6(15), 13299-13307.

248. Cui, J., Daniel, D., Grinthal, A., Lin, K., & Aizenberg, J. (2015). Dynamic Polymer Systems With Self-Regulated Secretion For The Control Of Surface Properties And Material Healing. *Nature Materials*, *14*(8), 790-795.

249. Howell, C., Vu, T. L., Lin, J. J., Kolle, S., Juthani, N., Watson, E., ... & Aizenberg, J. (2014). Self-Replenishing Vascularized Fouling-Release Surfaces. ACS Applied Materials & Interfaces, 6(15), 13299-13307.

250. Maccallum, N., Howell, C., Kim, P., Sun, D., Friedlander, R., Ranisau, J., ... & Aizenberg, J. (2015). Liquid-Infused Silicone As A Biofouling-Free Medical Material. *ACS Biomaterials Science & Engineering*, *1*(1), 43-51.

251. Sotiri, I., Overton, J. C., Waterhouse, A., & Howell, C. (2016). Immobilized Liquid Layers: A New Approach To Anti-Adhesion Surfaces For Medical Applications. *Experimental Biology And Medicine*, *241*(9), 909-918.

252. Khanafer, K., Duprey, A., Schlicht, M., & Berguer, R. (2009). Effects Of Strain Rate, Mixing Ratio, And Stress–Strain Definition On The Mechanical Behavior Of The Polydimethylsiloxane (PDMS) Material As Related To Its Biological

Applications. *Biomedical Microdevices*, *11*, 503-508.

253. Darby, D. R., Cai, Z., Mason, C. R., & Pham, J. T. (2022). Modulus And Adhesion Of Sylgard 184, Solaris, And Ecoflex 00-30 Silicone Elastomers With Varied Mixing Ratios. *Journal Of Applied Polymer Science*, *139*(25), E52412.

254. Jeong, S. H., Zhang, S., Hjort, K., Hilborn, J., & Wu, Z. (2016). PDMS-Based Elastomer Tuned Soft, Stretchable, And Sticky For Epidermal Electronics. Advanced Materials, 28(28), 5830-5836.

255. Ahmadzadeh, S. M. H., & Hukins, D. W. (2014). Feasibility Of Using Mixtures Of Silicone Elastomers And Silicone Oils To Model The Mechanical Behaviour Of Biological Tissues. Proceedings Of The Institution Of Mechanical Engineers, Part H: Journal Of Engineering In Medicine, 228(7), 730-734.

256. Vincent, L., & Engler, A. J. (2017). Effect Of Substrate Modulus On Cell Function And Differentiation. Comprehensive Biomaterials 5, 51-63.

257. Anon, (2023) Tissue-Mimicking Phantoms - OBEL (Uwa.Edu.Au) Optical And Biomedical Engineering Laboratory School Of Electrical, Electronic And Computer Engineering, The University Of Western Australia, Australia.

258. Oldenburg, A. L., Toublan, F. J. J., Suslick, K. S., Wei, A., & Boppart, S. A. (2005). Magnetomotive Contrast For In Vivo Optical Coherence Tomography. Optics Express, 13(17), 6597-6614.

259. Liang, X., Oldenburg, A. L., Crecea, V., *Et Al* (2008). Optical Micro-Scale Mapping Of Dynamic Biomechanical Tissue Properties. Optics Express, 16(15), 11052-11065.

260. Moučka, R., Sedlačík, M., Osička, J., & Pata, V. (2021). Mechanical Properties Of Bulk Sylgard 184 And Its Extension With Silicone Oil. Scientific Reports, 11.

261. Davoodi, E., Montazerian, H., Khademhosseini, A., & Toyserkani, E. (2020). Sacrificial 3D Printing Of Shrinkable Silicone Elastomers For Enhanced Feature Resolution In Flexible Tissue Scaffolds. Acta Biomaterialia, 117, 261-272.

262. Ustbas, B., Kilic, D., Bozkurt, A., Aribal, M. E., & Akbulut, O. (2018). Silicone-Based Composite Materials Simulate Breast Tissue To Be Used As Ultrasonography Training Phantoms. Ultrasonics, 88, 9-15.

263. Zhang, C., Liu, L., Zhang, Z., Pal, K., & Kim, J. K. (2011). Effect Of Silica And Silicone Oil On The Mechanical And Thermal Properties Of Silicone Rubber. Journal Of Macromolecular Science, Part B, 50(6), 1144-1153.

264. Liu, Z., & Yeung, K. (2008). The Preconditioning And Stress Relaxation Of Skin Tissue. Journal Of Biomedical & Pharmaceutical Engineering, 2(1), 22-28.

265. Wolf, K. J., Weiss, J. D., Uzel, S. G., Skylar-Scott, M. A., & Lewis, J. A. (2022). Biomanufacturing human tissues via organ building blocks. *Cell Stem Cell*, *29*(5), 667-677.

266. Delingette, H. (1998). Toward Realistic Soft-Tissue Modeling In Medical

Simulation. *Proceedings Of The IEEE*, *86*(3), 512-523.

267. Bischoff, J.E., Arruda, E.M. & Grosh, K. (2004) A Rheological Network Model For The Continuum Anisotropic And Viscoelastic Behavior Of Soft Tissue. Biomech Model Mechanobiol 3, 56–65 (2004).

268. Payne, A. R., & Whittaker, R. E. (1971). Low Strain Dynamic Properties Of Filled Rubbers. Rubber Chemistry And Technology, 44(2), 440-478.

269. Lüders, W. (1860). "Über Die Äusserung Der Elasticität An Stahlartigen Eisenstäben, Und Über Eine Beim Biegen Solcher Stäbe Beobachtete Molecularbewegung" [On The Manifestation Of Elasticity In Steel-Like Iron Rods, And On A Molecular Movement Observed In The Bending Of Such Rods]. Polytechnisches Journal (In German). 155 (1): 18–22.

270. Portevin, A., & Le Chatelier, F. (1924). Le Traitement Thermique Des Alliages Légers D'aluminium À Base De Cuivre. *Revue De Métallurgie*, *21*(4), 233-246.

271. Marckmann, G., Chagnon, G., Le Saux, M., & Charrier, P. (2016). Experimental Investigation And Theoretical Modelling Of Induced Anisotropy During Stress-Softening Of Rubber. *International Journal Of Solids And Structures*, *97*, 554-565.

272. Palmieri, G., Sasso, M., Chiappini, G., & Amodio, D. (2009). Mullins effect characterization of elastomers by Multi-axial cyclic tests and optical experimental methods. *Mechanics of materials*, *41*(9), 1059-1067.

273. Muñoz, S., Moreno, M. (2022). Advances in Cruciform Biaxial Testing of Fibre-Reinforced Polymers. *Polymers*, *14*(4), 686.

274. Edsberg, L. E., Mates, R. E., Baier, R. E., & Lauren, M. (1999). Mechanical characteristics of human skin subjected to static versus cyclic normal pressures. *Journal of rehabilitation research and development*, *36*(2).

275. Cheng, S., Clarke, E. C., & Bilston, L. E. (2009). The Effects Of Preconditioning Strain On Measured Tissue Properties. *Journal Of Biomechanics*, *42*(9), 1360-1362.

276. Gough, J. (2000). *Stress-Strain Behaviour Of Rubber* (Doctoral Dissertation, Queen Mary University Of London).

277. Peixoto, T., Carneiro, S., Fangueiro, R., Guedes, R. M., Paiva, M. C., & Lopes, M. A. (2022). Engineering Hybrid Textile Braids For Tendon And Ligament Repair Application. *Journal Of Applied Polymer Science*, *139*(17), 52013.

278. Rutherford, K. J., Akutagawa, K., Ramier, J. L., Tunnicliffe, L. B., & Busfield, J. J. (2023). The Influence Of Carbon Black Colloidal Properties On The Parameters Of The Kraus Model. *Polymers*, *15*(7), 1675.

279. Jiang, B. (2014). Effect Of The Microstructure Of A Filled Rubber On Its Overall Mechanical Properties. Acta Mechanica, 225(4-5), 1121-1140.

280. Wang, M. J. (1999). The Role Of Filler Networking In Dynamic Properties Of Filled

Rubber. Rubber Chemistry And Technology, 72(2), 430-448.

281. Garnier, P., Le Cam, J. B., & Grediac, M. (2013). The Influence Of Cyclic Loading Conditions On The Viscoelastic Properties Of Filled Rubber. Mechanics Of Materials, 56, 84-94.

282. Ramier, J., Gauthier, C., Chazeau, L., Stelandre, L., & Guy, L. (2007). Payne effect in silica-filled styrene–butadiene rubber: influence of surface treatment. *Journal of Polymer Science Part B: Polymer Physics*, *45*(3), 286-298.

283. Morozov, I., Lauke, B., & Heinrich, G. (2010). A New Structural Model Of Carbon Black Framework In Rubbers. Computational Materials Science, 47(3), 817-825.

284. Morozov, I., Svistkov, A. (2010) Structural-Phenomenological Model Of The Mechanical Behavior Of Rubber. Composites: Mechanics, Computations, Applications, An International Journal, 1(1), 1–17 (2010)

285. Bouzidi, S., & Bechir, H. (2022). Modeling Payne effect on basis of linearization of a visco-hyperelastic model. *Modelling and Simulation in Materials Science and Engineering*, *30*(3), 035003.

286. Fazekas, B., & Goda, T. J. (2021). Constitutive Modelling Of Rubbers: Mullins Effect, Residual Strain, Time-Temperature Dependence. International Journal Of Mechanical Sciences, 210, 106735.

287. Diani, J., Fayolle, B., & Gilormini, P. (2009). A review on the Mullins effect. *European Polymer Journal*, *45*(3), 601-612.

288. Merabia, S., Sotta, P., & Long, D. R. (2010). Unique Plastic And Recovery Behavior Of Nanofilled Elastomers And Thermoplastic Elastomers (Payne And Mullins Effects). *Journal Of Polymer Science Part B: Polymer Physics*, *48*(13), 1495-1508.

289. Lanir, Y. (1976). Biaxial stress-relaxation in skin. *Annals of biomedical engineering*, *4*, 250-270.

290. Subramanian, K. H., & Duncan, A. J. (2000). Tensile Properties For Application To Type I And Type II Waste Tank Flaw Stability Analysis (U) (Vol. 232). WSRC-TR-2000.

291. Coër, J., Manach, P. Y., Laurent, H., Oliveira, M. C., & Menezes, L. F. (2013). Piobert–Lüders Plateau And Portevin–Le Chatelier Effect In An Al–Mg Alloy In Simple Shear. Mechanics Research Communications, 48, 1-7.

292. Torres, V. M., Lanasa, J. A., Vogt, B. D., & Hickey, R. J. (2021). Controlling Nanostructure And Mechanical Properties In Triblock Copolymer/Monomer Blends Via Reaction-Induced Phase Transitions. *Soft Matter*, *17*(6), 1505-1512.

293. Brinson, H. F., & Brinson, L. C. (2008). Polymer Engineering Science And Viscoelasticity. *An Introduction*, 99-157.

294. Davis, J. R. (Ed.). (2004). *Tensile Testing*. ASM International.

295. Ait-Amokhtar, H., Fressengeas, C., & Boudrahem, S. (2008). The Dynamics Of Portevin–Le Chatelier Bands In An Al–Mg Alloy From Infrared Thermography. Materials Science And Engineering: A, 488(1-2), 540-546.

296. Huang, W. M. (2010). Thermo-Moisture Responsive Polyurethane Shape Memory Polymer For Biomedical Devices. *The Open Medical Devices Journal*, *2*(1).

297. Gossweiler, G. R., Brown, C. L., Hewage, G. B., Sapiro-Gheiler, E., Trautman, W. J., Welshofer, G. W., & Craig, S. L. (2015). Mechanochemically Active Soft Robots. *ACS Applied Materials & Interfaces*, *7*(40), 22431-22435.

298. Hong, Y., Velegol, D., Chaturvedi, N., & Sen, A. (2010). Biomimetic Behavior Of Synthetic Particles: From Microscopic Randomness To Macroscopic Control. *Physical Chemistry Chemical Physics*, *12*(7), 1423-1435.

299. Miranda, I., Souza, A., Sousa, P., Ribeiro, J., Castanheira, E. M., Lima, R., & Minas, G. (2021). Properties And Applications Of PDMS For Biomedical Engineering: A Review. *Journal Of Functional Biomaterials*, *13*(1), 2.

300. Victor, A., Ribeiro, J. E., & Araújo, F. F. (2019). Study Of PDMS Characterization And Its Applications In Biomedicine: A Review. *Journal Of Mechanical Engineering And Biomechanics*, *4*(1), 1-9.

301. Conrad, H. (1963). Effect Of Stress On The Lüders Band Velocity In Low Carbon Steels. *Journal Of The Mechanics And Physics Of Solids*, *11*(6), 437-440.

302. Abbadi, M., Hähner, P., & Zeghloul, A. (2002). On The Characteristics Of Portevin–Le Chatelier Bands In Aluminum Alloy 5182 Under Stress-Controlled And Strain-Controlled Tensile Testing. *Materials Science And Engineering: A*, *337*(1-2), 194-201.

303. Ren, S. C., Morgeneyer, T. F., Mazière, M., Forest, S., & Rousselier, G. (2021). Effect Of Lüders And Portevin–Le Chatelier Localization Bands On Plasticity And Fracture Of Notched Steel Specimens Studied By DIC And FE Simulations. *International Journal Of Plasticity*, *136*, 102880.

304. Nayan, N., Narayana Murty, S.V.S., Sarkar, R. Et Al. The Anisotropy Of Serrated Flow Behavior Of Al-Cu-Li (AA2198) Alloy. Metall Mater Trans A 50, 5066–5078 (2019). Https://Doi.Org/10.1007/S11661-019-05431-6

305. Daly CH. Biomechanical Properties Of Dermis. J Invest Dermatol. 1982 Jul;79 Suppl 1:17s-20s. Doi: 10.1111/1523-1747.Ep12544620. PMID: 7086188.

306. Reinehr, C.P.H., De Mattos Milman, L., Campos, V. (2021). Understanding Skin And Drug Delivery. In: Kalil, C.L.P.V., Campos, V. (Eds) Drug Delivery In Dermatology. Springer, Cham. Https://Doi.Org/10.1007/978-3-030-81807-4_1

307. Jalkanen, V., Andersson, B. M., Bergh, A., Ljungberg, B., & Lindahl, O. A. (2006). Prostate Tissue Stiffness As Measured With A Resonance Sensor System: A Study On Silicone And Human Prostate Tissue In Vitro. Medical And Biological Engineering And Computing, 44, 593-603.

308. Omata S (1990) New Type Tactile Sensor For Sensing Hardness Like The Human Hand And Its Application For Living Tissue. In: Technical Digest Of The 9th Sensor Symposium, Pp 257–260

309. Belyaev, O., Herden, H., Meier, J. J., Muller, C. A., Seelig, M. H., Herzog, T., ... & Uhl, W. (2010). Assessment of pancreatic hardness—surgeon versus durometer. *Journal of Surgical Research*, *158*(1), 53-60.

310. Escoffier, C., de Rigal, J., Rochefort, A., Vasselet, R., Lévêque, J. L., & Agache, P. G. (1989). Age-related mechanical properties of human skin: an in vivo study. *Journal of Investigative Dermatology*, *93*(3), 353-357.

311. Viidik A. Functional Properties Of Collagenous Tissues. Int Rev Connect Tissue Res. 1973; 6:127-215. Doi: 10.1016/B978-0-12-363706-2.50010-6. PMID: 4593853

312. Yazdi SJ, Baqersad J. Mechanical Modeling And Characterization Of Human Skin: A Review. J Biomech. 2022 Jan; 130:110864. Doi: 10.1016/J.Jbiomech.2021.110864. Epub 2021 Nov 13. PMID: 34844034.

313. Leveque JL, De Rigal J, Agache PG, Monneur C. Influence Of Ageing On The In Vivo Extensibility Of Human Skin At A Low Stress. Arch Dermatol Res. 1980;269(2):127-35. Doi: 10.1007/BF00406532. PMID: 7458404.

314. Moronkeji, K., Akhtar, R. (2015). Mechanical Properties Of Aging Human Skin. In: Derby, B., Akhtar, R. (Eds) Mechanical Properties Of Aging Soft Tissues. Engineering Materials And Processes. Springer, Cham. Https://Doi.Org/10.1007/978-3-319-03970-1_10

315. Remache, D., Caliez, M., Gratton, M., & Dos Santos, S. (2018). The effects of cyclic tensile and stress-relaxation tests on porcine skin. *Journal of the mechanical behavior of biomedical materials*, *77*, 242-249.

316. Xu, F., Seffen, K. A., & Lu, T. J. (2008). Temperature-Dependent Mechanical Behaviors of Skin Tissue. *IAENG International Journal of Computer Science*, *35*(1).

317. Wang, Y. Z., Li, M. J., & Liu, D. (2021). Thermo-mechanical interaction on transient heating of skin tissue with variable thermal material properties. *European Journal of Mechanics-A/Solids*, *86*, 104173.

318. Fatemi, M., Manduca, A., & Greenleaf, J. F. (2003). Imaging elastic properties of biological tissues by low-frequency harmonic vibration. *Proceedings of the IEEE*, *91*(10), 1503-1519.

319. Huang, Y. P., & Zheng, Y. P. (2015). *Measurement of soft tissue elasticity in vivo: techniques and applications*. CRC Press.

320. Palmeri, M. L., & Nightingale, K. R. (2011). Acoustic radiation force-based elasticity imaging methods. *Interface focus*, *1*(4), 553-564.

321. Boyer, G., Laquièze, L., Le Bot, A., Laquièze, S., & Zahouani, H. (2009). Dynamic indentation on human skin in vivo: ageing effects. *Skin Research and Technology*, *15*(1), 55-67.

322. Douglas WR. Of Pigs And Men And Research: A Review Of Applications And Analogies Of The Pig, Sus Scrofa, In Human Medical Research. Space Life Sci. 1972 Jun;3(3):226-34. Doi: 10.1007/BF00928167. PMID: 4556756.

323. Wei JC, Cartmill ID, Kendall MA, Crichton ML. In Vivo, In Situ And Ex Vivo Comparison Of Porcine Skin For Microprojection Array Penetration Depth, Delivery Efficiency And Elastic Modulus Assessment. J Mech Behav Biomed Mater. 2022 Jun; 130:105187. Doi: 10.1016/J.Jmbbm.2022.105187. Epub 2022 Mar 25. PMID: 35364362.

324. Kim, J., Srinivasan, M.A. (2005). Characterization Of Viscoelastic Soft Tissue Properties From In Vivo Animal Experiments And Inverse FE Parameter Estimation. In: Duncan, J.S., Gerig, G. (Eds) Medical Image Computing And Computer-Assisted Intervention – MICCAI 2005. MICCAI 2005. Lecture Notes In Computer Science, Vol 3750. Springer, Berlin, Heidelberg. Https://Doi.Org/10.1007/11566489_74

325. Snedeker, J. G., Barbezat, M., Niederer, P., Schmidlin, F. R., & Farshad, M. (2005). Strain energy density as a rupture criterion for the kidney: impact tests on porcine organs, finite element simulation, and a baseline comparison between human and porcine tissues. *Journal of Biomechanics*, *38*(5), 993-1001.

326. Jachowicz J, Mcmullen R, Prettypaul D. Indentometric Analysis Of In Vivo Skin And Comparison With Artificial Skin Models. Skin Res Technol 2007; 13: 299– 309.

327. Norfleet, J., Fenoglietto, F. L., & Mazzeo, M. (2015). Simulated Human Tissue Performance. In *MODSIM World Meeting 2015*.

328. Alkhouli, N., Mansfield, J., Green, E., et al (2013). The mechanical properties of human adipose tissues and their relationships to the structure and composition of the extracellular matrix. *American Journal of Physiology-Endocrinology and Metabolism*, *305*(12), E1427-E1435.

329. Sommer, G., Eder, M., Kovacs, L., Pathak, H., Bonitz, L., Mueller, C., ... & Holzapfel, G. A. (2013). Multi-axial mechanical properties and constitutive modeling of human adipose tissue: a basis for preoperative simulations in plastic and reconstructive surgery. *Acta biomaterialia*, *9*(11), 9036-9048.

330. Geerligs, M., Peters, G. W., Ackermans, P. A., Oomens, C. W., & Baaijens, F. (2008). Linear Viscoelastic Behavior Of Subcutaneous Adipose Tissue. Biorheology, 45(6), 677-688.

331. Delalleau, A., Josse, G., Lagarde, J. M., Zahouani, H., & Bergheau, J. M. (2006). Characterization of the mechanical properties of skin by inverse analysis combined with the indentation test. *Journal of biomechanics*, *39*(9), 1603-1610.

332. Zahouani, H., Pailler-Mattei, C., Sohm, B., Vargiolu, R., Cenizo, V., & Debret, R. (2009). Characterization of the mechanical properties of a dermal equivalent compared with human skin in vivo by indentation and static friction tests. *Skin research and technology*, *15*(1), 68-76.

333. Chattrairat, A., Kandare, E., Aimmanee, S., Tran, P., & Das, R. (2022). Development and characterisation of hybrid composite skin simulants based on short polyethylene fibre and

bioactive glass particle-reinforced silicone. *Journal of the Mechanical Behavior of Biomedical Materials*, *136*, 105424.

334. Piaggesi, A., Romanelli, M., Schipani, E., Campi, F., Magliaro, A., Baccetti, F., & Navalesi, R. (1999). Hardness Of Plantar Skin In Diabetic Neuropathic Feet. *Journal Of Diabetes And Its Complications*, *13*(3), 129-134.

335. Strzalkowski, N. D., Triano, J. J., Lam, C. K., Templeton, C. A., & Bent, L. R. (2015). Thresholds Of Skin Sensitivity Are Partially Influenced By Mechanical Properties Of The Skin On The Foot Sole. *Physiological Reports*, *3*(6), E12425.

336. Aghassi, D., Monoson, T., & Braverman, I. (1995). Reproducible Measurements To Quantify Cutaneous Involvement In Scleroderma. *Archives Of Dermatology*, *131*(10), 1160-1166.

337. Periyasamy, R., Anand, S., & Ammini, A. C. (2012). The effect of aging on the hardness of foot sole skin: a preliminary study. *The Foot*, *22*(2), 95-99.

338. Qi, H. J., Joyce, K., & Boyce, M. C. (2003). Durometer Hardness And The Stress-Strain Behavior Of Elastomeric Materials. *Rubber Chemistry And Technology*, *76*(2), 419-435.

339. Morgans, R., Lackovic, S., & Cobbold, P. (1999). Understanding the IRDH and Shore methods in rubber hardness testing: rubber division.

340. Reisfeld, P. L. (1994). A hard subject: use of a durometer to assess skin hardness. Journal of the American Academy of Dermatology, 31(3 Pt 1), 515-515.

341. Foitzik, K., Langan, E. A., & Paus, R. (2009). Prolactin and the skin: a dermatological perspective on an ancient pleiotropic peptide hormone. *Journal of Investigative Dermatology*, *129*(5), 1071-1087.

342. Larson, K. 2019. White paper. Can You Estimate Modulus From Durometer Hardness for Silicones? Yes, but only roughly … and you must choose your modulus carefully! The Dow Chemical Company. All rights reserved. S90799/E26340 Form No. 11-3716-01 A S2D. 2-3. https://www.dow.com/content/dam/dcc/documents/en-us/tech-art/11/11-37/11-3716-01-durometer-hardness-for-silicones.pdf?iframe=true

343. Bergström, J.; Boyce, M. Constitutive modeling of the large strain time-dependent behavior of elastomers. *J.Mech. Phys. Solids* 1998, *5*, 931–954.

344. Haider, Y. M., Abdullah, Z. S., Jani, G. H., & Mokhtar, N. (2019). Evaluation of some mechanical properties of a maxillofacial silicon elastomer reinforced with polyester powder. *International Journal of Dentistry*, *2019*, 1-6.

345. Gent, A. N. (1958). On the relation between indentation hardness and Young's modulus. *Rubber Chemistry and Technology*, *31*(4), 896-906.

346. Madhani, A. J., Niemeyer, G., & Salisbury, J. K. (1998, October). The black falcon: a teleoperated surgical instrument for minimally invasive surgery. In *Proceedings. 1998 ieee/rsj international conference on intelligent robots and systems. innovations in theory, practice and applications (cat. no. 98ch36190)* (Vol. 2, pp. 936-944). IEEE.

347. Brown, J. D., Rosen, J., Kim, Y. S., Chang, L., Sinanan, M. N., & Hannaford, B. (2003). In-vivo and in-situ compressive properties of porcine abdominal soft tissues. In *Medicine meets virtual reality 11* (pp. 26-32). IOS Press.

348. Bello, M., Welch, C. F., Goodwin, L. A., & Keller, J. (2014). Sylgard® mixing study (No. LA-UR-14-26638). Los Alamos National Lab. (LANL), Los Alamos, NM (United States).

349. Gąsior-Głogowska, M.; Komorowska, M.; Hanuza, J.; Mączka, M.; Zając, A.; Ptak, M.; Będziński, R.; Kobielarz, M.; Maksymowicz, K.; Kuropka, P.; et al. FT-raman spectroscopic study of human skin subjected to uni-axial stress. *J. Mech. Behav. Biomed. Mater.* **2013**, *18*, 240–252.

350. Diridollou, S.; Black, D.; Lagarde, J.; Gall, Y.; Berson, M.; Vabre, V.; Patat, F.; Vaillant, L. Sex- and site-dependent variations in the thickness and mechanical properties of human skin in vivo. *Int. J. Cosmet. Sci.* **2000**, *6*, 421–435.

351. Ferguson, J., & Barbenel, J. C. (1981). Skin surface patterns and the directional mechanical properties of the dermis. In *Bioengineering and the Skin: Based on the Proceedings of the European Society for Dermatological Research Symposium, held at the Welsh National School of Medicine, Cardiff, 19–21 July 1979* (pp. 83-92). Dordrecht: Springer Netherlands.

352. Alexander, H., & Cook, T. H. (1977). Accounting for natural tension in the mechanical testing of human skin. *Journal of Investigative Dermatology*, *69*(3), 310-314.

353. Stark, H. L. (1977). Directional variations in the extensibility of human skin. *British Journal of Plastic Surgery*, *30*(2), 105-114.

354. Fratzl, P., Misof, K., Zizak, I., Rapp, G., Amenitsch, H., & Bernstorff, S. (1998). Fibrillar structure and mechanical properties of collagen. *Journal of structural biology*, *122*(1-2), 119-122.

355. Kolupaev, V. A., & Nierbauer, A. (2022). Multi-axial Tensile Properties of Soft Biological Tissues. *Biomedical Journal of Scientific & Technical Research*, *41*(4), 32818-32822.

356. Ratner, B. D. (2015). The biocompatibility of implant materials. In *Host response to biomaterials* (pp. 37-51). Academic Press.

357. Zare, M., Biau, S., Croq, M., & Roquelaure, Y. (2014). Development of a biomechanical method for ergonomic evaluation: comparison with observational methods. *World Academy of Science, Engineering and Technology International Journal of Social, Human Science and Engineering*, *8*, 223-7.

358. Larraga-García, B., Pérez-Jiménez, A., Ros-Dopico, S., Rubio-Bolívar, J., Quintana-Diaz, M., & Gutiérrez, Á. (2021). Design and Development of a Hemorrhagic Trauma Simulator for Lower Limbs: A Pilot Study. *Sensors*, *21*(11), 3816.

359. Heskin, L., Galvin, R., Conroy, J., Traynor, O., Madden, S., & Simms, C. (2022). Skeletal muscle surrogates for the acquisition of muscle repair skills in upper limb surgery. *Journal of the Mechanical Behavior of Biomedical Materials*, *131*, 105216.

360. Ogden, R. (2001). Pseudo-elasticity and Stress Softening. In Y. Fu & R. Ogden (Eds.), Nonlinear Elasticity: Theory and Applications (London Mathematical Society Lecture Note Series, pp. 491-522). Cambridge: Cambridge University Press. doi:10.1017/CBO9780511526466.014.

361. Trotta, A., Ni Annaidh, A. (2019). Mechanical Characterisation Of Human And Porcine Scalp Tissue At Dynamic Strain Rates. Journal Of The Mechanical Behavior Of Biomedical Materials, 100, 103381.

362. Dahms, Piechota, Dahiya, Lue, & Tanagho. (1998). Composition and biomechanical properties of the bladder acellular matrix graft: comparative analysis in rat, pig and human. *British journal of urology*, *82*(3), 411-419.

363. Samur, E., Sedef, M., Basdogan, C., Avtan, L., & Duzgun, O. (2005, May). A robotic indenter for minimally invasive characterization of soft tissues. In *International Congress Series* (Vol. 1281, pp. 713-718). Elsevier.

364. Ottensmeyer, M. P., Kerdok, A. E., Howe, R. D., & Dawson, S. L. (2004, June). The effects of testing environment on the viscoelastic properties of soft tissues. In *International Symposium on Medical Simulation* (pp. 9-18). Berlin, Heidelberg: Springer Berlin Heidelberg.

Appendices

Chapter 3 Appendix

Multi-axial data processing procedure

The Zwick Z2.5 tensiometer with a 200N load cell to gather data. Test expert is the programme used to control the tensiometer. Matlab is used to process the data.

All data is collected as per the standard BS EN 14704-2:2007.

The below is an account of the test apparatus and methodologies used to gather and process Multi-axial data.

Figure 1 shows a diagram of the data gathering probe and ring clamp sample holder, together with its dimensions.

The clamp is fixed the tensiometer base and the probe is fixed to the mobile crosshead gantry.

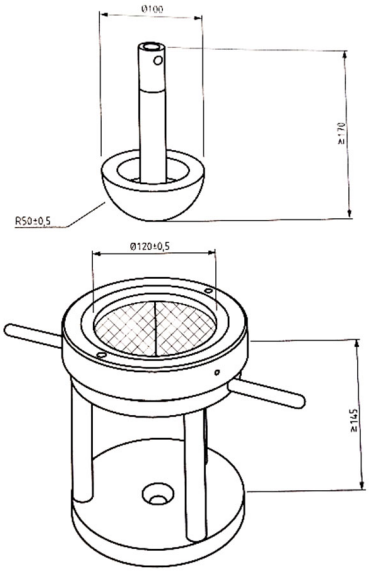

Figure 1. Data gathering probe (top) and ring clamp set up (bottom) used in all Multi-axial tests.

Apparatus and method summary

The data gathering probe is set 2 -5mm away from sample secured in the ring clamp.

The probe contacts the sample surface with a force up to 0.2N before gathering data.

The probe deforms the sample at a rate of 500mm per minute up to a maximum force of 5N before returning to the start position, in a series of 6 cycles of loading and unloading- a process involving 12 steps in total.

Cyclic loading for elastomeric and viscoelastic materials is known as preconditioning and involves a series of loading cycles to capture hysteresis curve data.

During the test, two behavioural characteristics are observed- Force decay and Unrecovered deformation.

Force decay

Force decay percentage is gathered at the maximum deformation (5N), during the 5th cycle after holding time of 60 sec.

The probe is held for 60 seconds gathering data on the samples' relaxation (the decay in resistive force).

Relaxation is the loss of stored elastic energy over time. True, Hookean elastic materials do not lose their energy while held at extension over time, so long as the extension is within the

elastic limit. Viscoelastic materials lose stored elastic energy quickly. The more 'viscoelastic' the material, the slower it responds to loading causing it to lose or gain its stored energy slower.

> "Stress relaxation is a time-dependent decrease in stress under a constant strain. This characteristic behavior of the polymer is studied by applying a fixed amount of deformation to a specimen and measuring the load required to maintain it as a function of time. Stress-relaxation data have been useful in many practical applications. A typical stress-time curve is shown in Fig. 7.5. At the beginning of the experiment, the strain is applied to the specimen at a constant rate to achieve the desired elongation. Once the specimen reaches the desired elongation, the strain is held constant for a predetermined amount of time. The stress decay, which occurs because of stress relaxation, is observed as a function of time. The stress values at different time intervals are recorded and the results are plotted to obtain a stress versus time curve."
> https://reader.elsevier.com/reader/sd/pii/B9781455731725000074?token=42A0D91FCADC34296454D3F8D8BEDE7DFB54DF579F4AC5B60C68AE0330D916D4772D6E864A4BF0FE9A57DE37236A39C5&originRegion=eu-west-1&originCreation=20230307104821

Unrecovered deformation (Hysteresis)

After the force decay data has been gathered (in cycle 5) and the probe has returned to the starting position, the probe holds its position for a further 60 seconds. The probe then completes the final 6th cycle holding at 0.2N to measure the change in load between the first loading cycle and the final unloading cycle. The difference between these two figures be can used to measure the amount of permanent (unrecovered) deformation, or 'bagging'.
The vectors that form the characteristic hysteresis loop also offer an insight into the materials behaviour under cyclic loading. Each sample set (T3 – T16 and O1 - O5) will have quite different hysteresis formation reflective of their variable mechanical and chemical configurations.

Once the data has been gathered from the test and securely stored, processing of the data can begin.

Raw test data *(RTD)* refers to the complete data set gathered from the Zwick test expert (III) program, presented in MS Excel format to allow for the easy creation of graphs and charts.

The Multi-axial data contained in the RTD includes;

1. Tool separation
2. Test time
3. Cycle number
4. Standard force
5. Standard travel

To create results tables, related graphs and charts, from the data, follows this procedure to populate the results table first.

Populating the results table

Using the RTD:

1. To find 'L', use the standard force data, find 0.2N and log the deformation in mm. Add to the results table in the L column.
2. To find 'V' and 'E', locate the maximum force (V), in Newtons, at the end of the 5^{th} cycle (9^{th} step) and log the deformation in mm (E). Add these to the results table in column V and E.
3. To find 'W', locate the maximum force, in Newtons, at the end of the holding period of the 5^{th} cycle. Add this to the results table in the W column.
4. To find 'Q', locate the data at the end of the final cycle (6^{th}) and log the displacement in mm at 0.2 Newtons. Add this to the results table in the Q column.

Once the results table has been populated, the remaining data can be calculated from 'L', 'V', 'E' and 'W'.

Where L is the undeformed measurement at 0.2N, V is the force at maximum deformation at the end of the 5^{th} cycle and E is the deformation at V in mm. W is the force decay in Newtons after 60 seconds in the final cycle. Q is the unrecovered deformation at 0.2N after the final unloading cycle given in mm.

Using the Results table:

1. To find 'S',
   $S = E - L$

2. To find 'A',

$$A = \frac{V-W}{V}\ 100$$

3. To find ‘P’,
   P = L

4. To find ‘C’,
   C = Q – L

To determine force degradation, create a separate table (with the title Force degradation) in the RTD page from ‘E’ down to ‘W’. Copy and paste:
Test time, cycle number, standard force and standard travel.
In the new table add a 5th column on the left showing the time, 0 – 60 seconds.

Using Excel; Create a rule to change the original test (OT) time to a new cycle-specific (CS) time (0-60 seconds), subtract the second line of the OT time from the first line of the OT time then add the first line of the CS time (zero). Double click the plus sign cursor to populate the rest of the CS time.
So;
OT2 – OT1 + CS1 = CS2

Use these data to create suitable graphs and charts for visual dissemination of the data.

- Hysteresis is shown as a cyclic graph.
- Force degradation is shown as a line graph
- Force decay is shown as a bar chart

Averaging the Multi-axial force degradation graphs

Open the relaxation excel file
Select a new column, top cell (G2)
Press = average
Double click (left mouse) on average cell then Select first row of data
Double click bottom right of the averaged cell to populate the remaining column
Right click the graph and ‘select data’
Press ‘add’ (edit series) series name it ‘average’
series X value is the time column (select the time and control shift down)
Y values are the average force (select the average force and control shift down)
Press ok to exit the window

Untick all other boxes in the left hand window EXCEPT average. Press ok.

Chapter 4 appendix

Results of hardness tests on fibre filled PDMS membranes

Indentation Results for PDMS A-10.

Indentation is a common method for the characterisation of elastomers used to measure skin hardness in vivo, and is also the standard measurement method used to evaluate the hardness of elastomers. Indentation by durometer was performed on all disc specimens to ASTM standard (D2240-03) guidelines. Due to the softness of specimens, a type 00 Shore hardness (H 00) calibrated durometer (‘Checkline', USA SN: 50168) with a spherical indenter tip measuring 2.5 mm in length and 2.3 mm in diameter and the device and mounting assembly arm had a total weight of 400 g. Each reading was taken using 6mm, triple-plied, 3 × 2mm specimens cut from the same sheet material. Each plied specimen was measured five times in different locations taken 6mm apart (12 mm from any edge) and recorded directly as a shore 00 hardness value before being converted to a force value in Newton’s.

	Control Group (0% Fibre addition)										Average Median	
Key	Specimen 1		Specimen 2		Specimen 3		Specimen 4		Specimen 5			
	H00	F(N)	H00	F(N)	H00	F(N)	H00	F(N)	H00	F(N)		
1	11	0.31	11	0.30	11	0.30	10.5	0.30	11	0.30		
2	9	0.28	11	0.30	12	0.31	9	0.28	11	0.30	H 00	Force (N)
3	12	0.31	12	0.31	11	0.30	9	0.29	10	0.29		
4	11	0.30	11	0.31	10	0.30	10	0.29	11	0.30		
5	11	0.30	12	0.31	10	0.30	9	0.28	11	0.30		
Average	10	0.30	11	0.31	11	0.30	9	0.29	10	0.30	10	0.30
Median	11	0.30	11	0.31	11	0.30	9	0.29	11	0.30	10	0.30

	Specimen Group 1 (1% Fibre addition)										Average Median	
Key	Specimen 1		Specimen 2		Specimen 3		Specimen 4		Specimen 5			
	H00	F(N)	H00	F(N)	H00	F(N)	H00	F(N)	H00	F(N)		
1	37	0.54	38	0.55	36	0.53	36	0.53	37	0.54		
2	37	0.54	38	0.55	36	0.53	36	0.53	37	0.54	H 00	Force (N)
3	37	0.54	38	0.55	37	0.54	36	0.53	37	0.54		
4	36	0.53	38	0.55	37	0.54	36	0.53	37	0.54		
5	36	0.53	38	0.55	37	0.54	36	0.53	37	0.54		
Average	36	0.54	38	0.55	36	0.54	36	0.53	37	0.54	37	0.54
Median	37	0.54	38	0.55	37	0.54	36	0.53	37	0.54	37	0.54

Key	Specimen Group 3 (3% Fibre addition)										Average Median	
	Specimen 1		Specimen 2		Specimen 3		Specimen 4		Specimen 5			
	H00	F(N)	H00	F(N)	H00	F(N)	H00	F(N)	H00	F(N)		
1	44	0.61	45	0.61	45	0.61	46	0.62	46	0.62		
2	45	0.62	45	0.62	47	0.63	47	0.63	47	0.63	H 00	Force (N)
3	46	0.62	47	0.63	47	0.63	46	0.62	47	0.63		
4	47	0.63	47	0.63	48	0.64	48	0.64	46	0.62		
5	48	0.64	48	0.64	47	0.63	48	0.64	46	0.62		
Average	46	0.62	46	0.63	47	0.63	47	0.63	46	0.63	46	0.63
Median	46	0.62	47	0.63	47.	0.63	47	0.63	46	0.62	46	0.63

Key	Specimen Group 4 (4% Fibre addition)										Average Median	
	Specimen 1		Specimen 2		Specimen 3		Specimen 4		Specimen 5			
	H00	F(N)	H00	F(N)	H00	F(N)	H00	F(N)	H00	F(N)		
1	50	0.66	49	0.65	49	0.65	48	0.64	50	0.66		
2	52	0.68	50	0.66	50	0.66	51	0.67	51	0.67	H 00	Force (N)
3	50	0.66	50	0.66	51	0.67	50	0.66	51	0.67		
4	52	0.68	51	0.67	52	0.68	49	0.65	52	0.68		
5	50	0.66	50	0.66	50	0.66	52	0.68	52	0.68		
Average	50	0.67	50	0.66	50	0.66	50	0.66	51	0.67	50	0.66
Median	50	0.66	50	0.66	50	0.66	50	0.66	51	0.67	50	0.66

Key	Specimen Group 2 (2% Fibre addition)										Average Median	
	Specimen 1		Specimen 2		Specimen 3		Specimen 4		Specimen 5			
	H00	F(N)	H00	F(N)	H00	F(N)	H00	F(N)	H00	F(N)		
1	41	0.58	44	0.60	41	0.58	41	0.58	41	0.58		
2	42	0.59	44	0.60	42	0.58	42	0.58	42	0.58	H 00	Force (N)
3	43	0.59	42	0.58	43	0.59	42	0.58	42	0.59		
4	43	0.59	44	0.60	43	0.60	42	0.59	43	0.59		
5	43	0.60	44	0.60	44	0.60	43	0.59	43	0.59		
Average	42	0.59	43	0.60	42	0.59	42	0.59	42	0.59	42	0.59
Median	43	0.59	44	0.60	43	0.59	42	0.58	42	0.59	42	0.59

Indentation Results for PDMS 00-30

Indentation is a common method for the characterisation of elastomers used to measure skin hardness in vivo, and is also the standard measurement method used to evaluate the hardness of elastomers. Indentation by durometer was performed on all disc specimens to ASTM standard (D2240-03) guidelines. Due to the softness of specimens, a type 00 Shore hardness (H 00) calibrated durometer (‘Checkline', USA SN: 50168) with a spherical indenter tip measuring 2.5 mm in length and 2.3 mm in diameter and the device and mounting assembly arm had a total weight of 400 g. Each reading was taken using 6mm, triple-plied, 3 × 2mm specimens cut from the same sheet material. Each plied specimen was measured five times in different locations taken 6mm apart (12

mm from any edge) and recorded directly as a shore 00 hardness value before being converted to a force value in Newton's.

Test equipment	HOO Harness reading from Durometer (00)
Conversion factor	F(N) = 0.203 + 0.00908 × H00
Formulation	PDMS 00-30 + Softener + Fibres

Key	Control Group (0% Fibre addition)										Average Median	
	Specimen 1		Specimen 2		Specimen 3		Specimen 4		Specimen 5			
	H 00	F(N)	H 00	F(N)	H 00	F(N)	H 00	F(N)	H 00	F(N)		
1	23	0.41	24	0.43	26	0.44	25	0.43	24	0.42	H 00	Force (N)
2	23	0.42	24	0.42	25	0.43	23	0.42	24	0.43		
3	24	0.42	24	0.43	24	0.43	23	0.41	25	0.43		
4	24	0.42	24	0.42	26	0.44	26	0.44	25	0.43		
5	24	0.42	24	0.43	25	0.43	25	0.43	23	0.42		
Average	23	0.42	24	0.42	25	0.43	24	0.43	24	0.42	24	0.42
Median	23	0.42	24	0.42	25	0.43	24	0.42	24	0.42	24	0.42

Key	Specimen Group 1 (1% Fibre addition)										Average Median	
	Specimen 1		Specimen 2		Specimen 3		Specimen 4		Specimen 5			
	H 00	F(N)	H 00	F(N)	H 00	F(N)	H 00	F(N)	H 00	F(N)		
1	35	0.52	35	0.52	35	0.53	35	0.53	36	0.53	H 00	Force (N)
2	36	0.53	35	0.53	36	0.53	36	0.53	36	0.53		
3	35	0.52	35	0.52	35	0.52	34	0.52	36	0.53		
4	36	0.53	35	0.53	36	0.53	36	0.53	36	0.53		
5	36	0.53	35	0.53	34	0.51	36	0.53	36	0.53		
Average	35	0.53	35	0.52	35	0.52	35	0.53	36	0.53	35	0.52
Median	35	0.53	35	0.52	35	0.53	35	0.53	36	0.53	36	0.52

Key	Specimen Group 2 (2% Fibre addition)										Average Median	
	Specimen 1		Specimen 2		Specimen 3		Specimen 4		Specimen 5			
	H 00	F(N)	H 00	F(N)	H 00	F(N)	H 00	F(N)	H 00	F(N)		
1	41	0.58	41	0.58	42	0.58	43	0.59	42	0.58	H 00	Force (N)
2	42	0.58	41	0.58	43	0.59	41	0.58	41	0.58		
3	42	0.58	42	0.58	43	0.60	42	0.59	42	0.58		
4	42	0.58	42	0.58	42	0.59	43	0.59	42	0.58		
5	40	0.57	41	0.58	42	0.59	42	0.59	43	0.59		
Average	41	0.58	41	0.58	42	0.59	42	0.59	41	0.58	41	0.58
Median	42	0.58	41	0.58	42	0.59	42	0.59	42	0.58	42	0.58

Key	Specimen Group 3 (3% Fibre addition)										Average Median	
	Specimen 1		Specimen 2		Specimen 3		Specimen 4		Specimen 5			
	H 00	F(N)	H 00	F(N)	H 00	F(N)	H 00	F(N)	H 00	F(N)		
1	45	0.61	46	0.62	45	0.61	46	0.62	45	0.61	H 00	Force (N)
2	45	0.61	44	0.60	45	0.61	45	0.61	46	0.62		
3	43	0.60	46	0.62	45	0.61	45	0.61	47	0.63		
4	44	0.60	47	0.63	45	0.61	46	0.62	46	0.62		
5	44	0.60	46	0.62	44	0.60	47	0.63	45	0.61		
Average	44	0.61	45	0.62	44	0.61	45	0.62	45	0.62	45	0.61
Median	44	0.61	46	0.62	45	0.61	45	0.62	46	0.62	45	0.61

Key	Specimen Group 4 (4% Fibre addition)										Average Median	
	Specimen 1		Specimen 2		Specimen 3		Specimen 4		Specimen 5			
	H 00	F(N)	H 00	F(N)	H 00	F(N)	H 00	F(N)	H 00	F(N)		
1	52	0.68	49	0.65	52	0.68	53	0.68	49	0.65	H 00	Force (N)
2	52	0.68	51	0.67	53	0.68	51	0.67	52	0.68		
3	52	0.68	50	0.66	53	0.69	51	0.67	52	0.68		
4	50	0.66	49	0.65	50	0.66	51	0.67	51	0.67		
5	51	0.67	51	0.67	49	0.65	51	0.67	50	0.66		
Average	51	0.67	50	0.66	51	0.67	51	0.67	50	0.66	51	0.66
Median	52	0.68	49	0.65	52	0.68	51	0.67	51	0.67	50	0.66

Tensile tests PDMS A10 with fibres

Results from tensile tests on fibre filled membranes

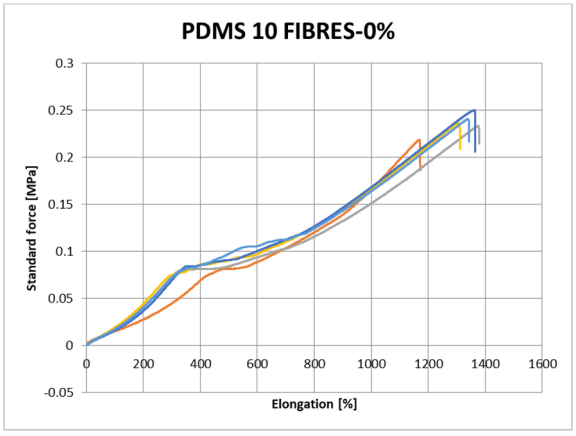

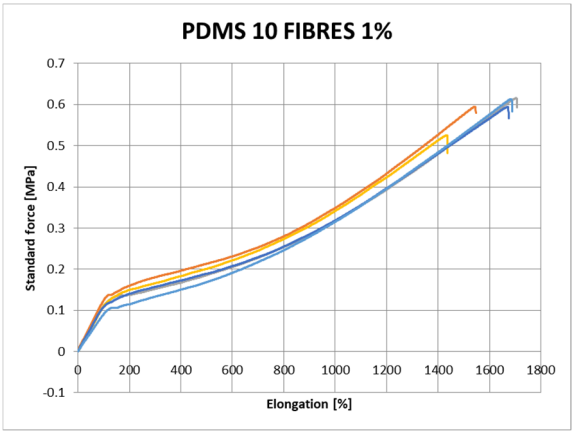

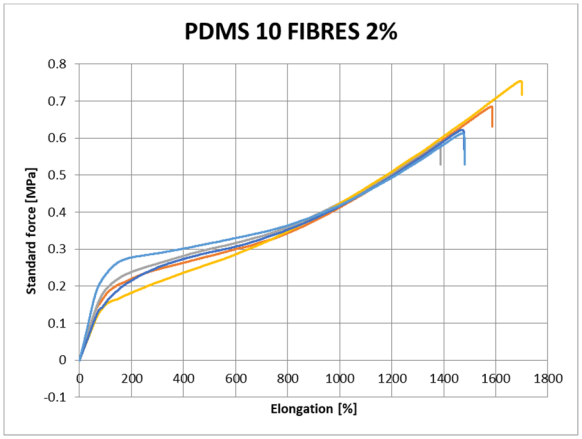

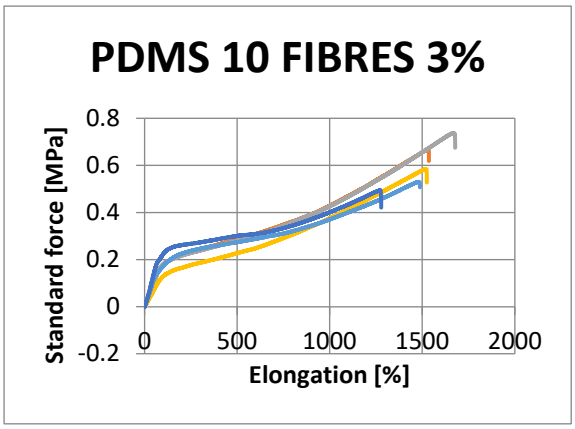

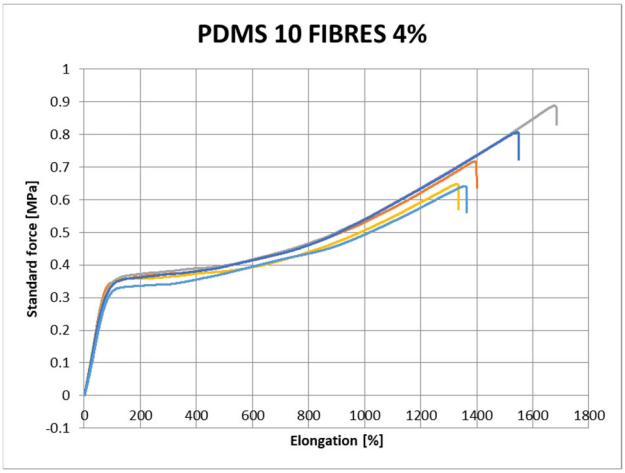

Multi-axial tests PDMS A10 with fibres

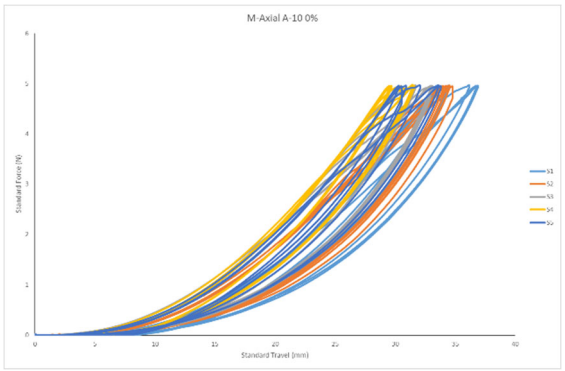

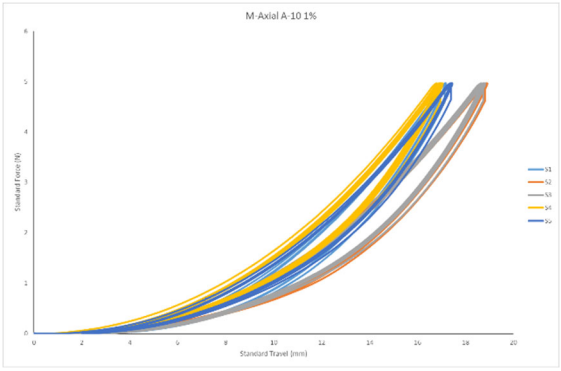

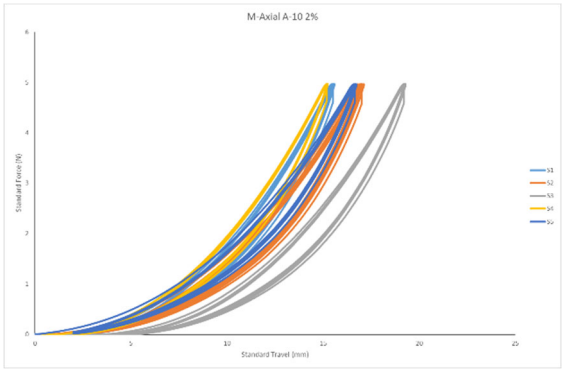

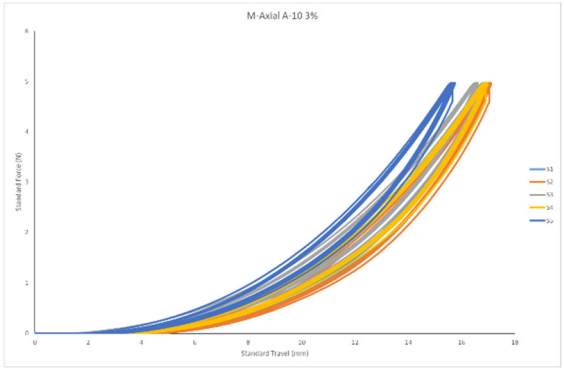

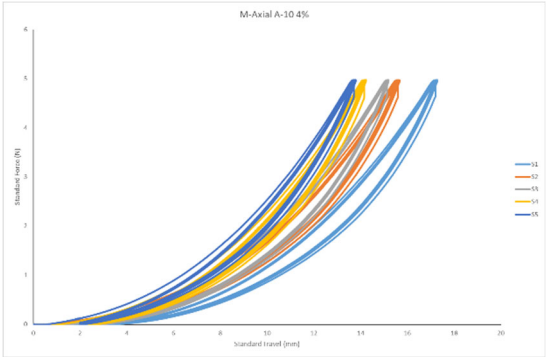

Tensile tests PDMS OO-30 with fibres

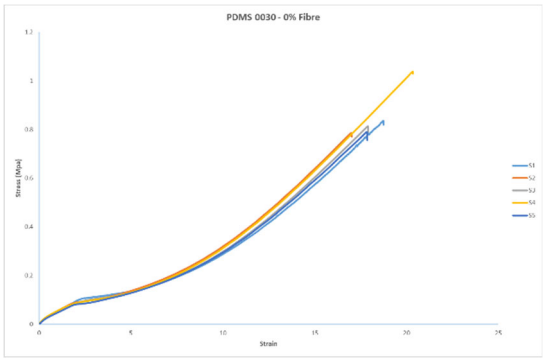

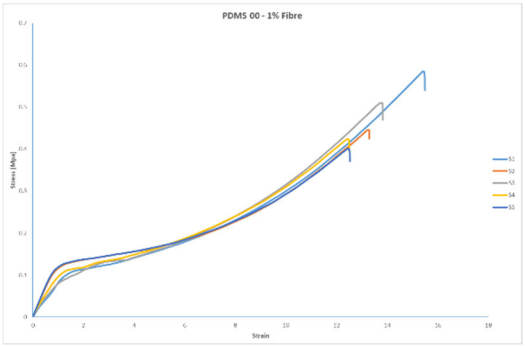

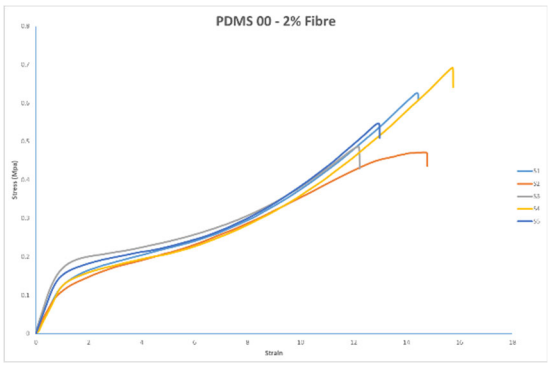

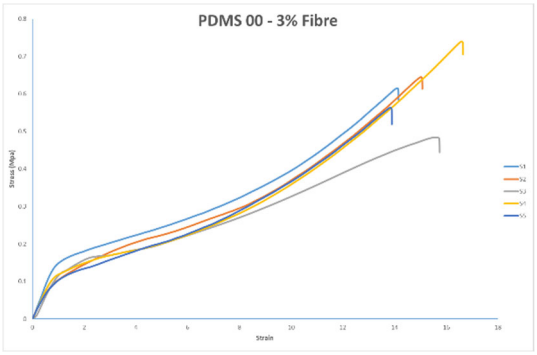

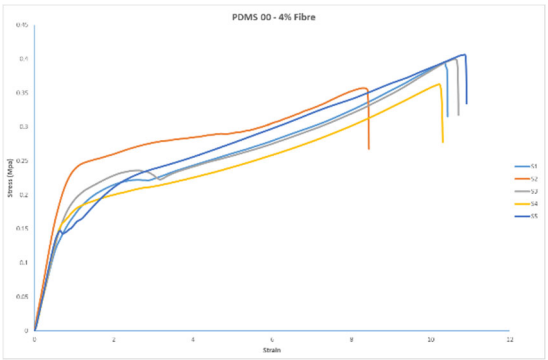

Hysteresis for PDMS with fibres

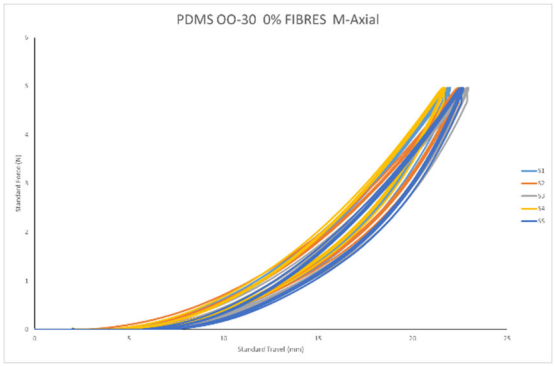

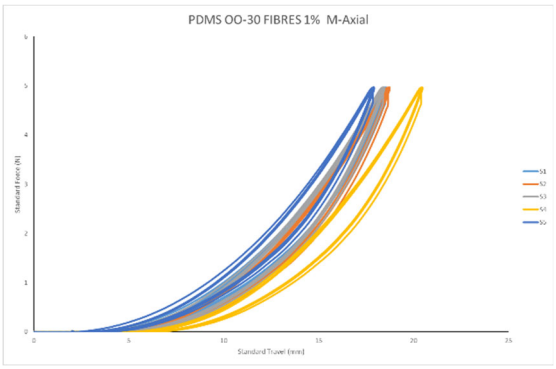

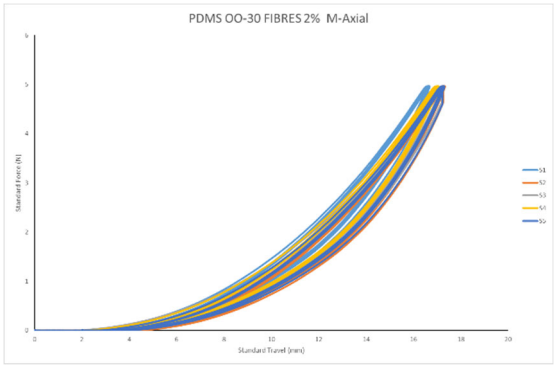

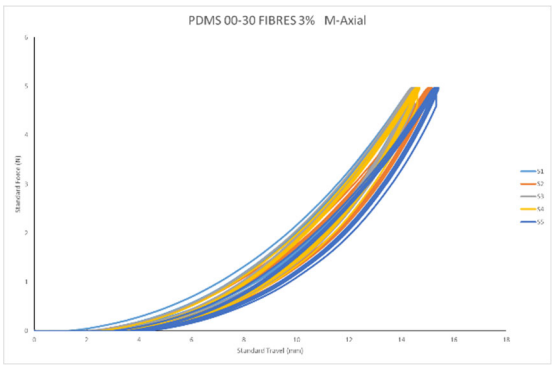

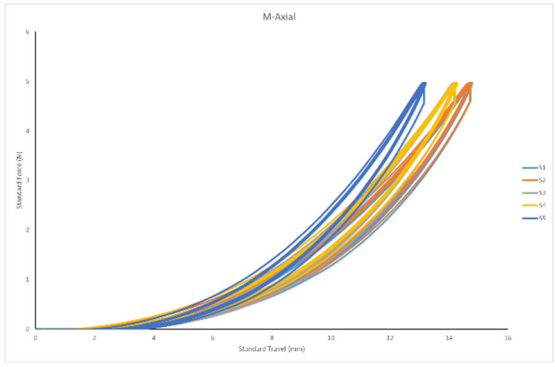

Chapter 5 appendix

Test schedule for covid19 specimen tracking manager

Mechanical testing

Tensile (UTS), Hardness (Indentation), Multi-axial test

500mm x 500mm specimen sheet makes x7 Multi-axial discs specimens (also used for hardness specimen testing) and x12 UTS dumbbell samples for tensile tests.

Same test specimen dimensions as (ISOBS37)

PDMS 0030/A10 + yarn/fabric

Legend Black text- original test group Pre-covid 19 (2019) Green text- New test group remade post-covid19 (2022)	
1. Yarn tests (single yarn thread) T1 Tensile extension Tensile tests x5 (UTS) Microscopic images x10 (x5 pre-test and x5 post-test UTS)	The Yarn, The Float and the Fabric Tests to determine the mechanical behaviour changes in lycra yarn architecture prior to embedding in PDMS matrix. Mechanical tests X20 Extension X5 Multi-axial **All specimens extended in wales direction only** **(0%, 50% and 100%)**
2. Multi-strand yarn tests knitted at both ends with a ladder float (6 strand) T2 Tensile extension Tensile test x5 (UTS) Microscopic images x10 (x5 pre-test and x5 post-test UTS)	
3. Knitted Fabric T3 Tensile tests Tensile tests x5 Course direction (UTS) Tensile tests x5 Wales direction (UTS) Multi-axial x5 Microscopic images x20 (x5 pre-test and x5 post-test UTS for each)	
4. 0% Pre-stretch Multi-strand yarn embedded PDMS 0030- T4 Tensile extension Course direction x5 (UTS) Wales direction x5 (UTS) Multi-axial x5 Indentation x5 Microscopic images x20 (x5 pre-test and x5 post-test UTS for each)	The (embedded) Float in PDMS 0030 only PDMS 0030 of previously described individual membranes. Embedded with multi-strand, uni-directional lycra yarn float.

Specimen	Dimensions
T4 V-1	2.8mm
T4 V-2	2.7mm
T4 V-3	2.6mm
T4 V-4	2.6mm
T4 V-5	2.6mm
Specimen	Dimensions
T4 P-1	2.7mm
T4 P-2	2.7mm
T4 P-3	2.7mm
T4 P-4	2.7mm
T4 P-5	2.7mm
Specimen	Dimensions
T4 D-1	2.3mm
T4 D-2	2.5mm
T4 D-3	2.4mm
T4 D-4	2.4mm
T4 D-5	2.4mm
Average specimen thickness	2.58mm

Specimen - Measurement	Hardness (HOO)	Average (logarithmic)
T4	37, 46, 47, 49, 49	45.6
T4-2	49, 47, 48, 47, 48	47.8
T4-3	46, 47, 47, 47, 46	46.6
T4-4	50, 51, 50, 49, 49	49.8
T4-5	48, 45, 48, 48, 49	47.6
Total average		**47.4**
Standard deviation		**4.2**

Mechanical tests

X30 Extension

X15 Multi-axial

X15 Indentation

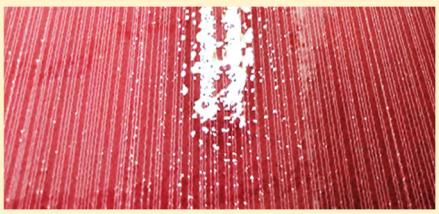

5. 50% Pre-stretch Multi-strand yarn embedded PDMS 0030 – T5

Tensile extension

Course direction x5 (UTS)

Wales direction x5 (UTS)

Multi-axial x5

Indentation x5

Microscopic images x20 (x5 pre-test and x5 post-test UTS for each)

Specimen	Dimensions
T5 V-1	2.9mm
T5 V-2	2.8mm
T5 V-3	2.8mm
T5 V-4	2.6mm

T5 V-5	2.6mm
Specimen	Dimensions
T5 P-1	3.1mm
T5 P-2	3.0mm
T5 P-3	3.0mm
T5 P-4	3.0mm
T5 P-5	3.0mm
Specimen	Dimensions
T5 D-1	3.0mm
T5 D-2	3.0mm
T5 D-3	2.9mm
T5 D-4	2.9mm
T5 D-5	2.9mm
Average specimen thickness	2.9mm

Specimen - Measurement	Hardness (HOO)	Average (logarithmic)
T5-1	46, 46, 46, 45, 46	45.8
T5-2	48, 47, 45, 48, 46,	46.8
T5-3	47, 45, 46, 46, 45	45.8
T5-4	48, 47, 47, 49, 47	47.6
T5-5	48, 46, 47, 47, 50	47.6
Total average		**46.7**
Standard deviation		**1.8**

6. 100% Pre-stretch Multi-strand yarn embedded PDMS 0030 – T6

Tensile extension

Course direction x5 (UTS)

Wales direction x5 (UTS)

Multi-axial x5

Indentation x5

Microscopic images x20 (x5 pre-test and x5 post-test UTS for each)

Specimen	Dimensions
T6 V-1	2.6mm
T6 V-2	2.6mm
T6 V-3	2.7mm
T6 V-4	2.7mm
T6 V-5	2.6mm
Specimen	Dimensions
T6 P-1	2.6mm
T6 P-2	2.5mm
T6 P-3	2.6mm

T6 P-4	2.7mm
T6 P-5	2.8mm
Specimen	Dimensions
T6 D-1	2.5mm
T6 D-2	2.7mm
T6 D-3	2.6mm
T6 D-4	2.7mm
T6 D-5	2.7mm
Average specimen thickness	2.64mm

Specimen - Measurement	Hardness (HOO)	Average (logarithmic)
T6-1	49, 50, 50, 50, 48	49.4
T6-2	46, 46, 46, 47, 48	46.6
T6-3	50, 47, 48, 50, 50	49
T6-4	50, 51, 51, 49, 50	50.2
T6-5	47, 50, 50, 49, 50	49.2
Total average		**48.8**
Standard deviation		**3.6**

7. 0% Pre-stretch fabric embedded PDMS 0030 – T7

Tensile extension

Course direction x5 (UTS)

Wales direction x5 (UTS)

Diagonal x5 (UTS)

Multi-axial x5

Indentation x5

Microscopic images x30 (x5 pre-test and x5 post-test UTS for each)

Specimen	Dimensions
T7 V-1	3.3mm
T7 V-2	3.3mm
T7 V-3	3.2mm
T7 V-4	3.3mm
T7 V-5	3.2mm
Specimen	Dimensions
T7 P-1	3.2mm
T7 P-2	3.1mm
T7 P-3	3.1mm
T7 P-4	3.3mm
T7 P-5	3.3mm
Specimen	Dimensions

The (embedded) Fabric PDMS 0030 only

Of previously described individual membrane.

Embedded with multi-strand, uni-directional lycra yarn float.

Mechanical tests

X45 Extension

X15 Multi-axial

X15 Indentation (fabric side up)

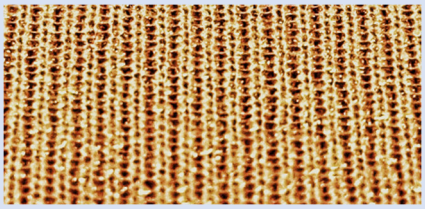

T7 D-1	3.3mm
T7 D-2	3.4mm
T7 D-3	3.3mm
T7 D-4	3.2mm
T7 D-5	3.3mm
Average specimen thickness	3.25mm

Specimen - Measurement	Hardness (HOO)	Average (logarithmic)
T7-1	47, 49, 47, 49, 48	48
T7-2	49, 48, 48, 49, 47	48.2
T7-3	47, 45, 46, 46, 50	46.8
T7-4	49, 48, 49, 48, 49	48.6
T7-5	47, 49, 46, 46, 50	47.6
Total average		**47.8**
Standard deviation		**1.8**

8. 50% Pre-stretch fabric embedded PDMS 00030 – T8

Tensile extension

Course direction x5 (UTS)

Wales direction x5 (UTS)

Diagonal x5 (UTS)

Multi-axial x5

Indentation x5

Microscopic images x30 (x5 pre-test and x5 post-test UTS for each)

Specimen	Dimensions
T8 V-1	3.4mm
T8 V-2	3.5mm
T8 V-3	3.5mm
T8 V-4	3.6mm
T8 V-5	3.5mm
Specimen	Dimensions
T8 P-1	3.2mm
T8 P-2	3.2mm
T8 P-3	3.2mm
T8 P-4	3.2mm
T8 P-5	3.2mm
Specimen	Dimensions
T8 D-1	3.4mm
T8 D-2	3.1mm
T8 D-3	3.2mm
T8 D-4	3.2mm
T8 D-5	3.7mm
Average specimen thickness	3.34mm

Specimen - Measurement	Hardness (HOO)	Average (logarithmic)
T8-1	46, 46, 46, 46, 45	45.8
T8-2	47, 48, 48, 48, 47	47.6
T8-3	46, 46, 47, 48, 48	47
T8-4	48, 48, 45, 47, 46,	46.8
T8-5	49, 47, 48, 48, 49,	48.2
Total average		**47.08**
Standard deviation		**2.4**

9. 100% Pre-stretch fabric embedded PDMS 0030 – T9

Tensile extension

Course direction x5 (UTS)

Wales direction x5 (UTS)

Diagonal x5 (UTS)

Multi-axial x5

Indentation x5

Microscopic images x30 (x5 pre-test and x5 post-test UTS for each)

Specimen	Dimensions
T9- V1	3.7mm
T9- V2	3.6mm
T9- V3	3.6mm
T9- V4	3.7mm
T9- V5	3.6mm
Specimen	Dimensions
T9 P-1	3.1mm
T9 P-2	3.1mm
T9 P-3	3.0mm
T9 P-4	3.4mm
T9 P-5	3.2mm
Specimen	Dimensions
T9 D-1	3.3mm
T9 D-2	3.4mm
T9 D-3	3.4mm
T9 D-4	3.5mm
T9 D-5	3.5mm
Average specimen thickness	3.4mm

Specimen - Measurement	Hardness (HOO)	Average (logarithmic)
T9-1	53, 53, 52, 53, 53	52.8
T9-2	53, 51, 52, 53, 52	52.4
T9-3	53, 54, 52, 53, 53	53
T9-4	54, 52, 53, 53, 52	52.8
T9-5	52, 53, 52, 53, 53	52.6
Total average		**52.7**
Standard deviation		**0.6**

10. PDMS A10 + PDMS 0030 laminated (no fabric or yarn) -T10

Tensile extension

Tensile test x5 (UTS)

Multi-axial x5

Indentation x5

Microscopic images x10 (x5 pre-test and x5 post-test UTS)

Specimen	Dimensions
T10 -1	2.7mm (2.1mm 00-30, 0.6mm A-10)
T10 -2	2.9mm (2.3mm 00-30, 0.6mm A-10)
T10 -3	2.8mm (2.2mm 00-30, 0.6mm A-10)
T10 -4	2.9mm (2.3mm 00-30, 0.6mm A-10)
T10 -5	2.7mm (2.1mm 00-30, 0.6mm A-10)
Average specimen thickness	2.8mm

Specimen - Measurement	Hardness (HOO)	Average (logarithmic)
T10-1	49, 51, 51, 48, 50	49.8
T10-2	51, 49, 51, 48, 50	49.8
T10-3	49, 51, 49, 49, 49	49.4
T10-4	49, 50, 48, 49, 51	49.4
T10-5	53, 52, 49, 48, 51	50.6
Total average		**49.8**
Standard deviation		**1.2**

PDMS lamination

Recreation of previously described individual membranes laminated together during the casting process.

Mechanical tests

X5 Extension

X5 Multi-axial

X5 Indentation

Emerging results

By increasing the 0030 thickness by just 0.2mm the maximum force and tear force increased by approximately 2N. From 12-15N

11. 0% Pre-stretch Multi-strand yarn embedded in PDMS A10 + PDMS 0030 laminated – T11

Tensile extension

Course direction x5 (UTS)

Wales direction x5 (UTS)

The (embedded) Float

PDMS lamination of previously described individual membranes

Embedded with multi-strand, uni-directional lycra yarn float.

Multi-axial x5

Indentation x5

Microscopic images x20 (x5 pre-test and x5 post-test UTS for each)

Specimen	Dimensions
T11 V -1	3mm (2.4mm 00-30, 0.6mm A-10)
T11 V -2	2.9mm (2.1mm 00-30, 0.8mm A-10)
T11 V -3	2.9mm (2.3mm 00-30, 0.6mm A-10)
T11 V -4	3mm (2.4mm 00-30, 0.6mm A-10)
T11 V -5	3.2mm (2.6mm 00-30, 0.6mm A-10)
Specimen	Dimensions
T11 P -1	2.9mm (2.3mm 00-30, 0.6mm A-10)
T11 P -2	2.9mm (2.3mm 00-30, 0.6mm A-10)
T11 P -3	3.2mm (2.6mm 00-30, 0.6mm A-10)
T11 P -4	3.4mm (2.8mm 00-30, 0.6mm A-10)
T11 P -5	3mm (2.3mm 00-30, 0.7mm A-10)
Average specimen thickness	3.04mm

Specimen -Measurement	Hardness (HOO)	Average (logarithmic)
T11-1	52, 49, 51, 50, 53	51
T11-2	51, 51, 50, 50, 50	50.4
T11-3	50, 51, 52, 53, 53	51.8
T11-4	50, 52, 51, 52, 52	51.4
T11-5	51, 52, 53, 53, 54	52.6
Total average		**51.4**
Standard deviation		**2.2**

Mechanical tests

X30 Extension

X15 Multi-axial

X15 Indentation

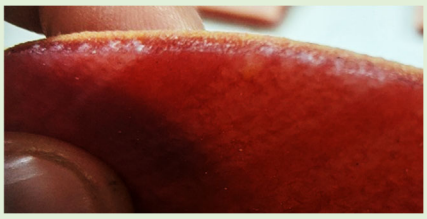

Maximum force at break increased by 10N to 25N for most specimens.

12. 50% Pre-stretch Multi-strand yarn embedded in PDMS A10 + PDMS 0030 laminated – T12

Tensile extension

Course direction x5 (UTS)

Wales direction x5 (UTS)

Multi-axial x5

Indentation x5

Microscopic images x20 (x5 pre-test and x5 post-test UTS for each)

Specimen	Dimensions
T12 V -1	2.9mm (2.2mm 00-30, 0.7mm A-10)
T12 V -2	2.8mm (2.2mm 00-30, 0.6mm A-10)
T12 V -3	3.2mm (2.5mm 00-30, 0.7mm A-10)
T12 V -4	3.2mm (2.5mm 00-30, 0.7mm A-10)
T12 V -5	3.2mm (2.5mm 00-30, 0.7mm A-10)
Specimen	Dimensions

T12 P -1	3.4mm (2.7mm 00-30, 0.7mm A-10)
T12 P -2	3.3mm (2.6mm 00-30, 0.7mm A-10)
T12 P -3	3.4mm (2.7mm 00-30, 0.7mm A-10)
T12 P -4	3.3mm (2.6mm 00-30, 0.7mm A-10)
T12 P -5	3.4mm (2.7mm 00-30, 0.7mm A-10)
Average specimen thickness	3.21mm

Specimen -Measurement	Hardness (HOO)	Average (logarithmic)
T12-1	50, 51, 53, 53, 53	52
T12-2	50, 51, 50, 52, 52	51
T12-3	52, 53, 51, 53, 52	52.2
T12-4	50, 51, 50, 49, 50	50
T12-5	50, 52, 53, 50, 51	51.2
Total average		**51.2**
Standard deviation		**2**

13. 100% Pre-stretch Multi-strand yarn embedded in PDMS A10 + PDMS 0030 laminated -T13

Tensile extension

Course direction x5 (UTS)

Wales direction x5 (UTS)

Multi-axial x5

Indentation x5

Microscopic images x20 (x5 pre-test and x5 post-test UTS for each)

Specimen	Dimensions
T13 V -1	3.3mm (2.7mm 00-30, 0.6mm A-10)
T13 V -2	3mm (2.4mm 00-30, 0.6mm A-10)
T13 V -3	3mm (2.4mm 00-30, 0.6mm A-10)
T13 V -4	3mm (2.4mm 00-30, 0.6mm A-10)
T13 V -5	2.9mm (2.3mm 00-30, 0.6mm A-10)
Specimen	Dimensions
T13 P -1	2.9mm (2.2mm 00-30, 0.7mm A-10)
T13 P -2	3mm (2.3mm 00-30, 0.7mm A-10)
T13 P -3	2.7mm (2.1mm 00-30, 0.6mm A-10) sub 1
T13 P -4	3.2mm (2.5mm 00-30, 0.7mm A-10)
T13 P -5	2.8mm (2.1mm 00-30, 0.7mm A-10) sub 2
Average specimen thickness	2.98mm

Specimen -Measurement	Hardness (HOO)	Average (logarithmic)
T13-1	52, 50, 53, 54, 55	52.8

T13-2	51, 52, 51, 52, 54	52
T13-3	55, 51, 53, 53, 51	52.6
T13-4	53, 52, 54, 52, 53	52.8
T13-5	52, 52, 53, 53, 53	52.6
Total average		**52.5**
Standard deviation		**0.8**

14. 0% Pre-stretch fabric embedded in PDMS A10 + PDMS 00-30 laminated – T14

Tensile extension

Course direction x5 (UTS)

Wales direction x5 (UTS)

Diagonal x5 (UTS)

Multi-axial x5

Indentation x5

Microscopic images x30 (x5 pre-test and x5 post-test UTS for each)

Specimen	Dimensions
T14 V-1	3.6mm (2.8mm 00-30, 0.8mm A-10)
T14 V-2	3.7mm (2.9mm 00-30, 0.8mm A-10)
T14 V-3	3.7mm (2.9mm 00-30, 0.8mm A-10)
T14 V-4	3.7mm (2.8mm 00-30, 0.9mm A-10)
T14 V-5	3.7mm (2.9mm 00-30, 0.8mm A-10)
Specimen	Dimensions
T14 P-1	3.4mm (2.6mm 00-30, 0.8mm A-10)
T14 P-2	4.3mm (2.9mm 00-30, 1.4mm A-10)
T14 P-3	4.3mm (2.9mm 00-30, 1.4mm A-10)
T14 P-4	4.2mm (2.8mm 00-30, 1.4mm A-10)
T14 P-5	4.1mm (2.9mm 00-30, 1.2mm A-10)
Specimen	Dimensions
T14 D-1	3.8mm (2.8mm 00-30, 1.0mm A-10)
T14 D-2	4.0mm (2.8mm 00-30, 1.2mm A-10)
T14 D-3	3.8mm (2.8mm 00-30, 1.2mm A-10)
T14 D-4	3.7mm (2.6mm 00-30, 1.1 mm A-10)
T14 D-5	3.7mm (2.7mm 00-30, 1.0mm A-10)
Average specimen thickness	3.84mm

Specimen - Measurement	Hardness (HOO)	Average (logarithmic)
T14-1	50, 52, 53, 53, 53	52.2
T14-2	54, 54, 54, 54, 53	53.8
T14-3	54, 53, 54, 54, 53	53.6

The (embedded) Fabric

PDMS lamination_of previously described individual membranes

Embedded with knitted (multi-directional) lycra yarn.

Mechanical tests

X45 Extension

X15 Multi-axial

X15 Indentation

T14-4	53, 54, 53, 51, 52	52.6
T14-5	55, 54, 54, 54, 53	54
Total average		53.2
Standard deviation		1.8

15. 50% Pre-stretch fabric embedded in PDMS A10 + PDMS 0030 laminated – T15

Tensile extension

Course direction x5 (UTS)

Wales direction x5 (UTS)

Diagonal x5 (UTS)

Multi-axial x5

Indentation x5

Microscopic images x30 (x5 pre-test and x5 post-test UTS for each)

Specimen	Dimensions
T15 V-1	3.6mm (2.6mm 00-30, 1.0mm A-10)
T15 V-2	3.5mm (2.7mm 00-30, 0.8mm A-10)
T15 V-3	3.5mm (2.7mm 00-30, 0.8mm A-10)
T15 V-4	3.6mm (2.7mm 00-30, 0.9mm A-10)
T15 V-5	3.6mm (2.7mm 00-30, 0.9mm A-10)
Specimen	Dimensions
T15 P-1	3.6mm (2.7mm 00-30, 0.9mm A-10)
T15 P-2	3.5mm (2.6mm 00-30, 0.9mm A-10)
T15 P-3	3.6mm (2.6mm 00-30, 1.0mm A-10)
T15 P-4	3.6mm (2.6mm 00-30, 1.0mm A-10)
T15 P-5	3.6mm (2.6mm 00-30, 1.0mm A-10)
Specimen	Dimensions
T15 D-1	3.5mm (2.8mm 00-30, 0.7mm A-10)
T15 D-2	3.5mm (2.7mm 00-30, 0.8mm A-10)
T15 D-3	3.6mm (2.7mm 00-30, 0.9mm A-10)
T15 D-4	3.6mm (2.8mm 00-30, 0.8mm A-10)
T15 D-5	3.6mm (2.7mm 00-30, 0.9mm A-10)
Average specimen thickness	3.56mm

Specimen - Measurement	Hardness (HOO)	Average (logarithmic)
T15-1	55, 56, 56, 56, 55	55.6
T15-2	55, 56, 55, 56, 57	55.8
T15-3	55, 56, 57, 57, 56	56.2

T15-4	56, 56, 55, 56, 57	56
T15-5	54, 56, 56, 57, 57	56
Total average		55.9
Standard deviation		0.6

16. 100% Pre-stretch fabric embedded in PDMS A10 + PDMS 0030 laminated – T16

Tensile extension

Course direction x5 (UTS)

Wales direction x5 (UTS)

Diagonal x5 (UTS)

Multi-axial x5

Indentation x5

Microscopic images x30 (x5 pre-test and x5 post-test UTS for each)

Specimen	Dimensions
T 16 V-1	3.3mm (2.5mm 00-30, 0.8mm A-10)
T 16 V-2	3.5mm (2.4mm 00-30, 1.1mm A-10)
T 16 V-3	3.6mm (2.5mm 00-30, 1.1mm A-10)
T 16 V-4	3.6mm (2.5mm 00-30, 1.1mm A-10)
T 16 V-5	3.6mm (2.5mm 00-30, 1.1mm A-10)
Specimen	Dimensions
T16 P-1	3.1mm (2.4mm 00-30, 0.7mm A-10)
T16 P-2	3.4mm (2.5mm 00-30, 0.9mm A-10)
T16 P-3	3.5mm (2.6mm 00-30, 0.9mm A-10)
T16 P-4	3.4mm (2.5mm 00-30, 0.9mm A-10)
T16 P-5	3.4mm (2.5mm 00-30, 0.9mm A-10)
Specimen	Dimensions
T16 D-1	3.2mm (2.3mm 00-30, 0.9mm A-10)
T16 D-2	3.2mm (2.3mm 00-30, 0.9mm A-10)
T16 D-3	3.2mm (2.3mm 00-30, 0.9mm A-10)
T16 D-4	3.2mm (2.2mm 00-30, 1.0mm A-10)
T16 D-5	3.2mm (2.2mm 00-30, 1.0mm A-10)
Average specimen thickness	3.36mm

Specimen - Measurement	Hardness (HOO)	Average (logarithmic)
T16-1	57, 59, 57, 58, 58	57.8
T16-2	58, 58, 59, 60, 60	59
T16-3	59, 60, 58, 58, 58	58.6
T16-4	60, 60, 59, 58, 58	59

T16-5	59, 59, 59, 58, 58	58.6
Total average		58.6
Standard deviation		1.2

Test Schedule Overview

X175 UTS tests (AS)

X70 Multi-axial tests (AS)

X65 (x5) Indentation tests (RA)

X350 Microscopic images (RA)

Materials

2 cones of Lycra yarn- Single cover 16/SC (‘S’ twist direction, single cover)/090

Cr:22/1/60 (lycra size)/60 (twists per meter) n66 (Nylon type)

20KG PDMS 00-30

20KG PDMS A-10

2KG Loose chopped strand polyester fibres

Specimen legend

V – Inline with direction of extension (Wales)

P – Perpendicular to direction of extension (Course)

D - Diagonal to direction of extension (45 degrees)

Hardness - Modulus converter and inverter using Gent's expansion equation

Table of results for Gent's expansion equation And Shahidi's inversion equation			
A. N. Gent (1958)		A. Shahidi (2022)	
Hardness Shore A	Modulus MPa	Hardness Shore A	Modulus MPa
-	-	1.64	0.05
-	-	3.835	0.1
5	0.127	5.933	0.15
-	-	7.942	0.2
10	0.253	9.867	0.25
15	0.394	11.713	0.3
-	-	13.485	0.35
-	-	15.187	0.4
-	-	16.824	0.45
-	-	18.398	0.5
20	0.552	19.914	0.55
-	-	21.375	0.6
-	-	22.784	0.65
-		24.142	0.7
25	0.732	25.454	0.75
-	-	26.722	0.8
-	-	27.946	0.85
-	-	29.131	0.9
30	0.937	30.277	0.95
35	1.174	31.387	1
40	1.45	40.809	1.5
45	1.777	47.955	2
50	2.169	53.562	2.5
55	2.648	58.078	3
60	3.246	61.794	3.5
65	4.016	64.904	4
-	-	67.547	4.5
70	5.045	69.819	5
75	6.479	-	-
80	8.63	-	-
85	12.227	-	-
90	19.411	-	-

Uni-axial specimen breaks multi-layered specimens without yarn or fabric

Uni-axial specimen breaks multi-layered specimens with embedded yarns

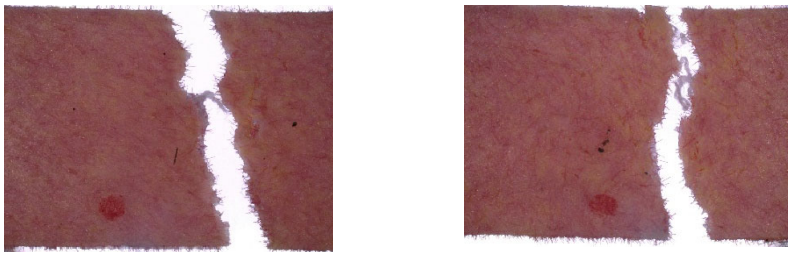

Uni-axial specimen breaks multi-layered specimens with embedded fabrics

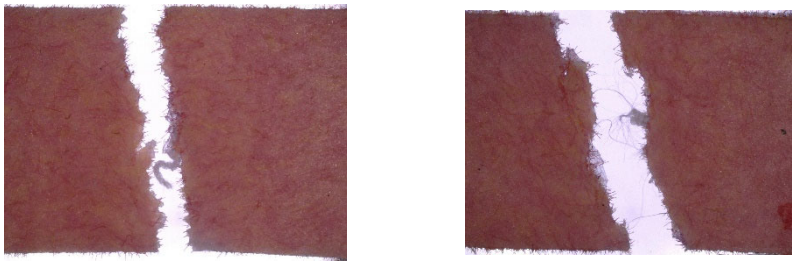

Chapter 6 appendix

Hardness test data log

+ 150% PDMS oil (3:2 ratio) (Test group O4)

Specimen	Dimensions
T1	2.6mm
T2	2.6mm
T3	2.7mm
T4	2.5mm
T5	2.6mm

Specimen - Measurement	Hardness (HOO)	Average (logarithmic)
T1	-	-
T2	-	-
T3	-	-
T4	-	-
T5	-	-
Total average		-

Specimen - Measurement	Hardness **(HOOO)**	Average (logarithmic)
T1	20, 20, 21, 20, 20	20.2
T2	18, 20, 20, 20, 20	19.6
T3	19, 20, 20, 20, 19	19.6
T4	20, 20, 20, 20, 19	19.8
T5	19, 21, 20, 20, 20	20
Total average		**19.84**

+ 50% PDMS oil (1:2 ratio) (Test group O2)

Specimen	Dimensions
T1	2.7mm
T2	2.7mm
T3	2.7mm
T4	2.7mm
T5	2.7mm

Specimen - Measurement	Hardness (HOO)	Average (logarithmic)
T1	16, 21, 20, 21, 20	19.6
T2	18, 20, 19, 19, 18	18.8
T3	18, 20, 19, 20, 21	19.6
T4	17, 20, 19, 20, 20	19.2
T5	17, 18, 20, 19, 19	18.6
Total average		19.9

Specimen - Measurement	Hardness **(HOOO)**	Average (logarithmic)
T1	40, 38, 39, 40, 39	39.2
T2	41, 39, 40, 40, 39	39.8
T3	39, 40, 39, 40, 39	39.4
T4	41, 41, 40, 39, 40	40.2
T5	41, 41, 39, 40, 41	40.4
Total average		**39.8**

(control group) (Test group **O1**)
Test sample dimensions

PDMS (control group)

Specimen	Dimensions
T1	4.1mm
T2	4.2mm
T3	4.1mm
T4	4.1mm
T5	4mm

Specimen - Measurement	Hardness **(HOO)**	Average (logarithmic)
T1	33, 35, 34, 35, 35	34.4
T2	40, 37, 35, 34, 36	36.4
T3	36, 35, 35, 35, 36	35.4
T4	35, 35, 34, 35, 35	34.8
T5	35, 34, 34, 33, 34	34
Total average		35

Specimen - Measurement	Hardness **(HOOO)**	Average (logarithmic)
T1	57, 56, 56, 56, 55	56
T2	56, 55, 57, 56, 57	56.2
T3	57, 55, 56, 57, 57	56.4
T4	56, 56, 56, 55, 55	55.6
T5	55, 57, 56, 54, 54	55.2
Total average		**55.88**

+ 200% PDMS oil (2:1 ratio) (Test group O5)

Specimen	Dimensions
T1	2.7mm
T2	2.7mm
T3	2.8mm
T4	2.8mm
T5	2.7mm

Specimen - Measurement	Hardness (HOO)	Average (logarithmic)
T1	-	-
T2	-	-
T3	-	-
T4	-	-
T5	-	-
Total average		

Specimen - Measurement	Hardness **(HOOO)**	Average (logarithmic)
T1	13, 13, 16, 12, 13	13.4
T2	12, 13, 10, 11, 13	11.8
T3	12, 12, 13, 12, 12	12.2
T4	13, 13, 11, 12, 13	12.4
T5	12, 12, 12, 10, 13	11.8
Total average		**12.32**

Tensile and Multi-axial tests for PDMS with oil

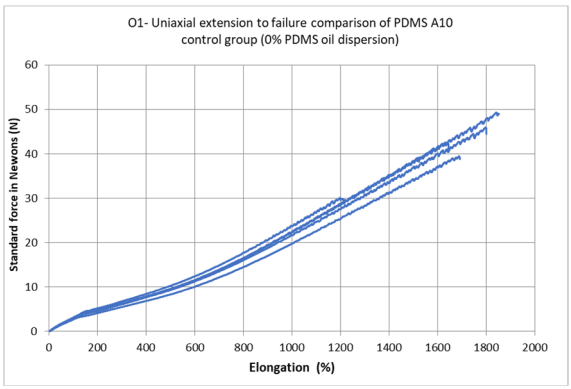

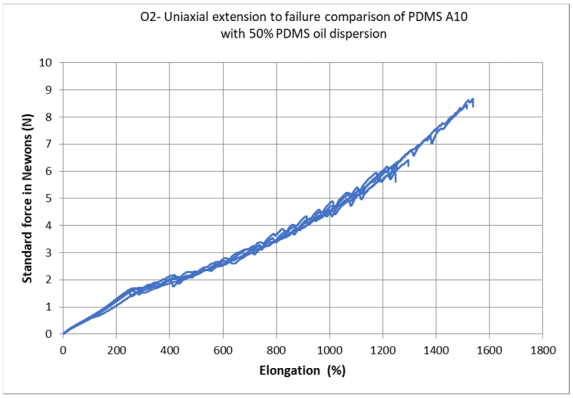

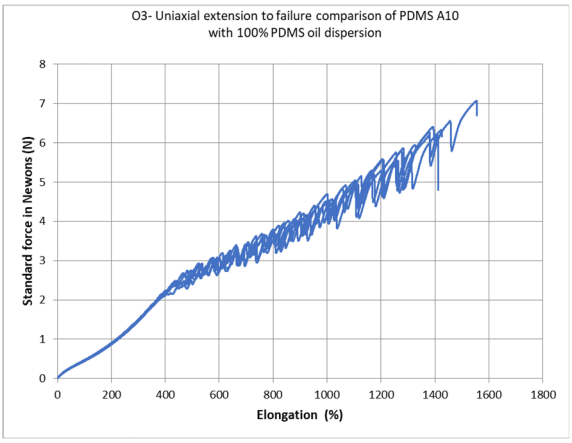

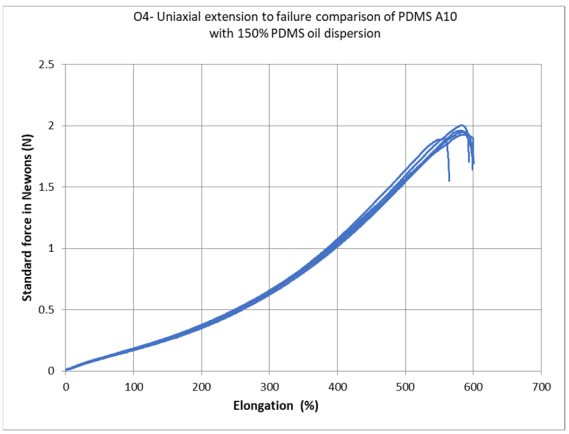

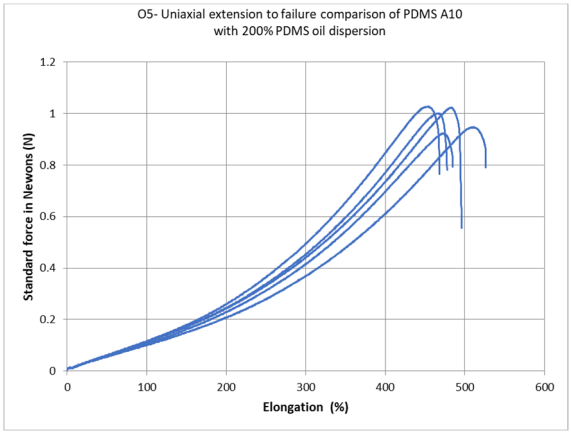

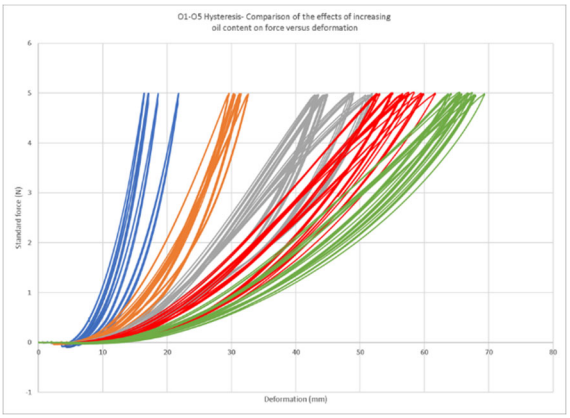

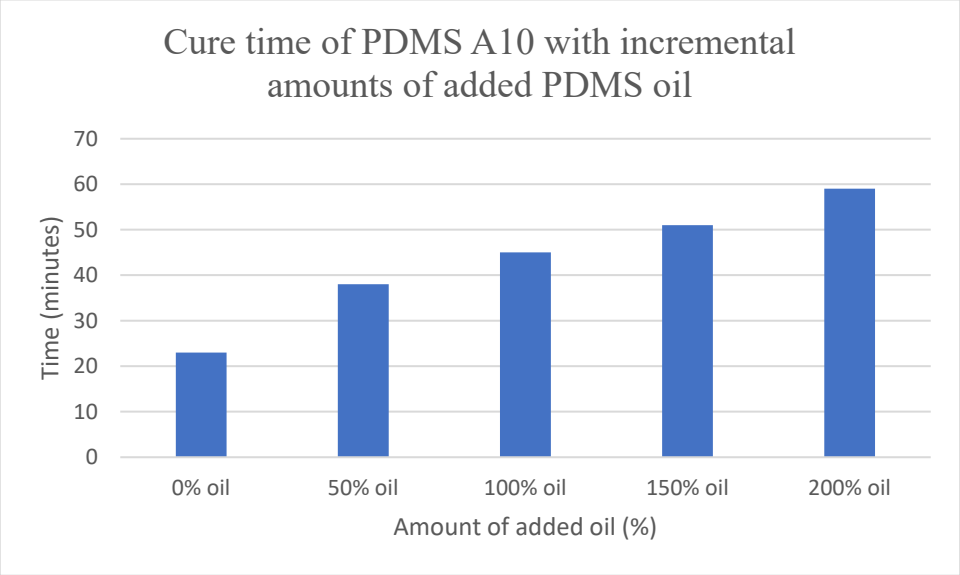
Cure time of PDMS A10 with incremental amounts of added PDMS oil
Time (minutes)
70
60
50
40
30
20
10
0
0% oil
50% oil
100% oil
150% oil
200% oil
Amount of added oil (%)